

On art, science, and the conservation of subterranean ecosystems

Stefano Mammola^{1,2,3}, Jagoba Malumbres-Olarte^{2,4}, Ilaria Vaccarelli^{1,5,6},
Veronica Nanni^{1,6}, Adrià Bellvert¹, Ivan Jarić^{7,8}

1 *Molecular Ecology Group, Water Research Institute, National Research Council, Verbania, Italy* **2** *Finnish Museum of Natural History, University of Helsinki, Helsinki, Finland* **3** *NBFC, National Biodiversity Future Center, Palermo, Italy* **4** *CE3C – Centre for Ecology, Evolution and Environmental Sciences, LIBRe – Laboratory for Integrative Biodiversity Research, CHANGE – Institute for Global Change and Sustainability, University of the Azores, Terceira, and University of Lisbon, 1749-016 Lisboa, Portugal* **5** *Department of Life, Health and Environmental Sciences, University of L'Aquila, L'Aquila, Italy* **6** *School for Advanced Studies IUSS, Science, Technology and Society Department, Pavia, Italy* **7** *Université Paris-Saclay, CNRS, AgroParisTech, Ecologie Systématique Evolution, Gif-sur-Yvette, France* **8** *Biology Centre of the Czech Academy of Sciences, Institute of Hydrobiology, České Budějovice, Czech Republic*

Corresponding author: Stefano Mammola (stefano.mammola@cnr.it)

Academic editor: Elizabeth Borda | Received 22 October 2024 | Accepted 3 February 2025 | Published 26 February 2025

<https://zoobank.org/E9975F62-B400-4DF1-A910-E4A56AD3F43A>

Citation: Mammola S, Malumbres-Olarte J, Vaccarelli I, Nanni V, Bellvert A, Jarić I (2025) On art, science, and the conservation of subterranean ecosystems. *Subterranean Biology* 51: 1–19. <https://doi.org/10.3897/subtbiol.51.139954>

Abstract

Caves, with their unique geologic and biological features, have inspired human imagination throughout history. From photography to movies, through comics, painting, and poetry, subterranean ecosystems feature prominently in various forms of artistic expression, often incorporating scientific ideas or concepts. Integrating art with science offers a powerful way to convey the uniqueness and importance of the organisms that inhabit subterranean ecosystems, emphasizing their importance as providers of key ecological and cultural services. This, in turn, would help promote their conservation. We discuss realized and un-realized connections between subterranean biologists and artists, aiming to achieve broader protection for subterranean ecosystems. We showcase the different art forms that depict subterranean environments, explain how each aligns with conservation science, and highlight the mutual benefits artists and researchers in subterranean biology can derive from collaboration. In doing so, we pose two important questions: How can we effectively bridge the cultural divide between subterranean scientists and artists? And how can we assess the effectiveness of art in enhancing science communication about subterranean ecosystems and their conservation? By addressing these questions, we envision a future where art and science intersect to safeguard the rich and diverse subterranean biological and cultural heritage.

Keywords

Artistic expression, conservation art, conservation science, environmental communication, interdisciplinarity, public engagement, scientific visualization, science communication

Art goes underground

“In 15,000 years, we have invented nothing!” Pablo Picasso is said to have exclaimed, shaking his head, upon seeing the Paleolithic art in Altamira cave, Spain – an anecdote widely regarded as apocryphal. However, it serves as a reminder that humans have been using cave walls as canvases for a very long time (Fig. 1a). Since then, caves have evolved from serving as artistic media to becoming central subjects in modern and contemporary art. From abstract paintings (Fig. 1b) to graffiti (Fig. 1c), through figurative art (Fig. 1d, e), comics (Fig. 1f), and music (Fig. 1g), caves and their biota have been prominently featured in various forms of artistic expression, which often incorporate scientific ideas or concepts. For instance, Sebastião Salgado’s “Genesis” photographic series includes haunting images of cave formations that emphasize the untouched beauty of subterranean landscapes. Werner Herzog’s documentary “Cave of Forgotten Dreams” explores the Chauvet Cave’s prehistoric art, offering a meditative look at the intersection of time, art, and human consciousness. In painting, the work of contemporary artist Anselm Kiefer frequently features cave-like structures, exploring themes of memory, history, and mythology; whereas in poetry, Seamus Heaney’s poem “The Underground” uses the imagery of caves and tunnels to explore themes of fear, wonder, and the unknown.

Caves and other subterranean ecosystems have increasingly become the protagonists of entire exhibitions, such as “Subterranean” at Amos Rex in Helsinki (2 April – 21 August 2022) and more recently, “Subterranean worlds” (*Mondes souterrains*) at Louvre Lens Museum in Paris (27 March – 22 July 2024) (Fig. 1h). While these expositions celebrated the beauty and mysteries of hidden subterranean worlds, they also underscored the growing pressures human activities pose on these ecosystems, drawing attention to the critical need for their conservation (Mammola et al. 2019). For example, the pamphlet of Amos Rex’s “Subterranean” exhibition emphasizes how *“Humanity has carved its own footprint beneath the surface of the earth [...]. These themes are central to the works of many contemporary artists who comment on political conflicts and globally unsustainable development”*. Given this example and others, we contend that the convergence of art and science for promoting the conservation of subterranean environments holds great promise. The question remains: how can artists and scientists collaborate most effectively to safeguard the rich heritage hidden beneath our feet?

The importance of art for subterranean science and conservation

The idea of bridging science and art to foster environmental education and improve communication is not new (e.g., Jacobson et al. 2007; Opermanis et al. 2015; Dixon et al. 2015). The intersection of art and science enriches both fields, making scien-

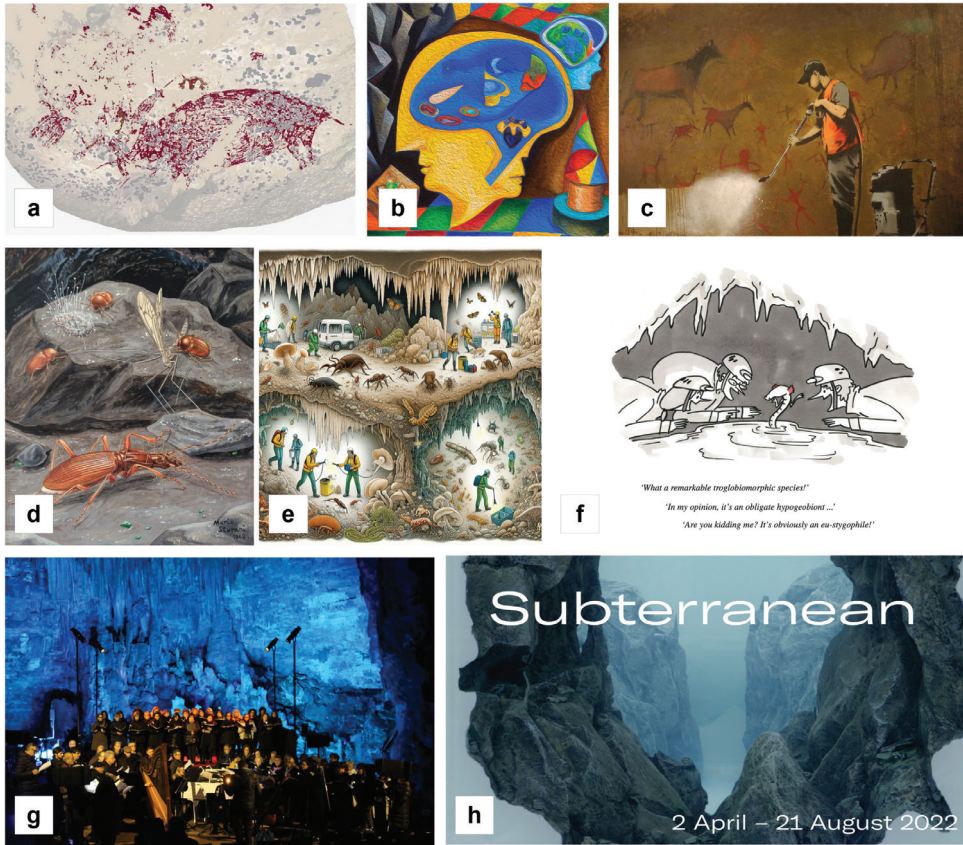


Figure 1. The breadth and scope of subterranean-related art. **a** Oldest known drawings on a cave wall in Indonesia, dating back 51,200 years (modified from Oktaviana et al. 2024) **b** “Pop Art Cubism Mind in Cave” (2022) by David S. Soriano (CC BY-SA 4.0) **c** street art by Banksy “Cave Painting Removal” (2008). Photo by Badjonni (CC BY-NC-SA 2.0) **d** the fauna of the Borna Maggiore di Pignetto cave, Italy, as depicted in a distemper painting by Mario Sturani (1906–1978). Courtesy of the Sturani family, published in Sturani (1942) **e** an example of figurative art created using artificial intelligence (DALL-E) with the prompt “Create an image about the impact of human activities on cave biota.” Such AI tools are increasingly being used by scientists, particularly for science communication (Box 1) **f** cartoon by Irene Frigo illustrating the often-self-inflicted challenge faced by subterranean scientists in deciding how to best refer to cave-dwelling animals. Courtesy of Irene Frigo, published in Martínez and Mammola (2021) **g** a concert in the Castellana Cave, Italy. Photo by Mafalda Baccaro (CC BY-NC-ND 2.0) **h** “Subterranean” (Amos Rex, Helsinki, 2 April – 21 August 2022), was an exhibition dedicated to the underground world. It included a section highlighting the impacts of human activities on subterranean ecosystems.

tific knowledge more approachable and engaging, while also helping to promote pro-conservation behaviors (e.g., Curtis et al. 2014; Tribot et al. 2022; Salazar et al. 2022; Matias et al. 2023; Ison et al. 2024). For example, a recent study by Franquesa-Soler et al. (2020) demonstrated the effectiveness of an arts-based educational program focused on the conservation of black howler monkeys (*Alouatta pigra*). They found that integrating artistic approaches grounded in scientific information led to greater knowl-

edge gains among children and higher overall satisfaction. Similarly, Marchio (2018) explored the role of aquarium keeping as a form of art in communicating science and conservation, whereby maintaining home aquariums helped participants learn about aquatic ecosystems and fostered a personal connection to conservation efforts.

These examples highlight how integrating art and science can engage audiences with underexplored species and ecosystems and foster personal connections to conservation. This approach could also benefit the subterranean world, which remains largely overlooked in public education and conservation efforts. In subterranean science, Danielopol (1998) was among the first to propose that integrating artistic perception with scientific facts could significantly enhance cultural education by emphasizing the unique organisms inhabiting subterranean ecosystems and highlighting their significance in cultural heritage and as public goods with multiple values. While Danielopol's idea compellingly highlights the potential synergy between art and science, it remains abstract, lacking concrete examples or actionable frameworks to fully realize its potential (but see a recent agenda by Gleeson [2024] focused on integrating art in groundwater hydrogeology). We suggest there are many benefits for subterranean scientists engaging with artists and *vice versa* (Fig. 2).

Subterranean ecosystems are invisible to most. As a result, they often end up being marginally represented in conservation policies and actions (e.g., Mammola et al. 2019, 2024; Sánchez-Fernández et al. 2021; Wynne et al. 2021; Fišer et al. 2022; Di Lorenzo et al. 2024). Art can illuminate the hidden subterranean world, reinforcing its ecological importance and interdependence with surface ecosystems (Glanville et al. 2023; Saccò et al. 2024). Artistic projects and exhibitions can draw attention to subterranean ecosystem degradation and galvanize public support for conservation. Furthermore, the emotional impact of art may drive financial backing (e.g., donations) for projects aimed at preserving subterranean biodiversity, especially given the often-limited resources allocated to subterranean conservation. Art can also foster interdisciplinary conservation efforts by encouraging collaboration between scientists, artists, and key stakeholders reliant on subterranean resources, such as farmers and water managers, who often use large quantities of groundwater but lack direct access to or knowledge of these environments.

Art is also central to scientific communication (Fig. 3). Subterranean science is a highly interdisciplinary field at the crossroads of hydrology, biology, geology, anthropology, and many other disciplines, making communication particularly challenging (Martínez and Mammola 2021). Art bridges the gap by transforming complex scientific ideas into accessible or engaging forms. By doing so, these concepts become more relatable and easier to understand, thus supporting education and raising awareness about critical issues surrounding subterranean conservation. Furthermore, art may act as a powerful source of inspiration, sparking curiosity and creativity, which can lead to deeper interest in scientific research and exploration of otherwise unreachable environments. This is particularly important for caves, as these environments are difficult to explore, requiring physical and technical skills, and are therefore only accessible to a small minority of scientists who can experience them directly (MacNeil and Bricc 2017). For example, artists

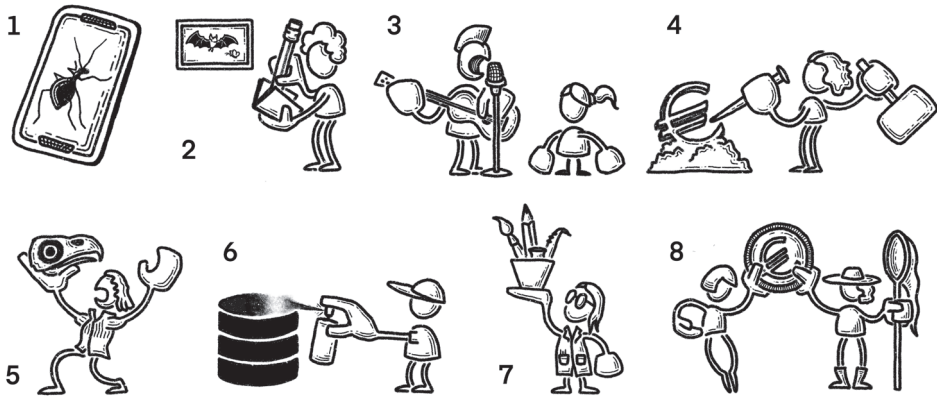


Figure 2. Conceptual illustration of synergies between art and subterranean science and conservation. Artistic disciplines can: **1** make subterranean science accessible **2** inspire scientific research **3** enhance education and awareness **4** strengthen conservation projects and attract funding **5** foster interdisciplinary conservation efforts; and **6** contribute to data generation. Conversely, subterranean science projects can: **7** offer material, inspiration, and collaboration opportunities for artists; and **8** support and fund artistic endeavours. Illustrations by Jagoba Malumbres-Olarte.

can play a crucial role during workshops, helping research groups communicate their projects effectively through graphic facilitation in project-specific workshops (Fig. 3e).

Finally, art may serve as a source of data, offering insights through visual documentation and creative interpretations of environmental changes and phenomena (Davis et al. 2025). This concept is well understood by archaeologists, anthropologists, and art historians, who have long used Paleolithic cave art to infer the lifestyles of early humans (Curtis 2007; Whitley 2009). Art can even, in certain circumstances, serve as a valuable source of ecological and conservation information. Figurative art and photography, for instance, have been used to investigate past changes in landscapes, habitats, and ecological conditions (Devrani and Singh 2014; Guagnin et al. 2016; Depauw et al. 2022; Warren et al. 2023). However, no concrete examples of such applications currently exist for subterranean ecosystems, highlighting untapped potential in this area. For example, the painting in Fig. 1d captures a mid-20th century snapshot of the Pugnetto cave community (Sturani 1942). Remarkably, this community continues to thrive today, with all the depicted species still abundant (Mammola et al. 2015, 2017), reflecting the stability and resilience of this unique ecosystem.

How can we effectively break the cultural divide between subterranean scientists and artists?

Integrating art into subterranean ecosystem research and conservation offers immense potential and benefits, but significant challenges remain. Subterranean scientists and artists often operate in distinct cultural contexts and “speak different languages” which

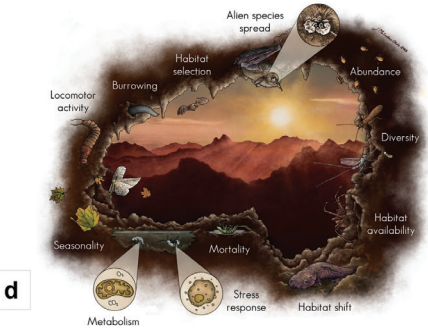


Figure 3. Examples of visual art used in scientific contexts to communicate about subterranean ecosystems and their conservation. **a** Photography: Photographs are a powerful tool for showcasing the hidden wonders of the subterranean world, often holding scientific value for cave research (e.g., Kambesis 2007). Pictured: *Troglolyphantes pluto* Di Caporiacco, 1938 (Araneae: Linyphiidae). Credit: Francesco Tomasinelli

can complicate collaborations. Fostering cross-pollination of ideas and exchanges among these professionals does not simply imply avoiding the typical “obscure” speleological jargon to ensure effective communication and idea-sharing (Martínez and Mammola 2021); it demands deliberate and concrete efforts to foster genuine partnerships. In essence, we must explore innovative ways to bring more artists into caves and cavers into studios, bridging these worlds to achieve shared goals.

To effectively integrate art into subterranean conservation, scientists should actively provide artists with the resources and information needed to create compelling and scientifically accurate works. This includes sharing research findings, data, insights, and materials about subterranean ecosystems to enhance the accuracy and depth of artistic interpretations. Recently, the emergence of artificial intelligence (AI) tools (Fig. 1e) has opened new avenues for collaboration between scientists and artists, promising to revolutionize how they operate, create, and interact (Wong 2024). These tools create opportunities to enhance artistic interpretations, but it is important to approach these tools with an awareness of their potential limitations and ethical considerations (Box 1). Given that subterranean ecosystems remain unfamiliar and inaccessible to most, additional efforts to connect artists with these environments are vital. Organizing tours of research sites, such as easily accessible or tourist caves, can provide firsthand inspiration, while inviting artists on research expeditions allows them to gain a deeper understanding of these ecosystems and their significance.

If budget limitations (see next paragraph) or logistical and technical challenges (e.g., caves are often in remote places, artists may lack speleological training) prevent

(<http://www.isopoda.net/>) **b** logos: Professional logos for labs, projects, and conferences related to subterranean research. Credits: Martin Turjak & SubBioLab (SubBioLab logo), Irene Frigo (DarCo and ICSB logos) **c** infographics: Infographics are powerful tools for teaching best practices in subterranean conservation. Pictured: Best practices for conserving biodiversity in cenotes and their caves (“*Conservación de la biodiversidad de los cenotes y sus cuevas*”). Credits: Nuno S. et al. (www.cenoteando.mx), available on Zenodo (<https://zenodo.org/records/10157871>; CC BY NC-ND) **d** graphical abstracts: Graphical abstracts provide concise visual summaries of complex scientific studies and help promote papers across different media (Yoon and Chung 2017). Pictured: A graphical abstract by Jagoba Malumbres-Olarte for a meta-analysis of climate change impacts on subterranean ecosystems (Vaccarelli et al. 2023) **e** graphic facilitation involves creating infographics that illustrate and connect the main ideas discussed in conferences, meetings, or workshops. Pictured: Infographic by Jagoba Malumbres-Olarte from a graphic facilitation workshop held by the DarCo research project, focusing on the conservation of subterranean ecosystems in Europe (see “Acknowledgements” for details) **f** conference Illustrations: Illustrations help summarize the main messages of scientific talks and are effective in promoting research, especially on social media. Pictured: Illustration by Jagoba Malumbres-Olarte of a talk by Alice Salussolia at the 26th International Conference on Subterranean Biology (Cagliari, Italy, 9–14 September 2024) titled “Genome skimming and amplicon sequencing: novel DNA-based techniques shed light on the taxonomy and phylogeny of the *N. thuringius* – *N. dolenianesis* species complex (Crustacea, Amphipoda, Niphargidae)”. Courtesy of Alice Salussolia **g** comics: Cartoons offer a whimsical yet effective way to deliver the core messages of scientific publications (McDermott et al. 2018) and promote biodiversity conservation (Small 2016). Pictured: A comic by Irene Frigo illustrating the impacts of human activities on subterranean fauna (Mammola et al. 2022a).

bringing artists into field sites, inviting them to scientific conferences and workshops offers an alternative way to share and visualize subterranean science to both academic audiences and the public. Direct invitations are crucial, as such events are often exclusive or poorly advertised beyond the niche community of subterranean biologists and speleologists. For instance, at the 26th International Conference on Subterranean Biology (Cagliari, Italy, 9–14 September 2024), a scientific illustrator was invited to depict a subterranean conservation workshop (Fig. 3e) and several talks (Fig. 3f). These exchanges benefit all parties: artists gain exposure, new ideas, and potential collaborators, while scientists enhance the reach and accessibility of their research. Scientists could organize workshops or lectures tailored for artists, simplifying complex scientific concepts for better understanding. Additionally, collaborative projects with scientists in research institutions provide artists with hands-on experience, fostering a more authentic integration of science in their art (see Clark et al. 2020 for an example).

For such collaborations to succeed, scientists and artists must often address the challenge of securing appropriate budgets to develop joint artistic-scientific work. While institutions and conferences can establish grants, fellowships, and artist residency programs to encourage these collaborations, an often more direct option is for scientists to allocate a portion of their research funding for art-related communication initiatives. These costs will, of course, vary depending on the form of art and level of engagement, with the extent of investment always determined by the total budget and funding scheme. In general, costs for illustrations are minimal compared to other non-primary research expenditures, such as high open-access publication fees (e.g., Van Noorden 2013), and thus often affordable through average research budgets. Other forms of art may be more costly and require more careful planning and valuation. In our experience, allocating about 5% of a project grant to communication expenditures (often art-related) typically allows for fruitful collaborations with artists. For smaller projects (e.g., less than \$50,000 USD), such an investment can cover costs to engage artists for logos, illustrations, videos, and other media. For larger grants, a similar percentage investment can potentially cover other expenditures, such as costs for inviting artists to field expeditions, workshops, and conferences, or even stipends for the artists. On a positive note, there is often a return on investment for these expenditures. Including artists in dissemination, communication, and education efforts not only enhances the quality of projects but may increase the likelihood of securing additional funding in the future.

While scientists often act as facilitators or “gatekeepers” of collaborations with artists, bridging the art-science cultural divide may – and should – also be initiated by artists. Artists can undertake projects focused on conservation and related scientific fields, using their own platforms and tapping into funding sources beyond traditional scientific grants. By challenging researchers’ communication methods or thinking outside the box, such projects can amplify the impact of their messages and reach broader audiences. Examples include comic books such as “*World without End*” by Blain and Jancovici (2022), which uses artistic tools from literary fiction to attract readers to the subjects of energy and climate, making them accessible and understandable. Indeed, collaboration

with conservationists or experts in the field is also fundamental to avoid scientific inaccuracies or misunderstandings when developing and executing these projects.

Finally, creating exhibitions fully dedicated to subterranean ecosystems – such as the aforementioned “Subterranean” (Amos Rex, Helsinki) and “Subterranean Worlds” (Louvre Lens, Paris) – is likely the most effective way to foster interdisciplinary collaboration and bring these important issues to a wider audience. A recent example, focused on a wide range of ecosystems beyond subterranean ones, is “In praise of diversity” (*Elogio della diversità*; Rome, 27 November 2024 – 30 March 2025), an exhibition devoted to the themes of biodiversity and One Health, funded by the National Biodiversity Future Center (NBFC) and curated by the University of La Sapienza. Large exhibitions such as this one have a broad reach and are capable of drawing attention to, and increasing awareness of, the diverse life forms on our planet and our relationship with biodiversity, thereby triggering both individual and collective responsibility. Importantly, the scope of such large-scale exhibitions often exceeds the capacity of a single scientific or artistic grant, necessitating broader involvement from public institutions, art organizations, and private sponsors to co-fund events that highlight the intersection of art and science.

Box 1. The role of AI in art and science collaboration.

At the time of writing, recent advancements in AI have opened new opportunities for collaboration between artists and scientists. This is an emerging and rapidly evolving field, with new tools constantly being developed, making it difficult to chart future trajectories. Many text-to-image AI tools, such as DALL-E and Midjourney, can already assist in creating complex, accurate, and engaging visualizations and animations of scientific data (Wong 2024). For instance, AI algorithms can process large datasets, simulate environmental changes, and generate dynamic visualizations, such as 3-dimensional models of subterranean ecosystems or time-lapse animations of ecological and geological processes therein. These capabilities provide unprecedented – and often costless – opportunities to bridge the gap between scientific rigor and artistic expression, which may be particularly useful for difficult-to-experience ecosystems such as caves.

However, these advancements come with important caveats and limitations. First, human supervision and validation (preferably by a team of artists and scientists) is crucial to avoid oversimplification or distortion of scientific concepts (see, e.g., Guo et al. 2024 for a recent example of a retracted article due to the misuse of AI-generated figures). Second, ethical concerns arise regarding the use of AI in art, particularly around intellectual property and authorship. When AI tools generate artwork, questions about ownership and the recognition of human creators must be addressed, emphasizing the importance of being transparent about the role of AI during the creative process. Third, the rise of AI may impact professional artists. While AI can support artists by automating repetitive tasks and enabling new creative possibilities, it may also pose a threat to traditional artistic roles, particularly in commercial fields where cost-efficiency often takes precedence. It is thus very important to positioning AI as a complementary tool rather than a replacement, ensuring it enhances human artistic contributions rather than diminishes them.

How can we test the effectiveness of art in enhancing communication about subterranean ecosystems and their conservation?

There is growing evidence that art is a powerful ally in scientific communication and that arts-based conservation education is central to successful conservation programs (Clark et al. 2020). Matias et al. (2023) conducted a meta-analysis showing that art contributes to coastal and marine conservation by engaging people, promoting dialogue, and increasing knowledge. Importantly, 19 out of 79 articles in their dataset assessed quantitatively the impact of artistic activities on audiences and conservation outcomes. One example is the Aula Verde Project, where artists, scientists, and environmental activists worked together to reconnect citizens with nature in urban areas. This effort resulted in the creation of a Land Art installation in Rome that serves both as a nature-based solution and a space for social interaction. The project evaluated the ecosystem services provided by this urban forest, demonstrating its potential over the next 50 years to store carbon (48 tons), remove air pollutants (11,000 grams), and prevent surface runoff (48 m³ per year) (Conte et al. 2024).

Yet, any reader who has made it this far may have noticed that this perspective focused on subterranean ecosystems does not present any quantitative data to complement the discussion. This is due to the lack of quantitative testing on how effective the synergies between subterranean science and art truly are. More broadly, there has been limited testing of the effectiveness of conservation actions in subterranean ecosystems (Mammola et al. 2022b; Meierhofer et al. 2024). A recent systematic review found that only 31% of recommended conservation actions for subterranean ecosystems have been rigorously tested for effectiveness (Mammola et al. 2022b). Similarly, Meierhofer et al. (2024) reported that just 34% of specific conservation actions for subterranean-dwelling bats have undergone testing. This lack of rigorous evaluation is particularly striking in the areas of education and communication, where the effectiveness of such activities has never been assessed (Mammola et al. 2022b; Meierhofer et al. 2024). This gap may discourage scientists from collaborating with artists, though examples of such partnerships in conservation science remain common despite the overall scarcity of evidence (see examples in Fig. 3). There are numerous ways to address this knowledge gap.

Scientometric approaches

A straightforward way to test the impact of art on science communication is through state-of-the-art scientometric approaches. Scientometrics, or the “science of science,” uses quantitative methods to analyze the performance and impact of scientific research, including researchers, journals, institutions, or fields of science (Fortunato et al. 2018). In our case, by examining a geographically and/or temporally coherent sample of literature focused on subterranean ecosystems – e.g., a sample of papers from journals like *Subterranean Biology* or *International Journal of Speleology* – researchers could compare the performance of papers containing artistic elements (e.g., illustrations, diagrams, or visual representations) to those without. Metrics such as citations, Altmetric scores,

and social media engagement could be used to evaluate the relative impact of artistic elements on publication performance (Kwok 2013; Bornmann 2014; Tahamtan et al. 2019). To ensure validity, the analyses would need to account for confounding factors, including both scientific and non-scientific characteristics of the papers (Tahamtan et al. 2019; Mammola et al. 2022c). Although primarily applicable within academia, this method would ultimately provide valuable quantitative evidence of the role art plays in enhancing the visibility and accessibility of scientific works. Given that publication metrics are a primary driver of career progression in academia, quantitative evidence of art's impact on the success of scientific outputs could serve as a strong incentive for researchers. In the long term, similar evidence might encourage more researchers to seek the help of and actively involve artists as collaborators, fostering a positive transformation in the relationship between these two fields.

Fundraising campaigns

Funding availability is a key limiting factor for conservation efforts (Waldron et al. 2017). Therefore, measuring conservation success through economic proxies offers a practical approach. For example, Kubo et al. (2022) demonstrated that advertisement design significantly impacts donor engagement in digital conservation fundraising. Their study tested the effectiveness of three types of advertisements: simple (control), seed money (indicating 55% progress of the fundraising target), and ecological (highlighting the threatened status of the target species). Drawing inspiration from this, similar fundraising campaigns could be designed for subterranean ecosystems to assess the impact of art. For instance, fundraising campaigns for cave conservation could be divided into those emphasizing artistic elements and control campaigns without them. The effectiveness of these campaigns could be evaluated in two ways: first, by comparing financial outcomes – do advertisements featuring artistic elements attract more donors? Second, by surveying donors and visitors to understand their motivations – does the presence of art influence their willingness to contribute or engage? These insights could illuminate how art enhances conservation efforts and public support, again representing a strong incentive for both artists and scientists to seek more collaborations and apply for joint grants and projects.

Social sciences

Beyond quantitative approaches, social science methods can provide deeper insights into how art shapes public perceptions of subterranean ecosystems and their conservation. Qualitative techniques such as interviews, focus groups, and online or in-person surveys in tourist caves can explore the emotional and cognitive effects of art (Dans and González 2019). For example, researchers could examine whether artistic representations evoke emotional responses – such as awe, curiosity, or empathy – that increase awareness of conservation issues. They could also assess whether art enhances memory retention of key ecological concepts or conservation messages. An-

other promising source of information is online data, particularly social media, which represents an emerging field of conservation culturomics (Ladle et al. 2016; Correia et al. 2021). Through the quantitative analysis of online digital data – such as social media, news platforms, webpage visitation rates, and internet search activity – culturomics can provide valuable insights into public values, awareness, interests, and attitudes related to art-science projects and initiatives, as well as the effectiveness of art-based public communication activities. For instance, it can be used to evaluate the effectiveness of social media campaigns promoting subterranean conservation issues by comparing public engagement with posts that feature artwork versus those that do not, or by conducting sentiment and topic analyses of social media content related to art-science activities. Simultaneously, public engagement can be evaluated beyond the digital realm by tracking participation in art exhibitions or theater performances focused on subterranean ecosystems. Understanding these emotional and cognitive dimensions offers valuable insight into how art fosters public engagement and support for subterranean conservation efforts.

A short final note on the potential environmental impacts of subterranean art

Subterranean ecosystems are particularly vulnerable to human disturbance due to their isolation and often pristine conditions. Introducing art, artists, and visitors into caves and subterranean sites can have localized impacts. For instance, organizing concerts or theater performances in tourist caves can lead to a large number of visitors temporarily occupying the subterranean environment (Fig. 1g). This activity can alter local thermal conditions, disturb native fauna, and introduce waste or external organic matter, including non-native fungi and bacteria (Piano et al. 2024). In extreme cases, tourists may even damage cave structures, such as speleothems, or harm cave art. An example is illustrated by the closure of caves such as Chauvet, Altamira, and Lascaux, whose delicate prehistoric wall art experienced microbial and fungal outbreaks due to mismanaged tourism and the improper removal of invasive microbial biofilms (Bastian et al. 2009). Furthermore, excessive or ill-suited artificial lighting can also promote the growth of photosynthetic organisms (often referred to as lampenflora) on cave walls (Baquedano Estévez et al. 2019; Piano et al. 2024). While these impacts are notable, they are likely minor compared to the long-term benefits of raising public awareness about subterranean ecosystems, which can have lasting effects on people's willingness to support conservation (Mammola et al. 2022). However, precautionary measures should always be taken to minimize these impacts (see, e.g., Chiarini et al. 2022; Piano et al. 2024 for a review of management options).

These measures include temporarily limiting the number of visitors allowed to access the subterranean artwork or exhibition to minimize several of the impacts mentioned above, adopting shoe and clothing cleaning practices at the entrance of the cave to prevent the introduction of alien organisms, using lighting systems that discour-

age the growth of lampenflora, and selecting less susceptible areas within caves for the placement of artworks. Furthermore, scientists can assist artists in creating more sustainable artwork by recommending eco-friendly materials and considering the geological and environmental context of the specific cave targeted for the art exhibition. In cases where caves are closed to the public for conservation purposes, cave replicas – full-scale reproductions of cave interiors and their art – offer an effective strategy to mitigate over-tourism. Notable examples include Altamira in Spain and Lascaux II, Lascaux IV, and Chauvet II in France, where teams of artists and scientists have recreated cave art using diverse approaches, including immersive technologies such as augmented reality and 3D projections. These replicas enable visitors to appreciate cave art while safeguarding the original sites' cultural artifacts and delicate subterranean ecosystems. Meanwhile, researchers continue to conduct scientific investigations in the natural caves, providing valuable insights to inform ongoing conservation efforts (Bastian et al. 2010; Geneste et al. 2014; Hughes et al. 2021).

When considering all these precautionary measures, it is important to remember that they are context-specific and must be tailored not only to the unique characteristics of the cave or subterranean site in question but also to the nature of the artwork itself.

Conclusions

Subterranean ecosystems have inspired artistic expression for millennia, from Paleolithic cave paintings to contemporary abstract performances. While there is no quantitative evidence yet that art directly advances subterranean conservation, our dual experiences as scientists who appreciate art – and as artists who appreciate science – suggest that deeper connections between these realms can have profound and long-lasting impacts on both scientific communication and conservation. Art has the unique ability to make complex scientific concepts more accessible, foster interdisciplinary collaboration, attract critical conservation funding, and even provide unexpected sources of data. By collaborating with artists, subterranean scientists can create more impactful visuals for research papers and presentations, engage the public through captivating storytelling, and inspire fresh insights that may drive new research directions. To maximize these benefits, scientists should nurture partnerships with artists. Allocating small portions of research budgets for art-related initiatives, inviting artists to conferences and workshops, and including them in cave expeditions are all meaningful steps toward fostering meaningful collaboration. Artists, in turn, can initiate collaborations by developing independent conservation projects, using their own platforms to advocate for subterranean conservation, and promoting innovative artistic approaches that challenge researchers to rethink scientific communication and engagement. Ultimately, these partnerships can spark creativity, generate new ideas, and ensure the unseen world beneath our feet garners the attention it deserves – for the advancement of both science and conservation.

Conflicts of interest

Stefano Mammola is a Subject Editor of *Subterranean Biology* but took no part in peer-review and editorial decisions for this manuscript.

Acknowledgments

We are grateful to Elizabeth Borda and Nuno Simões for their constructive feedback on the manuscript. Special thanks to Alice Salussolia, Irene Frigo, Matteo Sturani, Francesco Tomasinelli, and Maja Zagmajster for providing material for Fig. 3. This research was funded by Biodiversa+ (project ‘DarCo’), the European Biodiversity Partnership under the 2021–2022 BiodivProtect joint call for research proposals, co-funded by the European Commission (GA N°101052342) and with the funding organizations Ministry of Universities and Research (Italy), Agencia Estatal de Investigación – Fundación Biodiversidad (Spain), Fundo Regional para a Ciência e Tecnologia (Portugal), Suomen Akatemia – Ministry of the Environment (Finland), Belgian Science Policy Office (Belgium), Agence Nationale de la Recherche (France), Deutsche Forschungsgemeinschaft e.V. (Germany), Schweizerischer Nationalfonds (Grant No. 31BD30_209583, Switzerland), Fonds zur Förderung der Wissenschaftlichen Forschung (Austria), Ministry of Higher Education, Science and Innovation (Slovenia), and the Executive Agency for Higher Education, Research, Development and Innovation Funding (Romania). Additional support is provided by the P.R.I.N. 2022 “DEEP CHANGE” (2022MJSYF8), funded by the Ministry of Universities and Research (Italy). S.M. acknowledges further support of NBFC, funded by the Italian Ministry of University and Research, P.N.R.R., Missione 4, Componente 2, “Dalla ricerca all’impresa”, Investimento 1.4, Project CN00000033.

References

- Bastian F, Alabouvette C (2009) Lights and shadows on the conservation of a rock art cave: the case of Lascaux Cave. *International Journal of Speleology* 38(1): 55–60. <https://doi.org/10.5038/1827-806X.38.1.6>
- Bastian F, Jurado V, Nováková A, Alabouvette C, Sáiz-Jiménez C (2010) The microbiology of Lascaux cave. *Microbiology* 156(3): 644–652. <https://doi.org/10.1099/mic.0.036160-0>
- Baquedano Estévez C, Moreno Merino L, de la Losa Román A, Duran Valsero JJ (2019) The lampenflora in show caves and its treatment: an emerging ecological problem. *International Journal of Speleology* 48(3): 249–277. <https://doi.org/10.5038/1827-806X.48.3.2263>
- Bornmann L (2014) Do altmetrics point to the broader impact of research? An overview of benefits and disadvantages of altmetrics. *Journal of Informetrics* 8(4): 895–903. <https://doi.org/10.1016/j.joi.2014.09.005>

- Chiarini V, Duckeck J, De Waele J (2022) A global perspective on sustainable show cave tourism. *Geoheritage* 14(3): 82. <https://doi.org/10.1007/s12371-022-00717-5>
- Clark SE, Magrane E, Baumgartner T, Bennett SE, Bogan M, Edwards T, Dimmitt MA, Green H, Hedgcock C, Johnson BM, Johnson MR, Velo K, Wilder BT (2020) 6&6: a transdisciplinary approach to art-science collaboration. *BioScience* 70(9): 821–829. <https://doi.org/10.1093/biosci/biaa076>
- Conte A, Pace R, Li Q, Carloni S, Boetzkas A, Passatore L (2024) Aula Verde (tree room) as a link between art and science to raise public awareness of nature-based solutions. *Scientific Reports* 14(1): 2368. <https://doi.org/10.1038/s41598-024-51611-9>
- Correia RA, Ladle R, Jarić I, Malhado ACM, Mittermeier J, Roll U, Soriano-Redondo A, Veríssimo D, dos Santos JG, Fink C, Hausmann A, Vardi R, Di Minin E (2021) Digital data sources and methods for conservation culturomics. *Conservation Biology* 35(2): 398–411. <https://doi.org/10.1111/cobi.13706>
- Curtis G (2007) The cave painters: Probing the mysteries of the world's first artists. Anchor.
- Curtis DJ, Reid N, Reeve I (2014) Towards ecological sustainability: Observations on the role of the arts. *SAPI EN. S. Surveys and Perspectives Integrating Environment and Society* 7(1): 1–15.
- Danielopol DL (1998) Conservation and protection of the biota of karst: assimilation of scientific ideas through artistic perception. *Journal of Cave and Karst Studies* 60: 67.
- Dans EP, González PA (2019) Sustainable tourism and social value at World Heritage Sites: Towards a conservation plan for Altamira, Spain. *Annals of Tourism Research* 74: 68–80. <https://doi.org/10.1016/j.annals.2018.10.011>
- Davis CC, Kehoe J, Knaap AC, Atkins, CD (2025) Science× art: spotlighting unconventional collaborations. *Trends in Ecology & Evolution*, in press. <https://doi.org/10.1016/j.tree.2024.12.004>
- Depauw L, Blondeel H, De Lombaerde E, De Pauw K, Landuyt D, Lorer E, Vangansbeke P, Vanneste T, Verheyen K, De Frenne P (2022) The use of photos to investigate ecological change. *Journal of Ecology* 110: 1220–1236. <https://doi.org/10.1111/1365-2745.13876>
- Devrani R, Singh V (2014) Determining the geomorphic changes in Srinagar (Garhwal) Valley, NW Himalaya in last two centuries using landscape painting. *Zeitschrift Fur Geomorphologie* 58: 163–173. <https://doi.org/10.1127/0372-8854/2012/0099>
- Di Lorenzo T, et al.(2024) EU needs groundwater ecosystems guidelines. *Science* 386: 1103–1103. <https://doi.org/10.1126/science.ads8140>
- Dixon GN, McKeever BW, Holton AE, Clarke C, Eosco G (2015) The power of a picture: Overcoming scientific misinformation by communicating weight-of-evidence information with visual exemplars. *Journal of Communication* 65(4): 639–659. <https://doi.org/10.1111/jcom.12159>
- Fišer C, Borko Š, Delić T, Kos A, Premate E, Zagmajster M, Zakšek V, Altermatt F (2022) The European green deal misses Europe's subterranean biodiversity hotspots. *Nature Ecology & Evolution* 6(10): 1403–1404. <https://doi.org/10.1038/s41559-022-01859-z>
- Fortunato S, Bergstrom CT, Börner K, Evans JA, Helbing D, Milojević S, Petersen AM, Radicchi F, Sinatra R, Uzzi B, Vespignani A, Waltman L, Wang D, Barabási AL (2018) Science of science. *Science* 359(6379): eaao0185. <https://doi.org/10.1126/science.aao0185>

- Franquesa-Soler M, Jorge-Sales L, Aristizabal JF, Moreno-Casasola P, Serio-Silva JC (2020) Evidence-based conservation education in Mexican communities: Connecting arts and science. *PLoS One* 15: e0228382. <https://doi.org/10.1371/journal.pone.0228382>
- Geneste JM, Bardisa M (2014) The Conservation of Chauvet Cave, France. The Conservation, Research Organization and the Diffusion of Knowledge of a Cave Inaccessible to the Public. The conservation of subterranean cultural heritage, 173–183. <https://doi.org/10.1201/b17570-22>
- Glanville K, Sheldon F, Butler D, Capon S (2023) Effects and significance of groundwater for vegetation: A systematic review. *Science of the Total Environment* 875: 162577. <https://doi.org/10.1016/j.scitotenv.2023.162577>
- Gleeson T (2024) Groundwater connected art: practicing arts-based research to enrich how hydrogeology engages people, place and other disciplines. Preprint. *Earth ArXiv*. <https://doi.org/10.31223/X5TB1P>
- Guagnin M, Jennings R, Eager H, Parton A, Stimpson C, Stepanek C, Pfeiffer M, Groucutt HS, Drake NA, Alsharekh A, Petraglia MD (2016) Rock art imagery as a proxy for Holocene environmental change: A view from Shuwaymis, NW Saudi Arabia. *The Holocene* 26(11): 1822–1834. <https://doi.org/10.1177/0959683616645949>
- Guo X, Dong L, Hao D (2024) RETRACTED: cellular functions of spermatogonial stem cells in relation to JAK/STAT signaling pathway. *Frontiers in Cell and Developmental Biology* 11: 1339390. <https://doi.org/10.3389/fcell.2023.1339390>
- Hughes K, Mkono M, Myers D, Echantille S (2021) Are you for real?! Tourists' reactions to four replica cave sites in Europe. *Tourism Management Perspectives* 37: 100780. <https://doi.org/10.1016/j.tmp.2020.100780>
- Ison S, Cvitanovic C, Pecl G, Hobday AJ, van Putten I (2024) The role of visual framing in marine conservation communication. *Ocean & Coastal Management* 248: 106938. <https://doi.org/10.1016/j.ocecoaman.2023.106938>
- Jacobson SK, McDuff MD, Monroe MC (2007) Promoting conservation through the arts: Outreach for hearts and minds. *Conservation Biology* 21(1): 7–10. <https://doi.org/10.1111/j.1523-1739.2006.00596.x>
- Kambesis P (2007) The importance of cave exploration to scientific research. *Journal of Cave and Karst Studies* 69(1): 46–58.
- Kwok R (2013) Research impact: Altmetrics make their mark. *Nature* 500(7463): 491–493. <https://doi.org/10.1038/nj7463-491a>
- Ladle RJ, Correia RA, Do Y, Joo GJ, Malhado AC, Proulx R, Roberge JM, Jepson P (2016) Conservation culturomics. *Frontiers in Ecology and the Environment* 14(5): 269–275. <https://doi.org/10.1002/fee.1260>
- Mammola S, Elena P, Mauro GP, Isaia M (2015) Seasonal dynamics and micro-climatic preference of two Alpine endemic hypogean beetles. *International Journal of Speleology* 44(3): 239–249. <https://doi.org/10.5038/1827-806X.44.3.3>
- Mammola S, Piano E, Giachino PM, Isaia M (2017) An ecological survey of the invertebrate community at the epigeal/hypogean interface. *Subterranean Biology* 24: 27–52. <https://doi.org/10.3897/subtbiol.24.21585>
- Mammola S, Cardoso P, Culver DC, Deharveng L, Ferreira RL, Fišer C, Galassi DMP, Griebler C, Halse S, Humphreys WF, Isaia M, Malard F, Martinez A, Moldovan OT, Niemiller

- ML, Pavlek M, Reboleira ASPs, Souza-Silva M, Teeling EC, Wynne JJ, Zagamajster M (2019) Scientists' warning on the conservation of subterranean ecosystems. *BioScience* 69(8): 641–650. <https://doi.org/10.1093/biosci/biz064>
- Mammola S, Frigo I, Cardoso P (2022a) Life in the darkness of caves. *Frontiers for Young Minds* 10: 657265. <https://doi.org/10.3389/frym.2022.657265>
- Mammola S, Meierhofer MB, Borges PA, Colado R, Culver DC, Deharveng L, Delić T, Di Lorenzo T, Dražina T, Ferreira RL, Fiasca B, Fišer C, Galassi DMP, Garzoli L, Gerovasileiou V, Griebler C, Halse S, Howarth FG, Isaia M, Johnson JS, Komerički A, Martínez A, Milano F, Moldovan OT, Nanni V, Nicolosi G, Niemiller ML, Pallarés S, Pavlek M, Piano E, Pipan T, Sanchez-Fernandez D, Santangeli A, Schmidt SI, Wynne JJ, Zagamajster M, Zakšek V, Cardoso P (2022b) Towards evidence-based conservation of subterranean ecosystems. *Biological reviews* 97(4): 1476–1510. <https://doi.org/10.1111/brv.12851>
- Mammola S, Piano E, Doretto A, Caprio E, Chamberlain D (2022c) Measuring the influence of non-scientific features on citations. *Scientometrics* 127(7): 4123–4137. <https://doi.org/10.1007/s11192-022-04421-7>
- Mammola S, Altermatt F, Alther R, Amorim IR, Băncilă RI, Borges PA, Brad T, Brankovits D, Cardoso P, Cerasoli F, Chauveau CA, Delić T, Di Lorenzo T, Faille A, Fišer C, Flot JF, Gabriel R, Galassi DMP, Garzoli L, Griebler C, Konecny-Dupré L, Martínez A, Mori N, Nanni V, Ogorelec Ž, Pallarés S, Salussolia A, Saccò M, Stoch F, Vaccarelli I, Zagamajster M, Zित्रa C, Meierhofer MB, Sánchez-Fernández D, Malard F (2024) Perspectives and pitfalls in preserving subterranean biodiversity through protected areas. *npj Biodiversity* 3(1): 2. <https://doi.org/10.1038/s44185-023-00035-1>
- MacNeil RR, Brcic J (2017) Coping with the subterranean environment: A thematic content analysis of the narratives of cave explorers. *Journal of Human Performance in Extreme Environments* 13(1): 6. <https://doi.org/10.7771/2327-2937.1089>
- Marchio EA (2018) The art of aquarium keeping communicates science and conservation. *Frontiers in Communication* 3: 17. <https://doi.org/10.3389/fcomm.2018.00017>
- Martínez A, Mammola S (2021) Specialized terminology reduces the number of citations of scientific papers. *Proceedings of the Royal Society B* 288(1948): 20202581. <https://doi.org/10.1098/rspb.2020.2581>
- Matias A, Carrasco AR, Pinto B, Reis J (2023) The role of art in coastal and marine sustainability. *Cambridge Prisms: Coastal Futures* 1: e25. <https://doi.org/10.1017/cft.2023.13>
- McDermott JE, Partridge M, Bromberg Y (2018) Ten simple rules for drawing scientific comics. *PLoS Computational Biology* 14(1): e1005845. <https://doi.org/10.1371/journal.pcbi.1005845>
- Meierhofer MB, Johnson JS, Perez-Jimenez J, Ito F, Webela PW, Wiantoro S, Bernard E, Tanalgo KC, Hughes A, Cardoso P, Lilley T, Mammola S (2024) Effective conservation of subterranean-roosting bats. *Conservation Biology* 38(1): e14157. <https://doi.org/10.1111/cobi.14157>
- Oktaviana AA, Joannes-Boyau R, Hakim B, Burhan B, Sardi R, Adhityatama S, Hamrullah, Sumantri I, Tang M, Lebe R, Ilyas I, Abbas A, Jusdi A, Mahardian DE, Noerwidi S, Ririmasse MNR, Mahmud I, Duli A, Aksa LM, McGahan D, Setiawan P, Brumm A, Aubert M (2024) Narrative cave art in Indonesia by 51,200 years ago. *Nature* 631: 814–818. <https://doi.org/10.1038/s41586-024-07541-7>

- Opermanis O, Kalnins SN, Aunins A (2015) Merging science and arts to communicate nature conservation. *Journal for Nature Conservation* 28: 67–77. <https://doi.org/10.1016/j.jnc.2015.09.005>
- Piano E, Mammola S, Nicolosi G, Isaia M (2024) Advancing tourism sustainability in show caves. *Cell Reports Sustainability* 1(3): 100057. <https://doi.org/10.1016/j.crsus.2024.100057>
- Saccò M, Mammola S, Altermatt F, Alther R, Bolpagni R, Brancelj A, Brankovits D, Fišer C, Gerovasileiou V, Griebler C, Guareschi S, Hose GC, Korbel K, Lictevout E, Malard F, Martínez A, Niemiller ML, Robertson A, Tanalgo KC, Bichuette ME, Borko Š, Brad T, Campbell MA, Cardoso P, Celico F, Cooper SJB, Culver D, Di Lorenzo T, Galassi DMP, Guzik MT, Hartland A, Humphreys WF, Ferreira RL, Lunghi E, Nizzoli D, Perina G, Raghavan R, Richards Z, Reboleira ASPs, Rohde MM, Sánchez Fernández D, Schmidt SI, van der Heyde M, Weaver L, White NE, Zagamajster M, Hogg I, Ruhi A, Gagnon MM, Al-lentoft ME Reinecke R (2024) Groundwater is a hidden global keystone ecosystem. *Global Change Biology* 30(1): e17066. <https://doi.org/10.1111/gcb.17066>
- Small E (2016) The value of cartoons for biodiversity conservation. *Biodiversity* 17(3): 106–114. <https://doi.org/10.1080/14888386.2016.1203818>
- Salazar G, Monroe MC, Ennes M, Jones JA, Veríssimo D (2022) Testing the influence of visual framing on engagement and pro-environmental action. *Conservation Science and Practice* 4(10): e12812. <https://doi.org/10.1111/csp2.12812>
- Sánchez-Fernández D, Galassi DM, Wynne JJ, Cardoso P, Mammola S (2021) Don't forget subterranean ecosystems in climate change agendas. *Nature Climate Change* 11(6): 458–459. <https://doi.org/10.1038/s41558-021-01057-y>
- Sturani M (1942) *Caccia grossa tra le erbe*. Einaudi. Giulio Einaudi Editore, Torino, 113 pp. <https://doi.org/10.5962/bhl.title.70355>
- Tahamtan I, Safipour Afshar A, Ahamdzadeh K (2016) Factors affecting number of citations: A comprehensive review of the literature. *Scientometrics* 107(3): 1195–1225. <https://doi.org/10.1007/s11192-016-1889-2>
- Tribot AS, Faget D, Richard T, Changeux T (2022) The role of pre-19th century art in conservation biology: An untapped potential for connecting with nature. *Biological Conservation* 276: 109791. <https://doi.org/10.1016/j.biocon.2022.109791>
- Vaccarelli I, Colado R, Pallares S, Galassi DM, Sanchez-Fernandez D, Di Cicco M, Meierhofer MB, Piano E, Di Lorenzo T, Mammola S (2023) A global meta-analysis reveals multilevel and context-dependent effects of climate change on subterranean ecosystems. *One Earth* 6(11): 1510–1522. <https://doi.org/10.1016/j.oneear.2023.09.001>
- Van Noorden R (2013) The true cost of science publishing. *Nature* 495(7442): 426–429. <https://doi.org/10.1038/495426a>
- Waldron A, Miller DC, Redding D, Mooers A, Kuhn TS, Nibbelink N, Roberts JT, Tobias JA, Gittleman JL (2017) Reductions in global biodiversity loss predicted from conservation spending. *Nature* 551(7680): 364–367. <https://doi.org/10.1038/nature24295>
- Warren DR, Loeb HM, Betjemann P, Munck IA, Keeton WS, Shaw DC, Harvey EJ (2023) An interdisciplinary framework for evaluating 19th century landscape paintings for ecological research. *Ecosphere* 14(9): e4649. <https://doi.org/10.1002/ecs2.4649>

- Whitley DS (2009) *Cave paintings and the human spirit: The origin of creativity and belief*. Prometheus Books, New York, 322 pp.
- Wong C (2024) AI-generated images and video are here: how could they shape research? *Nature*. <https://doi.org/10.1038/d41586-024-00659-8>
- Wynne JJ, Howarth FG, Mammola S, Ferreira RL, Cardoso P, Lorenzo TD, Galassi DMP, Medellín RA, Miller BW, Sánchez-Fernández D, Bichuette ME, Biswas J, BlackEagle CW, Boonyanusith C, Amorim IR, Borges PAV, Boston PJ, Cal RN, Cheeptham N, Deharveng L, Eme D, Faille A, Fenolio D, Fišer C, Fišer Ž, Gon III SMO, Goudarzi F, Griebler C, Halse S, Hoch H, Kale E, Katz AD, Kováč L, Lilley TM, Manchi S, Manenti R, Martínez A, Meierhofer MB, Miller AZ, Moldovan OT, Niemiller ML, Peck SB, Pellegrini TG, Pipan T, Phillips-Lander CM, Poot C, Racey PA, Sendra A, Shear WA, Silva MS, Taiti S, Tian M, Venarsky MP, Pakarati SY, Zagamajster M, Zhao Y (2021) A conservation roadmap for the subterranean biome. *Conservation Letters* 14(5): e12834. <https://doi.org/10.1111/conl.12834>
- Yoon J, Chung E (2017) An investigation on graphical abstracts use in scholarly articles. *International Journal of Information Management* 37(1): 1371–1379. <https://doi.org/10.1016/j.ijinfomgt.2016.09.005>

A century later: Rediscovery and range expansion of *Typhlocaris lethaea* Parisi, 1920 (Crustacea, Decapoda) in subterranean karstic waters of Benghazi, northeastern Libya

Rosario Ruggieri¹, Houssein Elbaraasi², Mohammed H. Al Riaydh^{3,4,5},
Abdelsalam Elshaafi³, Awad Bilal³, Fathi Salloum³, Mohamed Abdelmalik³

1 Centro Ibleo di Ricerche Speleo-Idrogeologiche, via Torrenuova 87, 97100 Ragusa, Italy **2** Department of Zoology, Faculty of Science, University of Benghazi, Benghazi, Libya **3** Department of Earth Science, Faculty of Science, University of Benghazi, Benghazi, Libya **4** Diversity and Evolution, Institute of Ecology, Department of Life Sciences, Goethe University Frankfurt, Frankfurt, Germany **5** Senckenberg Research Institute and Natural History Museum, Department Messel Research and Mammalogy, Frankfurt, Germany

Corresponding author: Mohammed H. Al Riaydh (moha.alriaydh@stud.uni-frankfurt.de)

Academic editor: Fabio Stoch | Received 26 January 2025 | Accepted 2 February 2025 | Published 4 March 2025

<https://zoobank.org/5AC0B5D7-13A8-41CC-86F3-81B4156561ED>

Citation: Ruggieri R, Elbaraasi H, Al Riaydh MH, Elshaafi A, Bilal A, Salloum F, Abdelmalik M (2025) A century later: Rediscovery and range expansion of *Typhlocaris lethaea* Parisi, 1920 (Crustacea, Decapoda) in subterranean karstic waters of Benghazi, northeastern Libya. Subterranean Biology 51: 21–29. <https://doi.org/10.3897/subtbiol.51.147950>

Abstract

This study confirms the existence of the blind cave shrimp *Typhlocaris lethaea* Parisi, 1920, in Lethe Cave, Benghazi, Libya, nearly a century after its initial discovery, and documents its new distribution in the Al-Coeffiah caves. Field surveys conducted in 2023 and 2024 revealed its presence in the El-Khadim and Al-Jebah caves, extending its known range by 9 km. Specimens were found in subterranean lakes characterized by complete darkness, with water parameters including an average temperature of 22 °C, pH of 7.67, and salinity of 4.72 ppt. Two specimens were used for further analysis. These findings suggest that the species is more widespread than previously thought and highlight the potential hydrological connections within the karstic system. Additionally, the discovery of a depigmented isopod in El-Khadim cave suggests further hidden biodiversity. Given its IUCN data-deficient status, our findings emphasize the need for conservation efforts to protect these fragile ecosystems from human impacts, ensuring the preservation of Libya's unique subterranean biodiversity.

Keywords

Biospeleology, cave ecosystems, conservation biology, Libya, stygobiotic shrimp

Introduction

The subterranean ecosystem and its biodiversity are generally unfamiliar to the public, particularly to individuals without specialized knowledge of underground biology (Marmonier et al. 2023). A similar situation exists in the Benghazi Plain, north-eastern Libya. This area is heavily karstified by an intricate network of subterranean lakes and conduits. This is because of its geological setting, which is primarily composed of carbonate rocks of the Benghazi Formation (Salloum et al. 2022; El-Rayani et al. 2024). These conduits are mostly associated with the Bou-Atni and Al-Coeffiah areas east of Benghazi. The stygobiotic shrimp genus *Typhlocaris* (Calman 1909) (Malacostraca: Decapoda: Typhlocarididae) is exclusively located in the subterranean water habitats of the Mediterranean region (Tsurnamal 2008). All species exhibited stygomorphism, being characterized by the complete absence of eyes and pigmentation throughout the body. Additionally, they are distinguished by the presence of a longitudinal post-antennal suture, a structural characteristic that can be observed on the lateral surfaces of their carapaces (Bauer 2004; De Grave et al. 2008; De Grave and Fransen 2011; Guy-Haim et al. 2018). Currently, four valid species of this genus are known from four locations in the Mediterranean Sea (Fig. 1). Each location is inhabited by a distinct species with no congenetics in the open sea. Two species are known from the eastern coastline of the Mediterranean Sea: *T. galilea* (Calman 1909) from the Tabgha spring and *T. ayyaloni* (Tsurnamal 2008), discovered in a huge and natural network of pits known as Ayyalon cave, approximately 120 km south of Tabgha. The third species, *T. salentina* (Caroli 1923), was described from the Zinzulusa cave in southern Italy and was recently discovered in two other caves (Frogliia and Ungaro 2001). The fourth species, *T. lethaea* Parisi, 1920, was known from the Lethe (also known as Al Jekh) cave in Benghazi, Libya. Vito Zanan was the first ever to notice this decapod in the Lethe cave. He sent this to Bruno Parisi, who attributed it to *T. galilea*. Subsequently, Parisi sent one specimen to William Thomas Calman at the British Museum. After comparing it with the types of *T. galilea*, Calman concluded that it was a distinct species. After careful examination, Parisi described it under the name *T. lethaea* (Parisi 1920).

Unfortunately, the species was not reported in subsequent literature, and even Guy-Haim et al. (2018), in their molecular revision of the genus *Typhlocaris*, were unable to obtain any specimens of *T. lethaea*. For this reason, the International Union for Conservation of Nature (IUCN) Red List of Threatened Species classifies this species as data-deficient (De Grave 2013). Therefore, this short communication discusses the confirmation of the existence of the Lethe cave blind shrimp, *T. lethaea*, for the first time since 1920, and documents a novel and typical distribution of this species within the Al-Coeffiah caves in the Benghazi plain, Libya.

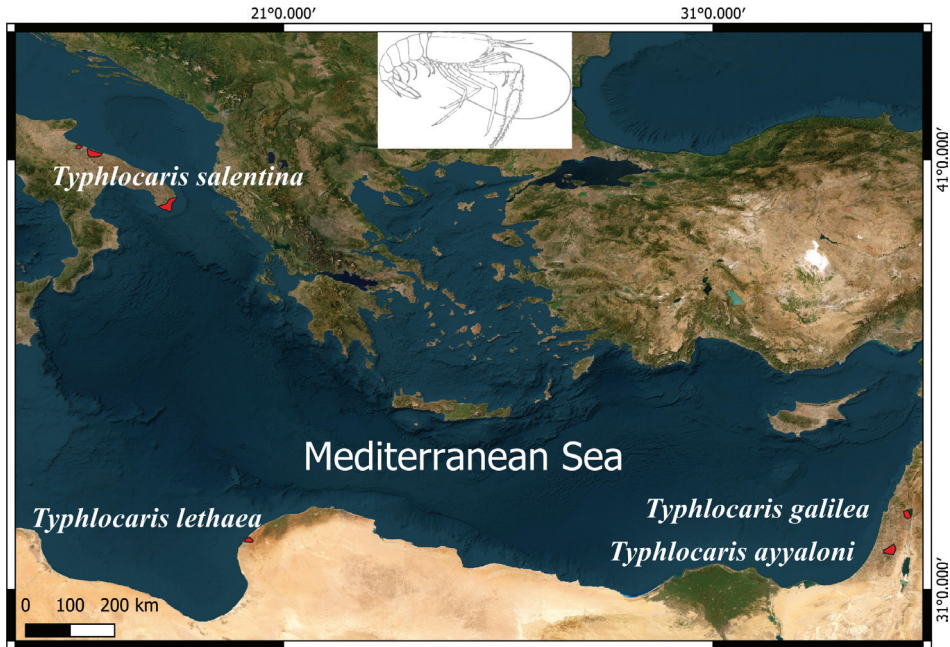


Figure 1. Distribution map of four *Typhlocaris* species from four locations around the Mediterranean Sea, modified after De Grave and Franssen (2011).

Materials and methods

Lethe cave

This cave is located in Bou-Atni area, south of Benghazi city, Libya, with coordinates 32°06'58.16"N, 20°09'24.44"E and an altitude of 30 m a.s.l. The cave was explored and surveyed by a research group from Centro Ibleo di Ricerche Speleo-Idrogeologiche di Ragusa, Italy (CIRS), and the Earth Science Department at the University of Benghazi (Benghazi, Libya) in 2007 and 2009. The cave is a part of several collapsed dolines lined up in NE – SW direction (Ruggieri and Abdelmalik 2009; Ruggieri 2010; Ruggieri et al. 2025), and the cave itself can be divided into two main branches. During the initial exploration of the Lethe cave in January 2007, several specimens (3-6 individuals) of genus *Typhlocaris*, likely belonging to the species *T. lethaea*, were observed on the sandy muddy bottom of the first branch of the subterranean lake, which is nourished by an underground aquifer of brackish water (Ruggieri and Abdelmalik 2009; Ruggieri 2010; Ruggieri et al. 2025). The specimens were located in dark sections a few meters from the platform landing stage. Given the clarity of the water, we were able to film and photograph one of them (Fig. 2A).

Al-Coeffiah caves

In 2023, two field visits were conducted in the Al-Coeffiah area northeast of Benghazi. Al-Coeffiah suburban's covers a surface area of about 835 km² and it is largely affected by many karstic features including caves and various sizes of dolines with complex

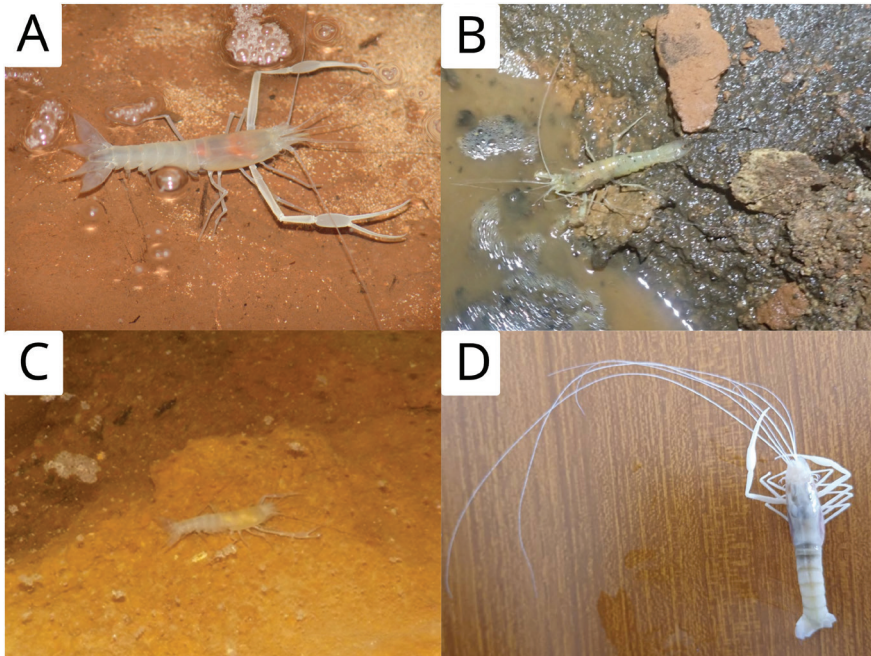


Figure 2. The rediscovered cave-dwelling shrimp *T. lethaea* during the survey of different caves in Bou-Atni and Al-Coeffiah areas, Benghazi plain, NE, Libya **A** *T. lethaea* observed on 2007 during the initial visit to the Lethe cave in Bou-Atni area (Photo by Iolanda Galletti) **B** *T. lethaea* reported on July 2023 during the exploration of the El-Khadim cave in Al-Coeffiah area (Photo by Rosario Ruggieri) **C** the same species reported on October 2023 during the exploration of the Al-Jebah cave in Al-Coeffiah area (Photo by Giovanni Gianninoto) **D** one of the two specimens collected during a recent visit to the El-Khadim cave, on the December 7th, 2024 (Photo by Houssein Elbaraasi).

underground drainage systems (Elshaafi et al. 2021; Salloum et al. 2022; El-Rayani et al. 2024). On July 2023 during a visit to explore El-Khadim doline-cave, which is located approximately 15 km northeast of Benghazi Port, at 32°11'50"N, 20°11'16"E, with an altitude of 21 m a.s.l (Fig. 3), a single specimen of *T. lethaea* was discovered and is reported here for the first time as a new record (Fig. 2B). The specimen was laid on a rocky muddy surface a few centimeters out of the water. Furthermore, during the above-mentioned exploration, an isopod measuring a few millimeters in size and completely white was observed in the same cave. On October 2023, during the exploration visit of the Al-Jebah collapse-doline cave at 32°11'59"N, 20°10'57"E, with an altitude of 21 m a.s.l, which is also located within Al-Coeffiah area, a single specimen of *T. lethaea* was observed again on muddy bottom of the cave (Fig. 2C).

Specimens collection

Recently, a group of researchers from the Departments of Zoology and Earth Sciences from the University of Benghazi conducted a second exploration visit to El-Khadim cave on December 7, 2024. The main aim of this study was to confirm the new

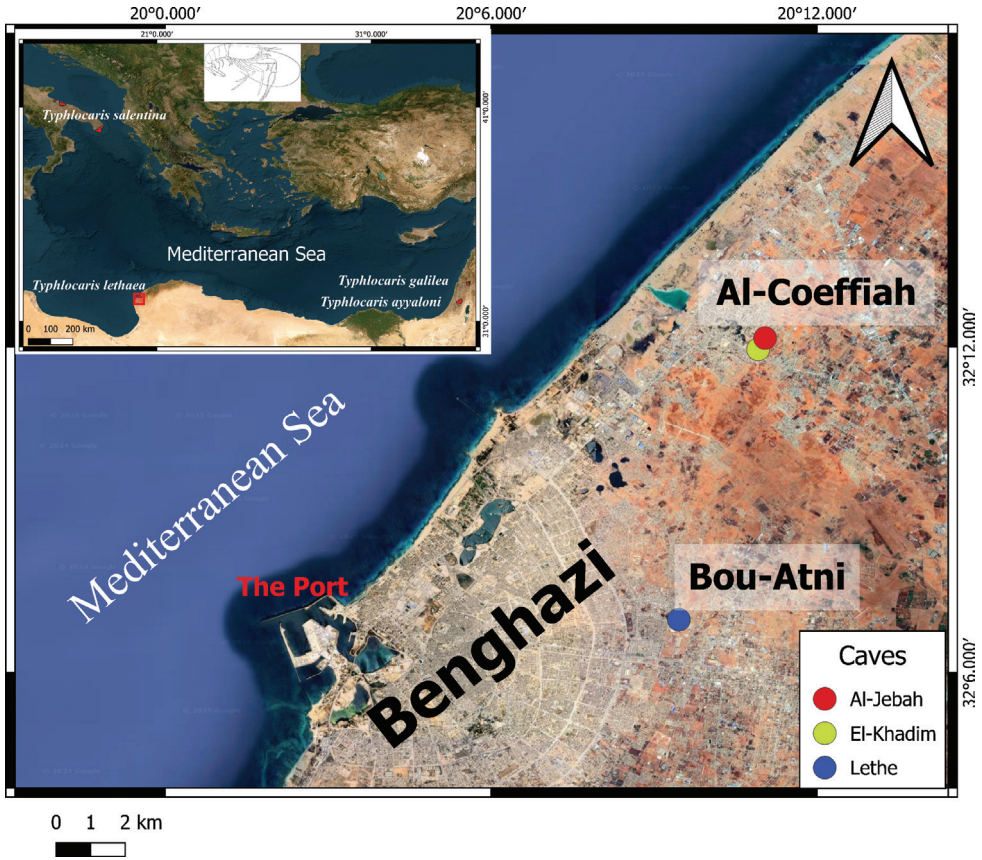


Figure 3. New records of *T. lethaea* based on field observations during the exploration of caves in the Bou-Atni area in 2007, and 2023 and 2024 in the Al-Coeffiah area.

distribution and collect samples of this species. Two specimens were collected using a dip net from the surface of the first subterranean lake, stored in 96% ethanol, and transferred to the Department of Zoology at the University of Benghazi for further investigation (Fig. 2D, Suppl. material 1). Water temperature, air temperature, pH, and salinity in the cave were measured to better understand shrimp habitats.

Results and discussion

Research on biodiversity and organisms in caves in Libya, specifically in Benghazi, has not yet been undertaken, resulting in a significant scientific gap regarding subterranean organisms. The Libyan blind shrimp *T. lethaea* is Benghazi's only endemic cave species to the south of the Mediterranean Basin. Information on this has been scarce since Parisi discovered it in the mysterious Lethe cave in 1920, leading to a widespread belief that it was extinct in its infancy. This paper presents for the first time, after almost 100 years, the confirmation of the existence of the stygobi-

ont species *T. lethaea* in Lethe cave and documents a new and unusual distribution in the newly explored El-Khadim cave and Al-Jebah cave in the Al-Coeffiah area, Benghazi, Libya. Our attempts to collect and confirm the presence of this decapod were successful. Although our visit was brief, this species was observed several times, indicating that its populations were abundant, particularly in the cave systems of the Al-Coeffiah area.

Caves are commonly characterized by a very special environment with complete darkness, high humidity, and low temperature fluctuations (De Grave & Fransen, 2011). The documented *T. lethaea* are commonly found to inhabit sandy and muddy bottoms on the surface of water mixed with organic debris and rocks. All our observations of this decapod Crustacean occurred in sections of caves characterized by complete darkness, such as *T. lethaea* reported from the El-Khadim and Al-Jebah caves (Al-Coeffiah area), and this is in good agreement with the conditions described in the original discovery in Lethe cave (Parisi, 1920). In this study, the average water and air temperatures were 22 and 21 °C, respectively. Average pH was 7.67. The average salinity of the water was 4.72 ppt. The two specimens collected from El-Khadim cave in 2024 were female, with a total length of 5 cm.

This study reports unusual findings for *T. lethaea* from a new area near Benghazi, and this new location extends the range of the species 9 km north of the original site in Benghazi (Bou-Atni) into the Al-Coeffiah area, 4 km southwest of the Mediterranean Sea coast (Fig. 3). The new record reported here, in combination with the detection of this species at a previously inventoried site (Lethe cave), suggests that this species is widely distributed in the subterranean waters of the karstic system of the Benghazi plain. We present a new record from a cave in Benghazi, expanding the range of *T. lethaea* to encompass much of the Benghazi area and altering its extinction risk status owing to the inclusion of this new locality.

Our records suggest that the hydrological systems of the Lethe caves (Bou-Atni area), El-Khadim and Al-Jebah caves (Al-Coeffiah area) are somehow interconnected, as both habitats harbor the same species of stygobiotic shrimp, *T. lethaea*, which is commonly observed. Furthermore, some biospeleological methods that study the DNA of subterranean stygobiotic animals and enable the establishment of biogeographic connections between underground watercourses should be used in conjunction with traditional hydrogeological methods to connect caves (Marin 2020; Marin and Turbanov 2021). This method can be applied in future research based on our findings, as well as other stygobiotic animals that may be prevalent in subterranean watercourses.

Existing knowledge on Libyan cave biodiversity has never been the focus of any research, and this study is considered a spark to open new areas for future research and scientific interest. Our observations in the studied caves and earlier observations from the same area are the only investigations of possible biodiversity in cave environments in Libya. Future research should fill the gaps in cave biology and ecology by potentially increasing the number of species and answering fundamental questions related to the biodiversity and health of underground populations.

Conclusions

The karstic underground system of Benghazi is unique because of its caves and fauna, which host aquatic and terrestrial cave-restricted species associated with subterranean aquifers and several cases of endemism. It is well known that the *Typhlocaris* species are classified as endangered and are listed in the IUCN Red List. The caves in which they live are not designated as protected areas or legally protected, and some caves have already been affected by human activity. Efforts must be made to engage local stakeholders in conservation actions to protect these unique cave ecosystems and the biological communities inhabiting them. Furthermore, this karst area remains outside the protected zones and is exposed to high groundwater pumping and pollution. Our findings confirm the existence of *T. lethaea* in Lethe cave, and the new unusual distribution in the Al-Coeffiah caves highlights the value of subterranean biodiversity, which increases its ecological significance and biological uniqueness, reinforcing its importance in conservation efforts. In addition, the biodiversity present in the karst system of the Benghazi plain may be further enriched by the discovery of a completely depigmented isopod, which was observed during the exploration of El-Khadim cave in July 2023. This species was not collected because of the absence of appropriate sampling equipment.

Acknowledgments

This work represents a contribution to the Cyrenaica Karst Project, an international cooperation between the Department of Earth Sciences at the University of Benghazi and the Hyblean Center of Speleo-Hydrogeological Research (CIRS), Italy. We are indebted to the University of Benghazi for logistical support, El-Diqa Lab for water chemical analysis from El-Khadim cave, and Mr. Jammal Alkomaty for his immense assistance during cave visits. Finally, we thank the Editor-in-Chief of Subterranean Biology, Fabio Stoch, for his valuable comments that improved this manuscript.

References

- Bauer RT (2004) Remarkable shrimps: adaptations and natural history of the carideans. University of Oklahoma Press, 316 pp.
- Calman WT (1909) V. on a blind prawn from the sea of Galilee (*Typhlocaris galilea*, g.et sp. n.). Transactions of the Linnean Society of London. 2nd Series. Zoology 11: 93–97. <https://doi.org/10.1111/j.1096-3642.1909.tb00194.x>
- Caroli E (1923) Di una specie italiana di *Typhlocaris* (*T. salentina* n.sp.) con osservazioni morfologiche e biologiche sul genere. Bollettino della Societa dei Naturalisti di Napoli 35: 265.
- El-Rayani E, Salloum F, Elshaafi A, Bilal A, Eldursi K (2024) Assessment of geohazards of karstified limestone in Al-Coeffiah area, Benghazi plain, NE Libya. Carbonates and Evaporites 39: 23. <https://doi.org/10.1007/s13146-024-00933-w>

- Elshaafi A, Bilal A, Awami Y, Salloum F (2021) Development of collapse dolines in Al Jabal Al Akhdar, NE Libya: geomorphic analysis and numerical modeling-based approach. *Carbonates and Evaporites* 36: 54. <https://doi.org/10.1007/s13146-021-00714-9>
- Froggia C, Ungaro N (2001) An unusual new record of *Typhlocaris salentina* (Caroli, 1923) (Decapoda: Typhlocarididae) from subterranean water of Apulia (Southern Italy). *Atti della Società Italiana di Scienze Naturali e del Museo Civico di Storia Naturale in Milano* 142: 103–108.
- De Grave S (2013) *Typhlocaris lethaea*. IUCN Red List of Threatened Species. <https://doi.org/10.2305/IUCN.UK.2013-1.RLTS.T197927A2505482.en>
- De Grave S, Fransen CHJM (2011) Carideorum catalogus: The recent species of the dendrobranchiate, stenopodidean, procarididean and caridean shrimps (Crustacea: Decapoda). *Zoologische Mededelingen* 85: 195–588.
- De Grave S, Cai Y, Anker A (2008) Global diversity of shrimps (Crustacea: Decapoda: Caridea) in freshwater. *Hydrobiologia* 595: 287–293. <https://doi.org/10.1007/s10750-007-9024-2>
- Guy-Haim T, Simon-Blecher N, Frumkin A, Naaman I, Achituv Y (2018) Multiple transgressions and slow evolution shape the phylogeographic pattern of the blind cave-dwelling shrimp *Typhlocaris*. *PeerJ* 6: e5268. <https://doi.org/10.7717/peerj.5268>
- Marin IN (2020) Stygobiotic atyid shrimps (Crustacea, Decapoda, Atyidae) from the Amtkel karst system, Western Abkhazia, Caucasus, with a redescription of *Xiphocaridinella osterloffii* and the description of two new co-occurring species. *Zoologicheskii Jurnal [Зоологический журнал]* 99: 1203–1222. <https://doi.org/10.31857/S0044513420100128>
- Marin IN, Turbanov I (2021) Molecular genetic analysis of stygobiotic shrimps of the genus *Xiphocaridinella* (Crustacea: Decapoda: Atyidae) reveals a connection between distant caves in Central Abkhazia, southwestern Caucasus. *International Journal of Speleology* 50: 301–311. <https://doi.org/10.5038/1827-806X.50.3.2378>
- Marmonier P, Galassi DMP, Korbel K, Close M, Datry T, Karwautz C (2023) Groundwater biodiversity and constraints to biological distribution. In: *Groundwater Ecology and Evolution*. Elsevier, 113–140. <https://doi.org/10.1016/B978-0-12-819119-4.00003-2>
- Parisi B (1920) Un nuovo crostaceo cavernicolo: *Typhlocaris lethaea* n. sp. *Atti della Società Italiana di Scienze Naturali e del Museo Civico di Storia Naturale in Milano* 59: 241–248.
- Ruggieri R (2010) Cyrenaica Karst Project. Report of the 2004 reconnaissance and 2007–2008–2009 campaigns of Karst and Speleological research.
- Ruggieri R, Abdelmalik M (2009) Cyrenaica karst project (north-eastern Lybia). In: White WB (Ed.) 15th International Congress of Speleology. The International Union of Speleology, Kerrville, Texas, 1667–1671.
- Ruggieri R, Elshaafi A, Bilal A, Salloum F, Elshari S (2025) The Cyrenaica karst project: Karst geomorphology and caves, Al-Jabal Al-Akhdar, NE Libya. *Journal of Pure & Applied Sciences* 25: 44–51. <https://doi.org/10.51984/jopas.v25i2.3787>
- Salloum FM, Al Amin AA, El-Shawaihdi MH, Amawy MA El, Muftah AM, Al Riaydh MH (2022) Impact of structural fabric on development of karst aquifer in Ayn Zayanah-Al Coeffiah area in Benghazi plain, NE Libya. *Carbonates and Evaporites* 37: 65. <https://doi.org/10.1007/s13146-022-00811-3>
- Tsurnamal (2008) A new species of the stygobiotic blind prawn *Typhlocaris* Calman, 1909 (Decapoda, Palaemonidae, Typhlocaridinae) from Israel. *Crustaceana* 81: 487–501. <https://doi.org/10.1163/156854008783797534>

Supplementary material I

Movie

Authors: Rosario Ruggieri, Houssein Elbaraasi, Mohammed H. Al Riaydh, Abdelsalam Elshaafi, Awad Bilal, Fathi Salloum, Mohamed Abdelmalik

Data type: multimedia

Copyright notice: This dataset is made available under the Open Database License (<http://opendatacommons.org/licenses/odbl/1.0/>). The Open Database License (ODbL) is a license agreement intended to allow users to freely share, modify, and use this Dataset while maintaining this same freedom for others, provided that the original source and author(s) are credited.

Link: <https://doi.org/10.3897/subtbiol.51.147950.suppl1>

Isotopic variability of $\delta^{13}\text{C}$ and $\delta^{15}\text{N}$ signals in cave systems: insights from the blind tetra *Astyanax mexicanus*

Jorge Hernández-Lozano¹, Fernando Córdova-Tapia², Ramses Miranda-Gamboa¹,
María de Lourdes Vázquez-Cruz¹, Carlos Garita-Alvarado¹,
Norman Mercado-Silva³, Claudia Patricia Ornelas-García¹

1 Colección Nacional de Peces, Departamento de Zoología, Instituto de Biología, Universidad Nacional Autónoma de México, Ciudad de México, Mexico **2** Laboratorio de Limnología, Instituto de Ciencias del Mar y Limnología, Universidad Nacional Autónoma de México, Ciudad de México, Mexico **3** Centro de Investigación en Biodiversidad y Conservación, Universidad Autónoma del Estado de Morelos, Cuernavaca, Morelos, Mexico

Corresponding authors: Fernando Córdova-Tapia (fcordova@cmarl.unam.mx);

Claudia Patricia Ornelas-García (patricia.ornelas.g@ib.unam.mx)

Academic editor: Maria Elina Bichuette | Received 3 November 2024 | Accepted 20 January 2025 | Published 17 March 2025

<https://zoobank.org/CE8894E0-36DA-4360-ACB8-93CAC6AF5617>

Citation: Hernández-Lozano J, Córdova-Tapia F, Miranda-Gamboa R, Vázquez-Cruz MdeL, Garita-Alvarado C, Mercado-Silva N, Ornelas-García CP (2025) Isotopic variability of $\delta^{13}\text{C}$ and $\delta^{15}\text{N}$ signals in cave systems: insights from the blind tetra *Astyanax mexicanus*. Subterranean Biology 51: 31–47. <https://doi.org/10.3897/subtbiol.51.140856>

Abstract

Stable isotope analysis allows the study of element cycles in ecosystems and trophic ecology. $\delta^{13}\text{C}$ reflects the diversity of primary productivity, while $\delta^{15}\text{N}$ is a good indicator of trophic levels of organisms. Caves have limited resources due to the absence of light, reducing the trophic chains in these ecosystems. These extreme conditions impose strong selection pressures on cave-dwelling organisms, known as troglolites, which exhibit specific adaptations such as vision and pigment loss, and metabolic and physiological differences with their surface counterparts. The species *Astyanax mexicanus* corresponds to a model organism in the study of regressive evolution, which presents two different ecotypes, a widely distributed surface morph, and a cave-dwelling morph present in at least 34 caves in three karst regions of San Luis Potosí and Tamaulipas, Mexico. In the present study, we characterized the $\delta^{13}\text{C}$ and $\delta^{15}\text{N}$ of seven cave populations of *A. mexicanus*, corresponding to two karst regions: Sierra de El Abra and Sierra de Guatemala, representing distinct genetic cavefish lineages. We also developed a Nutrient Input Index (NI), to assess whether cave geomorphology influences resource availability. We found isotopic differences between caves and regions analyzed. Caves in the Sierra de El Abra showed higher $\delta^{15}\text{N}$ values and wider trophic niche ranges compared with those in the Sierra de Guatemala, reflecting a more complex trophic network tentatively

associated also with its geological history. In addition, a relationship was observed between the proximity of pools to the surface and the $\delta^{13}\text{C}$ values, which could suggest differences in NI directly associated with cave geomorphology, impacting selective forces across the different cave systems.

Keywords

Cavefish, Layman metrics, Resource acquisition, Subterranean environment, Trophic ecology

Introduction

Caves are formed by different types of rocks and through various geological processes, with dissolution as the main forming agent, and limestone and dolomite as the substrates of the largest and most prevalent formations (Moldovan et al. 2018; Culver and Pipan 2019a). They represent distinctive ecosystems characterized by their physical structure and biological functioning (Moldovan et al. 2018). The geological setting, external terrestrial conditions including vegetation type, fauna, and soil, as well as hydrological features such as erosion, water flow, and material transport, delineate the cave ecosystem's boundaries, define its diverse habitats, and regulate the movement of energy and matter within the systems (Rouch 1987; Simon 2019).

Water bodies within caves exhibit variations in temperature, flow rate, and chemical composition depending on their connection to the surface. The terrestrial environment of caves can be classified into five zones: entrance, twilight, transition, deep zone, and stagnant air (White and Culver 2019), illustrating a gradient from the entrance towards deeper regions where light diminishes and temperature and humidity stabilize (Howarth 1983). Consequently, the terrestrial and aquatic habitats within caves should not be perceived as discrete systems but rather as a continuum characterized by relatively constrained energy flow (Poulson and Lavoie 2000).

These systems are characterized by perpetual darkness and oligotrophy, resulting from the limited availability of organic matter and low energy density (Moldovan et al. 2018). Consequently, the trophic structure of caves is considered less complex in terms of energy and nutrient dynamics compared to the surface environments (Moldovan et al. 2018), the latter playing a significant role in sustaining cave ecosystems (Kováč 2018). This connectivity is notably pronounced in limestone formations, where water percolation is a key characteristic (Dunne et al. 2002; Romero 2009; Kováč 2018). The combination of cave zones and available nutrient sources is important for species adaptation, imposing strong selective pressures for their evolution (Howarth and Moldovan 2018; Culver and Pipan 2019b).

In cave ecosystems, two distinct trophic networks have been described: detritus-based systems, which rely on decaying plant or animal matter, and chemoautotrophic systems, which are supported by bacteria capable of converting inorganic carbon (such as carbon dioxide or bicarbonate) into organic compounds (Venarsky and Huntsman 2018). Detritus-based cave ecosystems primarily operate through classical photosynthetic pathways, wherein organic material is transported by water flow from the surface, and also percolation, root growth inwards, and active or passive transport by animals (Simon et al. 2003; Culver and Pipan 2019b; Fong 2019; Simon 2019). In contrast,

chemoautotrophy-based cave ecosystems are sustained by bacteria that derive energy from the oxidation of inorganic compounds, notably sulfur (the most common) and methane. These bacteria transform carbon dioxide or bicarbonate into microbial biomass, facilitating primary productivity, particularly in the deepest zones of large caves (Sarbu et al. 1996; Venarsky and Huntsman 2018; Engel 2019).

Stable isotope ratio analysis (SIRA) stands as a valuable tool utilized to study element cycles in ecosystems, and trophic dynamics, particularly in elucidating the trophic positions of species within food webs (Boecklen et al. 2011; Brand and Coplen 2012). Specifically, the isotopic signatures of carbon ($\delta^{13}\text{C}$) and nitrogen ($\delta^{15}\text{N}$) provide insights into the organic carbon sources and trophic levels, respectively (Peterson and Fry 1987). This analytical approach has greatly advanced our understanding of trophic interactions and ecological roles in aquatic ecosystems (Vander-Zanden and Rasmussen 1999; Pilger et al. 2010; Cucherousset et al. 2012; Ornelas-García et al. 2018). For instance, $\delta^{13}\text{C}$ signals indicate the horizontal size of a food web (reflecting the diversity of primary producers) while $\delta^{15}\text{N}$ signals represent the number of vertical levels, where primary and secondary consumers are located (Bearhop et al. 2004; Boecklen et al. 2011). Additionally, stable isotopes facilitate the assessment of species' trophic niche areas (Córdova-Tapia and Zambrano 2016), which represents the extent of diversity in a food chain and an approximation of the variety and abundance of nutrients (Bearhop et al. 2004; Jackson et al. 2011). One of the most prominent methods for studying these isotopic signals is the so-called "Layman metrics", which comprise a suite of six measures delineating the structure, size of the ecological niche, and various trophic levels present within food webs (Layman and Post 2008).

In Mexico, one of the most studied cave-dwelling species is the Mexican tetra, *Astyanax mexicanus*, which has two morphs: a surface ecotype widely distributed in northern Mexico and the southern United States (Ornelas-García et al. 2008; Ornelas-García and Pedraza-Lara 2016), and a cave ecotype known from at least 34 distinct cave populations distributed in three karstic regions, between the states of San Luis Potosí and Tamaulipas: Sierra de La Colmena, Sierra de El Abra, and Sierra de Guatemala (Elliott 2018; Miranda-Gamboa et al. 2023). One unique aspect of this organism is that its cave populations evolved through at least three independent events (Garduño-Sánchez et al. 2023), providing a valuable opportunity to study parallel regressive evolution (Hernández-Lozano et al. 2024). The cave ecotype exhibits troglobitic traits, such as loss of vision and pigmentation (Jeffery 2009; McGaugh et al. 2014), as well as some features related to complex traits, including reduced sleep (Keene and Duboué 2018; Keene et al. 2024) and reduced aggressive behavior in certain populations (Elipot et al. 2013). One of the most notable adaptations in these cave populations is their ability to tolerate prolonged periods of starvation, which drives both metabolic and behavioral adaptations for resource acquisition in cave environments (Borowsky 2018; Pozo-Morales et al. 2024). Despite significant evidence for nutrient scarcity in these habitats, little is known about the trophic ecology, particularly nutrient availability, and whether these nutrient constraints differ among cave populations.

In this study, Stable Isotope Ratio Analysis (SIRA) is employed to investigate the trophic ecology of seven cavefish populations of *A. mexicanus* across two karstic geo-

graphic regions: the Sierra de El Abra and the Sierra de Guatemala. The primary goals of this research are: 1) to discern differences in trophic ecology among distinct populations of *A. mexicanus* inhabiting seven caves; 2) to determine differences between two cave systems, each representing a distinct lineage, considering their evolutionary backgrounds; and 3) to develop an index for nutrient influx based on cave geomorphology and evaluate its correlation with isotopic values to explore the potential impact of cave geomorphology on resource availability. This study represents a pioneering effort in elucidating the trophic structure of cavefish in Mexico.

Methods

Study Area

The Sierra de El Abra and Sierra de Guatemala systems are karst mountains in north-eastern Mexico along the eastern margin of the Sierra Madre Oriental (Fig. 1). The Sierra de El Abra system is located within the Biosphere Reserve Sierra de El Abra-Tanchipa San Luis Potosí and Tamaulipas, while the Sierra de Guatemala system is situated in the Biosphere Reserve El Cielo, Tamaulipas. These systems are characterized by their highly cavernous nature and are home to one of the world's highest

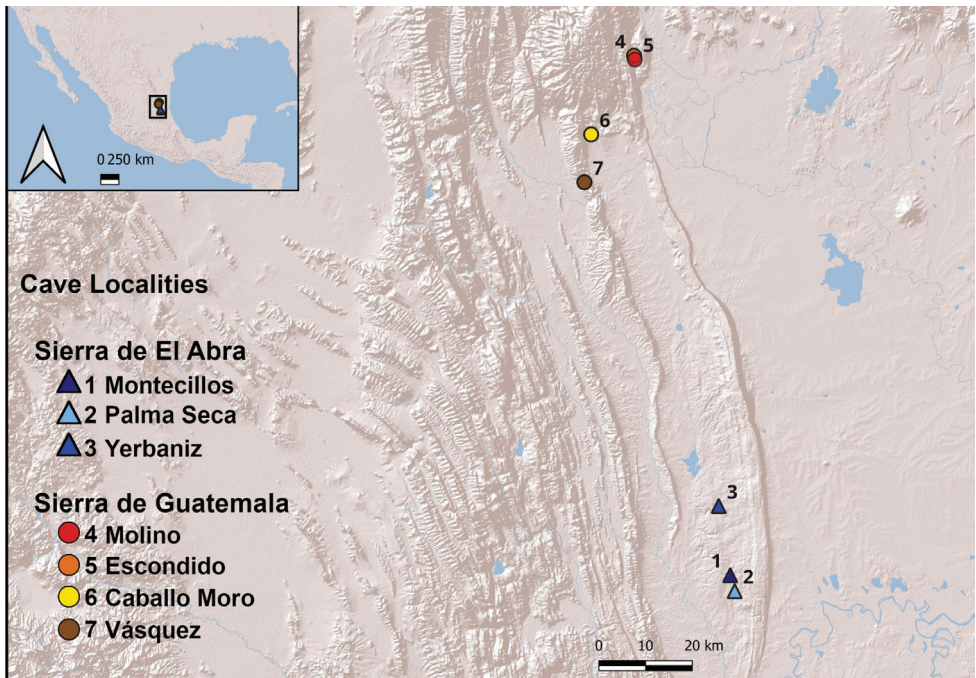


Figure 1. Geographic location of the sampled caves. Triangles represent caves in Sierra de El Abra system. Circles represent caves in the Sierra de Guatemala system.

flowing karst springs (Gary and Sharp 2006). There are currently 30 known populations of *A. mexicanus* in both regions (Elliott 2018; Miranda-Gamboa et al. 2023).

Sampling

Sampling was conducted between January and May, 2017, corresponding to the dry season. A total of 47 fish samples were collected from seven caves. In the Sierra de El Abra system, fish were sampled from Montecillos ($n = 3$), Palma Seca ($n = 13$), and Yerbaniz ($n = 5$), while in the Sierra de Guatemala system, fish were sampled from Caballo Moro ($n = 5$), Escondido ($n = 8$), Molino ($n = 8$), and Vásquez ($n = 5$) (Fig. 1). Fish were captured using hand nets, then photographed, weighed, sexed, and euthanized to obtain muscle tissue for stable isotope analysis. All sampling procedures were conducted under permit SGPA/DGVS/02438/16, issued by the Mexican Authority (SEMARNAT). All fish were treated following the Official Mexican Standards for the humane treatment of animals during collection (NOM-051-ZOO-1995).

Stable isotopes

Muscle tissues of fish were dehydrated by placing them in salt (NaCl) for transportation and then frozen at $-80\text{ }^{\circ}\text{C}$ until processing. To remove salt residues, the samples were hydrated in milliQ water, and then dried at $60\text{ }^{\circ}\text{C}$ for 48 hours. Once the samples were dry, they were ground into a fine powder and stored in sterile 2 mL tubes for further analysis. The samples were analyzed for their carbon and nitrogen signature using continuous flow isotope ratio mass spectrometry at the Center of Stable Isotopes at the University of New Mexico. The mean standard deviation between the samples and laboratory standards was 0.04‰ for $\delta^{13}\text{C}$ and 0.07‰ for $\delta^{15}\text{N}$.

Nutrient input index

Previous studies have estimated some geomorphological features of the caves used in this study, such as depth and entrance elevation in order to estimate the cave's age (Espinasa and Espinasa 2015; Elliot 2018). Following this, we developed the nutrient input index (NI) to estimate the influx of allochthonous material into subterranean pools, based on the geomorphological characteristics of caves, such as the proximity of pools to the surface, cave depth and phreatic level:

$$NI = \frac{DEP}{BLC - DC}$$

Where NI is the Nutrient Input Index; DEP is the distance from the cave entrance to the first fish pool; BLC is the local base level of the cave, which represents the minimum elevation of the local phreatic mantle (groundwater level determined by

local geology), estimated in relation to the minimum elevation of the nearest rivers (Goudie 2003); and DC is the cave's depth. The latter two geomorphological characteristics were obtained from published literature: BLC was sourced from Espinasa and Espinasa (2015), and DC from Elliot (2018). For the DEP, seven topographic cave maps were downloaded from data provided by the Association for Mexican Cave Studies (AMCS 2022, <http://www.mexicancaves.org/>, accessed in 2022). The total distance traversed in both vertical and horizontal directions within the cave passages was measured using the imageJ v.1.54 software (Schneider et al. 2012), calibrated with the assigned scale for each map (Suppl. material 1). The NI index compares the two distance values, DEP and BLC-DC. If the calculated value is greater than 1, it indicates that the pool is closer to the entrance, resulting in a higher input of allochthonous material. Conversely, values less than 1 indicate that the pool is farther from the entrance and closer to the bottom of the cave, where the influence of autochthonous material is greater.

Statistical analysis

To investigate differences in the $\delta^{15}\text{N}$ and $\delta^{13}\text{C}$ signals between Sierra de El Abra and Sierra de Guatemala, a Kruskal-Wallis analysis of variance was conducted. Subsequently, pairwise comparisons were made using the Mann-Whitney U test to examine differences at the population level, with significance values corrected by a Bonferroni procedure (Dunn 1961). To explore the relationship between the NI and isotopic signals, we conducted linear regressions using the NI values for the different caves and the average values of the $\delta^{13}\text{C}$ and $\delta^{15}\text{N}$ isotopic signals. All statistical analyses were performed using the R software (R Core Team 2023).

Layman's metrics were used to conduct a trophic niche analysis, which included: nitrogen range (NR), carbon range (CR), total niche area (TA), mean distance to centroid (CD), mean distance to nearest neighbor (NND), and standard deviation of nearest neighbor distance (SDNND) (Layman and Post 2008). NR is the interval between the organism with the highest and lowest values of $\delta^{15}\text{N}$. It describes the population's ability to feed on items from different trophic levels. CR is the interval between the organism with the highest and lowest values of $\delta^{13}\text{C}$. It describes the population's ability to feed on items from different producers at the base of the food web. TA represents the total trophic niche area of the population and is related to feeding diversity. CD measures the average degree of diversity within the population based on the spacing between organisms. NND measures the overall density of organism clustering, with lower values suggesting greater trophic redundancy. SDNND is less affected by sample size than NND and suggests a more uniform distribution of trophic niches (Jackson et al. 2001; Layman and Post 2008). In addition, a Bayesian trophic niche analysis was conducted using standard ellipse areas (SEA) to account for the potential effect of sample size, following the methodology of Jackson et al. (2011). Two Markov chain Monte Carlo (MCMC) simulations were run with 10,000 permutations each, and the first 1,000 values were discarded as burn-in.

Results

The analysis of variance revealed significant statistical differences for both stable isotopes among populations ($\delta^{15}\text{N}$: $H = 25.74$, $p < 0.01$; $\delta^{13}\text{C}$: $H = 15.34$, $p = 0.01$). At the population level, Yerbaniz cave had the lowest $\delta^{15}\text{N}$ value within the Sierra de El Abra system, while Montecillos had the highest $\delta^{15}\text{N}$ value ($9.2\text{‰} \pm 0.7$ and $10.9\text{‰} \pm 0.6$, respectively), making it the most $\delta^{15}\text{N}$ enriched population between the two geographic regions. Among the caves in the Sierra de El Abra, significant differences were found between Yerbaniz and Montecillos caves ($U = 0$, $p < 0.05$) and between Yerbaniz and Palma Seca ($U = 5.5$, $p = 0.01$) (Table 1). Within the Guatemala system, Molino cave had the lowest $\delta^{15}\text{N}$ value ($8.6\text{‰} \pm 0.4$), with significant differences observed between Molino and all others caves in the Sierra Guatemala: Caballo Moro ($U = 0$, $p < 0.01$), Vásquez ($U = 0$, $p < 0.01$), and Escondido ($U = 7.5$, $p = 0.01$). When comparing between the Sierra de El Abra and Sierra de Guatemala systems, we observed significant differences between Montecillos from Sierra de El Abra and the other two caves from Sierra de Guatemala: Molino ($U = 0$, $p = 0.01$) and Vásquez ($U = 0.5$, $p < 0.05$). We also recovered differences between Palma Seca from Sierra de El Abra and Molino from Sierra de Guatemala ($U = 1$, $p < 0.01$). The above suggests a link between isotopic variation and lineages associated with geographic systems.

Montecillos had the lowest $\delta^{13}\text{C}$ value across both geographic regions ($-29.8\text{‰} \pm 2.4$). Within the Sierra de El Abra system, significant differences were found between the Montecillos and the Palma Seca caves ($U = 2$, $p < 0.05$). In the Sierra de Guatemala system, significant differences were observed between Molino and Escondido caves ($U = 11.5$, $p < 0.05$). Between systems, differences were found between Montecillos and Caballo Moro caves ($U = 0$, $p < 0.05$), as well as between Montecillos and Escondido ($U = 0$, $p = 0.01$).

The Layman metrics showed that the trophic niche area (TA) in the Sierra de El Abra region was broader and exhibited lower trophic redundancy (CD, NND, and SDNND) compared to the Sierra de Guatemala region (Table 2). At the population level, Palma Seca cave has the widest niche amplitude in both geographic systems (7.06), whereas Vásquez has the narrowest niche (0.42). In general, the populations

Table 1. Statistical differences in $\delta^{13}\text{C}$ and $\delta^{15}\text{N}$ among sites and systems. The p values obtained from paired comparisons between caves are shown. Values with * are statistically significant.

	$\delta^{13}\text{C}$ $\delta^{15}\text{N}$	Guatemala				El Abra		
		Molino	Caballo Moro	Vásquez	Escondido	Montecillos	Palma Seca	Yerbaniz
Sierra de Guatemala	Molino		0.88	0.99	<0.05*	0.19	0.92	1
	Caballo Moro	<0.01*		0.99	0.69	<0.05*	0.99	0.9
	Vásquez	<0.01*	1		0.26	0.13	0.99	0.99
	Escondido	0.01*	0.76	0.60		0.01*	0.21	0.09
Sierra de El Abra	Montecillos	0.01*	0.07	<0.05*	0.12		<0.05*	0.29
	Palma Seca	0.01*	0.16	0.08	0.30	0.31		0.95
	Yerbaniz	0.07	0.11	0.14	0.10	<0.05*	0.01*	

Table 2. Layman metrics for each population and system. NR: nitrogen range, CR: carbon range, TA: total niche area, CD: mean distance to centroid, NND: mean distance to nearest neighbor, SDNND: standard deviation of nearest neighbor distance, $\delta^{15}\text{N}$: mean isotopic signature of nitrogen, $\delta^{13}\text{C}$: mean isotopic signatures of carbon, NI: nutrient input index.

	Trophic niche analysis						Nutrient index		
	NR	CR	TA	CD	NND	SDNND	$\delta^{15}\text{N}$	$\delta^{13}\text{C}$	NI
Sierra de El Abra	1.73	3.4	3.27	1.57	2.01	0.95			
Montecillos	1.2	4.2	2.49	1.93	2.18	1.69	10.9	-29.8	60
Palma Seca	2.5	6.1	7.06	1.62	0.74	0.42	9.1	-27.23	67
Yerbaniz	1.6	2.4	1.79	0.95	0.99	0.09	10.4	-26.43	-4.4
Sierra de Guatemala	1.45	2.5	1.41	1.01	1.05	0.45			
Caballo Moro	1.3	2	0.9	0.72	0.69	0.29	9.97	-26.11	1.2
Escondido	3.2	5.9	6.53	1.7	1.03	0.7	8.55	-27.22	-6.2
Molino	1.1	4	2.29	1.3	0.45	0.17	9.98	-27.7	20
Vásquez	0.6	1.4	0.42	0.48	0.43	0.22	9.94	-26.76	-4.1

showed overlap in their trophic niche areas; however, Montecillos did not overlap with any other populations (Fig. 2A). The NI index showed that populations living in deeper caves (i.e., Vásquez) have negative index values (Table 2). Escondido cave has the lowest value (NI=-6.2), followed by Yerbaniz (NI=-4.4), and Vásquez (NI=-4.1). In contrast, populations with pools closer to the cave entrances have higher NI index values, such as Montecillos (NI = 60) and Palma Seca (NI = 67).

Taken together, the Bayesian Standard Ellipse Area (SEA_b) and Layman's analyses showed differences between populations (Fig. 2B) and regions (Suppl. material 2). At the population level, Montecillos showed the highest values for total niche area based on SEA_b , which were consistent with other metrics such as mean distance to centroid (CD), mean distance to nearest neighbour (NND) and standard deviation of nearest neighbour distance (SDNND). While in Layman's metrics the highest values for niche area (TA) were found at Palma Seca. Vásquez showed the lowest SEA_b values, consistent with Layman's analyses. When comparing the two regions, the Sierra de El Abra system has a wider niche area (TA) and lower trophic redundancy (CD, NND, and SDNND) than the Sierra de Guatemala region.

Contrasting relationships were observed between the isotopic signals of $\delta^{15}\text{N}$ and $\delta^{13}\text{C}$, and the NI index. For nitrogen, the analysis indicated a trend where nitrogen values increased as the index values rose (Fig. 3A); however, this relationship was not statistically significant. In contrast, a significant negative relationship was observed for the carbon signal (Fig. 3B).

Discussion

Stable isotope analyses of nitrogen ($\delta^{15}\text{N}$) and carbon ($\delta^{13}\text{C}$) provide useful information for understanding the trophic structure of ecosystems, as they provide insights into trophic positions and food sources (Post 2002). This study represents

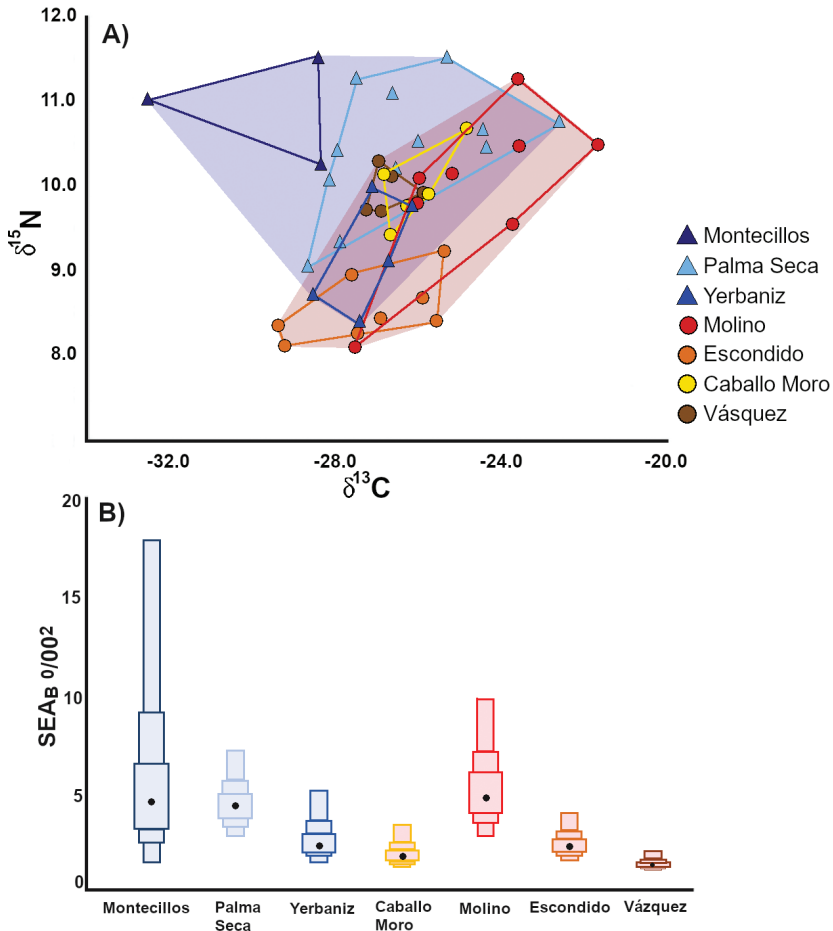


Figure 2. Trophic niche analysis of isotopic signals **A** bi-plot of $\delta^{15}\text{N}$ and $\delta^{13}\text{C}$: triangles represent populations from the Sierra El Abra, enclosed by the blue polygon, while circles represent populations from the Sierra de Guatemala, enclosed by the red polygon **B** standard ellipse area (SEAB_n) of the total niche area for each population. The black dot indicates the mean. Populations from the Sierra El Abra are depicted in blue tones, while those from the Sierra de Guatemala are depicted in red tones.

the first attempt to understand the trophic ecology of two independent lineages of cave populations of *A. mexicanus*. We found differences in the isotopic signals among regions and populations. Overall, the Sierra de El Abra region displayed a broader trophic niche area and lower trophic redundancy, with a relationship between cave geomorphology and isotopic values.

Comparing our regions, there is a 2.3‰ $\delta^{15}\text{N}$ difference between the most enriched population (Montecillos) and the least enriched population (Molino). The $\delta^{15}\text{N}$ helps explain the vertical complexity of the trophic network by identifying the trophic levels formed by producers and predators (Layman and Post 2008; Jackson et al. 2011). It has been observed that a difference of 3‰ - 4‰ in $\delta^{15}\text{N}$ typically exists between trophic

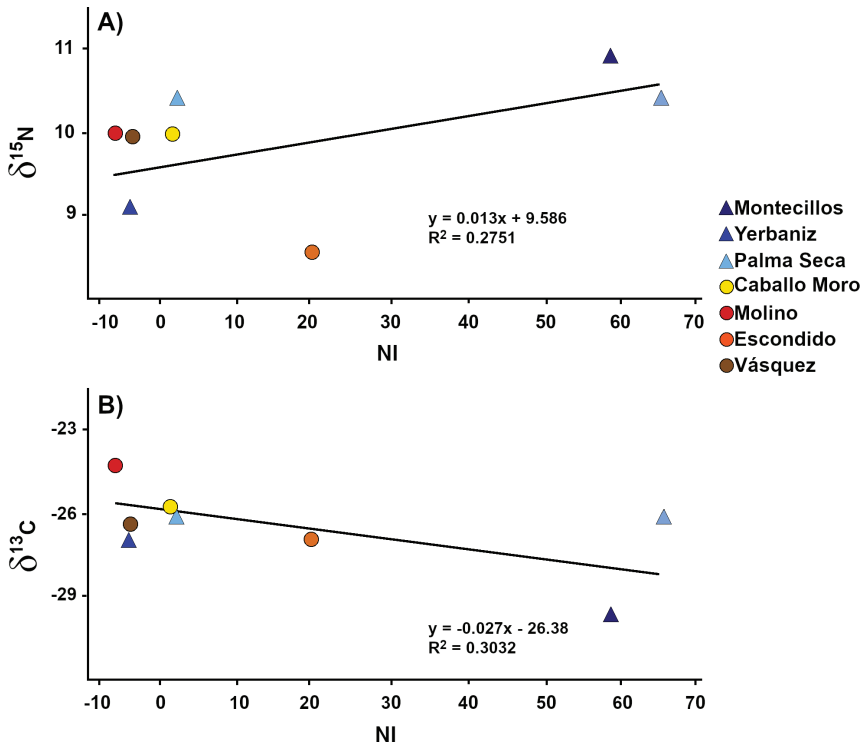


Figure 3. Linear regression of isotopic signals $\delta^{15}\text{N}$ (**A**) and $\delta^{13}\text{C}$ (**B**) against the nutrient input index (NI). Triangles represent populations from the Abra system, while circles represent populations from the Guatemala system.

levels (Vander-Zanden and Rasmussen 1999; Post 2002), suggesting that cavefish trophic levels may be similar in different caves. However, the isotopic signal of a consumer alone is generally insufficient to accurately infer trophic position without an appropriate isotopic baseline, typically comprising primary producers and primary consumers (potential prey) (Vander-Zanden and Rasmussen 1999; Post 2002). Differences in $\delta^{15}\text{N}$ and $\delta^{13}\text{C}$ among caves within the same region may reflect variations in the trophic resource availability, local ecological processes such as differences in trophic networks or environmental conditions in each cave, and the differential use of habitats or resources by local populations (Wilson et al. 2021). On the other hand, the differences observed between the Sierra de El Abra and Sierra de Guatemala regions could be linked to divergence processes among lineages driven by evolutionary history, geographic isolation, or ecological landscape differences that affect resource availability and trophic interactions. Together, these findings suggest that local ecological processes, such as resource availability and the structure of trophic networks, can be as influential as geographic or evolutionary factors in driving the observed isotopic variation.

Previous studies have reported that *A. mexicanus* cavefish primarily feed on detritus in pools but are also active predators, particularly during the early stages of

their life when they mainly consume microcrustaceans, isopods, and arthropods (Espinasa et al. 2017). It is suggested that active predation during the juvenile stage allows them to feed adequately until adulthood (Espinasa et al. 2017). However, during multiple expeditions across a year, these fish have also been observed to be opportunistic feeders, consuming animals that fall into the pools, such as arthropods, fish, and detritus, which could explain the variation in $\delta^{15}\text{N}$ among populations (Wilson et al. 2021). Moreover, studies of the stomach microbiome in cave populations have suggested that these cavefish may exhibit omnivorous habits (Ornelas-García et al. 2018). Other cave vertebrates like the cave salamander *Eurycea spelaea* feed on bat guano, providing nutritional value comparable to potential invertebrate prey (Fenolio et al. 2006), for the *A. mexicanus*, bat guano has been suggested as a food source (Espinasa et al. 2017). Therefore, while our findings are insightful, future studies should consider examining the entire trophic network or corroborating isotopic signals with stomach content analysis.

The $\delta^{13}\text{C}$ signal helps us understand the diversity of carbon sources within the trophic network (Bearhop et al. 2004; Layman and Post 2008; Jackson et al. 2011). Our results showed slight variations in the $\delta^{13}\text{C}$ signal, ranging from -29.8‰ in Montecillos to -24.7‰ in Escondido. These values are similar to those reported for plant material in other anchialine karst systems ($\delta^{13}\text{C} = -35\text{‰}$ to -25‰ , Brankovits et al. 2017), but differ from those associated with methanotrophic bacteria ($\delta^{13}\text{C} = -75\text{‰}$ to -45‰ ; Brankovits et al. 2017; Chavéz-Solis et al. 2020). Based on this, we can infer that the primary source of carbon in these caves is plant material originated from the surface, even in the deepest caves such as Vásquez ($\delta^{13}\text{C} = -26.76\text{‰}$, depth = 270 m). In these cases, the decomposing plant material may be part of the fish diet or the diet of primary consumers, which in turn could be prey for *Astyanax* cavefish. That said, we acknowledge that other primary sources of carbon may exist for subterranean foodwebs (e.g., DOC and POC percolating from the surface, and microbial biomass) (Pacioglu et al. 2023) which could be contributing to observed *Astyanax* isotopic values. Given the nature of our sampling scheme, we were not able to isolate individual sources. It would be interesting to separate these sources and contrast their importance among cave systems; such effort will require a much different sampling approach to what we were able to apply in our investigation. Additionally, it is important to consider that our results could be affected by seasonality, as has been reported in previous trophic studies in *Astyanax* cavefish (Wilson et al. 2021).

Trophic niche analysis based on Layman's metrics revealed that the Sierra de El Abra had a broader total niche area and lower trophic redundancy compared to the Sierra de Guatemala system. This metric is commonly used to quantify the ecological niche occupied by a population and is related to trophic diversity (Bearhop et al. 2004; Layman and Post 2008; Jackson et al. 2011). According to our results, the Palma Seca cave population in the Sierra de El Abra system had the highest total niche area (6.10), in contrast to the Vásquez population in the Sierra de Guatemala system, which had the lowest value (0.42) and is the deepest cave of the study. Moreover, Vásquez also exhibited the lowest standard deviation in the trophic niches values among individu-

als (SDNND = 0.22), which indicates higher trophic redundancy and, consequently, more intense competition for resources within the population (Bearhop et al. 2004; Layman and Post 2008; Jackson et al. 2011). This can be explained by the fact that in deeper caves (DC), it is more difficult for allochthonous material to reach the pools.

The negative and significant relationship between $\delta^{13}\text{C}$ and the NI index is consistent with the idea that the deeper the cave, the more difficult it is for plant sources to enter from the surface. Although no significant relationship was found for $\delta^{15}\text{N}$, the trend suggests that caves with shallower depths and shorter distances from the basin entrance may support more complex trophic networks. Habitats close to the entrance of caves, where access to resources is easier, typically have higher biodiversity (Simões et al. 2015). Larger caves have greater zonation and may also exhibit high diversity, with different organisms highly specialized for troglobitic life inhabiting each zone (Ferreira 2000; Souza-Silva et al. 2011; Simões et al. 2015; Culver and Pipan 2019b).

Based on these observations, we propose that the influx of allochthonous material significantly influences the trophic ecology dynamics within each cave. This influx is driven by factors such as the transport of plant material by water currents, rainwater percolation, and the ease with which fauna can access the cave (White and Culver 2019). This is reflected in the NI index obtained, with positive NI index values in Montecillos and Palma Seca in the Sierra de El Abra system, and Molino and Caballo Moro in the Sierra de Guatemala system. Conversely, caves with negative NI index values, such as Yerbaniz, Escondido, and Vásquez, differ on attributes such as size, distance from the entrance to the pool, and depth. Additionally, nutrient input may come directly from groundwater. In this sense, the NI index suggested in the present study represents a pioneer metric to estimate the trophic ecology in the cave systems, thus, this index can be useful for indirectly describing the trophic ecology of cave systems. To corroborate this, it would be necessary to conduct a more exhaustive study of the trophic networks, incorporating direct measurements of resource inputs and analyses of other cave systems. However, we consider this a promising approach to infer the intensity of selective pressures on the organisms inhabiting these systems, based on the geomorphology of karst systems as a whole.

Additionally, both geographic regions have complex hydrological patterns that could allow interconnection between different caves (Elliott 2018). These patterns may also be influenced by seasonal changes, such as the rainy season, when the water levels of external aquatic bodies rise, as reported for other tropical caves (Souza-Silva et al. 2011; Simões et al. 2015). Furthermore, in the future we could evaluate the season differences in organic matter and its influence in the trophic ecology variation of cavefish of *A. mexicanus*.

Conclusion

The isotopic signals of $\delta^{15}\text{N}$ and $\delta^{13}\text{C}$ revealed differences among the analyzed caves, suggesting that each cave may have distinct nutrient cycle dynamics. Layman's metrics indicated that populations in the Sierra de El Abra system occupy a larger trophic niche area with lower trophic redundancy compared to those in Sierra de Guatemala system.

Despite variations in $\delta^{15}\text{N}$ values, our results suggest that the trophic level among the *Astyanax* cavefish populations is the same. Additionally, the isotopic signals appear to be influenced by geomorphological characteristics of caves, such as depth and distance from the entrance to the pool, which may directly affect nutrient input in each cave.

Acknowledgements

We sincerely thank María Ángeles Verde, Ulises Rivera Arroyo, Lorenzo Ortis Armas, Dalía Zaragoza Guzmán, Oscar Baeza Blancas, and Carlos Pedraza Lara for their assistance with sampling. We also want to thank Roberto Munguía Steyer for his observations and recommendations in the early draft.

This research was supported by Project No. 191986, Fronteras de la Ciencia – CONACyT and the Programa de Apoyo a Proyectos de Investigación e Innovación Tecnológica (PAPIIT), UNAM No. IN212419. JHL received a postgraduate scholarship from the Programa Nacional de Posgrados de Calidad (PNPC), a program sponsored by CONACyT.

References

- AMCS [Association for Mexican Cave Studies] (2022) A Project of the National Speleological Society. <http://www.mexicancaves.org/maps/> [Accessed on 10.02.2022]
- Bearhop S, Adams CE, Waldron S, Fuller RA, Macleod H (2004) Determining trophic niche width: A novel approach using stable isotope analysis. *Journal of Animal Ecology* 73(5): 1007–1012. <https://doi.org/10.1111/j.0021-8790.2004.00861.x>
- Boecklen WJ, Yarnes CT, Cook BA, James AC (2011) On the use of stable isotopes in trophic ecology. *The Annual Review of Ecology, Evolution, and Systematics* 42(4): 11–40. <https://doi.org/10.1146/annurev-ecolsys-102209-144726>
- Borowsky RL (2018) Cavefishes. *Current Biology* 28(2): 60–64. <https://doi.org/10.1016/j.cub.2017.12.011>
- Brand WA, Coplen TB (2012) Stable isotope deltas: tiny, yet robust signatures in nature. *Isotopes in Environmental and Health studies* 48(3): 393–409. <https://doi.org/10.1080/10256016.2012.666977>
- Brankovits D, Pohlman JW, Niemann H, Leigh MB, Leewis MC, Becker KW, Iliffe TM, Alvarez F, Lehmann MF, Phillips B (2017) Methane-and dissolved organic carbon-fueled microbial loop supports a tropical subterranean estuary ecosystem. *Nature Communications* 8(1): 1835. <https://doi.org/10.1038/s41467-017-01776-x>
- Chávez-Solís EM, Solís C, Simões N, Mascaró M (2020) Distribution patterns, carbon sources and niche partitioning in cave shrimps (Atyidae: Typhlatya). *Scientific Reports* 10(1): 1–16. <https://doi.org/10.1038/s41598-020-69562-2>
- Córdova-Tapia F, Zambrano L (2016) Fish functional groups in a tropical wetland of the Yucatan Peninsula, Mexico. *Neotropical Ichthyology* 14(2): e150162. <https://doi.org/10.1590/1982-0224-20150162>

- Cucherousset JS, Bouletreau A, Martino JM, Roussel FS (2012) Using stable isotope analyses to determine the ecological effects of non-native fishes. *Fisheries Management and Ecology* 19: 111–119. <https://doi.org/10.1111/j.1365-2400.2011.00824.x>
- Culver DC, Pipan T (2019a) Sources of Energy in Subterranean Environments. In: Culver. DC, Pipan T (Eds) *The Biology of Caves and Other Subterranean Habitats*. Biology of Habitats Series. UK: Oxford University Press, 24–42. <https://doi.org/10.1093/oso/9780198820765.003.0002>
- Culver DC, Pipan T (2019b) Colonization and Speciation in Subterranean Environments. In: Culver. DC, Pipan T (Eds) *The Biology of Caves and Other Subterranean Habitats*. Biology of Habitats Series. UK: Oxford University Press, 147–178. <https://doi.org/10.1093/oso/9780198820765.003.0007>
- Dytham C (2011) *Choosing and using statistics: a biologist's guide*. John Wiley & Sons. Wiley Publishers, UK, 320 pp.
- Dunn OJ (1961) Multiple Comparisons among Means. *Journal of the American Statistical Association* 56(293): 52–64. <https://doi.org/10.1080/01621459.1961.10482090>
- Dunne JA, Williams RJ, Martinez ND (2002) Food-web structure and network theory: the role of connectance and size. *PNAS* 99: 12917–12922. <https://doi.org/10.1073/pnas.192407699>
- Elipot Y, Hinaux H, Callebert J, Rétaux, S (2013) Evolutionary shift from fighting to foraging in blind cavefish through changes in the serotonin network. *Current Biology* 23: 1–10. <https://doi.org/10.1016/j.cub.2012.10.044>
- Elliot WR (2018) *The Astyanax caves of México: cavefish of Tamaulipas, San Luis Potosí and Guerrero* (First). Association for Mexican Cave Studies, 325 pp.
- Engel AS (2019) Microbes. In: White BW, Culver DC (Eds) *Encyclopedia of Caves*. Academic Press of Elsevier, 490–499. <https://doi.org/10.1016/B978-0-12-814124-3.00083-2>
- Espinasa L, Espinasa M (2016) Hydrogeology of Caves in the Sierra de El Abra Region. In: Keene AC, Yoshizawa M, McGaugh SE (Eds) *Biology and Evolution of the Mexican Cavefish*. Academic Press, San Diego, USA, 1–5. <https://doi.org/10.1016/B978-0-12-802148-4.00002-5>
- Espinasa L, Bonaroti N, Wong J, Pottin K, Queinnec E, Rétaux S (2017) Contrasting feeding habits of post-larval and adult *Astyanax* cavefish. *Subterranean Biology* 21(1): 1–17. <https://doi.org/10.3897/subtbiol.21.11046>
- Fenolio DB, Graening GO, Collier BA, Stout JF (2006) Coprophagy in a cave-adapted salamander; the importance of bat guano examined through nutritional and stable isotope analyses. *Proceedings of the Royal Society B: Biological Sciences* 273(1585): 439–443. <https://doi.org/10.1098/rspb.2005.3341>
- Ferreira RL, Martins RP, Yanega D (2000) Ecology of bat guano arthropod communities in a Brazilian dry cave. In *Ecotropica* 6(2): 105–116.
- Fong DW (2019) Food sources. In: Culver. DC, Pipan T (Eds) *The Biology of Caves and Other Subterranean Habitats*. Biology of Habitats Series. UK: Oxford University Press, 429–434. <https://doi.org/10.1016/B978-0-12-814124-3.00051-0>
- Gary M, Sharp JM (2006) Volcanogenic karstification of Sistema Zacatón, Mexico (Vol. 404, 79–79). *Special Papers-Geological Society of America*. [https://doi.org/10.1130/2006.2404\(08\)](https://doi.org/10.1130/2006.2404(08))
- Goudie A (2003) *Geomorphological techniques*. Routledge. London, UK, 592 pp. <https://doi.org/10.4324/9780203430590>

- Hernández-Lozano J, Garita-Alvarado CA, Munguía-Steyer R, Garduño-Sánchez M, Ornelas-García CP (2024) Parallel phenotypic evolution of two independent cavefish lineages of *Astyanax mexicanus* (De Filippi, 1854) (Characiformes: Characidae). *Biological Journal of the Linnean Society* 2024: blae059. <https://doi.org/10.1093/biolinnean/blae059>
- Howarth FG (1983) Ecology of cave arthropods. *Annual Review of Entomology* 28: 365–389. <https://doi.org/10.1146/annurev.en.28.010183.002053>
- Howarth FG, Moldovan OT (2018) The ecological classification of cave animals and their adaptations. In: Moldovan OT, Kováč L, Halse S (Eds) *Cave ecology*. Springer Nature, Switzerland, 41–67. https://doi.org/10.1007/978-3-319-98852-8_4
- Jackson AL, Inger R, Parnell AC, Bearhop S (2011) Comparing isotopic niche widths among and within communities: SIBER - Stable Isotope Bayesian Ellipses in R. *Journal of Animal Ecology* 80(3): 595–602. <https://doi.org/10.1111/j.1365-2656.2011.01806.x>
- Jeffery WR (2009) Regressive evolution in *Astyanax* cavefish. *Annual review of genetics* 43(1): 25–47. <https://doi.org/10.1146/annurev-genet-102108-134216>
- Keene AC, Duboue ER (2018) The origins and evolution of sleep. *Journal of Experimental Biology* 221(11): jeb159533. <https://doi.org/10.1242/jeb.159533>
- Keene AC, Duboue ER, Foulkes NS, Bertolucci C (2024) Evolved Loss of Sleep and Circadian Rhythms in Cavefish. In: Gehrman P, Keene AC, Grant, SF (Eds) *Genetics of Sleep and Sleep Disorders*. Cham: Springer International Publishing, 133–157. https://doi.org/10.1007/978-3-031-62723-1_5
- Kováč L (2018) Caves as Oligotrophic Ecosystems. In: Moldovan OT, Kováč L, Halse S (Eds) *Cave Ecology*. Springer International Publishing, 297–308. https://doi.org/10.1007/978-3-319-98852-8_13
- Layman CA, Post DM (2008) Can stable isotope ratios provide for community-wide measures of trophic structure? reply. *Ecology* 89(8): 2358–2359. <https://doi.org/10.1890/08-0167.1>
- McGaugh SE, Gross JB, Aken B, Blin M, Borowsky R, Chalopin D, Hinaux H, Jeffery WR, Keene A, Ma L, Minx P, Murphy D, O’Quin KE, Rétaux S, Rohner N, Searle SMJ, Stahl BA, Tabin C, Volf JN, Yoshihawa M, Warren WC (2014) The cavefish genome reveals candidate genes for eye loss. *Nature Communications* 5(1): 5307. <https://doi.org/10.1038/ncomms6307>
- Miranda-Gamboa R, Espinasa L, de los Angeles Verde-Ramírez M., Hernández-Lozano J, Lacaille JL, Espinasa M, & Ornelas-García CP (2023) A new cave population of *Astyanax mexicanus* from Northern Sierra de El Abra, Tamaulipas, México. *Subterranean Biology* 45: 95–117. <https://doi.org/10.3897/subtbiol.45.98434>
- Moldovan OT, Kováč L, Halse S (2018) Preamble. In: Moldovan OT, Kováč L, Halse S (Eds) *Cave Ecology* (Vol. 235, 1–5). Springer International Publishing. <https://doi.org/10.1007/978-3-319-98852-8>
- Ornelas-García CP, Pedraza-Lara C (2015) Phylogeny and evolutionary history of *Astyanax mexicanus*. In: Keene AC, Yoshizawa M, McGaugh SE (Eds) *Biology and Evolution of the Mexican Cavefish*. Academic Press, San Diego, USA, 77–90. <https://doi.org/10.1016/B978-0-12-802148-4.00004-9>
- Ornelas-García CP, Domínguez-Domínguez O, Doadrio I (2008) Evolutionary history of the fish genus *Astyanax* baird & Girard (1854) (Actinopterygii, Characidae) in mesoamerica reveals multiple morphological homoplasies. *BMC Evolutionary Biology* 8(340): 1–17. <https://doi.org/10.1186/1471-2148-8-340>

- Ornelas-García CP, Córdova-Tapia F, Zambrano L, Bermúdez-González MP, Mercado-Silva N, Mendoza-Garfias B, Bautista A (2018) Trophic specialization and morphological divergence between two sympatric species in Lake Catemaco, Mexico. *Ecology and Evolution* 8(10): 4867–4875. <https://doi.org/10.1002/ece3.4042>
- Pacioglu O, Tuşa IM, Popa I, Içtuş C, Plăvan G, Boufahja F, Baba ŞC (2023) Aquatic subterranean food webs: a review. *Global Ecology and Conservation* 48: e02704. <https://doi.org/10.1016/j.gecco.2023.e02704>
- Peterson BJ, Fry B (1987) Stable isotopes in ecosystem studies. *Annual Review of Ecology and Systematics* 18: 293–320. <https://doi.org/10.1146/annurev.es.18.110187.001453>
- Pilger TJ, Gido KB, Propst DL (2010) Diet and trophic niche overlap of native and nonnative fishes in the Gila River, USA: implications for native fish conservation. *Ecology of Freshwater Fish* 19: 300–321. <https://doi.org/10.1111/j.1600-0633.2010.00415.x>
- Post DM (2002) Using stable isotopes to estimate trophic position: models, methods, and assumptions. *Ecology* 83: 703–718. [https://doi.org/10.1890/0012-9658\(2002\)083\[0703:USITE T\]2.0.CO;2](https://doi.org/10.1890/0012-9658(2002)083[0703:USITE T]2.0.CO;2)
- Poulson TL, Lavoie KH (2000) The trophic basis of subsurface ecosystems. In: Wilkens H, Culver DC, Halse S (Eds) *Subterranean ecosystems* (First, 231–249). Academic Press of Elsevier.
- Pozo-Morales M, Cobham AE, Centola C, McKinney MC, Liu P, Perazzol C, Singh SP (2024) Starvation-resistant cavefish reveal conserved mechanisms of starvation-induced hepatic lipotoxicity. *Life Science Alliance* 7(5): e202302458. <https://doi.org/10.26508/lsa.202302458>
- Romero A (2009) *Cave Biology: Live in Darkness*. Cambridge University Press. <https://doi.org/10.1017/CBO9780511596841>
- R Core Team (2023) *R: A Language and Environment for Statistical Computing*. R.
- Rouch R (1987) Sur l'écologie des eaux souterraines dans la karst. *Stygologia* 2(4).
- Sarbu SM, Kane TC, Kinkel BF (1996) A chemoautotrophically based cave ecosystem. *Science* 272: 5270. <https://doi.org/10.1126/science.272.5270.1953>
- Secretaría de Agricultura, Ganadería y Desarrollo Rural (1995) NOM-051-ZOO-1995. NORMA Oficial Mexicana. Trato humanitario en la movilización de animales.
- Simões MH, Souza-Silva M, Ferreira RL (2015) Cave physical attributes influencing the structure of terrestrial invertebrate communities in Neotropics. *Subterranean Biology* 16: 103–121. <https://doi.org/10.3897/subtbiol.16.5470>
- Simon KS (2019) Cave ecosystems. In: White BW, Culver DC (Eds) *Encyclopedia of Caves* (Third, 99–103). Academic Press of Elsevier. <https://doi.org/10.1016/B978-0-12-383832-2.00015-3>
- Simon KS, Benfield EF, Macko SA (2003) Food web structure and the role of epilithic films in cave streams. *Ecology* 84(9): 2395–2406. <https://doi.org/10.1890/02-334>
- Schneider CA, Rasband WS, Eliceiri KW (2012) NIH Image to ImageJ: 25 years of image analysis. *Nature methods* 9(7): 671–675. <https://doi.org/10.1038/nmeth.2089>
- Souza-Silva M, Martins RP, Ferreira RL (2011) Trophic dynamics in a neotropical limestone cave. *Subterranean Biology* 9(1): 127–138. <https://doi.org/10.3897/subtbiol.9.2515>
- Vander-Zanden MJ, Rasmussen JB (1999) Primary consumer ($\delta^{13}\text{C}$) and ($\delta^{15}\text{N}$) and the trophic position of aquatic consumers. *Ecology* 80(4): 1395–1404. [https://doi.org/10.1890/0012-9658\(1999\)080\[1395:PCCANA\]2.0.CO;2](https://doi.org/10.1890/0012-9658(1999)080[1395:PCCANA]2.0.CO;2)

- Venarsky MP, Huntsman BM (2018) Food webs in Caves. In: Moldovan OT, Kováč E, Halse S (Eds) Cave Ecology. Springer International Publishing, 309–328. https://doi.org/10.1007/978-3-319-98852-8_14
- Wilson EJ, Tobler M, Riesch R, Martínez-García L, García-De León FJ (2021) Natural history and trophic ecology of three populations of the Mexican cavefish, *Astyanax mexicanus*. Environmental Biology of Fishes 104: 1461–1474. <https://doi.org/10.1007/s10641-021-01163-y>
- White BW, Culver DC (2019) Cave, Definition of. In: White BW, Culver DC (Eds) Encyclopedia of Caves (Third, 103–107). Academic Press of Elsevier. www.elsevier.com

Supplementary material 1

Supporting data

Authors: Jorge Hernández-Lozano, Fernando Córdova-Tapia, Ramses Miranda-Gamboa, María de Lourdes Vázquez-Cruz, Carlos Garita-Alvarado, Norman Mercado-Silva, Claudia Patricia Ornelas-García

Data type: xlsx

Explanation note: **table S1**. Topographic information and maps used in this study.
table S2. Geomorphologic data and Nutrient Input Index values for each cave for this study.

Copyright notice: This dataset is made available under the Open Database License (<http://opendatacommons.org/licenses/odbl/1.0/>). The Open Database License (ODbL) is a license agreement intended to allow users to freely share, modify, and use this Dataset while maintaining this same freedom for others, provided that the original source and author(s) are credited.

Link: <https://doi.org/10.3897/subtbiol.51.140856.suppl1>

Supplementary material 2

SEA_B analysis of Layman's metrics for the two geographic regions, Sierra de El Abra and Sierra de Guatemala, plotted as a boxplot.

Authors: Jorge Hernández-Lozano, Fernando Córdova-Tapia, Ramses Miranda-Gamboa, María de Lourdes Vázquez-Cruz, Carlos Garita-Alvarado, Norman Mercado-Silva, Claudia Patricia Ornelas-García

Data type: docx

Copyright notice: This dataset is made available under the Open Database License (<http://opendatacommons.org/licenses/odbl/1.0/>). The Open Database License (ODbL) is a license agreement intended to allow users to freely share, modify, and use this Dataset while maintaining this same freedom for others, provided that the original source and author(s) are credited.

Link: <https://doi.org/10.3897/subtbiol.51.140856.suppl2>

On the troglobitic velvet worm *Speleoperipatus spelaeus* Peck, 1975 (Onychophora, Peripatidae): assessing the status of a Critically Endangered Jamaican invertebrate

Gonzalo Giribet¹, Pooja A. Anilkumar², Abbio Goodwin³, Ronald S. Stewart⁴,
Claud A. Watkis⁵, Damion Whyte³, Gustavo Hormiga²

1 Museum of Comparative Zoology & Department of Organismic and Evolutionary Biology, Harvard University, 26 Oxford Street, Cambridge, MA 02138, USA **2** Department of Biological Sciences, The George Washington University, 2029 G St. NW, Washington, DC, 20052, USA **3** Department of Life Sciences, University of the West Indies, Mona, Kingston, Jamaica **4** The Jamaican Caves Organisation, Ewarton, St. Catherine, Jamaica **5** Public Broadcasting Corporation of Jamaica, Kingston, Jamaica

Corresponding author: Gonzalo Giribet (ggiribet@g.harvard.edu)

Academic editor: Fabio Stoch | Received 21 February 2025 | Accepted 6 March 2025 | Published 24 March 2025

<https://zoobank.org/A8BB6BD3-FE66-4797-9C92-34E8205262FC>

Citation: Giribet G, Anilkumar PA, Goodwin A, Stewart RS, Watkis CA, Whyte D, Hormiga G (2025) On the troglobitic velvet worm *Speleoperipatus spelaeus* Peck, 1975 (Onychophora, Peripatidae): assessing the status of a Critically Endangered Jamaican invertebrate. Subterranean Biology 51: 49–59. <https://doi.org/10.3897/subtbiol.51.151034>

Abstract

The velvet worm *Speleoperipatus spelaeus* Peck, 1975 is one of the rarest velvet worm species reported, as it is only known from its type locality, Pedro Great Cave, Clarendon Parish, Jamaica. The type material of the species, the only four specimens available in known scientific collections, was obtained in the early 1970's, and since then, no additional specimens have been available for research. More recently, observations of three probably conspecific specimens by the Jamaican Caves Organisation, not collected, have been made in a different location, Swansea Cave, Saint Catherine Parish. Here we report and document five specimens of this rare species from the type locality, Pedro Great Cave, as well as some observations about their behavior. Placing this species in a phylogenetic context should be attempted in the future, to better understand the significance of *Speleoperipatus spelaeus* and its evolutionary origins, its relationship to the Swansea Cave specimens, and to determine what are its closest relatives and whether those are other Jamaican species or velvet worms from other geographical areas.

Keywords

Cave biogeography, Jamaican caves, Jamaican endemics, Onychophora, Terrestrial invertebrates, troglobiont

Introduction

Jamaica is the third largest island in the Caribbean, with limestone of Eocene age exposed over two thirds of the island, forming extensive karst systems (Brown and Ford 1973) with numerous caves and sinkholes (Fincham 1997) that are home to numerous troglobitic endemics. After Cuba, Jamaica has the richest known diversity of cave faunas on any island in the West Indies (Peck 1992). Velvet worms (the members of the phylum Onychophora) are mysterious terrestrial invertebrates best known for their velvety appearance and their unique mode of prey capture by shooting a stream of glue from their oral papillae (Guilding 1826; Read and Hughes 1987) (see Fig. 1). From the 232 currently accepted extant species (Oliveira 2023), many are considered short-range endemics (Harvey 2002), and only two are restricted to cave environments. Due to their restricted habitats, poor dispersal ability, and limited distribution, onychophorans have emerged as a model invertebrate taxon for conservation priority (Mesibov and Ruhberg 1991; New 1995; Hamer et al. 1997; Sosa-Bartuano et al. 2018; Trewick et al. 2018). Indeed, one of the few invertebrates supposedly extinct in a continental landmass is the Lion's Hill velvet worm, *Peripatopsis leonina* Purcell, 1899, from the Cape Peninsula in South Africa. This species has no known records subsequent to the early 1900's, as it inhabited an area that underwent substantial habitat change, including the development of recreational areas, the planting of pine forests, and the building of houses (Hamer et al. 1997).

Amongst the least known velvet worms are those that inhabit extreme environments, especially cave systems. These few velvet worm species may display typical troglobitic adaptations, specifically a lack of pigmentation, blindness, and a certain degree of appendage elongation. Tasmania has a non-troglobitic species that is blind and depigmented, *Leucopatus anophthalmus* (Ruhberg, Mesibov, Briscoe & Tait, 1991), a species of conservation interest (Mesibov and Ruhberg 1991). Blindness is also characteristic of the Indian species *Typhloperipatus williamsoni* (Kemp, 1914) from the foothills of the Himalayas. The South African *Opisthopatus camdebooii* Barnes & Daniels, 2022 is lightly pigmented, a near-surface-dwelling velvet worm species with a sunken and unpigmented eye, probably associated with an underground mode of life (Barnes and Daniels 2022). There is also a velvet worm species inhabiting a lava tube cave on the island of Santa Cruz, Galapagos, but this species has no obvious troglomorphic features, and it has also been found on surface environments (Espinasa et al. 2015). This unnamed species is closely related to *Oroperipatus eisenii* (Wheeler, 1898) from Mexico (Giribet et al. 2018), and how it arrived to Galapagos remains unanswered.

Only two true troglobiont velvet worm species are known, one for each of the two velvet worm families, Peripatidae and Peripatopsidae. Within the latter family, *Peripatopsis alba* Lawrence, 1931, was described based on two specimens collected in Table Mountain caves (Lawrence 1931), more specifically the Wynberg and Bat Cave systems of Table Mountain (Sharratt et al. 2000; Giribet et al. 2013; Lopes Ferreira et

al. 2020; Barnes and Daniels 2022), and the species has been found only a few times after its original discovery, including once by one of the authors of this note (GG). *Peripatopsis alba* is considered an exceptionally rare species and is classified as Vulnerable (V) on the IUCN Red List, as it occupies deep sections of the two cave systems on the Cape Peninsula, where it can be found on or under rocks.

Jamaica, like many other Antillean islands, is home to velvet worms, five in this case, all belonging to family Peripatidae, which Gosse (1851) considered “the greatest curiosity” of his many discoveries in his Naturalist’s Soujourn in Jamaica. But the first Jamaican velvet worm was not formally described for nearly half a century, when *Peripatus jamaicensis* Grabham & Cockerell, 1892 (now *Plicatoperipatus jamaicensis*) was published. This was followed by the description of three other species in three additional genera: *Peripatus swainsonae* Cockerell, 1893, *Epiperipatus lewisi* Arnett, 1961, and *Macroperipatus clarki* Arnett, 1961 (Grabham and Cockerell 1892; Grabham 1893; Arnett 1961). Jamaican onychophorans certainly raised awareness among local and visiting scientists and natural historians (e.g. Duerden 1901; Barbour 1910; Andrews 1912, 1933; Lynn 1936). But perhaps the greatest hit for the Jamaican onychophorans was the discovery of the second troglobitic velvet worm species, *Speleoperipatus spelaeus* Peck, 1975, by cave biologist Stewart B. Peck after a series of speleological expeditions to Jamaica in the 1970’s. This species was described based on four specimens from Pedro Great Cave (now Pedro Cave), Clarendon Parish, one collected on December 20th, 1972 (leg., S.B. Peck), one on March 25th, 1973 (leg., R. Norton & R. Zimmerman), and two on August 17th, 1974 (leg., S.B. Peck & family) (Peck 1975a, 1975b). No specimen has been reported from Pedro Cave since the last collection in 1974, and thus, *S. spelaeus* has since been considered among the rarest animals in Jamaica.

Results and discussion

Speleological research in Jamaica has flourished in the past two decades since the founding of the Jamaican Caves Organisation (JCO) by co-author RSS. This has led to the discovery, at Swansea Cave, Saint Catherine Parish, of one specimen of a blind, depigmented velvet worm observed on February 13th, 2010 and two additional specimens photographed on November 6th, 2021 (Fig. 1). These specimens remain unstudied, as no collection was conducted.

The two cave systems, Pedro and Swansea, are relatively close, separated by less than 6 km of linear distance through an area with numerous known caves (Fig. 2).

Driven by the discovery of additional specimens of blind, depigmented velvet worms in Swansea Cave by the JCO 36 years after *S. spelaeus* was last seen at Pedro Cave, and as part of ongoing research on Jamaican velvet worm diversity and systematics, a team of speleologists from Jamaica and foreign researchers returned to Pedro Cave in search of the elusive Jamaican blind velvet worm, currently listed as Critically Endangered (CE) by the IUCN (New 1996).



Figure 1. Swansea Cave specimen with prey (photographed on November 6th, 2021. Photos by J. Pael (JCO).

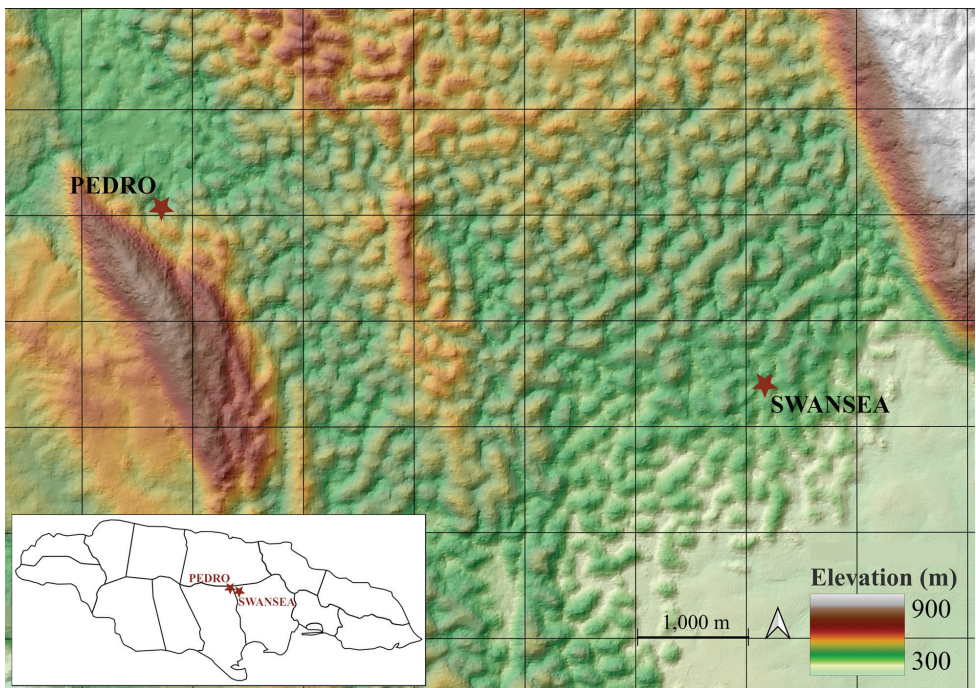


Figure 2. Map of the area from Pedro Cave to Swansea Cave.

The team of six researchers/crew explored Pedro Cave on January 18th, 2025, to assess the status of *S. spelaeus*—a species that had not been observed in this cave since 1974, and that was only known based on the four specimens from this cave studied by Peck (1975b), and by the observation of three specimens, probably

conspecific, from Swansea Cave by the JCO (Fig. 1). We searched the different sections of Pedro Cave and documented some of the fauna present in each section, which included, among other, a rare Opiliones in the family Zalmoxidae, *Ethobunus goodnighti* (Rambla, 1969), known from two specimens collected by S. B. Peck in 1968 in St. Clair Cave, St. Catherine Parish (Rambla 1969), and not documented since. The identified cave fauna includes non-adapted species, such as the Jamaican rock frog *Eleutherodactylus cundalli* Dunn, 1926 as well as some synanthropic species, such as *Oxidus gracilis* (C. L. Koch, 1847) (Myriapoda, Diplopoda, Paradoxosomatidae), abundant deep into the cave, the American cockroach *Periplaneta americana* (Linnaeus, 1758) (Insecta, Blattodea, Blattidae), as well as the cane toad *Rhinella marina* (Linnaeus, 1758) (Amphibia, Anura, Bufonidae), found ca. 200 meters from the entrance of the cave. Among the cave-adapted fauna, there were four bat species: the Jamaican fruit bat, *Artibeus jamaicensis* Leach, 1821; Leach's single leaf bat *Monophyllus redmani* Leach, 1821; the Antillean ghost-faced bat *Mormoops blainvillei* Leach, 1821; and MacLeay's mustached bat *Pteronotus macleayii* (Gray, 1839). The cave also hosts a number of arthropods, including the abundant spider *Gaucelmus cavernicola* (Petrunkevitch, 1910) (Araneae, Synotaxidae), three other spider species (including one Scytodidae, one Ctenidae, *Ctenus* cf. *catherine* Polotow & Brescovit, 2012, and one small mygalomorph), a whip-spider in the genus *Phrynus* closely resembling *P. levii* Quintero, 1981 (Amblypygi, Phrynidae), the extremely abundant cricket *Uvaroviella cavicola* Chopard, 1923 (Insecta, Orthoptera, Phalangopsidae), and an unidentified depigmented cockroach species (Fig. 3).

The Pedro Cave entrance was followed by the Belfry bifurcation and Bat Hall (Fig. 4). These areas showed abundant populations of bats, crickets, and the spider *Gaucelmus cavernicola*, although the whip-spider and ctenid spider species were also relatively abundant. *Gaucelmus cavernicola* is a common endemic Jamaican troglophile, recorded in numerous caves throughout at least ten Parishes (Peck 1975a; Gertsch 1984; Peck 1992). No velvet worms were located in these areas during this expedition or a prior exploration in 2024. A narrow passage then led to the Three Ways of the cave, where most of Peck velvet worm specimens had been located. It was in this section where several individuals of *S. spelaeus* were found walking on bat guano accumulated on top of a layer of clay (Fig. 5). Bat guano can be extremely variable, providing numerous microhabitats differentiated by fluctuating temperature, moisture, and pH (Bogdanowicz et al. 2020), and is considered one of the four cave ecosystems (Richards 2009). In the case of a predatory species like velvet worms, guano probably attracts possible prey. Five individuals were observed and photographed on or near the guano deposits with some running water from the cave roof, but the specimens were not properly measured to avoid specimen manipulation. One specimen quickly retreated into the crevices of a porous rock upon discovery, and another one buried itself in a clump of mud until it disappeared completely. This clearly indicates that the cave offers numerous hiding places for the velvet worms.

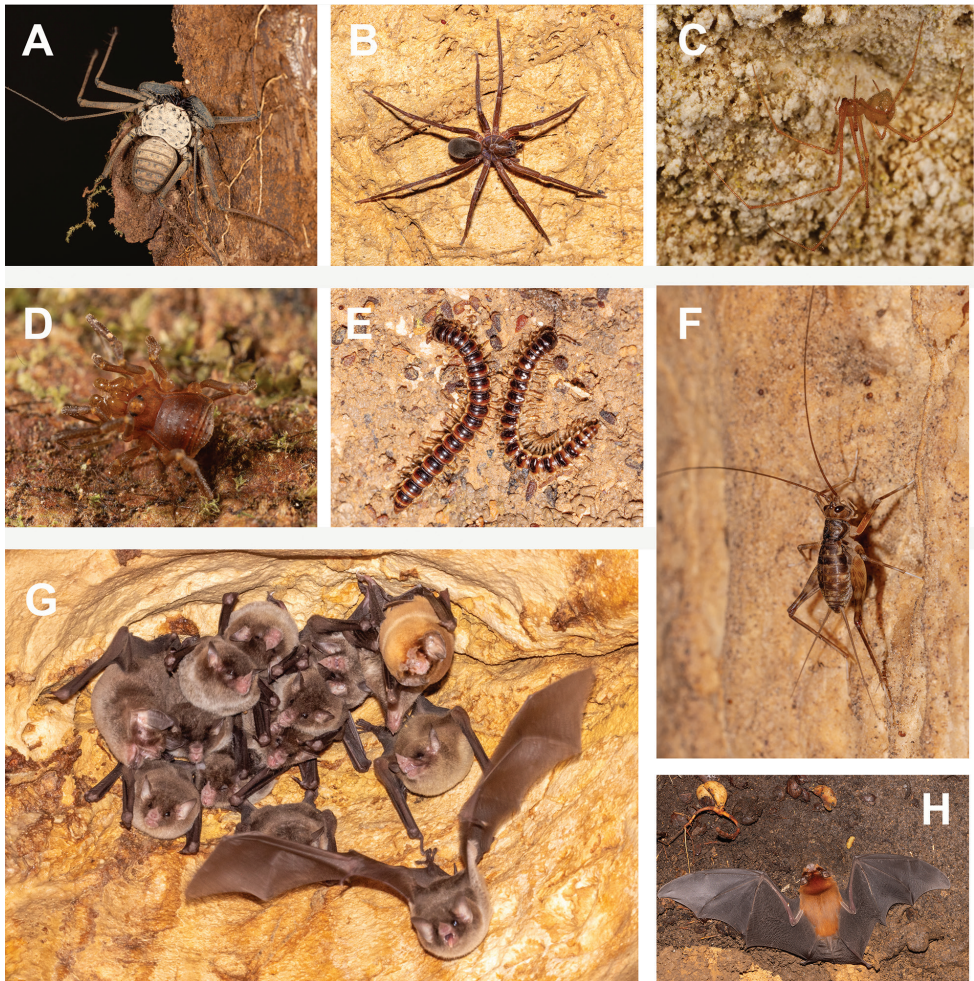


Figure 3. Examples of associated fauna found at Pedro Cave **A** *Phrynus* sp. (Chelicerata, Amblypygi) **B** *Ctenus* cf. *catherine* (Chelicerata, Araneae) **C** *Gaucelmus cavernicola* (Chelicerata, Araneae) **D** *Ethobunus goodnighti* (Chelicerata, Opiliones) **E** *Oxidus gracilis* (Myriapoda, Diplopoda) **F** *Uvaroviella cavicola* (Insecta, Orthoptera) **G** *Monophyllus redmani* and one *Mormoops blainvillei* (Mammalia, Chiroptera) **H** *Mormoops blainvillei* (Mammalia, Chiroptera). Photos **A, B, D–H** by G. Giribet; **C** by G. Hormiga.

The specimens varied in size as well as number of leg pairs and development of the last pair of legs, which could be fully developed (albeit small) to be highly reduced and pointing backwards without touching the ground while walking. From the specimens observed at Pedro Cave, three had 19 leg pairs, one had 23, and the largest individual had 22 leg pairs. The imaged Swansea individual had 21 leg pairs. However, all the specimens studied by Peck (1975b) had 22 or 23 leg pairs, with one individual showing 23 legs on the left side and 22 on the right. The three specimens with 19 leg pairs reported here require that diagnosis of the genus and the species be revised to include between 19 and 23 leg pairs (Table 1).

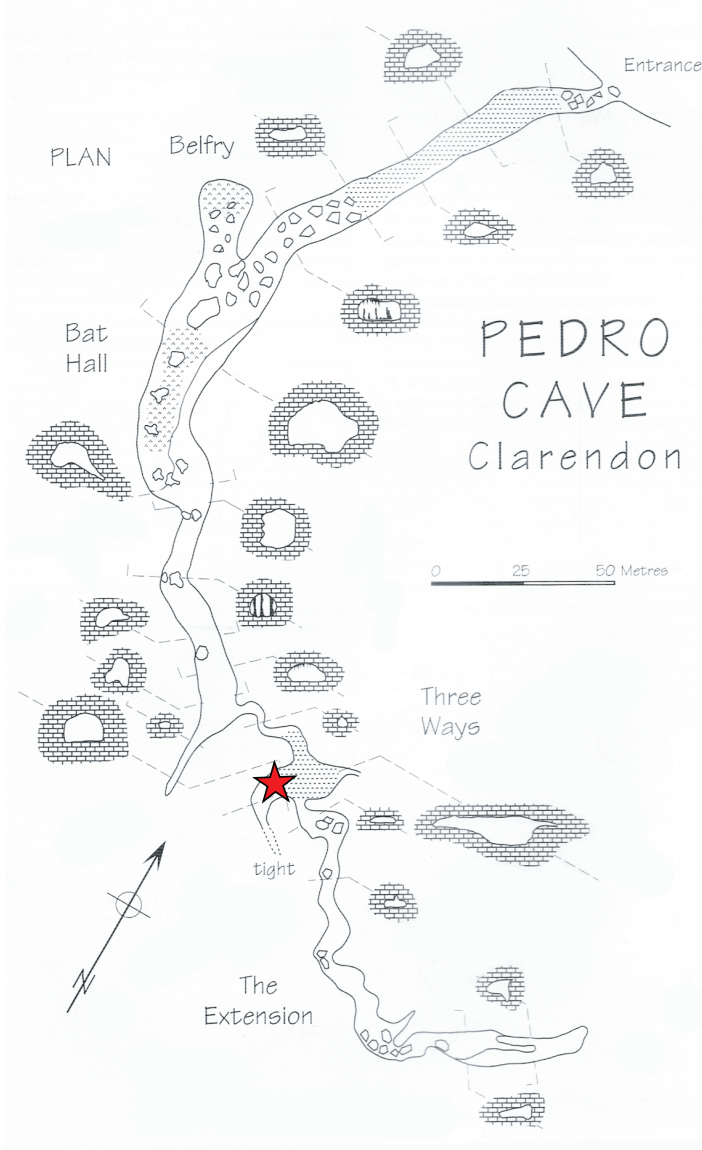


Figure 4. Map of Pedro Cave adapted from Fincham and Ashton (1967). The asterisk indicates the location of the *S. spelaeus* specimens.

Table 1. Specimens found at Pedro Cave (numbered) and Swansea Cave and leg pair numbers.

Specimen	Leg pairs
1	23 (last pair reduced)
2	19 (last pair reduced)
3	19
4	19
5	22
Swansea	21

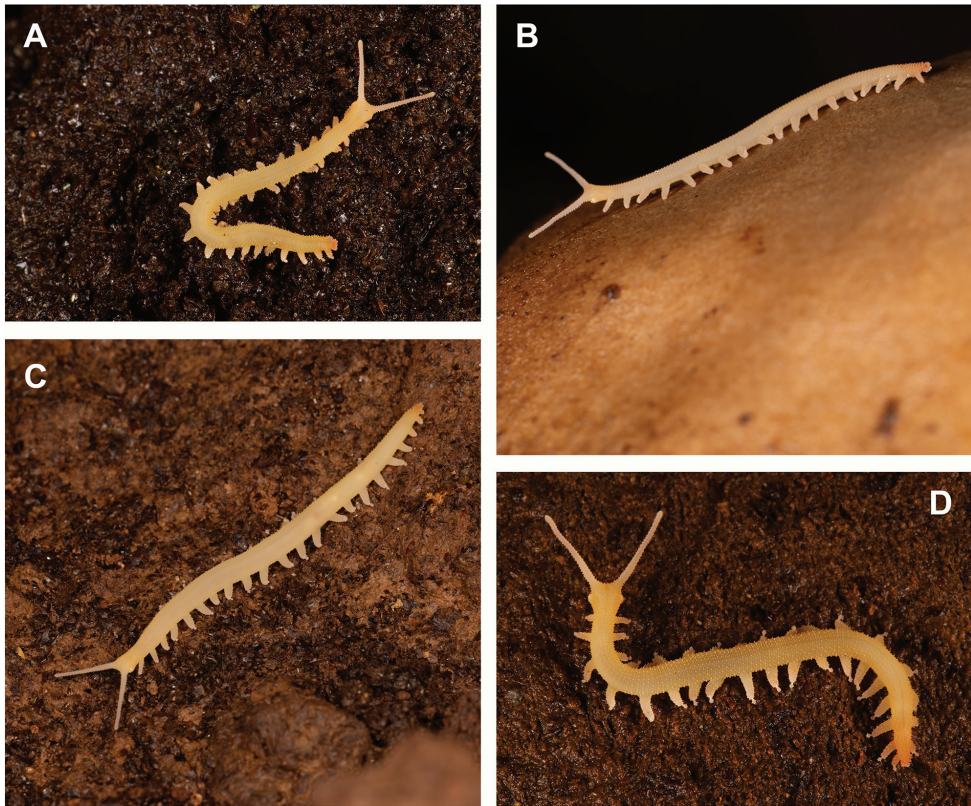


Figure 5. *Speleoperipatus spelaeus* from Pedro Cave **A** specimen 1 found on guano (23 leg pairs; note posterior diminutive legs) **B** specimen 2 (19 leg pairs) **C** specimen 5 (22 leg pairs) **D** specimen 3 (19 leg pairs). Photos **A, D** by G. Hormiga; **B, C** by G. Giribet.

Conclusion and future directions

Cave animals are often perceived as rare because they are seldom found due to the inherent difficulties of working in caves and low visitation rates, and therefore they display low detectability. The two troglomorphic velvet worm species are red-listed by the IUCN. *Speleoperipatus spelaeus* is currently considered as Critically Endangered (CE) because of its restricted habitat and the paucity of specimens known to science. However, the discovery of at least three individuals, probably conspecific, at a second location in Swansea Cave and the dedicated search at Pedro Cave resulting in the finding of five individuals in less than an hour of sampling, both suggest that the species may not be as rare as previously thought, and we expect that future work can help re-evaluate its status, Critically Endangered, as currently classified. We hope that, while continuing to apply conservation measures, this unique species can be properly evaluated for its ecology, distribution, and evolutionary history, as only then will we be able to properly understand the population size of this species and therefore its true

conservation perils. Furthermore, to better understand the significance of *Speleoperipatus spelaeus*, its distribution range, and its evolutionary origins it is imperative that the phylogenetic placement of this species is investigated to determine what are its closest relatives and whether those are other Jamaican species or velvet worms from other areas. Phylogenomic methods using ultraconserved elements (e.g., Sato et al. 2024) offer a powerful tool to infer the phylogenetic relationships of this remarkable species.

Acknowledgements

This work was supported by the National Science Foundation (grant numbers 2154245 and 2154246) “Collaborative Research: PurSUiT: Understanding the Neotropical Velvet Worms (Onychophora, Peripatidae, Neoplatida), a Cretaceous Radiation of Terrestrial Panarthropods” to GG and GH, which funded field work in Jamaica. PA, GG and GH received a research permit (Ref. #18/27) from the Jamaican National Environment and Planning Agency (NEPA) to conduct research on velvet worms and arachnids, and we show our gratitude for facilitating our research. Editor Fabio Stoch is acknowledged for his time and comments that helped improve this article. No specimen of *Speleoperipatus spelaeus* was collected during this research.

References

- Andrews EA (1912) The Jamaica *Peripatus*. Baltimore Johns Hopkins Univ. Cir. No. 2 1911: 51–55.
- Andrews EA (1933) *Peripatus* in Jamaica. *The Quarterly Review of Biology*, 155–163. <https://doi.org/10.1086/394431>
- Arnett RH (1961) The Onychophora of Jamaica. *Entomological News* 72: 213–220.
- Barbour T (1910) Notes on the herpetology of Jamaica. *Bulletin of the Museum of Comparative Zoology* 52: 273–301.
- Barnes A, Daniels SR (2022) Refining species boundaries among velvet worms (Onychophora, Peripatopsidae), with the description of two new species of *Opisthopatus* from South Africa. *Invertebrate Biology* 141(2): e12368. <https://doi.org/10.1111/ivb.12368>
- Bogdanowicz W, Worobiec E, Grooms C, Kimpe LE, Smol JP, Stewart RS, Suchecka E, Pomorski JJ, Blais JM, Clare EL, Fenton MB (2020) Pollen assemblage and environmental DNA changes: A 4300-year-old bat guano deposit from Jamaica. *Quaternary International* 558: 47–58. <https://doi.org/10.1016/j.quaint.2020.09.003>
- Brown MC, Ford DC (1973) Caves and groundwater patterns in a Tropical karst environment: Jamaica, West Indies. *American Journal of Science* 273: 622–633. <https://doi.org/10.2475/ajs.273.7.622>
- Duerden JE (1901) Abundance of *Peripatus* in Jamaica. *Nature* 63: 440–441. <https://doi.org/10.1038/063440d0>

- Espinasa L, Garvey R, Espinasa J, Fratto CA, Taylor S, Toulkeridis T, Addison A (2015) Cave dwelling Onychophora from a Lava Tube in the Galapagos. *Subterranean Biology* 15: 1–10. <https://doi.org/10.3897/subtbiol.15.8468>
- Fincham A, Ashton K (1967) The University of Leeds Hydrological Survey Expedition to Jamaica 1963. Cave Research Group of Gt. Britain (CRG): Transactions 9: 5–60.
- Fincham AG (1997) Jamaica Underground: The Caves, Sinkholes, and Underground Rivers of the Island. Press University of the West Indies, 464 pp. <https://doi.org/10.37234/RAQXRANV>
- Gertsch WJ (1984) The spider family Nesticidae (Araneae) in North America, Central America, and the West Indies. *Bulletin of the Texas Memorial Museum* 31: 1–91.
- Giribet G, Buckman-Young RS, Costa CS, Baker CM, Benavides LR, Branstetter MG, Daniels SR, Pinto-da-Rocha R (2018) The ‘*Peripatos*’ in Eurogondwana? – Lack of evidence that south-east Asian onychophorans walked through Europe. *Invertebrate Systematics* 32: 842–865. <https://doi.org/10.1071/IS18007>
- Giribet G, de Bivort BL, Hitchcock A, Swart P (2013) On *Speleosiro argasiformis*—a troglobitic Cyphophthalmi (Arachnida: Opiliones: Pettalidae) from Table Mountain, South Africa. *The Journal of Arachnology* 41: 416–419. <https://doi.org/10.1636/Ha12-78.1>
- Gosse PH (1851) A naturalists sojourn in Jamaica, London, 545 pp.
- Grabham M (1893) *Peripatus*. *Journal of the Institute of Jamaica* 1: 217–219.
- Grabham M, Cockerell TDA (1892) *Peripatus* re-discovered in Jamaica. *Nature* 46: 514. <https://doi.org/10.1038/046514a0>
- Guilting L (1826) Mollusca Caribbaeana. *The Zoological Journal* 2: 437–449.
- Hamer ML, Samways MJ, Ruhberg H (1997) A review of the Onychophora of South Africa, with discussion of their conservation. *Annals of the Natal Museum* 38: 283–312.
- Harvey MS (2002) Short-range endemism among the Australian fauna: some examples from non-marine environments. *Invertebrate Systematics* 16: 555–570. <https://doi.org/10.1071/Is02009>
- Lawrence RF (1931) A new peripatopsid from the Table Mountain caves. *Annals of the South African Museum* 30: 101–107.
- Lopes Ferreira R, Giribet G, Du Preez G, Ventouras O, Janion C, Souza Silva M (2020) The Wynberg Cave System, the most important site for cave fauna in South Africa at risk. *Subterranean Biology* 36: 73–81. <https://doi.org/10.3897/subtbiol.36.60162>
- Lynn WG (1936) A new location for *Peripatus* in Jamaica. *Psyche* 43: 119–125. <https://doi.org/10.1155/1936/85023>
- Mesibov R, Ruhberg H (1991) Ecology and conservation of *Tasmanipatus barretti* and *T. anophthalmus*, parapatric onychophorans (Onychophora: Peripatopsidae) from North-eastern Tasmania. *Papers and Proceedings of the Royal Society of Tasmania* 125: 11–16. <https://doi.org/10.26749/rstpp.125.11>
- New TR (1995) Onychophora in invertebrate conservation: priorities, practice and prospects. *Zoological Journal of the Linnean Society* 114: 77–89. <https://doi.org/10.1111/j.1096-3642.1995.tb00113.x>

- New TR (1996) *Speleoperipatus spelaeus*. The IUCN Red List of Threatened Species 1996: e.T20460A9202417. <https://doi.org/10.2305/IUCN.UK.1996.RLTS.T20460A9202417.en>
- Oliveira IdS (2023) An updated world checklist of velvet worms (Onychophora) with notes on nomenclature and status of names. *ZooKeys* 1184: 133–260. <https://doi.org/10.3897/zookeys.1184.107286>
- Peck SB (1975a) The invertebrate fauna of tropical American caves, Part III: Jamaica, an introduction. *International Journal of Speleology* 7: 303–326. <https://doi.org/10.5038/1827-806X.7.4.1>
- Peck SB (1975b) A review of the New World Onychophora with the description of a new cavernicolous genus and species from Jamaica. *Psyche* 82: 341–358. <https://doi.org/10.1155/1975/98614>
- Peck SB (1992) A synopsis of the invertebrate cave fauna of Jamaica. *National Speleological Society Bulletin* 54: 37–60.
- Rambla M (1969) Cave harvestmen from Jamaica (Opiliones: Phalangodidae). *Psyche* 76: 390–406. <https://doi.org/10.1155/1969/13496>
- Read VMSJ, Hughes RN (1987) Feeding behaviour and prey choice in *Macroperipatus torquatus* (Onychophora). *Proceedings Royal Society of London Series B: Biological Sciences* 230: 483–506. <https://doi.org/10.1098/rspb.1987.0030>
- Richards AM (2009) An ecological study of the cavernicolous fauna of the Nullarbor Plain Southern Australia. *Journal of Zoology* 164: 1–60. <https://doi.org/10.1111/j.1469-7998.1971.tb01297.x>
- Sato S, Derkarabetian S, Lord A, Giribet G (2024) An ultraconserved element probe set for velvet worms (Onychophora). *Molecular Phylogenetics and Evolution* 197: 108115. <https://doi.org/10.1016/j.ympev.2024.108115>
- Sharratt NJ, Picker MD, Samways MJ (2000) The invertebrate fauna of the sandstone caves of the Cape Peninsula (South Africa): patterns of endemism and conservation priorities. *Biodiversity and Conservation* 9: 107–143. <https://doi.org/10.1023/A:1008968518058>
- Sosa-Bartuano Á, Monge-Nájera J, Morera-Brenes B (2018) A proposed solution to the species problem in velvet worm conservation (Onychophora). *UNED Research Journal* 10: 193–197. <https://doi.org/10.22458/urj.v10i1.2027>
- Trewick S, Hitchmough R, Rolfe J, Stringer I (2018) Conservation status of New Zealand Onychophora ('peripatus' or velvet worm), 2018. *New Zealand Threat Classification Series* 26: 1–3.

Endless forms most wonderful: Four new cavernicolous planthopper species (Hemiptera, Fulgoromorpha, Cixiidae and Meenoplidae) from the Canary Islands

Hannelore Hoch¹, Heriberto López², Manuel Naranjo³,
Dora Aguín-Pombo⁴, Pedro Oromí⁵

1 Center for Integrative Biodiversity Discovery at Museum für Naturkunde, Leibniz Institute for Evolution and Biodiversity Science, Invalidenstr. 43, D-10115 Berlin, Germany **2** Island Ecology and Evolution Research Group (GEEI), Instituto de Productos Naturales y Agrobiología (IPNA-CSIC), E-38206, La Laguna, Tenerife, Canary Islands, Spain **3** Sociedad Entomológica Canaria Melansis, Av. Felo Monzón 21, P.1-4D, E-35019, Las Palmas de Gran Canaria, Gran Canaria, Spain **4** Faculty of Life Sciences, University of Madeira, 9000–390 Funchal, Madeira, Portugal **5** Depto. Biología Animal, Edafología y Geología, Universidad de La Laguna, E-38206 La Laguna, Tenerife, Spain

Corresponding authors: Hannelore Hoch (hhoch186@gmail.com); Heriberto López (herilope@ipna.csic.es)

Academic editor: Leonardo Latella | Received 11 December 2024 | Accepted 5 March 2025 | Published 28 March 2025

<https://zoobank.org/B0F56474-2B3D-4734-8516-AB8E5211F45C>

Citation: Hoch H, López H, Naranjo M, Aguín-Pombo D, Oromí P (2025) Endless forms most wonderful: Four new cavernicolous planthopper species (Hemiptera, Fulgoromorpha, Cixiidae and Meenoplidae) from the Canary Islands. *Subterranean Biology* 51: 61–101. <https://doi.org/10.3897/subtbiol.51.144111>

Abstract

The Canary Islands harbour a rich and diverse fauna of obligate subterranean arthropods (i.e. troglobionts). Among the insect taxa which have repeatedly undergone the evolutionary switch from life on the surface to underground environments are the Fulgoromorpha, or planthoppers: Cixiidae and Meenoplidae. Previously, a total of 13 troglobitic planthopper species have been described from El Hierro, La Palma, Tenerife and Gran Canaria. Here we describe three new troglobitic cixiid species: *Cixius palmirandus* **sp. nov.** from La Palma, *Cixius theseus* **sp. nov.** from El Hierro and *Tachycixius gomerobscurus* **sp. nov.** from La Gomera, and one new meenoplid species: *Meenoplus skotinophilus* **sp. nov.** from El Hierro. *Tachycixius gomerobscurus* **sp. nov.** is the first record of a subterranean adapted Fulgoromorpha on La Gomera. With now 17 documented species of strictly hypogean planthoppers, the Canary Islands hold the highest number of subterranean planthoppers of any region worldwide, representing ca. ¼ of all known species. We provide a key to all subterranean planthopper species known from the Canary Islands as well as information on their habitat, distribution, ecological classification and conservation status. As all highly specialized, narrow range troglobitic planthopper species must be regarded as vulnerable, if not endangered,

climate change poses a major risk of extinction. We hypothesize on island colonization and subterranean speciation underlying taxonomic diversity and high endemism. We conclude that the currently observed zoogeographic patterns imply the existence of an ancient fauna which is now extinct.

Keywords

Conservation, lava tubes, mesovoid shallow substratum, root feeders, subterranean adaptation, troglobionts, troglomorphy

Introduction

The Canary Islands are of purely volcanic origin, emerging the different islands from the sea level during the past 20.2 million years (Carracedo and Troll 2016). They are located in the Eastern Atlantic (27°37'–29°25'N, 13°20'–29°25'W), comparatively close to the adjacent continent: the most easterly island, Fuerteventura, lies just 100 km off the Northwest African coast. The seven main islands differ considerably in age (1.12–20.2 Ma), size (269–2034 km²), and altitude (670–3714 m a.s.l.) (Machado 2022). Due to their geographical position in the Eastern Atlantic, the climate is essentially subtropical, although with considerable local variation in respect to precipitation and temperature. Distinct vegetational zones are recognized and range from arid and semi-arid scrub to humid laurel and pine forest and to subalpine areas on the higher central and western islands (Fernández-Palacios et al. 2001). Plants and animals which initially colonized the islands in many cases gave rise to radiations which have brought forth many endemic species: 41% of the ca. 1400 native vascular plant species and 45% of the ca. 7900 native terrestrial invertebrate species are endemic (Canarian Government [2024]). Less obvious, yet no less spectacular are geologic features: lava tubes and their unique species communities. Lava tube caves form in basaltic low-viscosity flows known as „pahoehoe“ (Dutton 1884), or as ropy lava. They range in size from few centimeters in diameter to large tunnels of several meters high and decades of kilometers long (for formation of lava tubes see Peterson and Swanson 1974). Roots from the surface vegetation entering these hollow underground spaces provide a food resource for animals which inhabit the caves throughout their entire life cycle or parts of it (Howarth 1973).

The subterranean environment of the Canary Islands is rich in adapted arthropods – to date more than 230 troglobionts have been documented (e.g. Oromí 2004; 2008; Oromí et al. 2021). Yet it remains much less well investigated than surface biotopes, given the large number of lava tubes and existence of an extended mesovoid shallow substratum. Accordingly, in numerous taxa new species continue to be discovered with nearly any new survey, e.g., in the Curculionidae (*Oromia* Alonso-Zarazaga, 1987; García et al. 2020; *Baezia* Alonso-Zarazaga & García, 1999; García et al. 2021; *Laparocerus* Schoenherr, 1834; Machado 2022).

Insects frequently encountered in lava tubes on the Canary Islands are planthoppers of the families Cixiidae and Meenoplidae. While some do not differ in their external morphology from surface dwelling species of the taxon, and are likely occasional

visitors to the caves (troglonexes), others display characteristic troglomorphies, such as reduction or loss of compound eyes, reduced and non-functional wings, and light bodily pigmentation, and are considered troglobionts (Sket 2008; Howarth and Moldovan 2018b), spending their entire life cycle in subterranean habitats.

Hitherto, a total of 13 subterranean adapted planthopper species belonging to the Cixiidae and the Meenoplidae have been described from El Hierro, La Palma, Tenerife and Gran Canaria islands (Remane and Hoch 1988; Hoch and Asche 1993; Hoch et al. 2012).

Recent biospeleological investigations in the western islands of the archipelago have revealed the existence of at least four previously unknown subterranean species, three in the Cixiidae, from La Palma, El Hierro and La Gomera, and one in the Meenoplidae, from El Hierro (see Fig. 1). The descriptions of these new species and providing information on their ecology and conservation status is the main objective of this article.

Outside the Canary Islands, strictly hypogean planthoppers are known from many parts of the world: from all continents except North America and Antarctica, and from several island archipelagoes – e.g., Hawaii, Galápagos, Samoa, Azores, Cape Verde (see Le Cesne et al. 2024; Bourgoin 2024).

Troglobitic planthoppers feed by sucking sap from roots (Howarth 1983; Hoch 1994), and it has been hypothesized that the utilization of roots as a novel food resource may have triggered the evolutionary switch from epigeal to underground way of life (Howarth 1986). Within the subterranean communities, planthopper nymphs and adults are primary consumers, constituting prey for troglobitic scavengers and predators (Stone et al. 2005).

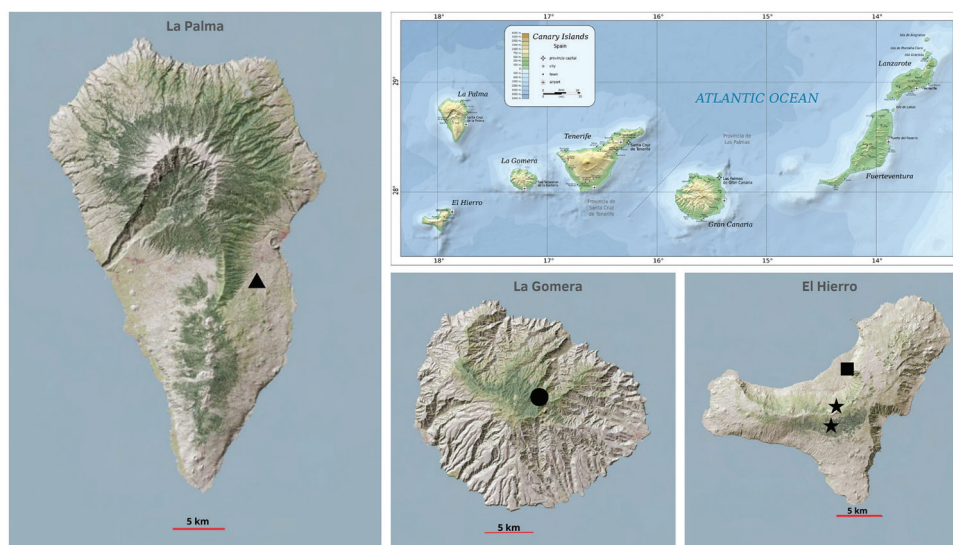


Figure 1. The Canary Islands and distribution of the new species described. Black triangle: *Cixius palmirandus* Hoch & Naranjo, sp. nov.; Black circle: *Tachycixius gomerobscurus* Hoch & Oromí, sp. nov.; Black stars: *Cixius theusis* Hoch & Aguin-Pombo, sp. nov.; Black square: *Meenoplus skotinophilus* Hoch & López, sp. nov. (https://commons.wikimedia.org/wiki/File:Map_of_the_Canary_Islands.svg; https://catalogo.idecanarias.es/geonetwork/srv/spa/catalog.search#/metadata/spagrafcan_MTLWMS_20160101).

Apart from living in lava tubes, these planthoppers have been documented from the „milieu souterrain superficiel“ (sensu Juberthie et al. 1980) or mesovoid shallow substratum (Culver and Pipan 2009) (henceforth referred to as MSS), which comprises a network of voids and cracks at the interface between soil and rock layer, and is characterized by similar conditions as those in deeper fissures or caves (Figs 2A–F, 3A–H).

Material and methods

Collecting, preservation, permanent storage

All the specimens used in this study were obtained in fieldwork carried out over many years in several islands of the Canary archipelago. Part of the studied specimens were collected inside lava tube caves by applying multiple sampling techniques (Wynne et al. 2019), mainly searching in those parts of the caves where roots appear abundantly, and then transferred immediately into vials containing absolute or 70% ethanol. Other specimens were collected using special permanent pitfall traps installed in the MSS (Fig. 3), according to López and Oromí (2010). For permanent storage, after dissection and examination, abdomen and genitalia were transferred to polyethylene vials containing glycerine, and individually associated with the specimen vial.

Morphological examination techniques, visualization

Measurements and examinations of external body features were made from the specimen in ethanol, without further manipulation. Measurements of body length refer to the distance between anterior margin of head and tip of anal segment in the male, and tip of ovipositor in the female. Terminology of wing venation follows Bourgoïn et al. (2015). To prepare male genitalia for dissection, the genital capsule was removed from the specimen, macerated for 24h in 10% KOH at room temperature, washed in water, transferred to glycerine for storage, or to glycerine-jelly for drawings. Examinations and drawings were made using a Leitz stereomicroscope with *camera lucida* attachment.

Photographs

Habitus images of *Tachycixius gomerobscurus* sp. nov. (Fig. 8) were generated with a Leica Z16 microscope, with Planapo 2.0 X/WD 39 mm objective, with the aid of stacking software Helicon Focus 6.7.1. at the Museum für Naturkunde, Berlin.

Mitochondrial COI sequencing/barcoding

Non-destructive DNA extractions were performed for three individuals of *Meenoplus skotinophilus* Hoch and López sp. nov. to obtain their barcode sequences. The digestion of each voucher was done overnight at 60 °C with a pK buffer (ratio



Figure 2. Habitat types of hypogean cave planthoppers on the Canary Islands **A** Galería Honda de Miranda, La Palma (*Cixius palmirandus* sp. nov.) (Photo: Rafael García, used with permission) **B** Camino de San Salvador, MSS, El Hierro (*Cixius theseus* sp. nov.) (Photo: Pedro Oromí) **C, D** Reventón Oscuro, La Gomera (*Tachycixius gomerobscurus* sp. nov.), slope inside the laurel forest where the MSS traps (**D**, see also Fig. 3) are installed (Photos: P. Oromí (**C**); Salvador de La Cruz (**D**), used with permission) **E, F** Sima de Guinea, El Hierro (*Meenoplus skotinophilus* sp. nov.) **E** location **F** entrance (Photos: Miguel Ángel Rodríguez, used with permission).

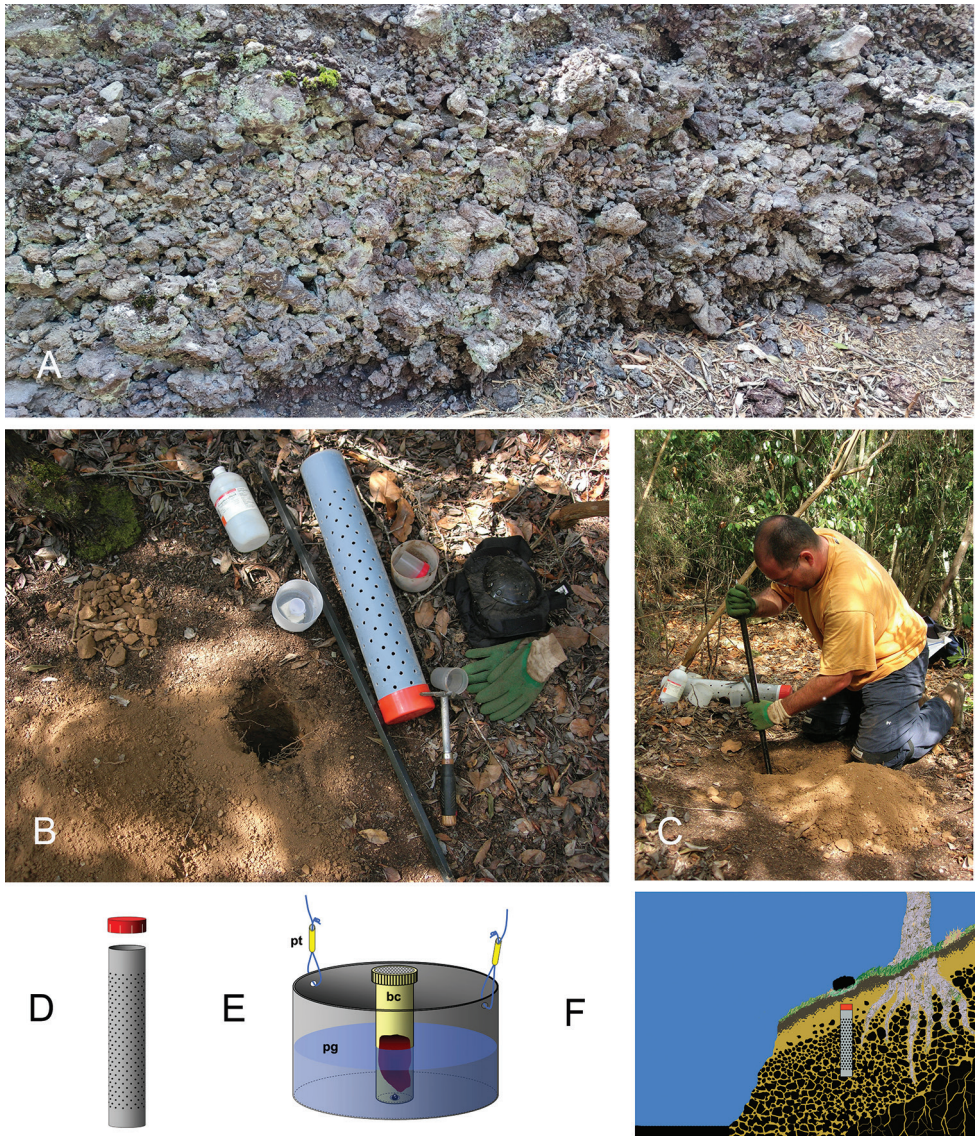


Figure 3. Collecting in the MSS **A** Detail of the MSS of El Hierro (Photo: Heriberto López) **B** Components of MSS trap and basic tools for installation **C** H. López installing a MSS trap in La Gomera island (Photos: Salvador de La Cruz, used with permission) **D** MSS trap: PVC pipe with multiple holes and silicone cover **E** sample collection container consisting of bait container (bc), nylon cords tied with small plastic tubes (pt) and tray with propylene glycol (pg) **F** trap installed in the MSS close to a road cut. **D, F** after López and Oromí (2010).

1/10). The supernatant (DNA lysate) was transferred to the corresponding well within a deep-well plate and the (DNA-extracted) vouchers were maintained in the vials with ethanol for further morphological studies. For the DNA extractions

of these specimens, we used the Mag-Bind Blood and Tissue DNA HDQ 96 kit (Omega Bio-Tek GA, USA) in the KingFisher robotic system (ThermoFisher Scientific inc.), and the Tecan Infinite 200 Pro (Configuration: Infinite M Nano+) to measure the DNA concentrations of the extracts. PCR amplification for the barcode region was done using degenerate Folmer barcode primers (Fol-degen-for: 'TCNACNAAAYCAYAARRAYATYGG'; Fol-degen-rev: 'TANACYTCNGGRT-GNCCRAA RAA YCA'; Folmer et al. (1994), Yu et al. (2012)). For PCR reaction, 2 μ L of diluted (1/10) DNA extract was amplified with 23 μ L of PCR mix (for a total volume of 25 μ L), comprised of 14.4 μ L of water, 2.5 μ L of 10 \times NH₄ buffer (Bioline), 1.5 μ L of 50 mM MgCl₂ (Bioline), 2 μ L of 2.5 mM dNTPs (Bioline), 0.5 μ L of BSA (20 mg/ml), 1 μ L of each primer (10 μ M), and 0.1 μ L of Taq polymerase (BIOTAQ™ DNA Polymerase, Bioline). The PCR conditions were: initial denaturing step at 95 °C for 2 minutes, 40 amplification cycles (94 °C for 30 seconds, 46 °C for 35 seconds, 72 °C for 45 seconds), and a final step at 72 °C for 5 minutes. PCR success was checked by running products on a 1% TAE agarose gel, and successfully amplified products were cleaned following EXO I/rAP PCR cleanup protocol. The purified PCR product for each voucher was Sanger sequenced with ABI technology in Macrogen, Spain (<https://dna.macrogen.com>).

The obtained sequences were edited on Geneious Prime version 2020.0.3 (www.geneious.com), and then processed in BOLD (<https://www.boldsystems.org>) and Genbank (<https://www.ncbi.nlm.nih.gov/genbank/>) with the IDS tool using default setting parameters, to explore if *Meenoplus skotinophilus* sp. nov. has closely related species included in these databases of barcode reference sequences.

Depository

Specimens are deposited in the following collections:

- DZUL** University of La Laguna, La Laguna, Tenerife, Canary Islands, Spain;
IPNA Institute of Natural Products and Agrobiology (IPNA-CSIC), La Laguna, Tenerife, Canary Islands, Spain;
UMACI University of Madeira Collection of Insects, Funchal, Madeira, Portugal.

Results

The three new species of Cixiidae described herein are *Cixius palmirandus* sp. nov. from La Palma, *Cixius theseus* sp. nov. from El Hierro and *Tachycixius gomerobscurus* sp. nov. from La Gomera; and the new Meenoplidae is *Meenoplus skotinophilus* sp. nov. from El Hierro (for distribution see Fig. 1; for a synopsis see Suppl. material 1: table S1). *Tachycixius gomerobscurus* sp. nov. is the first record of a hypogean planthopper from La Gomera.

Taxonomy

Cixiidae Spinola, 1839

Cixius palmirandus Hoch & Naranjo, sp. nov.

<https://zoobank.org/95A7D931-15AE-4D57-ACA2-DB8969D0E9FD>

Figs 4, 5A–F

Material examined. *Holotype*: SPAIN • male; Canary Islands, La Palma, Cueva Honda de Miranda; 28.63744940, -17.78849367; 17 Oct. 2015; M. Naranjo leg. (50353 **DZUL**).

Diagnosis. *Cixius palmirandus* is similar to the other cavernicolous *Cixius* species from La Palma, *C. palmeros* Hoch & Asche, 1993 and *C. pinarcoladus* Hoch & Asche, 1993 in habitus (degree of troglomorphy), body size, general configuration of the male genital morphology, but differs in several characters: upper portion of frons smooth (vs. pustulate as in *C. palmeros* and *C. pinarcoladus*), mesonotum with lateral carinae attaining posterior margin (unlike in *C. palmeros*), tegmen with Y-vein (Pcu, A1, Pcu + A1) complete (vs Y-vein incomplete in *C. palmeros* and *C. pinarcoladus*), genital styles with expanded distal portion highly elongate (vs spoon-shaped in *C. palmeros* and *C. pinarcoladus*), and aedeagus shaft ventrally with an obtuse ridge which is apically rounded, concave and distinctly curved ventrally (vs apically with an obtuse tip, as in *C. palmeros*, or directed straight caudally, as in *C. pinarcoladus*).

Description. *Habitus.* Strongly troglomorphic with compound eyes absent, tegmina, wings and bodily pigmentation strongly reduced.

Body length. Male 3.9 mm (n = 1)

Colouration. Head, thorax and abdomen stramineous/yellowish, lateral carinae of head and lateral carinae of pronotum in anterior portion slightly darker. Antennae and legs whitish, tegmina translucent with costal vein yellowish, other veins unpigmented.

Head. Vertex short and wide, not separated from frons by a transverse carina, i.e., frons continuously rounded into vertex. Vertex laterally near posterior margin of head with two shallowly concave areas. Frons convex, in ventral view ca. twice as wide as medially long, smooth, without median carina, lateral carinae strongly ridged, directed laterally. Frontoclypeal suture highly vaulted. Post- und anteclypeus smooth, without median carina. Post- and anteclypeus together ca. 2.8 × longer than frons medially. Rostrum elongate, well surpassing hind coxae, 2nd joint longer than 3rd. Compound eyes and ocelli absent, the former position of the lateral ocelli faintly recognizable by a light roundish spot anteriorly of antennae. Antennae with scape very short, ring-like, pedicel globose, with sensory plaque organs feebly recognizable; antennae shielded anteriorly by lateral margins of frons.

Thorax. Pronotum short, ca. 4 × wider than medially long, and 1.5 × wider than maximum width of head; indistinctly tricarinate: median carina obtuse, lateral carinae distinct in anterior portion, diverging laterally, gradually vanishing; posterior margin of pronotum shallowly incised. Mesonotum slightly vaulted, ca. 1.3 × wider than medially long, in midline ca. 3 × the length of pronotum; tricarinate, with carinae obtuse

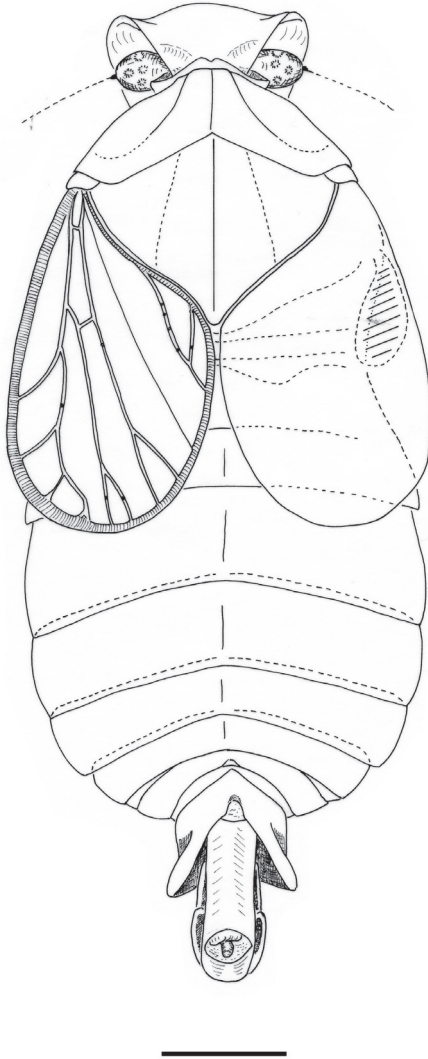


Figure 4. *Cixius palmirandus* Hoch & Naranjo, sp. nov. Habitus male (holotype). Scale bar: 0.5 mm.

and faintly recognizable, lateral carinae attaining posterior margin. Tegulae vestigial. Tegmina strongly reduced, venation as in Fig. 4. Costal vein in anterior and distal part of tegmen conspicuously wide; „Y-vein“ (Pcu, A1, Pcu + A1) preserved and recognizable. Tegmen ca. 1.6 × longer than maximally wide, attaining, respectively slightly surpassing posterior margin of third abdominal tergite. Longitudinal veins sparsely beset with bases of setae. Wings vestigial. Metatibiae laterally with 3 minute spines, distally with 6 teeth, grouped 5+1, lateral tooth longest. First and second metatarsal joints with 4 apical teeth, lateral ones longer than median ones. First metatarsal joint about as long as 2nd and 3rd joints together. Pretarsal claws slender, arolium small.

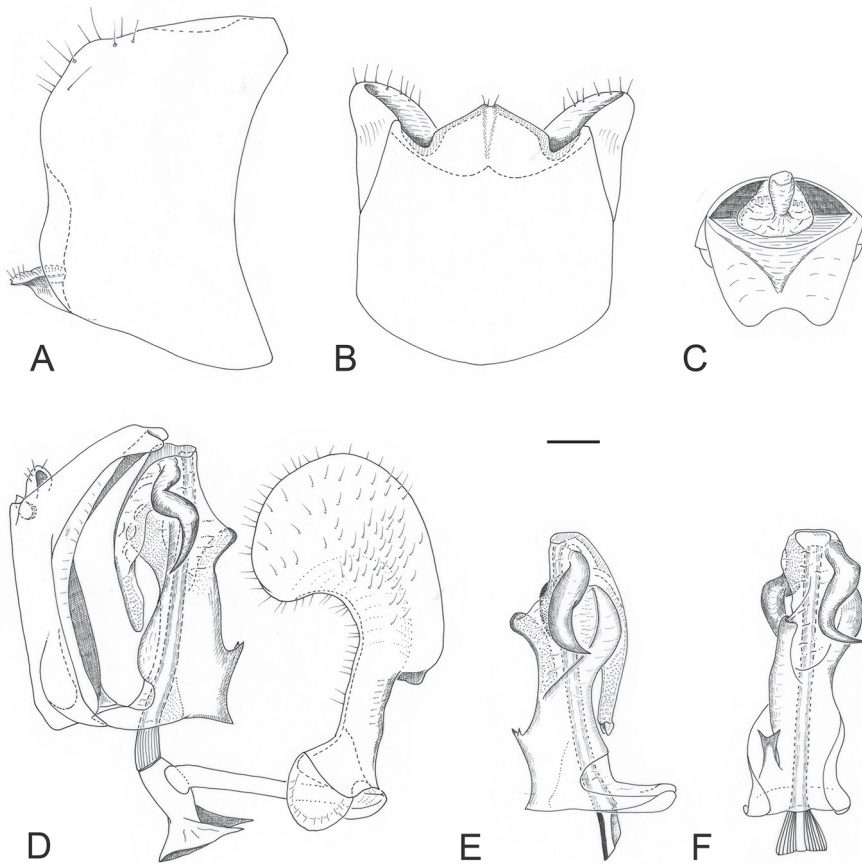


Figure 5. *Cixius palmirandus* Hoch & Naranjo, sp. nov. Male genitalia (holotype) **A** genital segment, right lateral aspect **B** same, ventral aspect **C** anal segment, caudal aspect **D** anal segment, aedeagus, genital style, *in situ*, left lateral aspect **E** aedeagus, right lateral aspect **F** same, ventral aspect. Scale bar: 0.1 mm.

Male genitalia. Genital segment bilaterally symmetrical, in caudal aspect ca. $1.6 \times$ higher than maximally wide, and in lateral aspect ca. $4 \times$ longer ventrally than dorsally, caudal margins laterodorsally slightly expanding into rounded lobes, their margins beset with a cluster of long setae; medioventral process wide at base, distally tapering, tip in ventral view slightly incised, dorsal surface of medioventral process concave. Anal segment tongue-shaped, lateral margins straight, without ventral lobes, parallel from base to level of anal style, distally slightly tapering; anal segment distally of anal style bent ventrally in a ca. 45° angle, caudal margin produced into two short rounded lobes. Genital styles narrow in basal third, distally expanding, expanded portion elongate, distally rounded, medially concave; genital styles with dorsal margin of narrow portion and external surface of expanded portion densely beset with setae. Genital styles in repose joining in midline over nearly their whole length ventrally, nearly completely covering the aedeagus. Aedeagus with basal part (shaft) tubular, slender,

slightly compressed in basal two thirds, ventrally near base with two small rigid spines directed caudally; shaft ventrally with an obtuse longitudinal ridge which is apically rounded and in upper part slightly curved ventrally. Shaft subapically with a bulbous projection dorsally and right laterally, shaft apically with two sturdy movable spinose processes: left lateral one shallowly S-shaped, tip in repose directed basally, right lateral one slightly shorter than left lateral one, strongly curved and in repose directed right-lateroventrally, its tip pointing right laterally. Distal part of aedeagus (flagellum) in repose bent dorsally, narrow, surpassing midlength of shaft, but not attaining base of shaft; dorsally with a longitudinal ridge which is produced into a short, stout spine at apex, tip of flagellum directed right laterally.

Female. Unknown.

Etymology. The species epithet is an adjective in nominative singular, and a combination from the island of the type locality, La Palma, and the name of the cave, Cueva Honda de Miranda. The gender is masculine.

Distribution. Known from the type locality in the east of La Palma, municipality of Breña Alta (Fig. 1). Endemic to La Palma.

Ecology and behavior. Cueva Honda de Miranda is a lava tube located at 417 m a.s.l. in the eastern slope of the island. The potential vegetation in this area corresponds to a dry laurel forest (*Visneo mocanerae-Arbutus canariensis sigmetum*) (Del Arco and Rodríguez 2018). Currently, this space is occupied by agricultural plots and substitution scrub. The cave is a labyrinthic lava tube with over 20 galleries and 1 km of total development (Dumpiérrez et al 2000), in which seven troglobiont species have been recorded so far: the amphipod *Palmorchestia hypogaea* Stock & Martín, 1988, the isopod *Halophiloscia microphthalmia* Taiti & López, 2008, the cockroach *Loboptera fortunata* Krauss, 1892, the thread-legged bug *Collartida tanausu* Ribes, Oromí & Ribes, 1998, and the beetles *Licinopsis angustula* Machado, 1987, *Domene benahoarensis* Oromí & Martín, 1990 and *Laparocerus dacilae* García, 1998. The gallery with the presence of *C. palmirandus* is located relatively close to the entrance to the cave, in which predominates a wide section, a high relative humidity and the presence of roots. The only specimen collected of *C. palmirandus* was dead but in good conditions for the formal descriptions of the new species. In this sector, an American cockroach nymph (*Periplaneta americana*) was observed, which may indicate local contamination by sewage.

Ecological classification. *Cixius palmirandus* sp. nov. displays several troglomorphic characters: absence of compound eyes and ocelli, strongly reduced tegmina and vestigial wings, and light body coloration. Although there is no information on the behaviour of the species, it is certainly unable to fly. The phenotypical configuration of eyes and wings suggests that it is restricted to the subterranean environment and likely to complete the entire life cycle underground. According to the criteria provided by Sket (2008), and more recently by Howarth and Moldovan (2018 a, b), we regard *C. palmirandus* sp. nov. as an obligate cavernicole, or troglobiont.

Conservation status. Cueva Honda de Miranda is located in an area of the island where the potential vegetation should be dry laurel forest (Del Arco and Delgado 2018), but it is currently heavily transformed into a rural environment dotted with scattered

homes and agricultural fields. The sewage sanitation system in the area is non-existent, and wastewater is generally discharged directly into underground wells, which are gradually contaminating the subsurface. Additionally, the chemicals used in the fields also accumulate in the subterranean environment over the years. Under these circumstances, the underground habitat loses its suitability for native subterranean species, as they are very sensitive to such habitat alterations. Furthermore, with this degradation, the underground habitat begins to be colonized by invasive species that thrive in these types of contaminated environments, competing with and displacing the native subterranean fauna. The detection of *Periplaneta americana* (Linné, 1758) in some areas of Cueva Honda de Miranda is a clear indication that its subterranean environment is likely undergoing such environmental degradation process. Nevertheless, there is no regular monitoring of the subterranean species populations present in the cave, which would provide precise information on whether they are experiencing some decline (Rafael García, personal comment). The sporadic sampling conducted so far in the cave has allowed for the capture of the only known specimen of *Cixius palmirandus* sp. nov., but the lack of continuity in these sampling efforts does not allow us to determine whether this species is scarce due to being rare, due to naturally low populations, or because they have indeed suffered a decline due to the deterioration of the subterranean environment. According to the IUCN criteria for assessing whether a species falls into one of the threat categories on its Red List, *Cixius palmirandus* meets criterion D2 (see IUCN 2022) due to its very restricted area of occupancy, which is less than 20 km², and the fact that it is known from only one location. Such circumstances make this species highly vulnerable to the impacts of human activities and stochastic events in a short time frame, potentially leading to its classification as Critically Endangered or even Extinct in the near future. Given these conditions, this new species should be classified as Vulnerable according to the IUCN criteria.

Remarks. The only known individual of this species, a male, was apparently collected and preserved in ethanol soon after the adult molt: the larval skin is still partially attached, and the cuticle still soft, thus the frons is distorted and the arista of the antennae are missing. However, the male genital capsule appears to be fully sclerotized.

***Cixius theseus* Hoch & Aguín-Pombo, sp. nov.**

<https://zoobank.org/45F9D8C4-9242-4FC7-8B14-BFE941C28AB5>

Figs 6 A, B, 7A–G

Material examined. *Holotype*: SPAIN • male; Canary Islands, El Hierro, Municipality of Frontera, Camino de San Salvador, MSS; 27.73294972, -18.01168166; 28 Aug. 2007; H. López and P. Oromí leg. (IPNA). *Paratype*: SPAIN • female; same data as holotype (50354 DZUL).

Additional material. SPAIN • 1 nymph III instar, 3 nymph IV instar; same data as holotype (IPNA).

Diagnosis. *Cixius theseus* sp. nov. is similar to the other cavernicolous *Cixius* species from El Hierro, *C. ariadne* Hoch & Asche, 1993 and *C. nycticolus* Hoch & Asche,

1993 in habitus (degree of troglomorphy), body size, general configuration of the male and female morphology, but differs in several characters: Frons $2.3 \times$ wider than medially high and not pustulate (vs. $1.5 \times$ wider and pustulate in *C. ariadne*); tegmen with Y-vein preserved (vs. reduced in *C. ariadne*); in the male genitalia: caudal margin of anal segment medially incised (vs. rounded in *C. ariadne*), genital styles with distal expanded part dorsally rounded (vs. dorsally produced in *C. ariadne*), basal part of aedeagus (shaft) left laterally with a prominent longitudinal ridge (vs. without such a ridge in *C. ariadne*), and with bifurcate ventral projection slender (vs. wide in *C. ariadne*), right lateral subapical spinose process sturdy and in repose curved dorsally (vs. slender and in repose curved basally in *C. ariadne*) and, most prominently, distal part of aedeagus (flagellum) with a slender spinose process at ca. midlength (vs. without such a spinose process in *C. ariadne*); in the female genitalia: caudal margin of 7th sternite medially expanding into an obtusely angulate process (as in *C. nycticolus*, vs. caudal margin straight in *C. ariadne*), and wax-secreting field on 9th tergite medially separated by a narrow, longitudinal, membranous area (vs. wax-secreting field medially not separated but with a distinct median ridge in *C. ariadne* and *C. nycticolus*).

Description. Habitus. Strongly troglomorphic with compound eyes absent, tegmina, wings and bodily pigmentation strongly reduced.

Body length. Male 2.7 mm ($n = 1$). Female 3.3 mm ($n = 1$).

Colouration. Male. Head and thorax incl. legs light yellowish, lateral carinae of head and posterior margin of vertex brownish; antennae whitish; tegmina translucent, whitish, venation white-yellowish, veins beset with brownish setae; legs whitish, distal spines of hind tibiae and of metatarsal joints brownish; abdomen whitish, genital capsule slightly darker, yellowish brown. **Female.** Head with vertex light yellowish, frons yellowish, medially with a brownish longitudinal stripe; clypeus light brown; antennae yellowish with distinct reddish brown star-shaped sensory plaque organs; pronotum medially, i.e., between lateral carinae, yellowish, lateral portions slightly darker, yellowish brown; mesonotum light yellowish; tegmina translucent, venation whitish, beset with brownish setae; legs yellowish white; abdomen light yellowish, genital segment incl. ovipositor yellowish brown.

Head. Vertex short, ca. $3.5 \times$ wider at base than medially long, very faintly separated from frons by an obsolete transverse carina. Frons convex, ca. $2.3 \times$ wider than medially high, lateral carinae distinctly ridged and directed (antero-)laterally; frons smooth, without median carina, not pustulate. Frontoclypeal suture highly vaulted/arched. Post- and anteclypeus smooth, without median carina, together ca. $3.4 \times$ longer than frons. Rostrum elongate, 2nd joint longest; rostrum relatively shorter in the male: surpassing caudal margin of hind coxae only slightly, in the female with ca. half the length of 3rd joint. Compound eyes and ocelli absent. Antennae with scape very short, ring-like, pedicel subcylindrical, ca. $1.4 \times$ longer than wide, in the female with distinctly recognizable star-shaped sensory plaque organs.

Thorax. Pronotum faintly tricarinate, lateral carinae diverging laterally, gradually vanishing; pronotum ca. $1.8 \times$ wider than maximum width of head, and $4.2 \times$ wider than medially long, posterior margin concave, obtusely angulate. Mesonotum

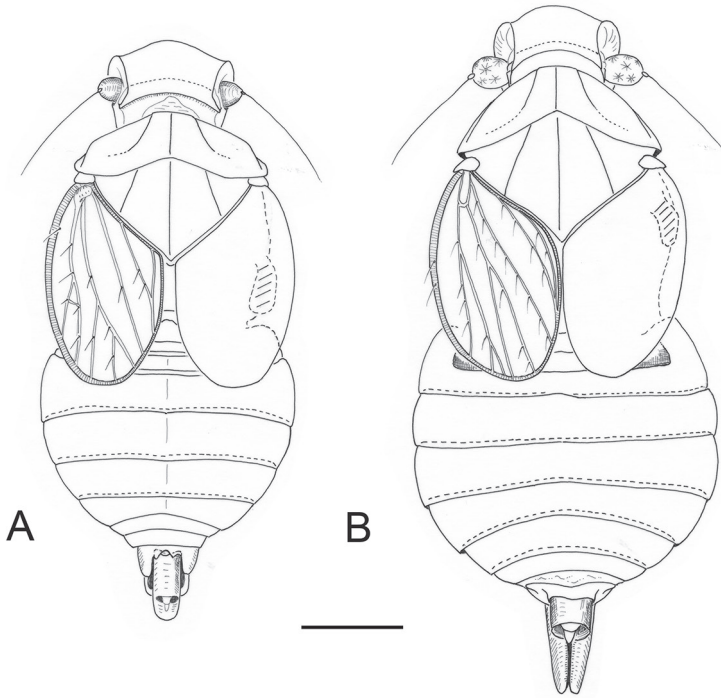


Figure 6. *Cixius theseus* Hoch & Aguín-Pombo, sp. nov. **A** habitus male (holotype) **B** habitus female (paratype). Scale bar: 0.5 mm.

tricarinate, carinae only faintly recognizable, lateral carinae reaching posterior margin, median carina feeble, obtuse, vanishing caudally; mesonotum in the male 1.5 ×, in the female 1.4 × wider than medially long, and in midline 2.3 × longer than length of pronotum. Tegulae small. Tegmina strongly reduced, their caudal margin attaining ca. midlength of 3rd abdominal tergite; tegmen longer than maximally wide: ca. 1.5 × in the male, and 1.65 × in the female; venation rudimentary, costal vein strong, basal cell closed, „Y-vein“ (Pcu, A1, Pcu + A1) preserved and recognizable, A1 and Pcu + A1 very close to posterior margin of tegmen; tegmina with numerous conspicuous setae along veins. Wings vestigial, very small.

Metatibiae laterally with 3 tiny spines, distally with 6 (in the male), and 6/7 (in the female) apical teeth, of which the lateral one is largest. First metatarsal joint in both sexes with 4, and second metatarsal joint with 4 (in the male) and 3/4 (in the female) distal spines. First metatarsal joint about as long as 2nd and 3rd metatarsal joints together. Pretarsal claws slender, arolium small.

Male genitalia. Genital segment in caudal aspect slightly higher than wide, medioventral process simple, in ventral aspect obtusely angulate. Anal segment in dorsal aspect rectangular, ca. 2 × longer than wide, with distal portion slightly bent ventrally, lateral margins parallel, distal margin medially incised. Genital styles slender at base, distally expanding dorsally, expanded part medially concave. Aedeagus with basal part (shaft) slender, more or less tubular, left laterally with a prominent, longitudinal,

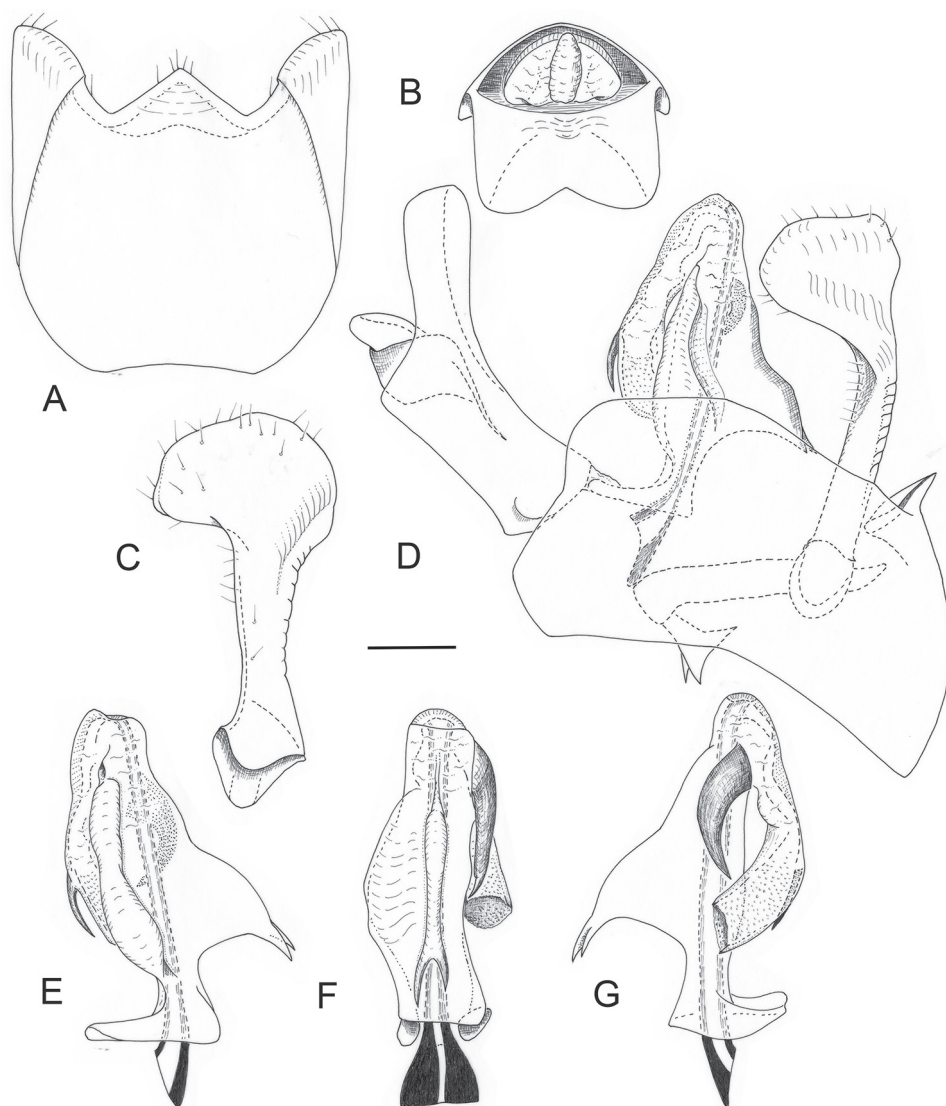


Figure 7. *Cixius theseus* Hoch & Aguín-Pombo, sp. nov. (holotype). Male genitalia **A** genital segment, ventral aspect **B** anal segment, caudal aspect **C** left genital style, maximum aspect **D** anal segment, genital segment, aedeagus and genital style, *in situ*, left lateral aspect **E** aedeagus, left lateral aspect **F** same, ventral aspect **G** same, right lateral aspect. Scale bar: 0.1 mm.

rounded ridge and ventrally with a bifurcate projection directed basally. Shaft subapically on its right side with a sturdy movable spinose process which in repose is curved basally, its tip pointing dorsally. Distal part of aedeagus (flagellum) tubular, in repose bent dorsally and to right side, surpassing midlength of shaft, with a slender, spinose process, in repose directed basally, left laterally at ca. midlength of flagellum; visible part of ejaculatory duct rugose; phallotreme wide, located apically.

Female genitalia. 7th sternite with anterior margin convex, highly vaulted cephally, rounded, caudal/posterior margin medially expanding caudally, expanded portion obtusely angulate. Ovipositor ensiform, slightly curved dorsally, caudally surpassing anal tube with less than 1/3 of its total length; anal segment tubular, short, in lateral view ca. 2 × higher than long, lateral margins more or less parallel; 9th tergite caudally truncate, wax-secreting field distinctly limited, slightly concave, medially separated by a narrow, longitudinal membranous portion.

Etymology. The species epithet is a noun in nominative singular and refers to Theseus, one of the heroes in Greek mythology, friend of Ariadne. The gender is masculine.

Distribution. Adults known only from the type locality (Camino San Salvador), in the laurel forest in the huge landslide of El Golfo, at the northwest of El Hierro (Fig. 1). Endemic to El Hierro.

Ecology and behaviour. El Hierro is the youngest island in the Canary archipelago, and the youth of the terrain is visibly apparent in much of its territory. Fields of recent lava abound, and a large part of the soil is made up of volcanic deposits where fine ash or more or less coarse lava clinker predominate, or a mixture of both in highly variable proportions. In the central, western, and northern parts of the island, it is very common to find terrains formed by a layer of lava clinker covered by fine ash or an already formed, thin edaphic soil. The scoria layer contains a dense network of interstices and cracks (Fig. 2, top right), well isolated from changes in humidity and temperature from the outside by the overlying fine pyroclasts or soil covering it. This type of MSS was described for the first time in El Hierro and named as “volcanic MSS” (Oromí et al. 1986). Under these circumstances, the layer of pyroclasts maintains a high humidity level and a rather constant temperature throughout the year, which allows for the establishment of fauna adapted to subterranean life. This configuration of volcanic deposits constitutes the most common type of MSS in El Hierro, extending across large areas of the island. In Camino de San Salvador, where *Cixius theseus* n.sp. was discovered, the MSS was exposed when the terrain was cut to build a road (Fig. 2B). The location is in the laurel forest whose dominant trees are *Morella faya* (Aiton) Wilbur and *Erica canariensis* Rivas-Mart., Osorio and Wildpret, and herbaceous plants in the vicinity of the traps are *Pericallis murrayi* (Bornm.) B. Nord. and *Urtica morifolia* Poir. The traps were set over the talus of the road crossing the laurel forest, at 1230 m a.s.l. Although a good representation of the entire troglobiont fauna present on the island has been collected in nearby areas using MSS traps, only the capture of this new cixiid species should be noted in Camino de San Salvador.

Ecological classification. *Cixius theseus* displays a high degree of troglomorphy: compound eyes and ocelli absent, tegmina strongly reduced, vestigial wings as well as light, almost white body coloration. This blind and flightless species is most likely restricted to subterranean environments throughout its entire life cycle. According to the criteria provided by Sket (2008) and Howarth and Moldovan (2018 a, b) we regard *Cixius theseus* as an obligate cavernicole, or troglobiont.

Conservation status. Although only a few individuals of *Cixius theseus* are known, this new species apparently would not have conservation problems for several reasons: i) the volcanic MSS is widely distributed throughout the northern slope of the island, so

habitat availability is not a limiting factor; ii) in general, this entire slope of the island with laurel forest is well-preserved and there are no houses that could be contaminating the subsurface with sewage; iii) since cixiids feed by sucking fluids from roots, the presence of laurel forest in high density across this area ensures a constant food supply. The initial results from the MSS traps in San Salvador showed very poor capture of troglobitic species, which led us to their deactivation soon, a reason why very few specimens of this new species are known. However, *Cixius theseus* also clearly meets criterion D2 as in the case of *Cixius palmirandus*, so it should be classified as Vulnerable according to the IUCN criteria.

Remarks. From the type locality, 4 unpigmented, eyeless cixiid nymphs (III. and IV. instar) were collected, which are here preliminarily identified as *C. theseus* sp. nov. (IPNA). Morphologically very similar nymphs have been recorded from another locality („Mercader, MSS4; 27 Jan. 2012; H. López leg.“ and „Mercader, MSS3; 18 Jun. 2012; P. Oromí and H. López leg.“), 1075 m a.s.l. (27.71294456, -18.02217521), on the southern slope of the island, 2.3 km far from San Salvador. Whether these are conspecific with *C. theseus* cannot be confirmed on the basis of morphological characters alone. It remains to be investigated whether *C. theseus* sp. nov. is more widely distributed on El Hierro.

***Tachycixius gomerobscurus* Hoch & Oromí, sp. nov.**

<https://zoobank.org/98930191-9075-4A0B-85F9-8799BEFD79C8>

Figs 8 A, B, 9, 10A–G

Material examined. Holotype: SPAIN • male; Canary Islands, La Gomera, Reventón Oscuro, MSS T3; 28.12468504, -17.21638908; 2 Jan. 2012; P. Oromí leg. (50355 DZUL).

Paratypes: • Same data as holotype, except • 1 male, 1 female; 5 Feb. 2009; P. Oromí and H. López leg. (34924 DZUL) • 1 male (6962 DZUL), 2 males (7014 DZUL), 3 males (7074 DZUL); 30 Jun. 2009; P. Oromí and H. López leg. • 1 male; 1 Jul. 2009; P. Oromí and H. López leg. (34935 DZUL) • 2 males; T3; 4 Jan. 2010; P. Oromí leg. (7009 DZUL) • 1 female; 8 Jun. 2010; P. Oromí and H. López leg. (UMACI) • 1 male, 1 female; T1; 9 Jan. 2011; P. Oromí and H. López leg. (UMACI) • 1 male, 3 females; T1; 30 Jul. 2011; P. Oromí leg. (IPNA) • 1 male, 1 female; T3; 2 Jan. 2012; P. Oromí leg. (7038 DZUL) • 1 male, 1 female; T3; 26 Mar. 2015; P. Oromí leg. (UMACI) • 1 female; 17 Sep. 2015; P. Oromí leg. (DZUL) • 1 male; 31 Jul. 2024; P. Oromí leg. (IPNA: BC3166).

Additional material. • Same data as holotype, except • 3 nymphs V instar (6962 DZUL), 4 nymphs V instar; T1; 30 Jul. 2009; P. Oromí and H. López leg. (UMACI) • 3 nymphs V instar and 1 nymph IV instar; T3; 4 Jan. 2010; P. Oromí leg. (UMACI) • 1 nymph V instar and 1 nymph IV instar; T3; 8 Jul. 2010; P. Oromí and H. López leg. (UMACI) • 1 nymph V instar; 9 Jan. 2011; P. Oromí and H. López leg. (UMACI) • 1 nymph V instar; T1; 30 Jul. 2011; P. Oromí leg. (IPNA: BC2984) • 2 nymphs IV and V instar; T3; 2 Jan. 2012; P. Oromí leg. (IPNA: BC2982, BC2983) • 1 nymph V instar; T1; Jun. 2013; P. Oromí leg. (UMACI) • 2 nymphs III and IV instar; T1-4; 17 Nov. 2013; P. Oromí leg. (IPNA: BC2985, BC2986) • 1 nymph V instar; 17 Sep. 2015; P. Oromí leg. (UMACI) • 1 male; 31 Jul. 2024; P. Oromí leg. (IPNA: BC3165).



Figure 8. *Tachycixius gomerobscurus* Hoch & Oromí, sp. nov. **A** habitus male **B** head and thorax, dorsal aspect.

T1, T2, T3 are the different MSS traps set along ca. 100 m in the same location.

Diagnosis. In general appearance and in the overall configuration of male and female genital structures *Tachycixius gomerobscurus* sp. nov. resembles *T. crypticus* and *T. retrusus* from Tenerife, but differs in the following characters: shape of vertex: vertex short, anterior margin very shallowly rounded (vs strongly convex towards frons in *T. crypticus* and *T. retrusus*); colouration of tegmina: less vividly coloured than in *T. crypticus* and *T. retrusus*; reduction of hind wings much stronger than in *T. crypticus* and *T. retrusus*; male genitalia: caudal margin of anal segment medially strongly concave (vs shallowly concave in *T. crypticus* and straight in *T. retrusus*); shaft of aedeagus with 3 subapical movable spines (vs. 2 such spines in *T. crypticus* and *T. retrusus*); female genitalia: 9th tergite medioventrally deeply incised, membranous excavation acutely triangular (vs 9th tergite medioventrally only shallowly incised, membranous excavation dorsally shallowly rounded in *T. crypticus* and *T. retrusus*); 9th tergite with wax-secreting field medially with a short, but distinct median ridge (vs without such a ridge in *T. crypticus* and *T. retrusus*).

Description. Habitus. In general appearance resembling *Tachycixius crypticus* Hoch & Asche, 1993 and *T. retrusus* Hoch & Asche, 1993 from Tenerife, although less vividly coloured; weakly troglomorphic (i.e. hypogeomorphic, see Deharveng and Bedos 2018): compound eyes present, but small, tegmina covering most of the abdomen but not attaining tip of anal tube in the male, respectively tip of ovipositor in the female; hind wings strongly reduced, vestigial.

Body length. Male 3.8–4.05 mm (n = 4). Female 4.3–5.2 mm (n = 6).

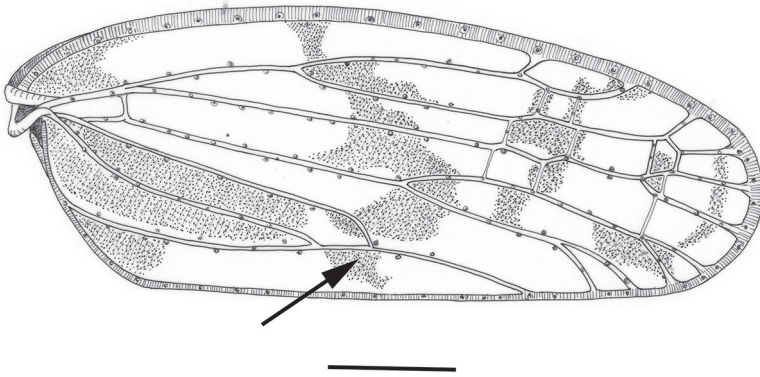


Figure 9. *Tachycixius gomerobscurus* Hoch & Oromí, sp. nov. Right tegmen (male). For meaning of arrow see text. Scale bar: 0.5 mm.

Colouration. Vertex, frons and head laterally light yellowish, with lateral carinae of vertex and frons and posterior margin of vertex slightly darker; antennae (pedicel) whitish; compound eyes reddish-dark brown; pro- and mesonotum light yellowish, otherwise thorax incl. Legs whitish, tips of lateral and distal spines of tibia, as well as distal spines of first and second metatarsal joints dark brown. Tegmina translucent, light yellowish, venation whitish, bases of setae along veins and margin of tegmen slightly darker, brownish; tegmen with anterior portion of triangle formed by cubitus posterior (CuP) and posterior margin of tegmen profusely brownish, and three irregularly limited, faint fuscous transverse bands: one at level of tegmen midlength, one at level of pterostigma, and one more or less parallel to distal margin (see remarks). Abdomen incl. genitalia light yellowish, or yellowish-brown, respectively.

Head. Vertex short, about $3.5 \times$ wider at base than medially long, anteriorly rounded, with a faint median carina, areolet small, slightly concave, medially separated by an obtuse median carina; vertex indistinctly separated from frons by an obsolete transverse carina. Frons $1.2 \times$ wider than medially high, with a distinct median carina, lateral carinae foliately produced laterally. Post- and anteclypeus with an obtuse median carina; together ca. $1.5 \times$ longer than frons. Frontoclypeal suture strongly arched. Compound eyes present, compared to epigeal *Tachycixius* species reduced in relative size, pigmented, lateral ocelli distinct, median frontal ocellus rudimentary. Rostrum elongate, well surpassing hind coxae, in males attaining anterior margin of 9th abdominal segment, in females attaining level of caudal margin of 9th tergite. Antennae with scape short, ring-like, and pedicel cylindrical, ca. $1.4 \times$ longer than wide, with sensory plaque organs arranged in several rows.

Thorax. Pronotum tricarinate, lateral carinae ridged and diverging laterally near posterior margin of pronotum; pronotum short, medially ca. $1.8 \times$ longer than vertex, and $1.7 \times$ wider than maximum width of head (incl. compound eyes), posterior margin concave, medially forming an obtuse angle. Mesonotum tricarinate, carinae faint, lateral carinae attaining posterior margin of mesonotum; mesonotum $1.2 \times$ wider than

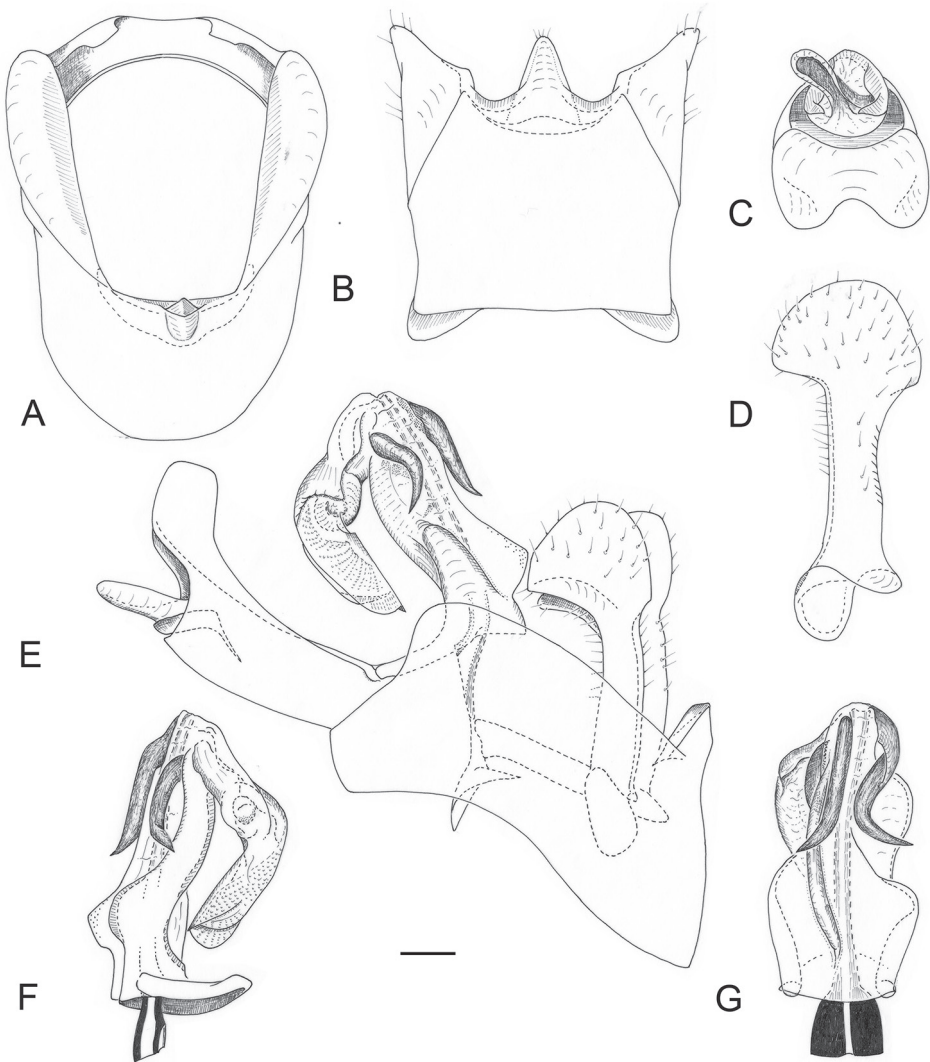


Figure 10. *Tachycixius gomerobscurus* Hoch & Oromí, sp. nov. Male genitalia **A** genital segment, caudal aspect **B** same, ventral aspect **C** anal segment, caudal aspect **D** left genital style, maximum aspect **E** anal segment, genital segment, aedeagus and genital styles, *in situ*, left lateral aspect **F** aedeagus, right lateral aspect **G** same, ventral aspect. Scale bar: 0.1 mm.

medially long, and medially $3.2 \times$ longer than pronotum. Tegulae small. Tegmina distally reduced, in both sexes attaining caudal margin of anal segment, ca. $2.5 \times$ longer than maximally wide; venation well developed, variable among specimens (in all specimens studied except for 1 female, the CuP vein does not connect to posterior margin of tegmen as is the case for most Cixiidae, but merges with PCu + A1 (= common stem of Y-vein, see Fig. 6, arrow), see remarks; basal cell closed, pterostigma faintly recog-

nizable; veins beset with or accompanied by numerous conspicuous bases of setae, on distal margin also between veins. Hind wings very small, vestigial, not surpassing posterior margin of metanotum. Metatibiae laterally in the majority of specimens studied with 3 small spines (variation: configurations 4/3 and 3/2 were observed in one female each), distally with 6 sturdy spines (in one female with 7 spines on one leg) (arranged in a row, lateral one strongest); metabasitarsus distally with 7–8 (bilaterally and individually variable), 2nd metatarsal joint distally with 7–8 spines (bilaterally and individually variable), each of the median 4 bearing one macroseta. Metabasitarsus slightly longer than 2nd and 3rd metatarsal joints together. Pretarsal claws short, stout, arolium small.

Male genitalia. Genital segment in caudal view ca. 1.3 × higher than wide, and in lateral view ventrally ca. 4.6 × longer than dorsally, caudal margins laterodorsally produced into 2 rounded lobes directed laterocaudally; medioventral process slender, triangular, dorsal surface with a faint median ridge. Anal segment elongate, narrow, in distal third bent ventrocaudally, in dorsal view ca. 2 × longer than wide at base, lateral margins in dorsal view more or less parallel, caudally of anal style converging, distal margin broadly rounded, ventral portion distally of anal style in caudal aspect strongly vaulted, with caudal margin medially concave; anal style elongate, slender. Genital styles narrow at base, distal third expanding dorsally, expanded portion caudally rounded, dorsally with an obtuse angle, medially concave. Aedeagus. Basal part of aedeagus (shaft) in proximal half wide, with three more or less compressed velum-like projections: one left laterally, extending from base to ca. midlength of shaft, one ventrally which is wide at base, narrowing at ca. midlength of shaft and extending from base almost to apex, and one right laterally which is broadly rounded and directed right laterocaudally. Shaft in distal half on right side with a compressed lobe extending right laterally, and subapically with 3 sturdy movable spinose processes: one left laterally, in repose curved dorsally, one ventrally, in repose directed basally, its tip pointing left laterally, and one right laterally, which is double-S-shaped, in repose curved basally and to right side. Distal portion of aedeagus (flagellum) well surpassing midlength of shaft, medially almost rectangularly bent and directed right laterally; without any spinose processes; distal portion of flagellum on ventral side expanding into a lobate, rounded protrusion, visible part of ejaculatory duct rugose, phallosome wide, exposed dorsally.

Female genitalia. Seventh sternite subtriangular, anterior margin broadly rounded, caudal margin medially straight; ovipositor ensiform, slightly curved dorsally, caudally slightly surpassing anal segment; anal segment tubular, short, stout, dorsoventrally only slightly depressed; ninth tergite caudally truncate, wax-secreting field indistinctly limited, shallowly concave, with a short, but distinct median ridge; 9th tergite medioventrally deeply incised, membranous excavation acutely triangular, attaining dorsal third of 9th tergite.

Etymology. The species epithet is an adjective in nominative singular and a combination of Gomera and *oscurus*, the Spanish word for *dark*, probably used to create the toponym of this shadowy location inside the laurel forest. The gender is masculine.

Distribution. Known only from the type locality, Reventón Oscuro, municipality of Hermigua, in Garajonay National Park (Fig. 1). Endemic to La Gomera.

Ecology and behaviour. The MSS in Reventón Oscuro and in other places of Garajonay National Park is of the colluvial type, originated by accumulation of stone fragments at the base of rocky walls, and covered over time by soil (Juberthie et al. 1980, Mammola et al. 2016). The three traps set in Reventón Oscuro are on a steep slope inside a dense, humid and moderately dark laurel forest at 1035 m a.s.l. with a thin but rich organic soil covering the colluvium. All traps were set very close to tree trunks in order to protect them from gravitational collapse, and the colluvium was rich in small roots throughout its sampled depth (70–80 cm). La Gomera is the only island of the archipelago without lava tube caves due to the absence of volcanism in the last 2.5 Ma, but the MSS in the laurel forest is rich in troglobionts (Medina and Oromí 1990, Pipan et al. 2010, Gilgado et al. 2011, García et al. 2020). In this sense, Reventón Oscuro is the most diverse (13 species) among all Canary Island's MSS stations, as well as the most abundant in individuals (PO, HL unpublished data).

Ecological classification. *Tachycixius gomerobscurus* displays several troglomorphic characters, although not as strongly as *Tachycixius lavatubus* Remane & Hoch, 1988, *Cixius palmirandus* or *C. theseus*: the integument shows remnants of brownish pigmentation, the compound eyes are reduced in size, yet present, and ommatidia are pigmented; the lateral ocelli are distinct, the frontal ocellus is rudimentary. The tegmina are reduced distally, and hind wings are vestigial, much shorter than in the other MSS-dwelling species *T. crypticus* and *T. retrusus*. Although there are no observations on the behaviour of the species, we assume that individuals are unable to fly, but may be able to perceive visual input. As *T. gomerobscurus* has been collected from traps in the MSS, and given the presence of reduced but pigmented eyes, little is known about its behaviour. Despite its comparatively mild degree of troglomorphy, we assume that *T. gomerobscurus* is restricted to subterranean environments, and we therefore regard it preliminarily as an obligate hypogeomorphic troglobiont.

Conservation status. Over the past 15 years, nearly 40 individuals (both adults and nymphs) of this new species have been collected using MSS traps baited with liver or blue cheese. These individuals probably fell into the traps by chance rather than being attracted to the bait, as these planthoppers feed by sucking fluids from roots. The MSS site of Reventón Oscuro is the location in the Canary Islands where we have captured the largest number of troglobitic planthoppers using MSS traps, and the number of captures has remained relatively constant over the years. All evidence suggests that this species likely has a high density of individuals in this area. The region where this new species has been collected is a very well preserved national park, where a dense laurel forest ensures a consistent food supply in the subterranean habitat (roots). The limited known distribution of *T. gomerobscurus* on La Gomera is primarily due to the scarce sampling performed in the MSS at other sites on the island, being uncertain whether or not it has a broader distribution. However, although this species lives in a well-preserved habitat where it could apparently have a good population size, the IUCN recommends classifying it as Vulnerable according to criterion D2, since only one population is known distributed in a small area, which could completely disappear or enter a higher threat category if such a limited area were suddenly affected by impacts of human activities and/or stochastic events.

Remarks. The peculiar venation pattern observed in all but one specimens studied (the CuP merging with PCu + A1, i.e., the common stem of the „Y“ -vein instead of connecting to the posterior margin of tegmen) is very unusual not only for Cixiidae, but the Fulgoromorpha. It is likely a mutation in connection with the distal reduction of the tegmen, which has affected the overall venation pattern.

Some variation is observed in the colouration of body and tegmina: 2 specimens, 1 male and 1 female (coll. 2 Jan. 2012; T3) show very weak pigmentation of body and tegmina, and appear to have freshly molted into adult.

Meenoplidae Fieber, 1872

Meenoplus skotinophilus Hoch & López, sp. nov.

<https://zoobank.org/7FA676EF-33CF-4D9C-A0DC-51C57D897EDE>

Figs 11A, B, 12A, B, 13A–G, 14A, B

Material examined. Holotype: SPAIN • male; Canary Islands, El Hierro, Cueva de Guinea; 27.77448369, -17.99866804; 22 Mar. 2021; H. López and C. Andújar leg. (IPNA). **Paratypes:** SPAIN • 2 males, 10 females; same data as holotype; (1♂ 50356 DZUL; 3♀ 50357, 50358, 50359 DZUL; 1♂7♀ IPNA).

Additional material. SPAIN • 14 nymphs IV instar, 5 nymphs V instar; same data as holotype; (16 nymphs DZUL; 3 nymphs (IPNA: BC1267, BC1268; BC1269)).

Diagnosis. *Meenoplus skotinophilus* is similar in general appearance and degree of troglomorphy to *Meenoplus claustrorophilus* from La Palma, but differs from this species by the distally stronger reduced tegmina and lighter overall pigmentation. From the other two cavernicolous *Meenoplus* species on El Hierro (*M. cancavus* und *M. charon*), it differs distinctly by its degree of troglomorphy (compound eyes present, tegmina and wings well developed, tegmina surpassing tip of abdomen). While the general configuration of the male and female genitalia is similar in all four species (*M. claustrorophilus*, *M. skotinophilus*, *M. cancavus* und *M. charon*), *Meenoplus skotinophilus* differs from these by the following characters of the male genitalia: ventrocaudal lobes of anal segment with median tips subacute and well separated (vs rounded and nearly apposed in the other species), aedeagus with apical margins of phallosome angulate (vs rounded in the other species), and of the female genitalia: ventral valvulae distally with a beak-shaped, sturdy and acute tip pointing mediad (vs bearing a minute tip), and with proximal portion broadly lobate and finely serrate (vs rounded and smooth in the other species).

Description. Habitus. Troglomorphies weakly defined except for compound eyes and pigmentation, tegmina and wings well developed, in repose surpassing the tip of the abdomen. In general appearance, intermediate between epigeal Meenoplidae and strongly troglomorphic species, such as e.g., *Meenoplus cancavus* Remane & Hoch, 1988 and *M. charon* Hoch & Asche, 1993.

Body length. Male 2.8–2.9 mm (n = 3). Female 3.2–3.5 mm (n = 6).

Colouration. Head, pro- and mesonotum as well as male and female genitalia yellowish-brown, otherwise thorax und pregenital abdomen white. Compound eyes red. Teg-

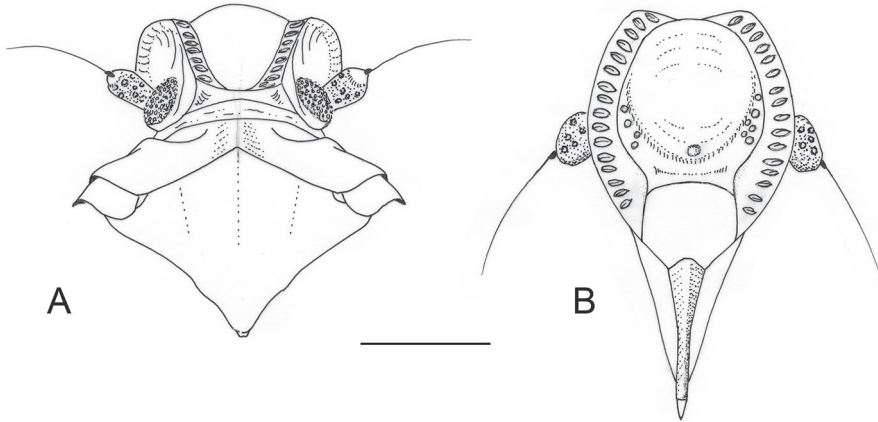


Figure 11. *Meenoplus skotinophilus* Hoch & López, sp. nov. **A** head and thorax, dorsal aspect **B** head, ventral aspect. Scale bar: 0.5 mm.

mina translucent, pale stramineous in males, light brown in females; venation as well as areas along veins and between sensory pits yellowish-brown. Wings hyaline, venation yellowish-brown. Legs stramineous, apical spines of tibia and tarsal joints I–II, light brown.

Head. Vertex very short, ca. 12 times wider than medially long, distinctly separated from frons by a ridged transverse carina. Frons strongly convex, anterior portion bulbous, about as wide as medially high, at and below level of antennae with a short row of small and hardly visible sensory pits irregular in number (4–6). Lateral carinae of frons foliately ridged and directed anterolaterad, anteriorly with a distinct row of large sensory pits; lateral lamelliform carinae continuing onto postclypeus. Frons smooth, without median carina, postclypeus shallowly, anteclypeus steeply vaulted. Compound eyes small, lateral ocelli vestigial, median frontal ocellus strongly reduced, its former position marked by a light circular spot at the lower portion of the frontal bulbous area. Scape short, ring-like, pedicel cylindrical, ca. 1.7 times longer than wide.

Thorax. Pronotum medially about 3.5 times the length of vertex, posterior margin obtusely angulate; pronotum weakly tricarinate, median carina very feeble. Tegulae, tegmina and wings well developed; tegmina distally surpassing tip of abdomen with ca. 1/5 their total length. Tegmen with rows of sensory pits along the distal part of the costal vein, along ScP+R (+Ma), RP (+MA) and along PCu, A1, and their common stem PCu + A1 („Y-vein“). Metatibiae laterally unarmed, with 8 apical teeth. First metatarsal joint with 7 apical teeth, second metatarsal joint with 6 apical teeth.

Male genitalia. Genital segment in lateral aspect ventrally ca. 3 times as long as dorsally. Anal segment distally produced into two ventrocaudal lobes which converge medially, their median tips subacute and well separated from each other. Genital styles slender, narrow throughout, apically rounded, gently curved dorsad. Aedeagus tubular, stout, with phallosoma apically and dorsocaudally exposed, apical margins dorsally bluntly angulate.

Female genitalia. Strongly reduced, ventral valvifers produced into a rounded lobe; ventral valvulae with distal portion „bird-head-shaped“, i.e., caudally rounded

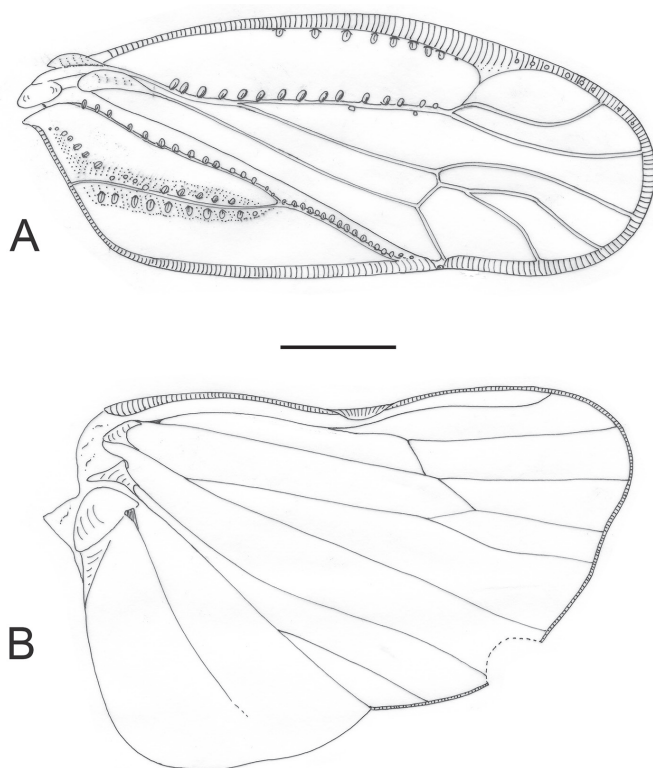


Figure 12. *Meenoplus skotinophilus* Hoch & López, sp. nov. **A** tegmen **B** wing. Scale bar: 0.5 mm.

and medially with an acute tip pointing mediad, and with proximal portion broadly lobate, with median margin straight and finely serrate, apposed.

Molecular identification. Mitochondrial COI barcode sequences of 635 pb were obtained for three individuals of *Meenoplus skotinophilus* (specimen codes BC1267, BC1268 and BC1269). These individuals have identical barcode sequences, so no interpopulation genetic divergence has been detected. Either in BOLD or GenBank, no matches with similarity values greater than 85% were detected, so the genetic information that we supply is actually new for the genetic lineage of the group of species that may belong *Meenoplus skotinophilus*. The sequences were deposited in GenBank (accession numbers PQ530856, PQ530856 y PQ530856), with the following base composition:

```
AATGAGCCAGATTAATAGGTATAACAAGAAGAATAATTATTCGAATT-
GAATTAATACAACCTGGTTCAATAATTAAAAATGATCAAATTTATA-
ACTCAATTGTTACATCACATGCATTCATTATAATTTTTTTTTTCAGT-
TATACCCATCCTAATCGGTGGATTGGAAATGACTTGACCTCTAAT-
GATTGGAGCACCTGATATAGCATTCCCACGAATAACAATATAAGCTTCT-
GAATATTACCTCCATCACTAATACTATTAATTTTCAGTTCATTTTCAG-
GTTTCAGGTACAGGTACAGGATGAACAATTTATCCACCATTAT-
```

CAAGAATTCCTGCACATTCTGGCCCATCTACTGACTTATC-
 TATCTTTTCCCTTCATATAGCAGGTGTAAGATCAATTCTAGGAG-
 CAATTAATTTTCATTTCAACTATTATTAATATACGACCTAAAATAATAA-
 CAATAGAAAAAATACCCCTATTTTGCTGATCAATTTTCATTACAG-
 CAATTTTACTTCTTCTATCATTACCTATTTCTTGCAGGAGCAATTAC-
 TATACTATTAAGTATCGAACTTTAATACATCATTTTTGGATCCAACAG-
 GAGGAGGAGACCCTATTTTATATCAACATTTATTT

Etymology. The species epithet is an adjective in nominative singular and a combination of the Greek words „skótos“ (= darkness) and „phílos“ (= friend). The gender is masculine.

Distribution. The species is known only from the type locality, Cueva de Guinea, municipality of Frontera (Fig. 1). Endemic to El Hierro.

Ecology and behaviour. *Meenoplus skotinophilus* has been discovered in a lowland area of Frontera with a wide lava flow seemingly originating from the base of Tibataje cliff and extending towards the sea. The point from which the lava flow emerged is apparently clear, but no volcanic cone can be seen there, probably being buried under abundant sediment dragged from the cliff. In the upper part of the lava flow, close to the cliff, there is a complex of lava tubes, mostly unconnected but clearly formed during this eruption. One of them is Cueva de Guinea, a hardly 25 m long lava tube with a small entrance on the roof. At first the floor is rocky with scattered stones fallen from the ceiling, while in the last wider room clayish sediments cover the original substrate. The humidity is high and there are many roots attached to the walls and hanging from the ceiling. All this creates a good environment for the establishment of a community of invertebrates with some troglobitic species, like blind weevils and spiders, actually under study, besides a rich population of *Meenoplus skotinophilus* n. sp. around the roots. Also, American cockroaches (*Periplaneta americana*) were observed, both living specimens and remains. Outside the cave the vegetation is typical of dry areas and lava flows at low altitudes, where *Euphorbia lamarckii* Sweet, *Schizogyne sericeae* (L. f.) DC. and *Rumex lunaria* L. predominate.

Ecological classification. *Meenoplus skotinophilus* displays several troglomorphic characters, such as small compound eyes, reduced ocelli, and light, yellowish-white body coloration. Tegmina are reduced distally, but wings are well developed. Although there are no observations on the behaviour of the species, we assume that individuals may be able to perceive some visual input, and may have retained the ability of some, even if not sustained flight. According to the degree of troglomorphy, we assume that *Meenoplus skotinophilus* is restricted to subterranean environments, and we therefore regard it preliminarily as an obligate cavernicole or troglobiont, but of the hypogeomorphic type.

Conservation status. The area surrounding the cave entrance is part of an archaeological complex transformed into an open-air ecomuseum, which features reconstructed homes of the island's earliest inhabitants as well as those of later colonizers. The site also includes a center for the rehabilitation of an endangered endemic giant lizard and a natural cave that has been adapted for tourist visits. The volume of visitors is significant, and all facilities are equipped with bathrooms without connection to a sewage system, the wastewa-

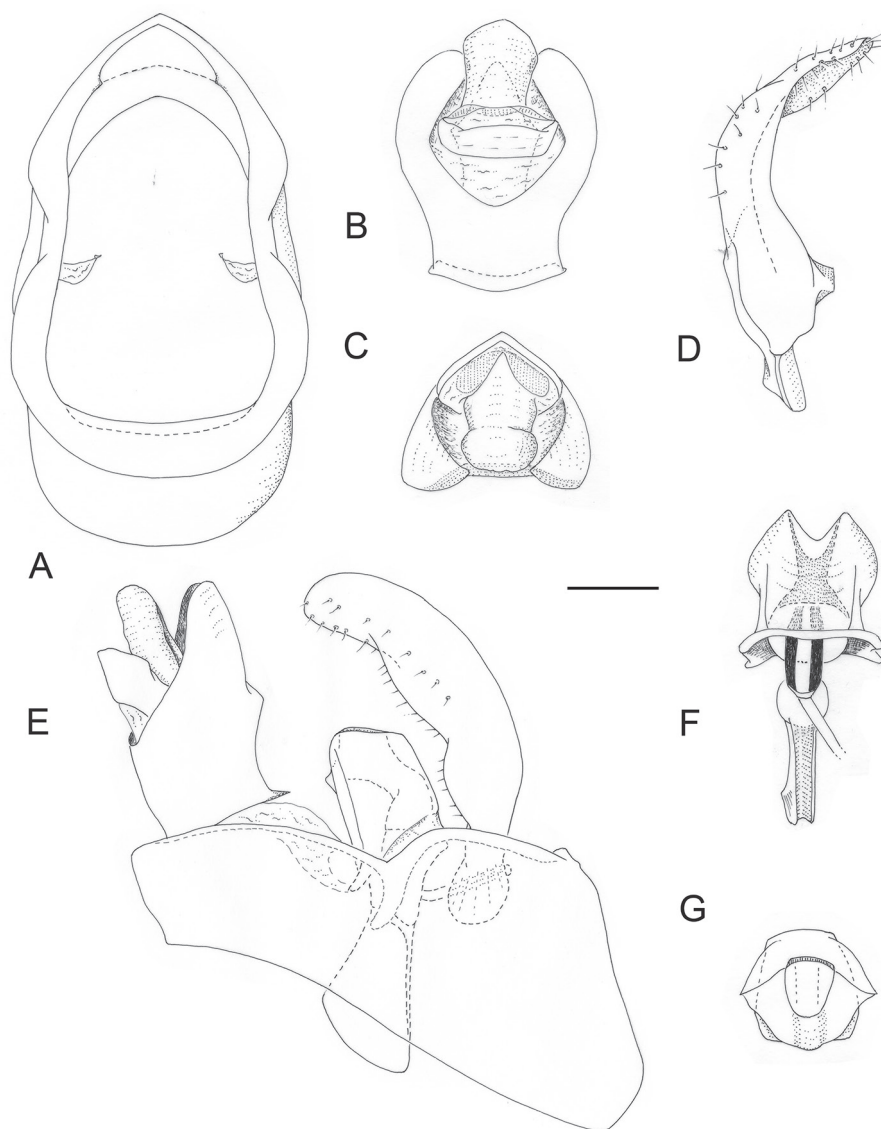


Figure 13. *Meenoplus skotinophilus* Hoch & López, sp. nov. Male genitalia **A** genital segment, caudal aspect **B** anal segment dorsal aspect **C** same, caudal aspect **D** left genital style, ventral aspect **E** anal segment, genital segment, aedeagus, genital style, *in situ*, left lateral aspect **F** aedeagus, ventral aspect **G** aedeagus, caudal aspect, view on phallotreme. Scale bar: 0.1 mm.

ter being discharged directly into underground wells. This practice gradually contaminates the underground environment, promoting the colonization of invasive species such as *Periplaneta americana* in both Cueva de Guinea and the nearby showcave. The deterioration of the subterranean environment poses a potential threat to native subterranean fauna, which

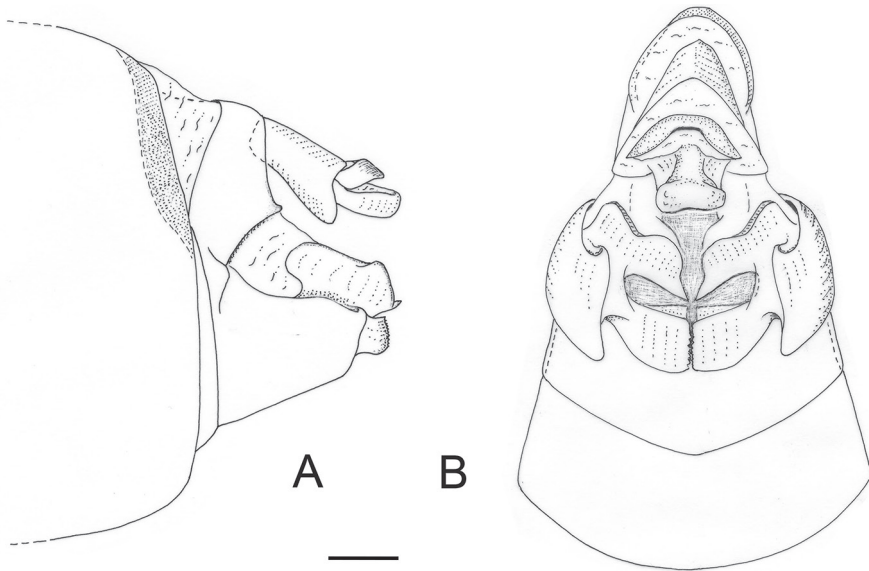


Figure 14. *Meenoplus skotinophilus* Hoch & López, sp. nov. Female genitalia **A** left lateral aspect **B** caudal aspect. Scale bar: 0.1 mm.

may either be displaced by invasive species or find their habitat unsuitable for survival. However, in the only sampling conducted in Cueva de Guinea *Meenoplus skotinophilus* was found abundantly, apparently with no serious threats at that time. To accurately apply the IUCN evaluation criteria to this species, it is essential to monitor its population in the short- to medium-term to determine whether it is indeed declining due to the aforementioned threats. However, *M. skotinophilus* should be included in the Vulnerable category based on IUCN criterion D2. In this case this is well justified given the intense tourist activity in the location where the only known population of this new species is found, being expected a strong negative pressure on its conservation in the short-medium term.

Remarks. Some nymphs of this new species have been selected for an ongoing genetic study with the aim of understanding the phylogenetic relationships between the three endemic species of *Meenoplus* present in El Hierro. This is a striking situation since it implies multiple speciation in the subterranean environment of a geologically very young island (1.12 Ma) in contrast to the absence of this genus on more mature islands rich in underground environments, such as Tenerife.

Key to the cavernicolous Fulgoromorpha species of the Canary Islands: adults of Cixiidae and Meenopidae

The key is based on morphological characters of external structures and male genitalia, and geographic distribution. For species described here figure numbers are given in brackets, for species described by Remane and Hoch (1988), Hoch and Asche (1993)

and Hoch et al. (2012) compare figures in original descriptions. All species display troglomorphies in varying degrees, such as the reduction of compound eyes (small to absent), tegmina, wings, and bodily pigment, and occur in cryptic or subterranean habitats (lava tubes, MSS).

- 1 Head and tegmina without sensory pits: Cixiidae 2
 – Head laterally and tegmina with sensory pits: Meenoplidae 12
 2(1) Apical margin of forewing (tegmen) without tubercles between apical veins:
Cixius Latreille, 1804 3
 – Apical margin of forewing (tegmen) with tubercles also between apical veins:
Tachycixius Wagner, 1939 9
 3(2) *Cixius* species from La Palma. All species of very similar habitus (as in e.g.,
 Fig. 4): strongly troglomorphic (absence of compound eyes and ocelli, light
 bodily coloration, and strongly reduced tegmina and wings), and similar
 configuration of the male genitalia: aedeagus shaft tubular, with 2 movable
 spinose process near apex, one right laterally and one left laterally; shaft ven-
 trally near base with one or two short rigid spines directed towards apex; flag-
 gellum of aedeagus slender, apically with or without a spinose process; geni-
 tal segment with medioventral process broadly triangular, apically slightly
 notched 4
 – *Cixius* species from El Hierro. All species with similar habitus, i.e. the degree
 of troglomorphy (see e.g., Fig. 6), and similar general configuration of male
 genitalia, e.g., medioventral process of genital segment broadly triangular,
 with blunt tip, anal segment elongate and distally bent ventrocaudally; shaft
 of aedeagus ventrally compressed, with a massive bifurcate projection direct-
 ed basad, and right laterally with a single movable spinose process near apex.
Cixius nycticolus Hoch & Asche, 1993 was described from 2 females and is
 thus not included in the key 8
 4(3) Flagellum of aedeagus with spinose process at apex 5
 – Flagellum of aedeagus without spinose process at apex 7
 5(4) Apical spinose processes of aedeagus shaft ventrally not exceeding midlength
 of shaft 6
 – Apical spinose processes of aedeagus shaft ventrally exceeding midlength of
 shaft, both processes in repose directed left laterally
 *Cixius tacandus* Hoch & Asche, 1993
 6(5) Aedeagus shaft more or less tubular ... *Cixius palmeros* Hoch & Asche, 1993
 – Aedeagus shaft ventrally distinctly compressed
 *Cixius raticolus* Hoch & Asche, 1993
 7(4) Aedeagus shaft tubular throughout, ventrally with two short spinose pro-
 cesses near base, the right lateral one of which is serrate
 *Cixius pinarcoladus* Hoch & Asche, 1993
 – Aedeagus shaft with a distinct constriction at ca. midlength, ventrally with
 one rigid, apically bifurcate spine ... *Cixius palmirandus* sp. nov. (Figs 4, 5)

- 8(3) Anal segment with distal margin rounded; aedeagus shaft with right lateral movable spine slender, in repose gently curved, directed basad, and bifurcate projection in ventral aspect with both spines equally long, left spine with an additional denticle near fork; flagellum of aedeagus not bearing any spinose processes ***Cixius ariadne* Hoch & Asche, 1993**
- Anal segment with distal margin medially shallowly incised; aedeagus shaft with right lateral movable spine sturdy, hook-shaped, with tip pointing baso-dorsally, and bifurcate projection in ventral aspect with left lateral spine longer than right lateral one, without any additional denticles; flagellum of aedeagus bearing a slender spinose process, arising slightly distad of midlength of flagellum and in repose directed basad ***Cixius theseus* sp. nov. (Figs 6, 7)**
- 9(2) *Tachycixius* from La Gomera... ***Tachycixius gomerobscurus* sp. nov. (Figs 8–10)**
- *Tachycixius* from Tenerife **10**
- 10(9) Strongly troglomorphic: body whitish, compound eyes and ocelli absent; tegmina short, venation reduced, in dorsal aspect not covering pregenital abdomen, wings vestigial. Male genitalia with aedeagus shaft bearing three subapical movable spinose processes near apex, one arising left laterally, and two right laterally..... ***Tachycixius lavatubus* Remane & Hoch, 1988**
- Mildly troglomorphic: compound eyes present, small, tegmina longer than maximally wide, venation well developed, in dorsal aspect covering pregenital abdomen, wings reduced, ca. half the length of tegmina, body pale yellow with brownish portions, tegmina with brownish pigmentation pattern. Male genitalia with aedeagus shaft bearing two subapical movable spinose processes right laterally near apex..... **11**
- 11(10) Male genitalia: anal segment with ventrocaudal margin medially concave; genital style club-shaped, with caudal margin forming a blunt triangle; shaft of aedeagus subapically on its left side with a small membranous velum ***Tachycixius crypticus* Hoch & Asche, 1993**
- Male genitalia: anal segment with ventrocaudal margin straight; genital style spoon-shaped with caudal margin evenly rounded; shaft of aedeagus subapically on its left side with a small ear-shaped projection..... ***Tachycixius retrusus* Hoch & Asche, 1993**
- 12(1) Troglomorphies weakly defined except for eyes and pigmentation; tegmina and hind wings well developed, tegmina in repose surpassing tip of abdomen, compound eyes present, but small..... **13**
- Strongly troglomorphic: Compound eyes and ocelli missing, vertex and frons smooth, tegmina reaching but not surpassing tip of abdomen, venation reduced, wings vestigial..... **14**
- 13(12) From La Palma ***Meenoplus claustrophilus* Hoch & Asche, 1993**
- From El Hierro ***Meenoplus skotinophilus* sp. nov. (Figs 11–14)**
- 14(12) From Gran Canaria..... ***Meenoplus roddenberryi* Hoch & Naranjo, 2012**
- From El Hierro **15**

- 15(14) Male genitalia with aedeagus in lateral aspect evenly rounded
 *Meenoplus cancavus* Remane & Hoch, 1988
 – Male genitalia with aedeagus in lateral aspect apically almost truncate
 *Meenoplus charon* Hoch & Asche, 1993

Discussion

Taxonomic diversity, or why are there so many cave planthopper species on the Canary Islands?

So far, a total of 70 subterranean planthopper species from 6 families (Cixiidae, Meenoplidae, Kinnaridae, Delphacidae, Hypochthonellidae and Flatidae) have been documented worldwide (Bourgoin 2024; Le Cesne et al. 2024). With now 17 documented species of cave-adapted planthoppers, the Canary Islands hold the highest number of subterranean planthoppers of any region worldwide, representing ca. $\frac{1}{4}$ of all known species.

Their taxonomic and geographic distribution as well as putative epigean relatives is shown in Suppl. material 1: table S1. It is striking that the majority of species (12 out of 17) occur on the youngest islands, La Palma and El Hierro.

The primary habitat of troglobitic planthoppers is the deep cave zone where permanent darkness, stable temperatures and stable high relative humidity prevail (Howarth 1983), and where roots of surface vegetation penetrate the overlying rock and are abundant. Nymphs as well as adults rely on these roots for nutrition. The roots also serve as transmission channels for the species-specific vibrational signals which planthoppers produce in order to bring the sexes together for mating (see Hoch and Howarth 1993, and references therein). Lava tubes with intact and extended deep cave zones are rather short-lived, and usually do not persist longer than a few hundred thousand years (Howarth 1973). They form during the active lava flow phase and are colonized by pioneer plants on the surface soon after cooling of the newly formed rock (Howarth 1983). On El Hierro and La Palma with their maximum ages of 1.1 to 1.7 million years (Carracedo and Troll 2016) thus extended areas of suitable cave planthopper habitat exist, providing ample opportunities for cave-adaptation of epigean ancestral species.

On both islands volcanic activity prevails, and in La Palma the most recent eruption in 2021 along the Cumbre Vieja ridge not only created a new volcano, Tajogaite, but certainly many new lava tubes. Lava tube entrances in younger flows which have not yet developed a dense vegetation cover, however, are also easier to locate and access by researchers, hence a certain degree of collectors' bias cannot be excluded.

Hoch and Asche (1993: 99) hypothesized „that in older and volcanically inactive islands progressive soil formation and erosion have presumably filled in the mesocaverns and dissected the cave passages causing much of the primary habitat of

rhizophagous troglobites to disappear“. The subsequent discovery of *Meenoplus roddenberryi* in Gran Canaria in 2012, however, challenged this view. *Meenoplus roddenberryi* specimens were found in a small, 30 m long artificial water mine, at ca. 1100 m a.s.l, embedded in deposits of basaltic rocks of an estimated age of 3.7–2.8 Myr (Cueto et al. 1990). This indicates that troglobitic planthoppers may retreat into the interconnected cracks and crevices upon the decay of larger caves. It has occurred much the same in La Gomera where neither lava tube caves nor modern MSS of the volcanic type exist due to the lack of recent volcanism (Medina and Oromí 1990, Ancochea et al. 2006). But most of these ancient terrains had been covered by recent basaltic lavas at the time, with macrocaverns suitable for the presence of proper cave-dwelling planthoppers, probable ancestors of the current ones occurring in colluvial MSS. Anyway, given the high diversity of allopatric species in El Hierro and La Palma, it is expected that more new species might be discovered. In fact, we have knowledge of additional troglobitic planthoppers from Gran Canaria, Tenerife and La Palma, hitherto represented exclusively by nymphs and thus not identifiable to species level. We also have indications that the troglobiont cixiid species *T. lavatubus*, widespread on Tenerife, may constitute a complex of various cryptic species in the geologically young areas of the island (Hoch, Oromí, López, unpublished data).

Island colonization and cave adaptation

In the present-day epigeal fauna of the Canary Islands the Cixiidae are represented by few taxa: *Cixius palmensis* Lindberg, 1960 endemic to La Palma; *Tachycixius canariensis* Lindberg, 1954 endemic to Tenerife and to be confirmed in Gran Canaria; *Hyalesthes* (with one widespread and several endemic species, Hoch and Remane 1985); and *Duilius seticulosus* (Lethierry, 1874) from Gran Canaria and Fuerteventura (Oromí et al. 2010; Bourgoïn 2024). Of these genera, only *Cixius* and *Tachycixius* have given rise to species that permanently inhabit subterranean environments (Hoch and Asche 1993). Hitherto, no epigeal Meenoplidae have been documented from any of the Canary Islands.

The distribution of cavernicolous planthopper species of the Canary Islands and potential epigeal relatives is shown in Suppl. material 1: table S1.

Based on morphological information, we hypothesize that in the Cixiidae at least five to six, and maximally as much as 12 successful underground colonization events have taken place.

In the Cixiidae, the minimum number are: 3 on Tenerife (*Tachycixius lavatubus*; *T. crypticus*; *T. retrusus*), 1 on La Gomera (*Tachycixius gomerobscurus*), 1 on La Palma (*Cixius palmeros* + *C. pinarcoladus* + *C. ratonicus* + *C. tacandus* + *C. palmirandus*) and 1 on El Hierro (*C. ariadne* + *C. nycticolus* + *C. theseus*).

On Tenerife, *T. crypticus* and *T. retrusus* seem to have evolved after a common *T. canariensis*-like ancestor, but very probably represent two separate subterranean invasions, given that all troglobitic arthropods from the Anaga peninsula are always local endemisms allopatric to other hypogean species from the rest of the island; the highly

different geologic origin and age of Anaga have somehow isolated its subterranean environments and, consequently, promoted the formation of its own fauna (Oromí and Martín 1992). The morphological similarity between these three species suggests a closer relationship (Hoch and Asche 1993); however, without a DNA-based molecular phylogeny it is impossible to determine which scenario underlies the current situation.

Also, for the five cavernicolous *Cixius* species on La Palma which are morphologically similar to each other, it cannot be determined at this point whether they represent five separate cave invasions, or whether the differentiation occurred subsequently to cave adaptation of a single species, which may or may not have been similar to *C. palmensis*, the only present-day epigean representative of the genus.

For the troglobitic *Cixius* species on El Hierro, *C. ariadne* and *C. theseus*, which are morphologically similar to each other, but clearly representing a lineage separate from the troglobitic *Cixius* species on La Palma, no epigean relative could yet be identified (*C. nycticolus* is not assessable due to the lack of information on male genital morphology). Also, for these two species it cannot be assessed on the basis of morphological information alone whether cave adaptation occurred once or twice.

In the Meenoplidae, the situation is even more puzzling. Albeit epigean species have not been reported from the Canary Islands, morphological information suggests that there must have been at least two lineages colonizing the Islands: one on Gran Canaria (ancestral to *Meenoplus roddenberryi* Hoch & Naranjo, 2012) and (at least) one on La Palma and El Hierro (ancestral to *Meenoplus claustrophilus*, *M. cancavus*, *M. charon* und *M. skotinophilus* which display high similarity in male genital characters). It is worth noting that these are the only three islands in the archipelago hosting *Collartida* (Hemiptera: Reduviidae) trogllobionts, another genus without epigean representatives (Davranoglou et al. 2022).

For the cavernicolous Meenoplidae we assume 3–4 underground colonization events: one on Gran Canaria (*M. roddenberryi*), one on La Palma (*M. claustrophilus*), one or two on El Hierro (*M. cancavus*, *M. charon*, *M. skotinophilus*). It remains uncertain whether *M. cancavus* and *M. charon* are the result of separate cave invasion events, or whether speciation occurred subsequent to cave adaptation. Both species are strongly troglomorphic and differ considerably in external morphology from the less troglomorphic *M. skotinophilus*.

The *Tachycixius* species occurring in colluvial MSS from the laurel forest (*T. gomeroobscurus* from La Gomera, *T. retrusus* and *T. crypticus* from Tenerife) fit with the hypogeomorphic morphotype (weakly troglomorphic, see Deharveng and Bedos 2018), while *T. lavatubus* occurring in caves of Tenerife is strongly troglomorphic. However, all the *Cixius* species (from La Palma and El Hierro), either inhabiting caves or the MSS, are highly troglomorphic. This pattern is not only true for planthoppers: many hypogean species from other groups (beetles, cockroaches, spiders) occurring in the Anaga peninsula (NE Tenerife) and La Gomera are always less troglomorphic than other congeneric species that live in more modern terrains of Tenerife, either in caves or in modern MSS (there are no recent terrains in La Gomera) (Medina and Oromí 1991; Hernández and Oromí 1993; Martín et al. 1999; Frisch and Oromí 2006).

A possible explanation is that the colluvial MSS from La Gomera and Tenerife are in old terrains covered by deep, organic rich soil inside a mature laurel forest, while in younger islands like La Palma and El Hierro any MSS is of volcanic type (Oromí et al. 1986) with less evolved soil upon and much scarcer organic matter. We hypothesize that selective pressure to evolve towards troglomorphism must be lower in rich colluvial MSS and higher in poorer volcanic MSS and lava tubes. The degree of troglomorphism does not depend on the age of the island, but on that of certain terrains within each island and their corresponding subterranean habitats.

Zoogeographic pattern and evolutionary process

In the present-day most of troglobitic planthoppers on the Canary Islands have no extant close epigeal relatives, and accordingly, are relicts, i.e. „persistent remnants of formerly widespread faunas ... existing in certain isolated areas or habitats“ (Lincoln et al. 1982).

Although current knowledge does not allow to determine whether initial cave adaptation was driven by allopatry (extinction of closely related epigeal populations: see *climatic relict hypothesis*, as postulated by e.g., Vandel 1964, or Barr 1968) or parapatry (by adaptive shift of troglomorphic populations in order to exploit novel food resources, as suggested by Howarth 1981, see also Howarth et al. 2019), it is clear that at some point, Meenoplidae must have been represented in the epigeal fauna of the Canary Islands. It is unlikely that epigeal Meenoplidae are still extant, but have not yet been recorded, as the Fulgoromorpha fauna of the Canary Islands can be regarded as well known (see Bourgoin 2024: www.flow.hemiptera-databases.org, version 8, last updated 2024-01-04). Hence it is rather more likely that the cavernicolous Meenoplidae of Gran Canaria, La Palma and El Hierro, as well as the cavernicolous Cixiidae from La Gomera and El Hierro, and *par-tim* of Tenerife (*T. lavatubus*) are indicative of an ancient fauna which is now extinct. This is a relatively common pattern concerning many other genera of a variety of arthropod groups represented in these islands only by subterranean adapted species (Oromí 2004).

Conservation

All cave-planthopper species of the Canary Islands are single-island endemics, and known from few, in most cases a single location, and from few specimens each.

According to the IUCN Red Data Book categories they classify as *vulnerable*, due to their narrow range and specialized habitat as well as their presumed small population size. Consequently, conservation efforts need to concentrate on the preservation of areas where cave planthoppers are known to exist, on the surface as well as underground.

Major threats to the cave environment are urbanization and development which may result in the destruction of the caves proper, but also alter the surface conditions by road construction, and loss of vegetation. Deposits of sanitary and chemical waste and water pollution may be harmful for cave organisms, including planthoppers. Even more disturbing are records of increasing periods of extreme droughts which have occurred over the past several years. Consequently, the stable, saturated atmosphere which is essential

for obligate terrestrial troglobionts (Howarth 1983) is no longer maintained in the larger cave passages as it has happened in Cueva de la Curva (El Hierro), from where *Cixius ariadne*, *Meenoplus charon* and two troglobitic weevils were exclusively known but are becoming very scarce due to breakage of the end of the lava tube by loader machines working on the surface (H. López and P. Oromí, personal observation). Cave planthoppers may be able to cope with short-term adverse conditions by retreating into the smaller crevices of the MSS, which are less prone to desiccation. Long-term climate change, however, will have lasting indirect and direct influence on the subterranean environment (Howarth et al., in press). Increasing temperatures and lower precipitation will cause alteration of surface plant communities, and plant species which provide adequate roots for food supply may vanish. Sporadic observations indicate that cave planthoppers may be temperature sensitive (Hoch, personal observation on troglobitic planthoppers in Hawaii), and thus, increasing average annual temperatures may result in their extirpation.

Perspectives

Although the Canary Islands hold the highest number of cave planthopper species of any region worldwide, there are indications (observations, images, yet without voucher specimens) that more new species await discovery. It is conceivable that the number of obligate subterranean planthopper species will eventually double. Particularly promising are caves in the north of La Palma, the El Golfo region on El Hierro, as well as the extended MSS on Tenerife, Gran Canaria and La Gomera. Conversely, the eastern islands of Fuerteventura and Lanzarote are much drier, their caves lack roots inside and planthoppers have never been found there.

Troglobitic planthoppers offer unique opportunities to study adaptation to specialized habitats, including their physiology and behaviour, and their evolutionary dynamics such as subterranean speciation (Hoch and Howarth 1993; Wessel et al. 2013; Le Cesne et al. 2024). Last but not least, cave planthoppers could be models for the study of global change biology. Especially studies on their physiology to better understand physiological constraints, and long-term monitoring to assess population dynamics could contribute to a better understanding of climate change impact on subterranean environments as has been postulated by Mammola et al (2019).

Funding

Publication fees were covered by the Spanish National Research Council, CSIC (Consejo Superior de Investigaciones Científicas).

Competing interests

The authors have declared that no competing interests exists.

Acknowledgements

We would like to express our sincere thanks to Carmelo Andújar, Daniel Suárez, Víctor Montalvo, Irene Santos and Eduardo Jiménez for their help in the fieldwork, to Miguel Ángel Rodríguez for showing us the location of Cueva de Guinea and to Octavio Fernández for guiding us in Cueva Honda de Miranda. Thanks also to Rafael García, Salvador de La Cruz, and Miguel Ángel Rodríguez for permission to use their photos (Fig. 2). We also thank our colleagues at the Museum für Naturkunde, Berlin: Bernhard Schurian for generating the habitus images of *Tachycixius gomerob-scurus*, Andreas Wessel for his help with image processing, and Jason Dunlop for English language editing. We are especially grateful to Manfred Asche, Museum für Naturkunde, Berlin, and to Frank Howarth (Portland, Oregon), formerly of Bishop Museum, Honolulu, for their constructive comments on earlier drafts of the manuscript. DNA barcoding was conducted under the project "CanaryBarcode: hacia el inventariado genómico de la biodiversidad de Canarias", funded by Agencia Canaria de Investigación, Innovación y Sociedad de la Información (ACIISI), Gobierno de Canarias (ProID2021010093), awarded to Brent C. Emerson. The fieldwork to get the specimens herein studied has been developed in different islands supported by collecting permits provided by the Cabildos of La Gomera, El Hierro and La Palma, by the Garajonay National Park, and by the Canarian Government.

The first part of the title is borrowed from the closing statement of Charles Darwin's book „On the origin of species by means of natural selection“ (Darwin 1859). The full text of the quotation is: „*There is grandeur in this view of life, with its several powers, having been originally breathed into a few forms or into one; and that, whilst this planet has gone cycling on according to the fixed law of gravity, from so simple a beginning **endless forms most beautiful and most wonderful** have been, and are being, evolved.*“

References

- Alonso-Zarazaga MA (1987) *Oromia hephaestos* n. gen., n. sp. de edafobio ciego de las Islas Canarias (Col., Curculionidae, Molytinae). *Vieraea* 17(1–2): 105–115. <https://www.museosdetenerife.org/assets/downloads/publication-f4ceb3ec3f.pdf>
- Alonso-Zarazaga MA, García R (1999) *Baezia litoralis* gen. n. y sp. n. de coleóptero edafobio de la isla de Tenerife (Col. Curculionidae, Molytinae). *Vulcania* 3: 48–55. <https://mdc.ulpgc.es/utills/getfile/collection/vul/id/14/filename/15.pdf>
- Ancochea E, Hernán F, Huertas MJ, Brändle JL, Herrera R (2006) A new chronostratigraphical and evolutionary model for La Gomera: Implications for the overall evolution of the Canarian Archipelago. *Journal of Volcanology and Geothermal Research* 157: 271–293. <https://doi.org/10.1016/j.jvolgeores.2006.04.001>
- Barr Jr TC (1968) Cave ecology and the evolution of troglobites. *Evolutionary Biology* 2: 35–102. https://doi.org/10.1007/978-1-4684-8094-8_2
- Bourgoin T (2024) FLOW (Fulgoromorpha Lists on The Web): a world knowledge base dedicated to Fulgoromorpha. [Retrieved 2024-10-31] <https://www.hemiptera-databases.org/flow/>

- Bourgoin T, Wang RR, Asche M, Hoch H, Soulier-Perkins A, Stroinski A, Yap S, Szwedo J (2015) From micropterism to hypopterism: recognition strategy and standardized homology-driven terminology of the forewing venation patterns in planthoppers (Hemiptera: Fulgoromorpha). *Zoormorphology* 134(1): 63–77. <https://doi.org/10.1007/s00435-014-0243-6>
- Canarian Government (2024) Biodiversity Data Bank of the Canary Islands. www.biodiversidadcanarias.es/biota [20/02/2024]
- Carracedo JC, Troll VR (2016) *The geology of the Canary Islands*. Elsevier, 636 pp.
- Cueto LA, Balcells R, Barrera JL (1990) *Mapa geológico de España – Telde*. Instituto Tecnológico Geominero de España, 101 pp.
- Culver DC, Pipan T (2009) *The Biology of Caves and Other Subterranean Habitats*. Oxford University Press, 254 pp. [1st ed.]
- Darwin C (1859) *On the origin of species by means of natural selection, or the preservation of favoured races in the struggle for life*. London: Murray. [1st ed.] <https://doi.org/10.5962/bhl.title.68064>
- Davranoglou L-R, Banar P, Suárez D, Martín S, Naranjo M (2022) A new cavernicolous assassin bug from the Canary Islands (Hemiptera: Reduviidae: Emesinae: Collartidini). *Zootaxa* 5115(3): 342–360. <https://doi.org/10.11646/zootaxa.5115.3.2>
- Deharveng L, Bedos A (2018) Diversity of terrestrial invertebrates in subterranean habitats. In: Moldovan O, Kovác L, Halse S (Eds) *Cave Ecology*. Springer Nature Switzerland, 107–172. https://doi.org/10.1007/978-3-319-98852-8_7
- Del Arco MJ, Rodríguez O (2018) *Vegetation of the Canary Islands*. Springer International Publishing, 437 pp. https://doi.org/10.1007/978-3-319-77255-4_6
- Dumpiérrez F, Fernández M, Fernández O, García R, González AJ, González E, Govantes F, Hernández JM, Martín M, Mata M (2000) Las cavidades volcánicas de los municipios de Breña Baja, Breña Alta y S/C de La Palma (La Palma, Islas Canarias). *Vulcania* 4: 1–45.
- Dutton CE (1884) Hawaiian Volcanoes. In: U.S. Geological Survey Annual Report 1882–1883, Washington, Govt. Print. Off., 75–219.
- Fernández-Palacios JM, Vera Á, Brito A (2001) 17. Los ecosistemas. In: Fernández-Palacios JM, Martín Esquivel JL (Eds) *Naturaleza de las islas Canarias*. Ecología y conservación. Turquesa Ediciones. Santa Cruz de Tenerife, 157–165.
- Fieber FX (1872) *Katalog der europäischen Cicadinen, nach Originalien mit Benützung der neuesten Literatur*. Druck und Verlag von Carl Gerold's Sohn, Wien (Austria), 19 pp.
- Folmer O, Black M, Hoeh W, Lutz R, Vrijenhoek R (1994) DNA primers for amplification of mitochondrial cytochrome c oxidase subunit I from diverse metazoan invertebrates. *Molecular Marine Biology and Biotechnology* 3(5): 294–299. <https://doi.org/10.1371/journal.pone.0013102>
- Frisch J, Oromí P (2006) New species of subterranean *Micranops* Cameron from the Canary Islands (Coleoptera, Staphylinidae, Paederinae), with a redescription of *Micranops bifossicapitatus* (Outerelo & Oromí, 1987). *Deutsche Entomologische Zeitschrift* 53(1): 23–37.
- García R (1998) *Laparocerus dacilae* n. sp. del subsuelo de La Palma, islas Canarias (Col., Curculionidae, Mylacini). *Vulcania* 2: 45–52.
- García, R, Andújar C, Oromí P, López H (2020) *Oromia orahan* (Curculionidae, Molytinae), a new subterranean species for the Canarian underground biodiversity. *Subterranean Biology* 35: 1–14. <https://doi.org/10.3897/subtbiol.35.52583>

- García R, Andújar C, Oromí P, Emerson B, López H (2021) Three new subterranean species of *Baezia* (Curculionidae, Molytinae) for the Canary Islands. *Subterranean Biology* 38:1–18. <https://doi.org/10.3897/subtbiol.38.61733>
- Gilgado JD, López H, Oromí P, Ortuño VM (2011) Description of the first larval instar of *Brosicus crassimargo* Wollaston, 1865 (Carabidae: Broscini) and notes about the presence of this species in the MSS of La Gomera (Canary Islands, Spain). *Entomologica fennica* 22: 46–55. <https://doi.org/10.33338/ef.84542>
- Hernández JJ, Oromí P (1993) Una nueva especie troglobia de *Domene* Fauvel (Coleoptera, Staphylinidae, Paederinae) de las Islas Canarias. *Vieraea* 22: 65–71.
- Hoch H (1994) Homoptera (Auchenorrhyncha Fulgoroidea). In: Juberthie C, Decu V (Eds) *Encyclopedia Biospeologica, Société de Biospéologie, Moulis-Bucarest*, 313–325.
- Hoch H, Asche M (1993) Evolution and speciation of cave-dwelling Fulgoroidea in the Canary Islands (Homoptera: Cixiidae and Meenoplidae). *Zoological Journal of the Linnean Society* 109: 53–101. <https://doi.org/10.1111/j.1096-3642.1993.tb01259.x>
- Hoch H, Howarth FG (1993) Evolutionary dynamics of behavioral divergence among populations of the Hawaiian cave-dwelling planthopper *Oliarus polyphemus* (Homoptera: Fulgoroidea: Cixiidae). *Pacific Science* 47(4): 303–318.
- Hoch H, Naranjo M, Oromí P (2012) Witness of a lost world: *Meenoplus roddenberryi* sp. nov., a new cavernicolous planthopper species (Hemiptera, Fulgoromorpha, Meenoplidae) from Gran Canaria. *Deutsche Entomologische Zeitschrift* 59(2): 207–215.
- Hoch H, Remane R (1985) Evolution und Speziation der Zikaden-Gattung *Hyalesthes* Signoret, 1865 (Homoptera, Auchenorrhyncha, Fulgoroidea, Cixiidae). *Marburger Entomologische Publikationen* 2(2): 1–427.
- Howarth FG (1973) The cavernicolous fauna of Hawaiian lava tubes. 1. Introduction. *Pacific Insects* 15: 139–151.
- Howarth FG (1980) The zoogeography of specialized cave animals: a bioclimatic model. *Evolution* 34(2): 394–406. <https://doi.org/10.1111/j.1558-5646.1980.tb04827.x>
- Howarth FG (1981) Non-relictual terrestrial troglobites in the tropical Hawaiian caves. In: *Proceedings of the 8th International Congress of Speleology, Huntsville, AL (USA), 1981*. National Speleological Society, 539–541.
- Howarth FG (1983) Ecology of cave arthropods. *Annual Review of Entomology* 28: 365–389. <https://doi.org/10.1146/annurev.en.28.010183.002053>
- Howarth FG (1986) The tropical cave environment and the evolution of troglobites. In: *Proceedings of the 9th International Congress of Speleology, Barcelona, Spain, 1986, Vol. 2*, 153–155.
- Howarth FG, Moldovan OT (2018a) Where cave animals live. In: Moldovan OT, Kovács L, Halse S (Eds) *Cave Ecology. Ecological Studies 235*. Springer Nature, Cham, Switzerland, 23–37. https://doi.org/10.1007/978-3-319-98852-8_2
- Howarth FG, Moldovan OT (2018b) The ecological classification of cave animals and their adaptations. In: Moldovan OT, Kovács L, Halse S (Eds) *Cave Ecology. Ecological Studies 235*. Springer Nature, Cham, Switzerland, 41–67. https://doi.org/10.1007/978-3-319-98852-8_2
- Howarth FG, Hoch H, Wessel A (2019) Adaptive shifts. In: Culver DC, White W (Eds) *Encyclopedia of Caves, 3rd edn*. Burlington: Elsevier Academic Press, 47–55. <https://doi.org/10.1016/B978-0-12-814124-3.00007-8>

- Howarth FG, Ferreira RL, Mammola S (in press) Impacts of climate change on subterranean ecology and biodiversity. Chapter 50. In: Demolin-Leite G (Ed.) Global Biome Conservation and Global Warming: Impacts on Ecology and Biodiversity. Elsevier, Cambridge, Mass.
- IUCN (2023) Red List of Threatened Species. Version 2022-2. <https://www.iucnredlist.org> [4 April 2023, date last accessed]
- Juberthie, C, Delay B, Bouillon M (1980) Extension du milieu souterrain en zone non-calcaire: description d'un nouveau milieu et de son peuplement par les coleoptères troglobies. *Mémoires de Biospéologie* 7: 19–52.
- Krauss H (1892) Systematisches Verzeichnis der canarischen Dermapteren und Orthopteren mit Diagnosen der neuen Gattungen und Arten. *Zoologischer Anzeiger* 15: 163–171.
- Le Cesne M, Hoch H, Zhang Y, Bourgoïn T (2024) Why cave planthoppers study matters: are Cixiidae a subtroglophile lineage? (Hemiptera, Fulgoromorpha) *Subterranean Biology* 48: 147–170. <https://doi.org/10.3897/subtbiol.48.117086>
- Lethierry LF (1874) Hémiptères nouveaux. *Petites Nouvelles Entomologiques*. Paris 1: 444.
- Lincoln RJ, Boxshall GA, Clark PF (1982) A dictionary of ecology, evolution and systematics. Cambridge University Press, 298 pp. <https://doi.org/10.1017/S0025315400047457>
- Lindberg H (1954) Hemiptera Insularum Canariensium. *Societas Scientiarum Fennica Commentationes Biologicae* 14(1): 1–304.
- Lindberg H (1960) Supplement Hemipterorum Insularum Canariensium. *Commentationes Biologicae*, Helsinki 22(6): 5–20.
- Linné C (1758) II. Hemiptera. In: Linné C 1758 – *Systema Naturae*. Editio Decima, reformata, 1: 434–439.
- López H, Oromí P (2010) A pitfall trap for sampling the mesovoid shallow substratum (MSS) fauna. *Speleobiology Notes* 2: 7–11.
- Machado A (1987) Consideraciones sobre el género *Licinopsis* Bedel, y descripción de nuevos taxones (Coleoptera, Caraboidea, Sphodrini). *Vieraea* 17: 393–408.
- Machado A (2022) The Macaronesian *Laparocerus*. Taxonomy, phylogeny and natural history. Turquesa Ediciones. Santa Cruz de Tenerife, 681 pp.
- Mammola S, Giachino PM, Piano E, Jones A, Barberis M, Badino G, Isaia M (2016) Ecology and sampling techniques of an understudied subterranean habitat: the Milieu Souterrain Superficiel (MSS). *The Science of Nature* 103: 88. <https://doi.org/10.1007/s00114-016-1413-9>
- Mammola S, Piano E, Cardoso P, Vernon P, Domínguez-Villar D, Culver DC, Pipan T, Isaia M (2019) Climate change going deep: The effects of global climatic alterations on cave ecosystems. *Anthropocene Review* 6(1–2): 98–116. <https://doi.org/10.1177/2053019619851594>
- Martín JL, Izquierdo I, Oromí P (1999) El género *Loboptera* en Canarias: descripción de cinco nuevas especies hipogeas (Blattaria, Blattellidae). *Vieraea* 27: 255–286.
- Medina AL, Oromí P (1990) First data on the superficial underground compartment in La Gomera (Canary Islands). *Mémoires de Biospéologie* 17: 87–91.
- Medina AL, Oromí P (1991) *Wolltinerfia anagae* n. sp., nuevo coleóptero hipogeo de la isla de Tenerife (Coleoptera, Carabidae). *Mémoires de Biospéologie* 18: 215–218.
- Oromí P (2004) Canary Islands: Biospeleology. In: Gunn J (Ed.) *Encyclopedia of caves and karst science*. Fitzroy Dearborn, New York, New York, 366–371. <https://doi.org/10.4324/9780203483855>

- Oromí P (2008) Biospeleology in Macaronesia. In: Espinasa-Pereña R, Pint J (Eds) Proceedings of the X, XI and XII International Symposia on Vulcanospeleology. Association for Mexican Cave Studies, Bulletin 19, and Sociedad Mexicana de Exploraciones Subterráneas, Boletín 7. Association for Mexican Cave Studies, Austin, Texas, 114–118.
- Oromí P, De la Cruz S, Báez M (2010) Hemiptera. In: Arechavaleta M, Rodriguez S, Zurita N, Garcia A (Eds) Lista de especies silvestres de Canarias. Hongos, plantas y animales terrestres. 2009. Gobierno de Canarias, Tenerife (Spain): 234–253.
- Oromí P, Martín JL (1990) Una nueva especie de *Domene* (Col., Staphylinidae) de cavidades volcánicas de La Palma (Islas Canarias). *Vieraea* 18: 21–26.
- Oromí P, Martín JL (1992) The Canary Islands subterranean fauna: characterization and composition. In: Camacho AI (Ed.) The Natural History of Biospeleology. C.S.I.C., Madrid, 527–567.
- Oromí P, Medina AL, Tejedor ML (1986) On the existence of a superficial underground compartment in the Canary Islands. Proceedings of the IX International Congress of Speleology, Barcelona 2: 147–151.
- Oromí P, Arechavaleta M, de la Cruz S, García R, Izquierdo I, López H, Macías-Hernández N, Martín JL, Martín S, Martínez A, Medina AL, Naranjo M, Pérez AJ, Zurita M (2021) Diversidad faunística del medio subterráneo volcánico, con especial énfasis en las Islas Canarias. *Boletín SEDECK* 16(3): 25–50.
- Peterson DW, Swanson DA (1974) Observed formation of lava tubes during 1970–71 at Kilaua Volcano, Hawaii. *Studies in Speleology* 2(6): 209–222.
- Pipán T, López H, Oromí P, Polack S, Culver DC (2010) Temperature variation and the presence of troglobionts in terrestrial shallow subterranean habitats. *Journal of Natural History* 45(3–4): 253–273. <https://doi.org/10.1080/00222933.2010.523797>
- Remane R, Hoch H (1988) Cave-dwelling Fulgoroidea (Homoptera: Auchenorrhyncha) from the Canary Islands. *Journal of Natural History* 22: 403–412. <https://doi.org/10.1080/00222938800770291>
- Ribes J, Oromí P, Ribes E (1998) Una nueva *Collartida* Villiers, 1949 subterránea de La Palma, islas Canarias (Heteroptera, Reduviidae, Emesinae). *Vieraea* 26: 99–105.
- Schoenherr CJ (1834) Genera et species Curculionidum, cum synonymia hujus familiae. Species nova ant hactenus minus cognitae, descriptionibus a Dom Leonardo Gyllenhal, C.H. Boheman, et entomologis allis illustratae 2(1): 1–326. <https://doi.org/10.5962/bhl.title.8952>
- Sket B (2008) Can we agree on an ecological classification of subterranean animals? *Journal of Natural History* 42(21): 1549–1563. <https://doi.org/10.1080/00222930801995762>
- Spinola M (1839) Essai sur les Fulgorelles, sous-tribu de la tribu des Cicadaïres, ordre des Rhynchotes. *Annales de la Société Entomologique de France*. Paris 8: 133–337.
- Stock JH, Martin JL (1988) A new cavehopper (Amphipoda: Talitridae) from lava tubes in La Palma, Canary Islands. *Journal of Natural History* 22(4): 1121–1133. <https://doi.org/10.1080/00222938800770701>
- Stone FD, Howarth FG, Hoch H, Asche M (2005) Root communities in lava tubes. In: Culver DC, White WB (Eds) *Encyclopedia of Caves*. Elsevier Academic Press, 477–484. <https://doi.org/10.1016/B978-0-12-383832-2.00097-9>

- Taiti S, López H (2008) New records and species of Halophilosciidae (Crustacea, Isopoda, Oniscidea) from the Canary Islands (Spain). In: Proceedings of the International Symposium of Terrestrial Isopod Biology ISTIB-07. Shaker-Verlag, Aachen, 43–58.
- Vandel A (1964) La biologie des animaux cavernicoles. Gauthier-Villars, Paris, 619 pp. <https://doi.org/10.1126/science.144.3626.1563-a>
- Wessel A, Hoch H, Asche M, von Rintelen T, Stelbrink B, Heck V, Stone FD, Howarth FG (2013) Rapid species radiation initiated by founder effects in Hawaiian cave planthoppers. *Proceedings of the National Academy of Sciences, USA* 110: 9391–9396. <https://doi.org/10.1073/pnas.1301657110>
- Wynne JJ, Howarth FG, Sommer S, Dickson BG (2019) Fifty years of cave arthropod sampling: techniques and best practices. *International Journal of Speleology* 48(1): 33–48. <https://doi.org/10.5038/1827-806x.48.1.2231>
- Yu DW, Ji Y, Emerson BC, Wang X, Ye C, Yang C, Ding Z (2012) Biodiversity soup: metabarcoding of arthropods for rapid biodiversity assessment and biomonitoring. *Methods in Ecology and Evolution* 3(4): 613–623. <https://doi.org/10.1111/j.2041-210X.2012.00198.x>

Supplementary material I

Canary Islands: Distribution of hypogean planthopper species and potential epigean relatives

Authors: Hannelore Hoch, Heriberto López, Manuel Naranjo, Dora Aguín-Pombo, Pedro Oromí

Data type: docx

Copyright notice: This dataset is made available under the Open Database License (<http://opendatacommons.org/licenses/odbl/1.0/>). The Open Database License (ODbL) is a license agreement intended to allow users to freely share, modify, and use this Dataset while maintaining this same freedom for others, provided that the original source and author(s) are credited.

Link: <https://doi.org/10.3897/subtbiol.51.144111.suppl1>

Seasonal abundance of the Monte Albo cave salamander *Speleomantes flavus* in Italy

Luca Coppari¹, Enrico Lunghi¹

¹ Department of Life, Health and Environmental Sciences (MeSVA), University of L'Aquila, L'Aquila, Italy

Corresponding author: Enrico Lunghi (enrico.lunghi@univaq.it)

Academic editor: Tiziana Di Lorenzo | Received 5 November 2024 | Accepted 19 March 2025 | Published 31 March 2025

<https://zoobank.org/8F3B66E7-7DD5-4F03-BE48-8E090612B04B>

Citation: Coppari L, Lunghi E (2025) Seasonal abundance of the Monte Albo cave salamander *Speleomantes flavus* in Italy. Subterranean Biology 51: 103–114. <https://doi.org/10.3897/subtbiol.51.141075>

Abstract

The Monte Albo cave salamander, *Speleomantes flavus*, is the species endemic to the namesake massif located in the northeastern part of Sardinia, Italy. *Speleomantes* are the only plethodontid species in Europe, a genus composed of eight troglomorphic species living in epigeal and subterranean environments. Most ecological studies on these species deal with species occupancy (i.e., presence/absence), while studies aiming to identify drivers for their abundance are lacking. Here, we present the first study aiming to determine which ecological factors influence the abundance of *S. flavus*. We identified three main hypotheses: (1) salamanders are more abundant where microclimatic conditions are the most suitable for their physiological requirements; (2) *Speleomantes* are more abundant where prey richness is the highest; and (3) salamanders tend to avoid potential predators. Our results suggested that cave air temperature, humidity, and illuminance are strongly affected by season, and individuals of *S. flavus* tended to aggregate in relatively cold and humid areas not far from the cave entrance. For most *Speleomantes*, there was a significant correlation between their abundance and the presence of the considered invertebrate species. This study produced the first information on which ecological features affect the abundance of *S. flavus* individuals. Additional studies extending to further *Speleomantes* populations and species may support our hypotheses, including factors not considered here.

Keywords

Abundance, *Hydromantes*, microhabitat, Plethodontidae, predator, prey, subterranean

Introduction

European cave salamanders (genus *Speleomantes*) are the only representative of the family Plethodontidae in Europe, of which the large majority is distributed throughout North America (Wake 2013). *Speleomantes* are a group of eight species endemic (or sub-endemic) to Italy: seven species (*S. ambrosii*, *S. italicus*, *S. flavus*, *S. supramontis*, *S. imperialis*, *S. sarrabusensis*, and *S. genei*) are distributed on mainland Italy and Sardinia, while *S. strinatii* occurs in Italy and a small portion of the French Provence (Lanza et al. 2006). *Speleomantes* are fully terrestrial amphibians with direct development and are characterized by the absence of lungs (Lanza et al. 2006). These specific features make *Speleomantes* very selective in terms of microclimatic conditions, as they require relatively low temperature and high moisture to guarantee the proper development of their eggs and to efficiently respire and osmoregulate through their skin (Spotila 1972; Lunghi et al. 2015b; Ficetola et al. 2018). These microclimatic conditions can be found in surface environments only during limited periods (mainly in spring and autumn), while they occur in deeper areas of many typologies of subterranean environments all year round (Culver and Pipan 2019). This circumstance was probably one of the leading causes that promoted the colonization of subterranean environments by *Speleomantes*, making them one of the most common troglophile vertebrate species in Europe and likely one of the main drivers of allochthonous organic matter that contributes to sustaining the local subterranean community (Lavoie et al. 2007; Barzaghi et al. 2017).

The colonization of subterranean environments by *Speleomantes* may have provided individuals with both advantages and disadvantages. Besides the pursuit of prolonged and constant suitable microclimatic conditions (Culver and Pipan 2019), *Speleomantes* may have the benefit of switching their trophic position at the top of the local trophic web (Manenti et al. 2020), strongly reducing the probability of being predated by most of their natural predators (Lunghi et al. 2018e; Di Nicola et al. 2024). On the other hand, individuals from subterranean environments found themselves the top predators in an oligotrophic ecosystem (Culver and Pipan 2019), being forced to move towards surface environments to increase the chance of finding potential prey (Manenti et al. 2015; Lunghi et al. 2018d), although being subjected to higher predatory risk (Manenti et al. 2016; Lunghi et al. 2018c; Lunghi and Corti 2021).

We present the first ecological study on multiple populations of The Monte Albo cave salamander *S. flavus* (Fig. 1A). In this study, we want to assess which are the main ecological factors affecting the abundance of salamanders over an entire calendar year. Specifically, we want to test the following hypotheses. The microclimatic selection hypothesis (MSH) predicts that *Speleomantes* tend to occupy cave sectors showing the best environmental conditions to maintain higher efficiency for their cutaneous respiration (Spotila 1972), so we expect a higher abundance where the most suitable conditions are realized (Ficetola et al. 2018). The best foraging hypothesis (BFH) predicts that *Speleomantes* tend to aggregate in areas characterized by the highest availability of food resources to increase the ecological opportunity and to minimize the effort to

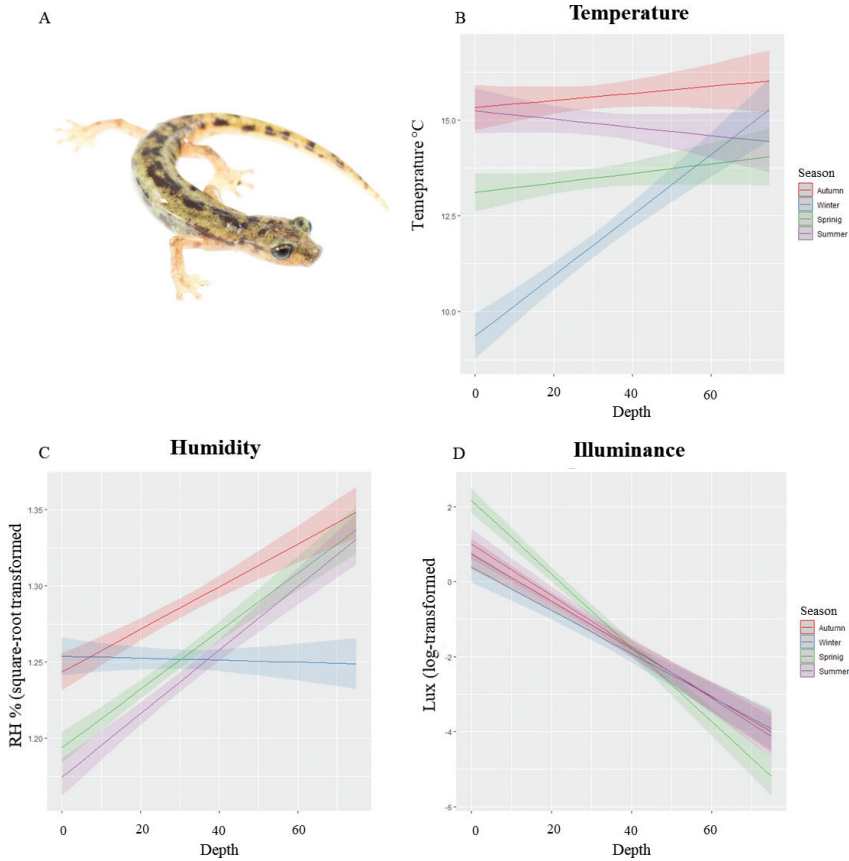


Figure 1. **A** an adult *Speleomantes flavus*. Photo credits: Simone Giachello **B–D** plot showing results of GLMM analyses performed on cave microclimatic conditions. Results show the seasonal trends for **B** air temperature (°C) **C** air humidity (%; square-root transformed) and **D** illuminance (lux; log-transformed). Shaded areas indicate 95% CI.

catch prey (Lunghi et al. 2018d; Lunghi et al. 2020c; Cianferoni and Lunghi 2023). The predation risk hypothesis (PRH) predicts that *Speleomantes* reduce their abundance in the presence of potential predators, and therefore, low individual abundance is expected when predators' diversity is higher.

Methods

Dataset and survey methods

We analyzed the data published by Lunghi et al. (2020a). This dataset contains information on the cave microclimate and on individuals of *Speleomantes flavus* (Fig. 1A) collected within seven natural caves located in the Monte Albo massif (Sardinia, Italy).

A total of 77 surveys (at least two per season) were conducted throughout the year, starting from October 2015 (autumn) to June 2016 (summer). A single researcher surveyed the inner cave environment, collecting data every three linear meters, starting from the entrance until the cave's end or the point in which the survey became too hard (e.g., too tight passages, employment of speleological equipment). Every cave section of 3 linear meters (hereafter, sector) was surveyed with a constant effort of 7.5 minutes per sector to standardize data on *Speleomantes* abundance (Banks-Leite et al. 2014). During sector surveys, the presence/absence of potential prey and predators was also recorded (see below). At the end of each sector (i.e., at its maximum distance from the cave entrance), three microclimatic variables were measured. Air temperature (°C) and relative humidity (%) were measured at the ground and 2.5 m of height using a TDP92 thermo-hygrometer (accuracy: 0.1 °C and 0.1%); this allowed us to take into account potential variation due to stratification of the microclimate (de Freitas 1982; Badino 2010). Maximum and minimum illuminance (lux) were measured in the most illuminated and the darkest points using a DVM1300 light meter (minimum recordable light: 0.1 lx). During sector surveys, we counted all salamanders observed; when possible, individuals were captured to determine the sex and to collect data on body size (snout-vent length; mm). Adult males were recognized by the presence of the mental gland, their characteristic secondary sexual trait (Lanza et al. 2006). No apparent external morphological character can easily distinguish between adult females and juveniles; their discrimination is only possible based on size (Lanza et al. 2006). Salamanders with snout-vent length (SVL) ≥ 55 mm were considered adult females, while those < 55 mm SVL were considered juveniles (Lunghi et al. 2018b). Some individuals ($N = 110$) were marked using a visual implant alpha tag (Lunghi and Veith 2017), and just 10 individuals were captured twice over a year (Lunghi et al. 2020a). Considering this low recapture rate, we assume that the dataset is not affected by the repeated preferences recorded for the recaptured individuals, and it genuinely provides an overview of the preferences of the studied populations. Within each sector, the presence of four cave invertebrates was also recorded. We considered the crane flies and the snail *Oxychilus oppressus* potential prey (Lunghi et al. 2018a; Lunghi et al. 2020b; Cianferoni and Lunghi 2023). The spiders *Meta bourneti* and *Tegenaria* sp. were considered potential predators, as some reports documented the predation on juvenile individuals of *Speleomantes* (Manenti et al. 2016; Lunghi and Corti 2021).

Analyses of cave microclimate

We first assessed the occurrence of specific microclimatic gradients during each season using Generalized Linear Mixed Models (GLMM) with R Studio (Douglas et al. 2015; Lunghi et al. 2015a; Team 2020). For each microclimatic variable (temperature, humidity, and illuminance), we averaged the two measures performed at the end of each cave sector. Before their use, the humidity was square-root transformed, and illuminance was logarithmically transformed to better fit a normal distribution, allowing their use in models with Gaussian distribution. In the first GLMM, we used

the average temperature as the dependent variable, while the sector depth (i.e., its maximum distance from the cave entrance), the season, and the interaction between them were independent variables. Due to multiple visits, cave and sector identity were included as random variables. Two additional GLMMs were performed, replacing the dependent variable once with mean humidity and once with mean illuminance; the other variables remained the same. Likelihood ratio tests were used to test the significance of model variables (Kuznetsova et al. 2016).

Analyses of *Speleomantes flavus* abundance

We used GLMM with negative binomial distribution to assess whether abiotic and biotic factors affect the abundance of *S. flavus* (Brooks et al. 2017). This type of model better fits zero-inflated count data that do not follow a normal distribution (Saphiro-Wilk test always $P > 0.05$). The count data on *S. flavus* abundance was used as the dependent variable, while season and its interaction with sector depth were independent factors. The season is considered a proxy for the variability of the cave microclimatic conditions as it strongly affects the inner cave environment, especially in its first parts (Lunghi et al. 2015a). Instead of adding each microclimatic variable as a further independent variable (making models more complex), we here used the “season” to represent specific microclimatic conditions (see Results, but also Lunghi et al. 2015a). The presence of potential prey and predators were added to the model, as they may have opposing effects on the salamanders’ abundance. Cave and sector identity were used as random factors. We used the Likelihood ratio test to assess the significance of the model variables. We then built a second model without including the non-significant variables; we chose the best one based on AIC criterion and the Likelihood ratio test. When the two models did not significantly diverge, we chose the most parsimonious (i.e., the less complex one). This analysis was repeated to assess the effect of those variables on each salamander group separately (adult males, adult females, and juveniles); to perform these GLMMs, unsexed adult individuals were discarded to avoid bias.

Results

Cave microclimate

The average mean sector temperature was significantly affected by the season ($F_{3,11.71} = 45.53$, $P < 0.001$), sector depth ($F_{1,192.61} = 8.78$, $P = 0.003$), and by the interaction between season and sector depth ($F_{3,1531.56} = 215.59$, $P < 0.001$). The mean sector temperature was significantly lower in winter ($\beta = -5.93$, $SE = 0.14$, $P < 0.001$) and spring ($\beta = -2.13$, $SE = 0.13$, $P < 0.001$). No difference was observed for summer ($P = 0.694$). The mean sector temperature was significantly higher near the cave entrance in summer ($\beta = -0.02$, $SE < 0.01$, $P < 0.001$), and in deeper sectors in winter ($\beta = 0.07$, $SE 0.01$, $P < 0.001$). No significant interaction was observed for spring ($P = 0.659$) (Fig. 1B).

The average mean sector humidity was significantly affected by the season ($F_{3,1544.64} = 66.34$, $P < 0.001$), sector depth ($F_{1,82.13} = 113.76$, $P < 0.001$), and by the interaction between season and sector depth ($F_{3,1544.62} = 48.17$, $P < 0.001$). The mean sector humidity was significantly lower in spring ($\beta = -0.06$, $SE = 0.01$, $P < 0.001$) and summer ($\beta = -0.07$, $SE = 0.01$, $P < 0.001$). No difference was observed for winter ($P = 0.198$). The mean humidity was slightly lower in cave deeper sectors during winter ($\beta < -0.01$, $SE < 0.01$, $P < 0.001$), while in spring and summer it was slightly higher in deeper sectors ($\beta < 0.01$, $SE < 0.01$, $P = 0.003$ and $\beta < 0.01$, $SE < 0.01$, $P < 0.001$, respectively) (Fig. 1C).

The average mean sector illuminance was significantly affected by the season ($F_{3,1540.22} = 22.5$, $P < 0.001$), sector depth ($F_{1,281.84} = 74.82$, $P < 0.001$), and by the interaction between season and sector depth ($F_{3,1540.18} = 14.10$, $P < 0.001$). The mean sector illuminance was significantly higher in spring ($\beta = 1.04$, $SE = 0.18$, $P < 0.001$), while no difference was observed during other seasons ($P > 0.05$). The mean sector illuminance was generally higher near the cave entrance ($\beta = -0.04$, $SE < 0.01$, $P < 0.001$), especially in spring ($\beta = -0.03$, $SE < 0.01$, $P < 0.001$). No significant interaction was observed with other seasons ($P > 0.25$) (Fig. 1D) (see Table 1).

Table 1. Estimated regression parameters, standard errors, t -values, and P -values for the GLMM analysis on the cave microclimatic conditions.

Dependent variable	Predictors	Estimate	Standard error	t -value	P -value
Temperature	Intercept (Autumn)	16.380	1.050	15.591	<0.001
	Winter	-5.932	0.141	-41.966	<0.001
	Spring	-2.127	0.132	-16.097	<0.001
	Summer	-0.056	0.141	-0.393	0.694
	Depth	-0.002	0.004	-0.500	0.618
	Winter*Depth	0.069	0.004	17.171	<0.001
	Spring*Depth	0.003	0.004	0.659	0.510
	Summer*Depth	-0.021	0.004	-5.246	<0.001
Humidity	Intercept (Autumn)	1.237	0.014	87.403	<0.001
	Winter	0.009	0.007	1.289	0.198
	Spring	-0.058	0.007	-8.722	<0.001
	Summer	-0.070	0.007	-9.810	<0.001
	Depth	0.002	<0.001	8.223	<0.001
	Winter*Depth	-0.001	<0.001	-7.072	<0.001
	Spring*Depth	0.001	<0.001	2.928	0.003
	Summer*Depth	0.001	<0.001	3.565	<0.001
Illuminance	Intercept (Autumn)	0.080	0.606	0.133	0.897
	Winter	-0.380	0.195	-1.950	0.051
	Spring	1.040	0.182	5.707	<0.001
	Summer	0.241	0.195	1.234	0.217
	Depth	-0.041	0.006	-6.352	<0.001
	Winter*Depth	0.006	0.006	1.146	0.252
	Spring*Depth	-0.025	0.005	-4.828	<0.001
	Summer*Depth	-0.005	0.006	-0.850	0.395

Speleomantes flavus abundance

We observed 831 individuals of *Speleomantes flavus*, of which 589 (94 adult males, 138 adult females, and 357 juveniles) were captured (Table 2). The best model did not include variables related to the two spider species and the *Oxychilus oppressus* (Table 3). The abundance of *Speleomantes flavus* was significantly lower in summer ($\beta = -1.51$, SE = 0.39, $P < 0.001$) and winter ($\beta = -1.23$, SE = 0.49, $P = 0.006$), while no difference was observed for spring ($P = 0.394$). *S. flavus* was more abundant towards the cave entrance ($\beta = -0.05$, SE = 0.02, $P = 0.006$) and in sectors in which crane flies were present ($\beta = 0.72$, SE = 0.21, $P < 0.001$). A tendency to increase its abundance in deeper sectors was observed in summer ($\beta = 0.04$, SE = 0.02, $P = 0.02$), while no effect was observed during the other seasons ($P > 0.569$) (Fig. 2A).

The best model for adult males did not include the variables related to the two prey species (*O. oppressus* and crane flies) and the interaction between sectors and seasons (Table 3). The abundance of adult males was significantly lower in winter ($\beta = -2.39$, SE = 0.79, $P = 0.002$), while no difference was observed during the other seasons ($P > 0.436$). Males were slightly less abundant near the cave entrance ($\beta = -0.04$, SE = 0.01, $P = 0.012$), while they were more abundant in sectors where *M. bourneti* ($\beta = 1.55$, SE = 0.56, $P = 0.006$) and *Teegenaria* sp. were present ($\beta = 1.24$, SE = 0.47, $P = 0.009$) (Fig. 2B).

The best model for adult females only included the variable related to the season (Table 3). The abundance of adult females was significantly lower in winter ($\beta = -1.55$, SE = 0.53, $P = 0.004$), while no difference was observed in other seasons ($P > 0.124$) (Fig. 2C).

The best model for juveniles did not include the variables related to crane flies and the spider *Teegenaria* sp. (Table 3). The abundance of juveniles was significantly lower in summer ($\beta = -0.99$, SE = 0.49, $P = 0.04$), while no difference was observed in other seasons ($P > 0.135$). Juveniles were more abundant in sectors where *M. bourneti* ($\beta = 0.82$, SE = 0.41, $P = 0.048$) and *O. oppressus* ($\beta = 0.93$, SE = 0.23, $P < 0.001$) were present. No apparent difference was observed for juvenile seasonal distribution ($P > 0.05$), but they showed a tendency to increase their abundance near the cave entrance in summer ($\beta = 0.04$, SE = 0.02, $P = 0.052$) (Fig. 2D).

Discussion

We demonstrated that the abundance and the distribution of the Monte Albo cave salamanders within caves mainly depend on microclimatic features (Lunghi et al. 2014; Ficaretola et al. 2018), which are strongly affected by climate seasonality. The considered microclimatic variables (air temperature, humidity, and illuminance) vary along the transect from the entrance to the deep cave zone (i.e., with increasing cave depth; Fig. 1) and are strongly dependent on climatic conditions occurring in adjacent surface environments (Culver and Pipan 2019). The microclimatic conditions characterizing the area nearest the entrance mostly resemble those occurring in surface

Table 2. Captured individuals of *Speleomantes flavus*. For each season, we indicate the number of adult males, adult females, juveniles, unsexed adults, and the total of observed individuals.

Season	Adult males	Adult females	Juveniles	Unsexed adults	Total individuals
Autumn	20	26	61	30	137
Winter	2	6	29	23	60
Spring	57	90	229	148	524
Summer	15	16	38	41	110

Table 3. Parameters related to model selection for *Speleomantes* abundances. We here compare the full model with a reduced model that does not include nonsignificant predictors assessed with a Likelihood Ratio Test.

Group	Model	Df	AIC	BIC	Log-Likelihood	Deviance	Chi-Square	Δ Df	P-value
<i>Speleomantes</i> total	Reduced	12	2008.10	2075.10	-992.06	1984.10			
	Full	15	2007.40	2091.10	-988.68	1977.40	6.76	3	0.08
<i>Speleomantes</i> males	Reduced	10	594.24	650.03	-287.12	574.24			
	Full	15	599.66	683.35	-284.83	569.66	4.58	5	0.47
<i>Speleomantes</i> females	Reduced	7	703.84	742.90	-344.92	689.84			
	Full	15	705.04	788.74	-337.52	675.04	14.80	8	0.06
<i>Speleomantes</i> juveniles	Reduced	13	1199.70	1272.20	-586.84	1173.70			
	Full	15	1200.10	1283.80	-585.07	1170.10	3.54	2	0.17

habitats in both magnitude of fluctuation and intensity. At the same time, external influences decrease, and the microclimate becomes stable with increased cave depth (Lunghi et al. 2015a). This was particularly true for air temperature, which showed an annual fluctuation of about 5 °C in the most profound areas (60–75 m). In contrast, within the first 15 m from the cave entrance, there was an annual variation of almost 20 °C (Lunghi et al. 2020a). The cave air temperature showed a marked and opposite trend towards the deep cave areas during summer (negative) and winter (positive), while in spring and autumn the temperatures slightly increased with depth from the cave entrance (Fig. 1B). Concerning the other microclimatic variables, we detected a constantly increasing trend for humidity, and a constantly decreasing trend for illuminance (Fig. 1C, D). The only exception for humidity occurred in winter, as seasonal precipitation reduced the gap between the conditions occurring at the two extremities of the cave environment (Fig. 1C).

Our analyses supported the predictions of the microclimate selection hypothesis (MSH). The abundance of *Speleomantes flavus* was strongly affected by seasonality (Fig. 2), one of the main factors responsible for microclimatic fluctuation within the first meters of caves (Lunghi et al. 2015a). Such influence remained evident even if individuals were analysed separately (Fig. 2). During summer, the season with the harsher environmental conditions for *Speleomantes* (Ficetola et al. 2018), individuals were generally less abundant and tended to concentrate in the most profound cave areas, where favourable microclimatic conditions occur year-round (Fig. 1). During

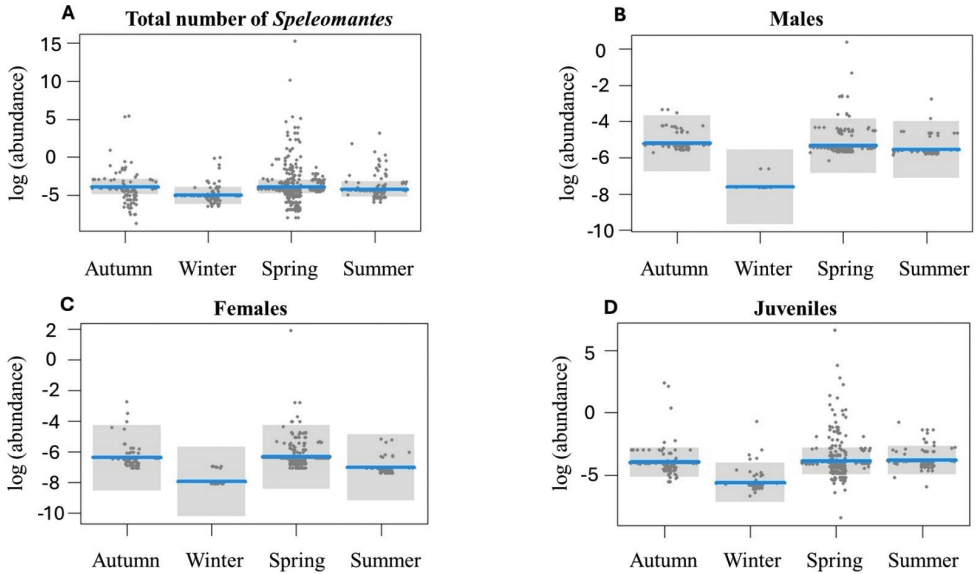


Figure 2. Plot showing results of *S. flavus* abundance during seasons **A** total number of *Speleomantes* **B** adult males **C** adult females; and **D** juveniles. Y axes show the log transformed abundances. Blue horizontal line represents mean values, while shaded areas indicate 95% CI.

winter, invertebrate abundance significantly decreases in surface environments (Driesen et al. 2013), and adults probably have no reason to leave the highly suitable deep cave areas to reach sub-optimal conditions if prey availability is scarce.

Our second hypothesis, the best foraging hypothesis (BFH), was partially supported, as only adults did not show a significant correlation with the presence of prey. Considering that most of the caves in the Palearctic region are oligotrophic (Culver and Pipan 2019), *Speleomantes* tend to concentrate in the cave areas that support the highest prey abundance, namely those nearest the entrance (Lunghi et al. 2017; Lunghi et al. 2020b). This is particularly true for young individuals, who prefer to occupy these sub-optimal microclimatic conditions to find higher prey availability (Salvidio and Pastorino 2002; Ficetola et al. 2013). We currently lack data to adequately explain the observed non-significant correlation between prey species and adult abundance, but we have a hypothesis that deserves to be tested. In our study, we only used the presence of two potential prey, the crane flies and the snail *Oxychilus oppressus*. Since *Speleomantes* exhibits an opportunistic and generalist foraging behavior (Cianferoni and Lunghi 2023), individuals may be more attracted by the quantity rather than the simple presence of potential prey species (Manenti et al. 2015). Future studies considering this feature may support our BFH hypothesis.

Our third and final hypothesis, the predation risk hypothesis (PRH), was not supported, as no *Speleomantes* group (males, females, juveniles, and overall) reduced its abundance in the presence of predators. *Speleomantes* are epigeal mesopredators that have switched their trophic position to the top of the trophic pyramid in colonized

subterranean environments (Manenti et al. 2020). Contrary to our expectation, the abundance of adult males and juveniles was positively related to the presence of these predator spiders. One of these potential predators is the orb-web cave spider *Meta bourneti*, a widespread species on Monte Albo (Lunghi 2018). *Meta* spiders are considered a good proxy for prey availability in subterranean environments (Manenti et al. 2015), and their positive correlation with some groups of *Speleomantes* can be an artifact due to the indirect correlation with prey abundance. Particularly, we expected to observe a negative relationship between juveniles and cave spiders due to the documented predation events (Manenti et al. 2016; Lunghi and Corti 2021). The predation risk for juvenile *Speleomantes* is probably lower than expected. Indeed, the only observed cases of predation of *Speleomantes* by cave spiders report salamanders that were likely to fall into the spider web, which gives a consistent advantage to the spider. Some other epigeal predators can use the first meters of the cave as a foraging area (Lunghi et al. 2018e; Di Nicola et al. 2024), but this is not an everyday event, and thus, it was not considered in our analysis. Additional studies are required to test whether predators' abundance can better predict *Speleomantes* abundance.

We conducted the first study that provided information on the ecological factors that influence the abundance of *Speleomantes flavus* in caves. Our results identified microclimatic suitability as the main driver, followed by the presence of specific invertebrate species. The highest activity of *S. flavus* occurs during the seasons in which the climatic conditions are the most suitable for the species (i.e., spring and autumn), and within the subterranean environments, individuals tend to be more abundant near the cave entrance, where prey availability is the highest. We did not observe a negative effect due to the presence of potential predators, supporting the hypothesis for the apical position of *Speleomantes* within the cave trophic pyramid. Our preliminary results should represent the starting point for future studies that consider additional ecological factors (e.g., prey/predator abundance) and test these same hypotheses in other *Speleomantes* species.

References

- Badino G (2010) Underground meteorology - "what's the weather underground?". *Acta Carsologica* 39: 427–448. <https://doi.org/10.3986/ac.v39i3.74>
- Banks-Leite C, Pardini R, Boscolo D, Righetto Cassano C, Püttker T, Santos Barros C, Barlow J (2014) Assessing the utility of statistical adjustments for imperfect detection in tropical conservation science. *Journal of Applied Ecology* 51: 849–859. <https://doi.org/10.1111/1365-2664.12272>
- Barzaghi B, Ficetola GF, Pennati R, Manenti R (2017) Biphase predators provide biomass subsidies in small freshwater habitats: a case study of spring and cave pools. *Freshwater Biology* 62: 1637–1644. <https://doi.org/10.1111/fwb.12975>
- Brooks ME, Kristensen K, van Benthem KJ, Magnusson A, Berg CW, Nielsen A, Skaug HJ, Maechler M, Bolker BM (2017) glmmTMB balances speed and flexibility among packages for zero-inflated generalized linear mixed modeling. *The R Journal* 9: 378–400. <https://doi.org/10.32614/RJ-2017-066>

- Cianferoni F, Lunghi E (2023) Inferring on *Speleomantes* foraging behavior from gut contents examination. *Animals* 13: 2782. <https://doi.org/10.3390/ani13172782>
- Culver DC, Pipan T (2019) The biology of caves and other subterranean habitats. Oxford University Press, New York, 336 pp. <https://doi.org/10.1093/oso/9780198820765.001.0001>
- de Freitas CR (1982) Cave climate: assessment of airflow and ventilation. *International Journal of Climatology* 2: 383–397. <https://doi.org/10.1002/joc.3370020408>
- Di Nicola MR, Mezzadri S, Cerullo A (2024) First evidence of Sette Fratelli cave salamander *Speleomantes sarrabusensis* (Urodela: Plethodontidae) consumption by the Sardinian grass snake *Natrix helvetica cetti* (Squamata: Natricidae). *Natural History Science*, 1–8. <https://doi.org/10.4081/nhs.2024.808>
- Douglas B, Maechler M, Bolker B, Walker S (2015) Fitting Linear Mixed-Effects Models using lme4. *Journal of Statistical Software* 67: 1–48. <https://doi.org/10.18637/jss.v067.i01>
- Driessen MM, Kirkpatrick JB, Mcquillan PB (2013) Shifts in composition of monthly invertebrate assemblages in moorland differed between lowland and montane locations but not fire-ages. *Environmental Entomology* 42: 58–73. <https://doi.org/10.1603/EN12322>
- Ficetola GF, Lunghi E, Canedoli C, Padoa-Schioppa E, Pennati R, Manenti R (2018) Differences between microhabitat and broad-scale patterns of niche evolution in terrestrial salamanders. *Scientific Reports* 8: 10575. <https://doi.org/10.1038/s41598-018-28796-x>
- Ficetola GF, Pennati R, Manenti R (2013) Spatial segregation among age classes in cave salamanders: habitat selection or social interactions? *Population Ecology* 55: 217–226. <https://doi.org/10.1007/s10144-012-0350-5>
- Kuznetsova A, Brockhoff B, Christensen HB (2016) lmerTest: Tests in Linear Mixed Effects Models. R package version 20–29 www.r-project.org. <https://doi.org/10.18637/jss.v082.i13>
- Lanza B, Pastorelli C, Laghi P, Cimmaruta R (2006) A review of systematics, taxonomy, genetics, biogeography and natural history of the genus *Speleomantes* Dubois, 1984 (Amphibia Caudata Plethodontidae). *Atti del museo civico di storia naturale di Trieste* 52: 5–135.
- Lavoie KH, Helf KL, Poulson TL (2007) The biology and ecology of North American cave crickets. *Journal of Cave and Karst Studies* 69: 114–134.
- Lunghi E (2018) Ecology and life history of *Meta bourneti* (Araneae: Tetragnathidae) from Monte Albo (Sardinia, Italy). *PeerJ* 6: e6049. <https://doi.org/10.7717/peerj.6049>
- Lunghi E, Cianferoni F, Ceccolini F, Mulargia M, Cogoni R, Barzaghi B, Cornago L, Avitabile D, Veith M, Manenti R, Ficetola GF, Corti C (2018a) Field-recorded data on the diet of six species of European *Hydromantes* cave salamanders. *Scientific Data* 5: 180083. <https://doi.org/10.1038/sdata.2018.83>
- Lunghi E, Corti C (2021) Predation of European cave salamanders (*Speleomantes*) by the spider *Meta bourneti*. *Spixiana* 44: 54.
- Lunghi E, Corti C, Manenti R, Barzaghi B, Buschetti S, Canedoli C, Cogoni R, De Falco G, Fais F, Manca A, Mirimin V, Mulargia M, Mulas C, Muraro M, Murgia R, Veith M, Ficetola GF (2018b) Comparative reproductive biology of European cave salamanders (genus *Hydromantes*): nesting selection and multiple annual breeding. *Salamandra* 54: 101–108.
- Lunghi E, Corti C, Mulargia M, Zhao Y, Manenti R, Ficetola GF, Veith M (2020a) Cave morphology, microclimate and abundance of five cave predators from the Monte Albo (Sardinia, Italy). *Biodiversity Data Journal* 8: e48623. <https://doi.org/10.3897/BDJ.8.e48623>

- Lunghi E, Ficetola GF, Mulargia M, Cogoni R, Veith M, Corti C, Manenti R (2018c) *Batrachobdella* leeches, environmental features and *Hydromantes* salamanders. International Journal for Parasitology: Parasites and Wildlife 7: 48–53. <https://doi.org/10.1016/j.ijppaw.2018.01.003>
- Lunghi E, Ficetola GF, Zhao Y, Manenti R (2020b) Are the neglected Tipuloidea crane flies (Diptera) an important component for subterranean environments? Diversity 12: 333. <https://doi.org/10.3390/d12090333>
- Lunghi E, Manenti R, Cianferoni F, Ceccolini F, Veith M, Corti C, Ficetola GF, Mancinelli G (2020c) Interspecific and inter-population variation in individual diet specialization: do environmental factors have a role? Ecology 101: e03088. <https://doi.org/10.1002/ecy.3088>
- Lunghi E, Manenti R, Ficetola GF (2014) Do cave features affect underground habitat exploitation by non-troglobite species? Acta Oecologica 55: 29–35. <https://doi.org/10.1016/j.actao.2013.11.003>
- Lunghi E, Manenti R, Ficetola GF (2015a) Seasonal variation in microhabitat of salamanders: environmental variation or shift of habitat selection? PeerJ 3: e1122. <https://doi.org/10.7717/peerj.1122>
- Lunghi E, Manenti R, Ficetola GF (2017) Cave features, seasonality and subterranean distribution of non-obligate cave dwellers. PeerJ 5: e3169. <https://doi.org/10.7717/peerj.3169>
- Lunghi E, Manenti R, Mulargia M, Veith M, Corti C, Ficetola GF (2018d) Environmental suitability models predict population density, performance and body condition for microendemic salamanders. Scientific Reports 8: 7527. <https://doi.org/10.1038/s41598-018-25704-1>
- Lunghi E, Mascia C, Mulargia M, Corti C (2018e) Is the Sardinian grass snake (*Natrix natrix cetti*) an active hunter in underground environments? Spixiana 41: 160.
- Lunghi E, Murgia R, De Falco G, Buschetti S, Mulas C, Mulargia M, Canedoli C, Manenti R, Ficetola GF (2015b) First data on nesting ecology and behaviour in the Imperial cave salamander *Hydromantes imperialis*. North-Western Journal of Zoology 11: 324–330.
- Lunghi E, Veith M (2017) Are Visual Implant Alpha tags adequate for individually marking European cave salamanders (genus *Hydromantes*)? Salamandra 53: 541–544.
- Manenti R, Lunghi E, Canedoli C, Bonaccorsi M, Ficetola GF (2016) Parasitism of the leech, *Batrachobdella algira* (Moquin-Tandon, 1846), on Sardinian cave salamanders (genus *Hydromantes*) (Caudata: plethodontidae). Herpetozoa 29: 27–35.
- Manenti R, Lunghi E, Ficetola GF (2015) Distribution of spiders in cave twilight zone depends on microclimatic features and trophic supply. Invertebrate Biology 134: 242–251. <https://doi.org/10.1111/ivb.12092>
- Manenti R, Melotto A, Guillaume O, Ficetola GF, Lunghi E (2020) Switching from mesopredator to apex predator: how do responses vary in amphibians adapted to cave living? Behavioral Ecology and Sociobiology 74: 126. <https://doi.org/10.1007/s00265-020-02909-x>
- Salvidio S, Pastorino MV (2002) Spatial segregation in the European plethodontid *Speleomantes strinatii* in relation to age and sex. Amphibia-Reptilia 23: 505–510.
- Spotila JR (1972) Role of temperature and water in the ecology of lungless salamanders. Ecological Monographs 42: 95–125. <https://doi.org/10.2307/1942232>
- Team R (2020) RStudio: Integrated Development for R. RStudio, PBC, Boston, MA.
- Wake DB (2013) The enigmatic history of the European, Asian and American plethodontid salamanders. Amphibia-Reptilia 34: 323–336. <https://doi.org/10.1163/15685381-00002893>

Three new cave-dwelling species of *Tyrannochthonius* Chamberlin, 1929 (Pseudoscorpiones, Chthoniidae) from Guangxi, China

Jianzhou Sun^{1,2}, Xiangbo Guo^{1,2}, Feng Zhang^{1,2}

1 Key Laboratory of Zoological Systematics and Application, College of Life Sciences, Hebei University, Baoding, Hebei 071002, China **2** Hebei Basic Science Center for Biotic Interaction, Hebei University, Baoding, Hebei 071002, China

Corresponding author: Feng Zhang (dudu06042001@163.com)

Academic editor: Zhizhong Gao | Received 11 January 2025 | Accepted 21 March 2025 | Published 7 April 2025

<https://zoobank.org/08B92375-2F90-4044-B807-1E8FE16E057F>

Citation: Sun J, Guo X, Zhang F (2025) Three new cave-dwelling species of *Tyrannochthonius* Chamberlin, 1929 (Pseudoscorpiones, Chthoniidae) from Guangxi, China. *Subterranean Biology* 51: 115–133. <https://doi.org/10.3897/subtbiol.51.146465>

Abstract

Three new *Tyrannochthonius* species are described, including detailed diagnosis and illustrations: *T. rudongyanensis* **sp. nov.**, *T. tiani* **sp. nov.**, and *T. yanwuensis* **sp. nov.** All samples were collected from the hypogean habitats in Guangxi, China. A distribution map of all *Tyrannochthonius* species in Guangxi is provided.

Keywords

Diversity, karst, morphology, taxonomy

Introduction

The Southwest China Karst region, spanning eight provinces in southwestern China and centred around the Yunnan-Guizhou Plateau and the southern hilly regions (Wang et al. 2019), is a hotspot for pseudoscorpion diversity. The first cave-dwelling pseudoscorpion species in China was described by Schawaller (1995), with only a few cave-dwelling pseudoscorpion species having been reported sporadically in the preceding years (Mahnert 2009; Mahnert and Li 2016; Gao et al. 2018, 2020). In recent years, the diversity of cave-dwelling pseudoscorpions in China has received unprecedented

attention, with the number of species showing an explosive growth trend (Li 2022; Hou et al. 2022, 2023a, 2023b; Feng et al. 2023; Sun et al. 2024; WPC 2025).

The genus *Tyrannochthonius* Chamberlin, 1929, belonging to the family Chthoniidae Daday, 1889, subfamily Chthoniinae Daday, 1889, and tribe Tyrannochthoniini Chamberlin, 1962, is a relatively common pseudoscorpion taxon living in caves in the Southwest China Karst region. A total of 42 *Tyrannochthonius* species have been recorded in China (including a subspecies), 38 of which are cave-dwelling species collected from caves in the Southwest China Karst region (WPC 2025). Among these 38 cave-dwelling species, 27 were from Guizhou (Gao et al. 2020; Li 2022; Hou et al. 2023a), while only one species, *Tyrannochthonius chixingi* Gao, Wynne & Zhang, 2018, is found in Guangxi (Gao et al. 2018).

This study describes three new cave-dwelling *Tyrannochthonius* species, based on specimens collected from caves in Guangxi by Prof. Mingyi Tian (South China Agricultural University, Guangdong Province) and our laboratory members. Detailed descriptions, illustrations, and a distribution map (Fig. 1) of these new species are provided.

Materials and methods

Specimen preparation and examination

The specimens examined for this study were preserved in 75% ethyl alcohol in a refrigerator at -20 °C and deposited in the Museum of Hebei University (MHBU) (Baoding, China). Photographs and measurements were obtained using a Leica M205A stereomicroscope equipped with a Leica DFC550 camera. Drawings were made using the Inkscape software (Ver. 1.0.2.0). Detailed examination was carried out using an Olympus BX53 general optical microscope. All images were edited and formatted using the Adobe Photoshop 2017 software.

Terminology

Terminology and measurements followed Chamberlin (1931) with some small modifications to the terminology of trichobothria (Harvey 1992; Judson 2007) and chelicera (Judson 2007). The chela and legs were measured in the lateral view and the others were taken in the dorsal view. The measurements of the specimens were predominantly provided in millimeters (mm) unless specified otherwise, whereas the measurements on the map were presented in kilometers (km). Proportions and measurements of chelicerae, carapace, and pedipalps correspond to length/breadth, and those of legs to length/depth.

The following abbreviations were used in the text: for chelal trichobothria: **b** = basal; **sb** = sub-basal; **st** = subterminal; **t** = terminal; **ib** = interior basal; **isb** = interior sub-basal; **ist** = interior sub-terminal; **it** = interior terminal; **eb** = exterior basal; **esb** = exterior sub-basal; **est** = exterior sub-terminal; **et** = exterior terminal. For other abbreviations: **dx**, duplex trichobothria.

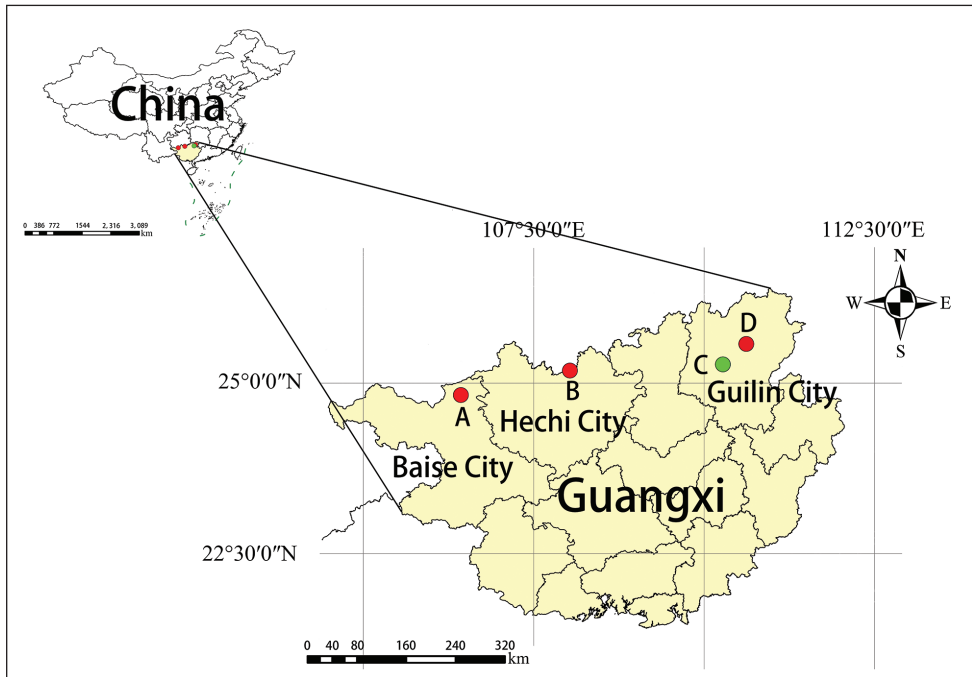


Figure 1. The distributions of the four novel *Tyrannochthonius* species in Guangxi, China **A** *Tyrannochthonius yanwuensis* sp. nov. **B** *Tyrannochthonius tiani* sp. nov. **C** *Tyrannochthonius chixingi* Gao, Wynne & Zhang, 2018 **D** *Tyrannochthonius rudongyanensis* sp. nov.

Results

Taxonomic section

Family Chthoniidae Daday, 1889

Subfamily Chthoniinae Daday, 1889

Tribe Tyrannochthoniini Chamberlin, 1962

Genus *Tyrannochthonius* Chamberlin, 1929

Type species. *Chthonius terribilis* With, 1906, by original designation.

***Tyrannochthonius rudongyanensis* sp. nov.**

<https://zoobank.org/02C48AA3-C896-4DCF-9D6A-30C7616EF12F>

Figs 2–5

Chinese name. 乳洞岩暴伪蝎

Type material. *Holotype* • ♂ (Ps.-MHBG-GX2019101001): CHINA, Guangxi, Guilin City, Xingan County, Rudongyan Cave [25.574192°N, 110.620256°E], 240 m a.s.l.,

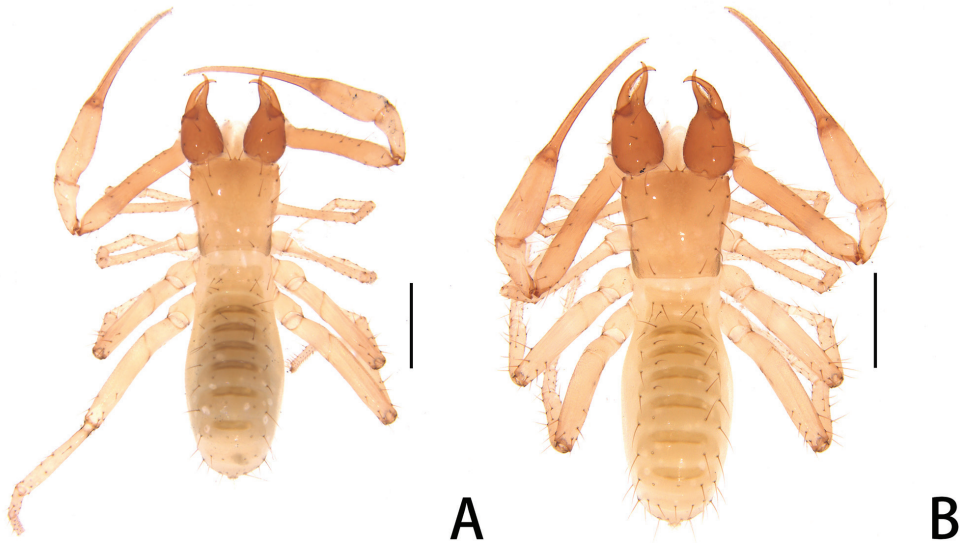


Figure 2. *Tyrannochthonius rudongyanensis* sp. nov. **A** holotype male (dorsal view) **B** paratype female (dorsal view). Scale bar: 0.50 mm.

10 October 2019, Zegang Feng & Lingchen Zhao leg. **Paratypes** • 2 ♀ (Ps.-MHBU-GX2019101002–03) all with the same data as the holotype • 3 ♀ (Ps.-MHBU-GX2023020401–03), Rudongyan Cave [25.570469°N, 110.627489°E], 213 m a.s.l., 04 February 2023, Xiangbo Guo, Jianzhou Sun, Tao Zheng & Songtao Shi leg.

Etymology. Named after the type locality, Rudongyan Cave.

Diagnosis. (♂♀) Moderately sized troglomorphic species with elongated appendages; carapace without eyes or eyespots; anterior margin of carapace thin, finely denticulated, epistome distinctly pointed, triangular; posterior margin of carapace with 2 setae; tergites I–IV each with four setae. Pedipalps slender, femur 6.29 (♂), 6.20–7.33 (♀) times longer than broad, length 0.88 (♂), 0.88–0.93 (♀); chela 7.23 (♂), 6.50–6.73 (♀) times longer than broad, length 1.23 (♂), 1.20–1.30 (♀); both chelal fingers with intercalary teeth; *sb* closer to *b* than *st*.

Description. Adult male (Figs 2–4).

Color generally pale yellow, chelicerae, carapace, pedipalps and tergites slightly darker black, soft parts pale.

Cephalothorax (Figs 3D, 4D): carapace nearly subquadrate, 1.00 times as long as broad, weakly constricted basally; posterior region with squamous sculpturing laterally, other area smooth, without furrows; anterior margin slightly serrate; epistome triangular, without eyes or eyespots; with 18 setae arranged s4s: 4: 4: 2: 2, most setae acuminate, sturdy, long and gently curved, anterolateral setae much shorter than others; with three pairs of lyrifissures, first and second pair situated middle and flank to the setae of ocular row, third pair situated lateral to the sole pair of setae of posterior row. Manducatory process with two acuminate distal setae, anterior seta more than 1/2

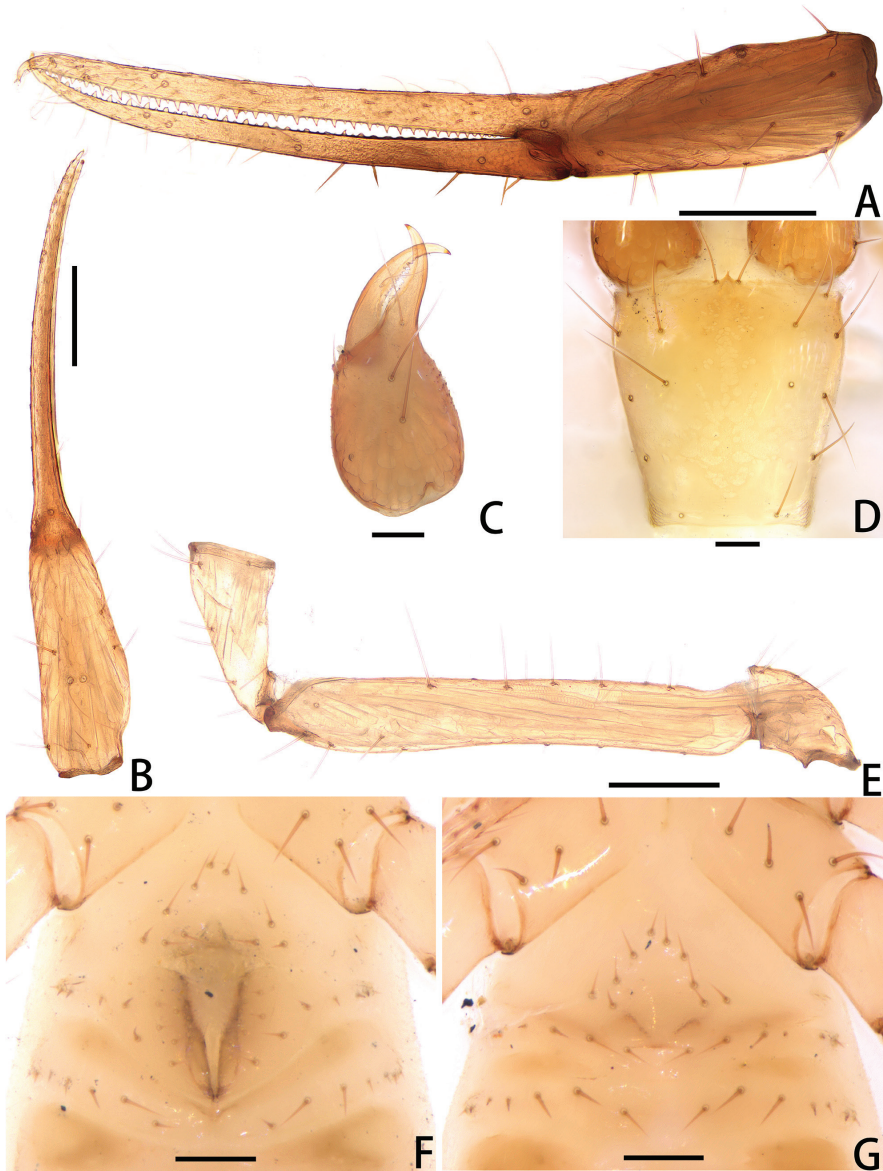


Figure 3. *Tyrannochthonius rudongyanensis* sp. nov., male (A–F), female (G): **A** left chela (lateral view) **B** left chela (dorsal view) **C** left chelicera (dorsal view) **D** carapace (dorsal view) **E** left pedipalp (minus chela, dorsal view) **F** male genital area (ventral view) **G** female genital area (ventral view). Scale bars: 0.20 mm (A, B, E); 0.10 mm (C, D, F, G).

length of medial seta; apex of coxa I with a rounded anteromedial process; coxae II with 12–13 terminally indented coxal spines on each side, set as an oblique and arched row, central spines slightly longer than the others (Fig. 4F); intercoxal tubercle absent; chaetotaxy of coxae: P 3, I 3, II 4, III 5, IV 5.

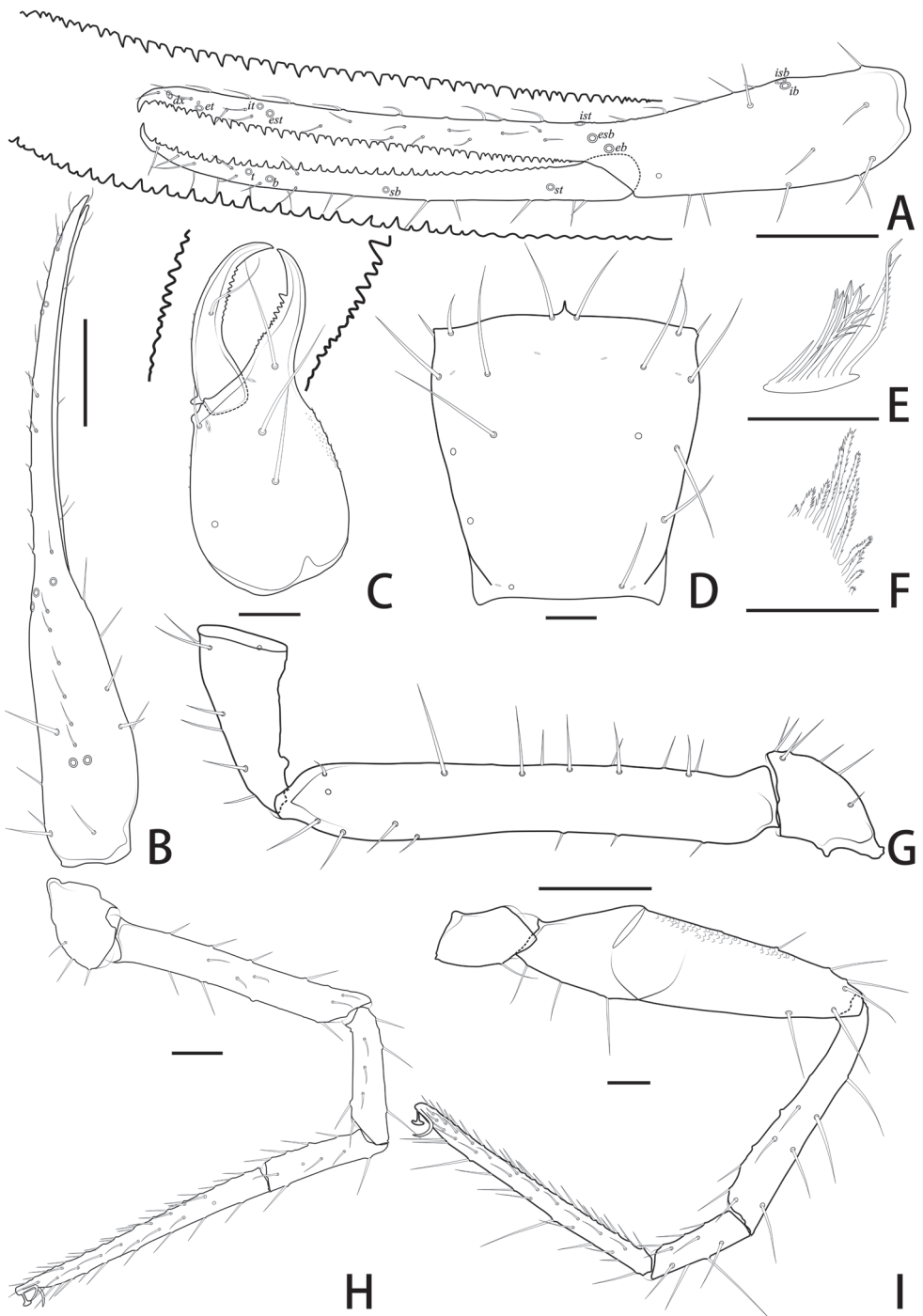


Figure 4. *Tyrannochthonius rudongyanensis* sp. nov., male: **A** left chela (lateral view), with details of teeth and trichobothrial pattern **B** left chela (dorsal view) **C** Left chelicera (dorsal view), with details of teeth **D** carapace (dorsal view) **E** rallum **F** coxal spines on coxae II (ventral view) **G** left pedipalp (minus chela, dorsal view) **H** leg I (lateral view) **I** leg IV (lateral view). Scale bars: 0.20 mm (**A, B, G**); 0.10 mm (**C-F, H, I**).

Chelicera (Figs 3C, 4C): almost as long as carapace, 2.04 times as long as broad; five setae and two lyrifissures (exterior condylar lyrifissure and exterior lyrifissure) present on hand, all setae acuminate, ventrobasal setae shorter than others; movable finger with one medial seta. Cheliceral hand with moderate wrinkle on both ventral and dorsal sides. Both fingers well provided with teeth, fixed finger with 14 teeth, distal one largest; movable finger with 13 contiguous small teeth; galea completely vestigial (Fig. 4C). Serrula exterior with 22 and serrula interior with 15 blades. Rallum with eight blades, the distal one longest, with fine barbules and slightly set apart from the other blades, latter tightly grouped and with long pinnae, some of which are subdivided (Fig. 4E).

Pedipalp (Figs 3A, B, E, 4A, B, G): trochanter 1.79, femur 6.29, patella 2.13, chela 7.23, hand 2.71 times as long as broad; femur 2.59 times as long as patella; movable chelal finger 1.72 times as long as hand and 0.64 times as long as chela. Setae generally long and acuminate. Chelal hand not constricted towards fingers, apodeme complex of movable chelal finger slightly sclerotized. Fixed chelal finger and hand with eight trichobothria, movable chelal finger with four trichobothria, *ib* and *isb* situated close together, submedially on dorsum of chelal hand; *eb*, *esb* and *ist* at base of fixed chelal finger; *esb* slightly distal *eb* and *ist* slightly distal to *esb*; *it* slightly distal to *est*, situated subdistally; *et* slightly near to tip of fixed chelal finger, slightly close to chelal teeth; *dx* situated distal to *et*; *sb* slightly closer to *b* than to *st*; *b* and *t* situated subdistally, *t* slightly distal to *it* and distal to *b*; *est* situated proximal to *b* and close to *it* (Figs 3A, 4A). Microsetae (chemosensory setae) present on dorsum of chelal hand (Figs 3B, 4B). Both chelal fingers with a row of teeth, spaced regularly along the margin, teeth smaller distally and proximally: fixed finger with 32 well-spaced, strongly pointed teeth and 28 intercalary microdenticles; movable finger with 18 well-spaced, strongly pointed teeth, plus 18 intercalary microdenticles and 11 vestigial, rounded and contiguous basal teeth.

Opisthosoma: generally typical, pleural membrane finely granulated. All tergites and sternites undivided; setae uniseriate and acuminate. Tergal chaetotaxy I–XII: 4: 4: 4: 4: 4: 4: 5: 5: 4: T2T: 0. Sternal chaetotaxy IV–XII: 12: 9: 7: 7: 7: 7: 7: -: 2. Genital region: sternite II with 11 setae scattered on median area, genital opening slit-like, sternite III with a row of 16 setae (Fig. 3F).

Legs (Fig. 4H–I): fine granulation present on anterodorsal faces of femur IV and patella IV. Leg I: femur 1.89 times as long as patella; tarsus 2.21 times as long as tibia. Leg IV: femoropatella 4.00 times as long as deep; tibia 5.90 times as long as deep; with basal tactile setae on both tarsal segments: basitarsus 3.57 times as long as deep (TS = 0.40), telotarsus 13.00 times as long as deep and 2.60 times as long as basitarsus (TS = 0.38). Setae of leg I (trochanter to tibia) 3: 12: 8: 10, setae of leg IV (trochanter to basitarsus) 1: 3: 6: 11: 9. Arolium not divided, slightly shorter than the simple claws.

Adult females (paratypes) (Figs 2B, 3G). Mostly same as males; tergal chaetotaxy I–XII: 4: 4: 4: 4: 4: 4: 4: 4–5: 4–5: 4–5: T2T: 0; sternal chaetotaxy IV–XII: 12–14: 10: 9–10: 9: 9: 8–10: 7: -: 2. Genital region: sternite II with 9–10 setae scattered on median area, sternite III with a row of six setae.

Dimensions (length/breadth or, in the case of the legs, length/depth in mm; ratios in parentheses). **Male**: body length 1.88. Pedipalps: trochanter 0.25/0.14 (1.79), femur 0.88/0.14 (6.29), patella 0.34/0.16 (2.13), chela 1.23/0.17 (7.23), hand 0.46/0.17

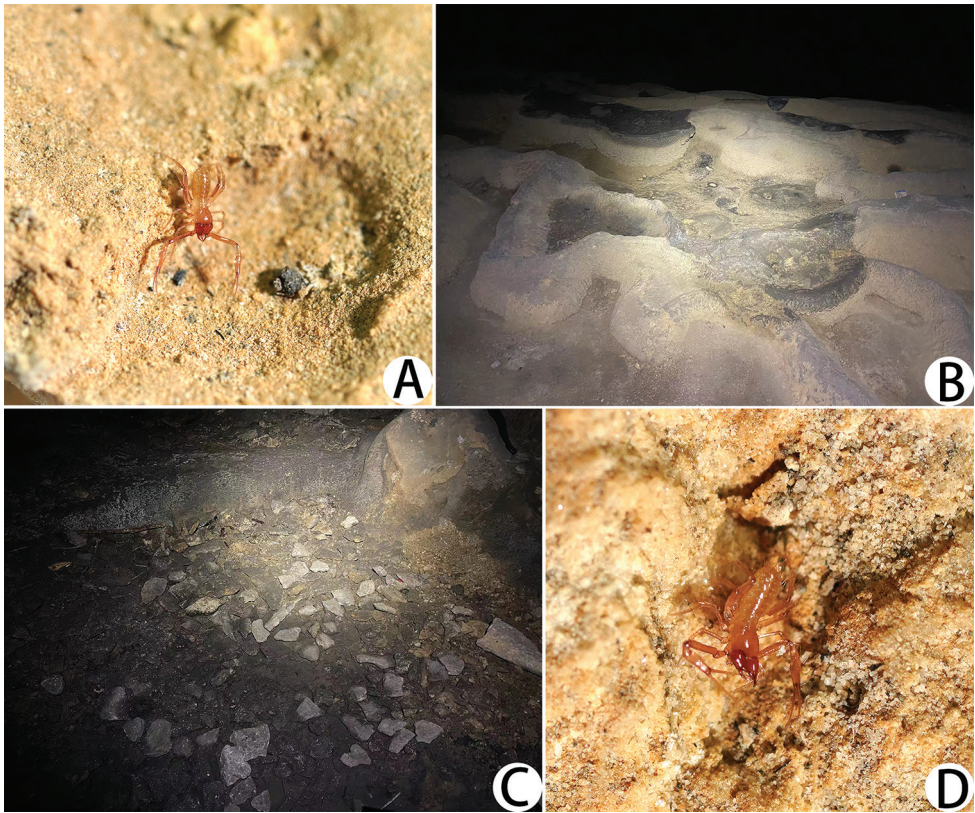


Figure 5. Rudongyan Cave, type locality of *Tyrannochthonius rudongyanensis* sp. nov., **A, D** live female *T. rudongyanensis* sp. nov. in its natural environment **B, C** areas where *T. rudongyanensis* sp. nov. specimens were collected.

(2.71), movable chelal finger length 0.79. Chelicera 0.49/0.24 (2.04), movable finger length 0.28. Carapace 0.54/0.54 (1.00). Leg I: trochanter 0.16/0.12 (1.33), femur 0.51/0.07 (7.29), patella 0.27/0.07 (3.86), tibia 0.24/0.06 (4.00), tarsus 0.53/0.05 (10.06). Leg IV: trochanter 0.23/0.14 (1.64), femoropatella 0.84/0.21 (4.00), tibia 0.59/0.10 (5.90), basitarsus 0.25/0.07 (3.57), telotarsus 0.65/0.05 (13.00).

Females: body length 1.73–1.84. Pedipalps: trochanter 0.25–0.27/0.15–0.16 (1.67–1.69), femur 0.88–0.93/0.12–0.15 (6.20–7.33), patella 0.34–0.37/0.15–0.18 (2.05–2.27), chela 1.20–1.30/0.18–0.20 (6.50–6.73), hand 0.46–0.50/0.18–0.20 (2.50–2.58), movable chelal finger length 0.77–0.83. Chelicera 0.54–0.61/0.25–0.27 (2.16–2.26), movable finger length 0.27–0.31. Carapace 0.55–0.58/0.54–0.58 (1.00–1.05). Leg I: trochanter 0.16–0.17/0.10–0.13 (1.31–1.60), femur 0.51–0.53/0.07–0.08 (6.50–7.57), patella 0.27–0.30/0.07 (3.86–4.29), tibia 0.23–0.25/0.06 (3.83–4.17), tarsus 0.53–0.56/0.05 (10.60–11.20). Leg IV: trochanter 0.20–0.24/0.11–0.16 (1.44–1.82), femoropatella 0.79–0.87/0.21 (3.36–3.76), tibia 0.56–0.60/0.09–0.10 (5.80–6.22), basitarsus 0.23–0.25/0.07–0.08 (3.00–3.29), telotarsus 0.62–0.67/0.05 (12.40–13.40).

Ecology. All the specimens were collected under clod and rocks inside the cave (Fig. 5).

Distribution. Known only from the type locality (Guangxi Zhuang Autonomous Region, China).

***Tyrannochthonius tiani* sp. nov.**

<https://zoobank.org/421F49B9-E565-41C7-B53C-2C908511F165>

Figs 6–8

Chinese name. 田氏暴伪蝎

Type material. *Holotype* • ♀ (Ps.-MHBG-GX2023120801): CHINA, Guangxi, Hechi City, Huanjiang County, The Mulun National Nature Reserve, Ganxiao Cave [25.18312°N, 108.03124°E], 695 m a.s.l., 08 December 2023, Mingyi Tian leg.

Etymology. This species is named for Prof Mingyi Tian, who participated in field work and collected the holotype specimen.

Diagnosis. (♀) Moderately sized troglomorphic species with elongated appendages; carapace without eyes or eyespots; anterior margin of carapace thin, finely denticulated, epistome distinctly triangular; posterior margin of carapace with two setae; tergites I–IV each with four setae. Pedipalps slender, femur 9.43 times longer than broad (length 1.32); chela 9.42 times longer than broad (length 1.79); both chelal fingers without intercalary teeth, and teeth with strongly heterodontate; *sb* slightly closer to *b* than to *st*.

Description. Adult female (Figs 6–8).

Color generally pale yellow, chelicerae, carapace, pedipalps and tergites slightly darker black, soft parts pale.

Cephalothorax (Figs 7E, 8D): carapace nearly subquadrate, 1.00 times as long as broad, weakly constricted basally; posterior region with squamous sculpturing laterally, other area smooth, without furrows; anterior margin slightly serrate; epistome triangular, without eyes or eyespots; with 18 setae arranged *s4s*: 4: 4: 2: 2, most setae acuminate, sturdy, long and gently curved, anterolateral setae much shorter than others; with three pairs of lyrifissures, first and second pair situated middle and flank to the setae of ocular row, third pair situated lateral to the sole pair of setae of posterior row. Manducatory process with two acuminate distal setae, anterior seta more than 1/2 length of medial seta; apex of coxa I with a rounded anteromedial process; coxae II with 10–11 terminally indented coxal spines on each side, set as an oblique and arched row, central spines slightly longer than the others (Fig. 8F); intercoxal tubercle absent; chaetotaxy of coxae: P 3, I 3, II 4, III 5, IV 5.

Chelicera (Figs 7D, 8C): almost as long as carapace, 2.58 times as long as broad; five setae and two lyrifissures (exterior condylar lyrifissure and exterior lyrifissure) present on hand, all setae acuminate, ventrobasal setae shorter than others; movable finger with one medial seta. Cheliceral hand with moderate wrinkle on both ventral and dorsal sides. Both fingers well provided with teeth, fixed finger with 18 teeth, distal one largest; movable finger with 11 contiguous small teeth; galea completely vestigial (Fig. 8C).



Figure 6. *Tyrannochthonius tiani* sp. nov., holotype female (dorsal view). Scale bar: 0.50 mm.

Serrula exterior with 19 and serrula interior with 16 blades. Rallum with eight blades, the distal one longest, with fine barbules and slightly set apart from the other blades, latter tightly grouped and with long pinnae, some of which are subdivided (Fig. 8E).

Pedipalp (Figs 7A, B, E, 8A, B, G): trochanter 1.88, femur 9.43, patella 3.53, chela 9.42, hand 2.79 times as long as broad; femur 2.20 times as long as patella; movable chelal finger 2.34 times as long as hand and 0.69 times as long as chela. Setae generally long and acuminate. Chelal hand not constricted towards fingers, apodeme complex of movable chelal finger slightly sclerotized. Fixed chelal finger and hand with eight trichobothria, movable chelal finger with four trichobothria, *ib* and *isb* situated close together, submedially on dorsum of chelal hand; *eb*, *esb* and *ist* at base of fixed chelal finger; *esb* slightly distal *eb* and *ist* slightly distal to *esb*; *it* slightly distal to *est*, situated subdistally; *et* slightly near to tip of fixed chelal finger, slightly close to chelal teeth; *dx* situated distal to *et*; *sb* slightly closer to *b* than to *st*; *b* and *t* situated subdistally, *t* slightly distal to *it* and distal to *b*; *est* situated proximal to *b* and close to *it* (Figs 7A, 8A). Microsetae (chemosensory setae) present on dorsum of chelal hand (Figs 7B, 8B). Both chelal fingers with a row of teeth, spaced regularly along the margin, teeth smaller distally and proximally: fixed finger with 41 well-spaced, strongly pointed teeth; movable finger with 32 well-spaced, strongly pointed teeth, plus five vestigial, rounded and contiguous basal teeth.

Opisthosoma: generally typical, pleural membrane finely granulated. All tergites and sternites undivided; setae uniseriate and acuminate. Tergal chaetotaxy I–XII: 4: 4: 4: 4: 4: 4:

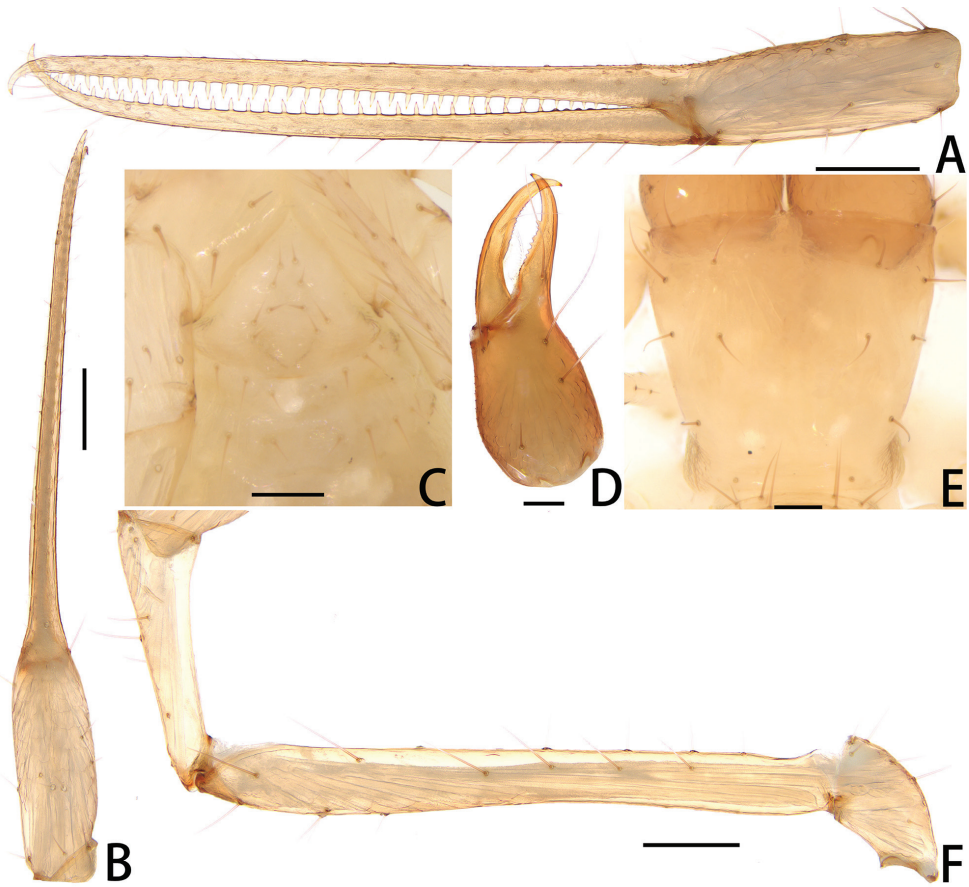


Figure 7. *Tyrannochthonius tiani* sp. nov., holotype female: **A** left chela (lateral view) **B** left chela (dorsal view) **C** female genital area (ventral view) **D** left chelicera (dorsal view) **E** carapace (dorsal view) **F** left pedipalp (minus chela, dorsal view). Scale bars: 0.20 mm (**A, B, F**); 0.10 mm (**C–E**).

5: 5: 5: 4: T2T: 0. Sternal chaetotaxy IV–XII: 10: 8: 8: 9: 9: 9: 9: -: 2. Genital region: sternite II with ten setae scattered on median area, sternite III with a row of 12 setae (Fig. 7C).

Legs (Fig. 8H–I): fine granulation present on anterodorsal faces of femur IV and patella IV. Leg I: femur 1.95 times as long as patella; tarsus 2.24 times as long as tibia. Leg IV: femoropatella 4.86 times as long as deep; tibia 7.44 times as long as deep; with basal tactile setae on both tarsal segments: basitarsus 4.00 times as long as deep (TS = 0.30), telotarsus 17.20 times as long as deep and 2.68 times as long as basitarsus (TS = 0.34). Setae of leg I (trochanter to tibia) 3: 16: 13: 11, setae of leg IV (trochanter to basitarsus) 4: 4: 5: 13: 10. Arolium not divided, slightly shorter than the simple claws.

Dimensions (length/breadth or, in the case of the legs, length/depth in mm; ratios in parentheses). **Female:** body length 1.60. Pedipalps: trochanter 0.32/0.17 (1.88), femur 1.32/0.14 (9.43), patella 0.60/0.17 (3.53), chela 1.79/0.19 (9.42), hand 0.53/0.19 (2.79), movable chelal finger length 1.24. Chelicera 0.75/0.29 (2.58), movable finger

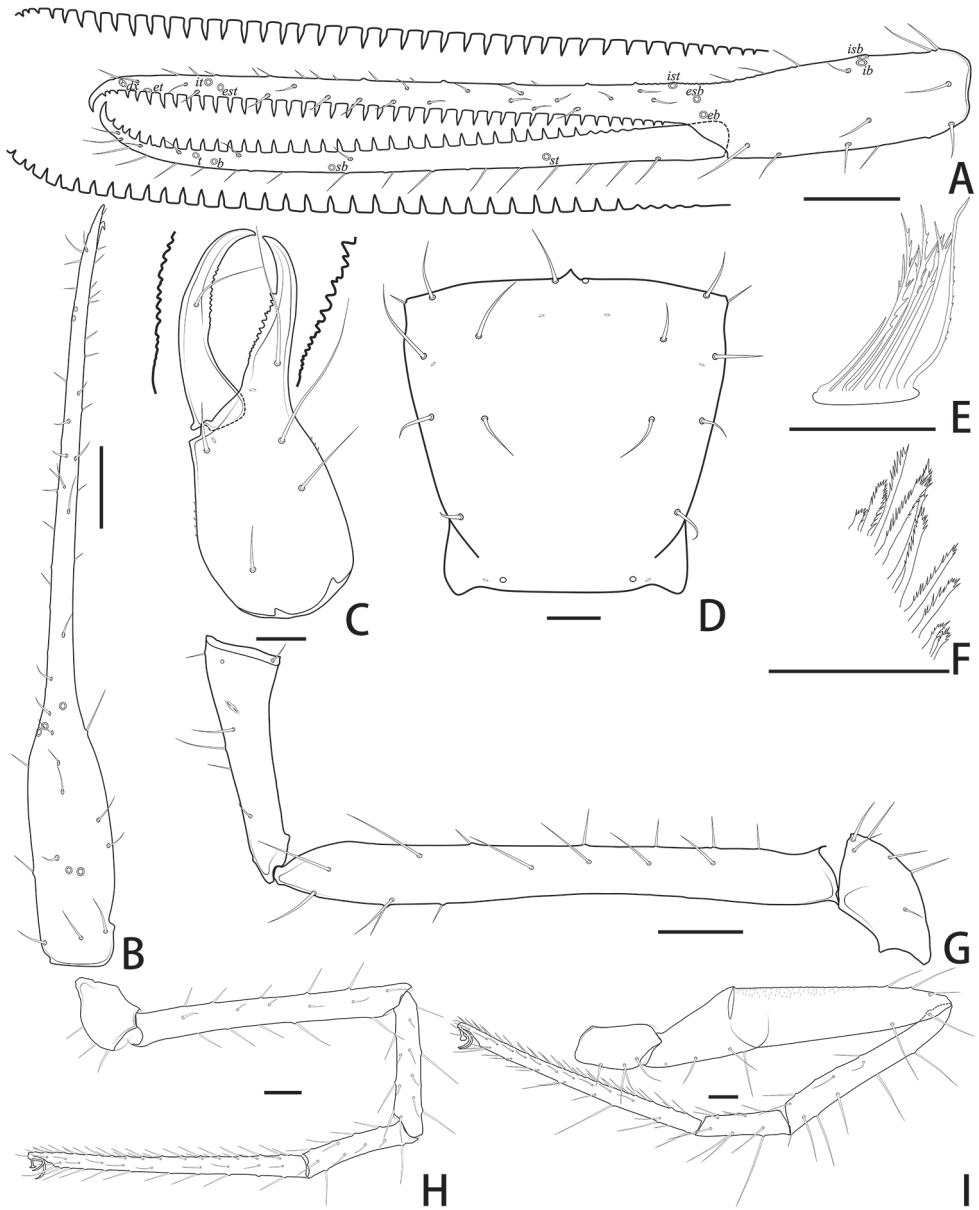


Figure 8. *Tyrannochthonius tiani* sp. nov., male: **A** left chela (lateral view), with details of teeth and trichobothrial pattern **B** left chela (dorsal view) **C** left chelicera (dorsal view), with details of teeth **D** carapace (dorsal view) **E** rallum **F** coxal spines on coxae II (ventral view) **G** left pedipalp (minus chela, dorsal view) **H** leg I (lateral view) **I** Leg IV (lateral view). Scale bars: 0.20 mm (**A, B, G**); 0.10 mm (**C-F, H, I**).

length 0.41. Carapace 0.60/0.60 (1.00). Leg I: trochanter 0.17/0.14 (1.21), femur 0.74/0.09 (8.22), patella 0.38/0.07 (5.43), tibia 0.33/0.06 (5.50), tarsus 0.74/0.06 (12.33). Leg IV: trochanter 0.29/0.15 (1.93), femoropatella 1.07/0.22 (4.86), tibia 0.67/0.09 (7.44), basitarsus 0.32/0.08 (4.00), telotarsus 0.86/0.05 (17.20).

Distribution. Known only from the type locality (Guangxi Zhuang Autonomous Region, China).

***Tyrannochthonius yanwuensis* sp. nov.**

<https://zoobank.org/EBD1FB4B-BB42-46FE-B171-0058D8485B56>

Figs 9–11

Chinese name. 岩屋暴伪蝎

Type material. *Holotype* • ♂ (Ps.-MHBU-GX2024042801): CHINA, Guangxi, Baise City, Leye County, Yanwu Cave [24.823900°N, 106.431500°E], 695 m a.s.l., 28 April 2024, Sunbin Huang, Mingzhi Zhao, Yan Li & Rong Chen leg.

Etymology. Named after the type locality, Yanwu Cave.

Diagnosis. (♂) Moderately sized troglomorphic species with elongated appendages; carapace without eyes or eyespots; anterior margin of carapace thin, finely denticulated, epistome distinctly triangular; posterior margin of carapace with two setae; tergites I–IV each with two setae. Pedipalps slender, femur 7.23 times longer than broad (length 0.94); chela 8.73 times longer than broad (length 1.31); both chelal fingers with intercalary teeth, and fixed finger teeth strongly heterodontate, movable finger teeth strongly retrorse; *sb* midway between *st* and *b*.

Description. Adult male (Figs 9–11).

Color generally pale yellow, chelicerae, carapace, pedipalps and tergites slightly darker black, soft parts pale.

Cephalothorax (Figs 10E, 11D): carapace nearly subquadrate, 0.96 times as long as broad, weakly constricted basally; posterior region with squamous sculpturing laterally, other area smooth, without furrows; anterior margin slightly serrate; epistome triangular, without eyes or eyespots; with 18 setae arranged s4s: 4: 4: 2: 2, most setae acuminate, sturdy, long and gently curved, anterolateral setae much shorter than others; with three pairs of lyrifissures, first and second pair situated middle and flank to the setae of ocular row, third pair situated lateral to the sole pair of setae of posterior row. Manducatory process with two acuminate distal setae, anterior seta more than 1/2 length of medial seta; apex of coxa I with a rounded anteromedial process; coxae II with 10–11 terminally indented coxal spines on each side, set as an oblique and arched row, central spines slightly longer than the others (Fig. 11F); intercoxal tubercle absent; chaetotaxy of coxae: P 3, I 3, II 4, III 5, IV 5.

Chelicera (Figs 10D, 11C): almost as long as carapace, 2.32 times as long as broad; five setae and two lyrifissures (exterior condylar lyrifissure and exterior lyrifissure) present on hand, all setae acuminate, ventrobasal setae shorter than others; movable finger with one medial seta. Cheliceral hand with moderate wrinkle on both ventral and dorsal sides. Both fingers well provided with teeth, fixed finger with 18 teeth, distal one largest; movable finger with 12 contiguous small teeth; galea completely vestigial (Fig. 11C). Serrula exterior with 23 and serrula interior with 16 blades. Rallum with eight blades, the distal one longest, with fine barbules and slightly set apart from the other blades, latter tightly grouped and with long pinnae, some of which are subdivided (Fig. 11E).



Figure 9. *Tyrannochthonius yanwuensis* sp. nov., holotype male (dorsal view). Scale bar: 0.50 mm.

Pedipalp (Figs 10A, B, E, 11A, B, G): trochanter 1.86, femur 7.23, patella 3.21, chela 8.73, hand 2.67 times as long as broad; femur 2.09 times as long as patella; movable chelal finger 2.22 times as long as hand and 0.68 times as long as chela. Setae generally long and acuminate. Chelal hand not constricted towards fingers, apodeme complex of movable chelal finger slightly sclerotized. Fixed chelal finger and hand with eight trichobothria, movable chelal finger with four trichobothria, *ib* and *isb* situated close together, submedially on dorsum of chelal hand; *eb*, *esb* and *ist* at base of fixed chelal finger; *esb* slightly distal *eb* and *ist* slightly distal to *esb*; *it* slightly distal to *est*, situated subdistally; *et* slightly near to tip of fixed chelal finger, slightly close to chelal teeth; *dx* situated distal to *et*; *sb* midway between *st* and *b*; *b* and *t* situated subdistally,

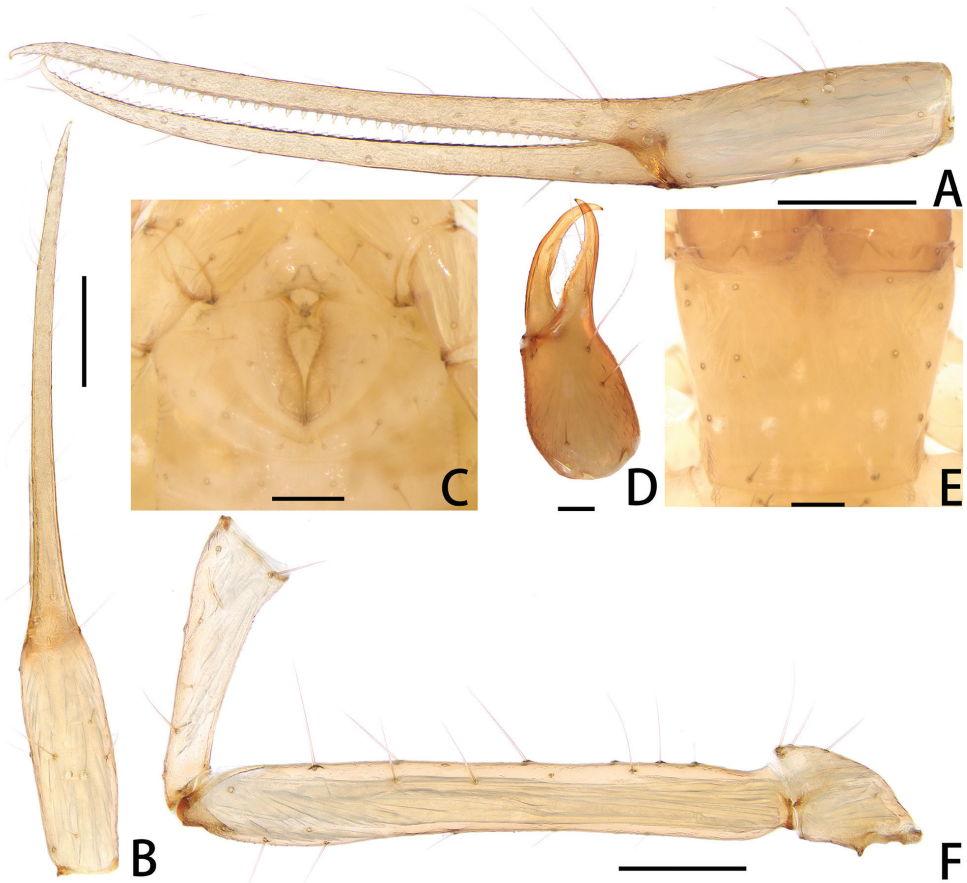


Figure 10. *Tyrannochthonius yanwuensis* sp. nov., holotype male: **A** left chela (lateral view) **B** left chela (dorsal view) **C** male genital area (ventral view) **D** left chelicera (dorsal view) **E** carapace (dorsal view) **F** left pedipalp (minus chela, dorsal view). Scale bars: 0.20 mm (**A, B, F**); 0.10 mm (**C–E**).

t slightly distal to *it* and distal to *b*; *est* situated proximal to *b* and close to *it* (Figs 10A, 11A). Microsetae (chemosensory setae) present on dorsum of chelal hand (Figs 10B, 11B). Both chelal fingers with a row of teeth, spaced regularly along the margin, teeth smaller distally and proximally: fixed finger with 45 well-spaced, strongly pointed teeth and six intercalary microdenticles at the terminal; movable finger with 47 well-spaced, pointed retrorse teeth with and seven intercalary microdenticles at the terminal.

Opisthosoma: generally typical, pleural membrane finely granulated. All tergites and sternites undivided; setae uniseriate and acuminate. Tergal chaetotaxy I–XII: 2: 2: 2: 4: 4: 4: 5: 5: 4: T2T: 0. Sternal chaetotaxy IV–XII: 10: 8: 8: 7: 7: 8: 7: -: 2. Genital region: sternite II with ten setae scattered on median area, genital opening slit-like, sternite III with a row of 16 setae (Fig. 10C).

Legs (Fig. 11H–I): Leg I: femur 1.90 times as long as patella; tarsus 2.27 times as long as tibia. Leg IV: femoropatella 3.90 times as long as deep; tibia 6.33 times as long

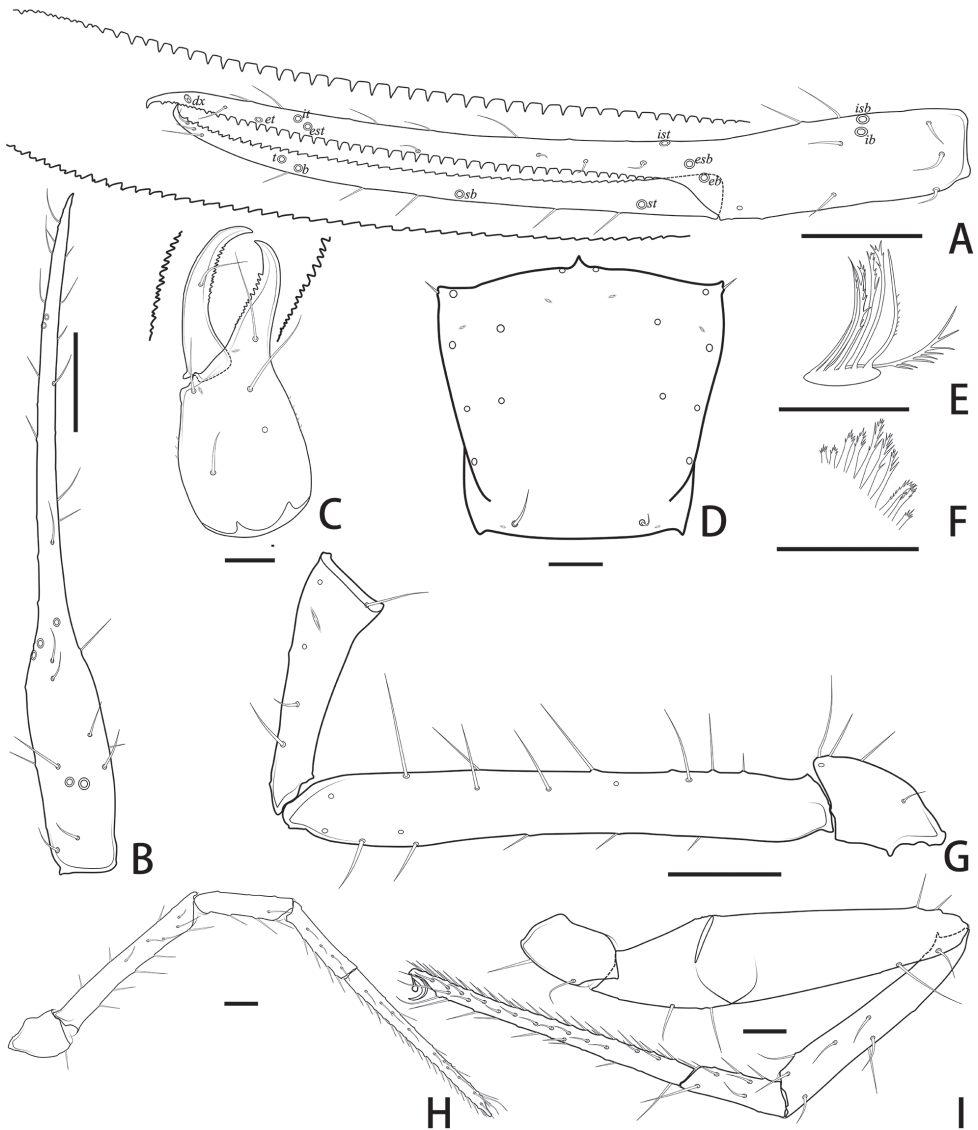


Figure 11. *Tyrannochthonius yanwuensis* sp. nov., male: **A** left chela (lateral view), with details of teeth and trichobothrial pattern **B** left chela (dorsal view) **C** left chelicera (dorsal view), with details of teeth **D** carapace (dorsal view) **E** rallum **F** coxal spines on coxae II (ventral view) **G** left pedipalp (minus chela, dorsal view) **H** leg I (lateral view) **I** leg IV (lateral view). Scale bars: 0.20 mm (**A**, **B**, **G**); 0.10 mm (**C**–**F**, **H**, **I**).

as deep; with basal tactile setae on both tarsal segments: basitarsus 4.17 times as long as deep ($TS = 0.28$), relotarsus 12.80 times as long as deep and 2.56 times as long as basitarsus ($TS = 0.28$). Setae of leg I (trochanter to tibia) 3: 13: 7: 9, setae of leg IV (trochanter to basitarsus) 2: 3: 5: 8: 9. Arolium not divided, slightly shorter than the simple claws.

Dimensions (length/breadth or, in the case of the legs, length/depth in mm; ratios in parentheses). **Male:** body length 1.36. Pedipalps: trochanter 0.26/0.14 (1.86), femur 0.94/0.13 (7.23), patella 0.45/0.14 (3.21), chela 1.31/0.15 (8.73), hand 0.40/0.15 (2.67), movable chelal finger length 0.89. Chelicera 0.58/0.25 (2.32), movable finger length 0.32. Carapace 0.51/0.53 (0.96). Leg I: trochanter 0.18/0.13 (1.38), femur 0.55/0.07 (7.86), patella 0.29/0.07 (4.14), tibia 0.26/0.05 (5.20), tarsus 0.59/0.05 (11.80). Leg IV: trochanter 0.24/0.16 (1.50), femoropatella 0.82/0.21 (3.90), tibia 0.57/0.09 (6.33), basitarsus 0.25/0.06 (4.17), telotarsus 0.64/0.05 (12.80).

Distribution. Known only from the type locality (Guangxi Zhuang Autonomous Region, China).

Discussion

In China, species of the genus *Tyrannochthonius* were reported exclusively in the southern regions, with the majority of species concentrated in the Yunnan-Guizhou Plateau, while only a few species occur in other regions. Before this study, only one *Tyrannochthonius* species was known from Guangxi; our research has expanded the number of hypogean species to four. The distinctions between these three new species and other known species are as follows:

1. *Tyrannochthonius rudongyanensis* sp. nov. closely resembles *T. multidentatus* Hou, Feng & Zhang, 2023 and *T. antridraconis* Mahnert, 2009 in the absence of eyes or eyespots, the presence of both chelal fingers with intercalary teeth, the presence of four setae on tergites I–IV, and the position of *sb*, which slightly closer to *b* than to *st*, but differs in the following characters: shorter pedipalpal femur (0.88 (♂), 0.88–0.93 (♀) vs 1.00–1.02 (♂), 1.10–1.12 (♀) in *T. multidentatus* and 1.18–1.29 (♂) in *T. antridraconis*), shorter pedipalpal chela (1.23 (♂), 1.20–1.30 (♀) vs. 1.48–1.49 (♂), 1.56–1.59 (♀) in *T. multidentatus* and 1.70–1.76 (♂), 1.68–1.70 (♀) in *T. antridraconis*) and, short and upright teeth (fixed chela finger with longer teeth and movable chela finger with macrodenticles, continuous, markedly retrorse teeth in *T. multidentatus*) (Hou et al. 2023a; Mahnert 2009).

2. *Tyrannochthonius tiani* sp. nov. closely resembles *T. nanxingensis* Hou, Feng & Zhang, 2023 in the absence of intercalary teeth, the presence of four setae on tergites I–III, and the position of *sb*, which is slightly closer to *b* than to *st*, but differs in the following characters: thinner chela (9.42 (♀) times longer than broad vs. 7.12 (♀) times longer than broad in *T. nanxingensis*) and the shape of the chela teeth (movable chela finger with macrodenticles teeth vs. with smaller teeth in *T. nanxingensis*) (Hou et al. 2023a).

3. *Tyrannochthonius yanwuensis* sp. nov. closely resembles *T. akaelus* Mahnert, 2009 by the presence of intercalary teeth on both chela fingers, the presence of two setae on tergites I–II, and the absence of eyes or eyespots, but differs in the following character: the number of setae on tergites III–IV (2:2 vs. 3:4 in *T. akaelus*) (Mahnert 2009).

Acknowledgements

We are grateful to Dr. Zegang Feng, Lingchen Zhao, Tao Zheng & Songtao Shi (Hebei University, Baoding, China) and Prof. Mingyi Tian, Sunbin Huang, Mingzhi Zhao, Yan Li & Rong Chen (South China Agricultural University, Guangdong Province) for their help during the fieldwork, to subject editor Dr. Zhizhong Gao and three reviewers Dr. Jan Andries Neethling, Dr. Mark S. Harvey and one anonymous reviewer for their helpful suggestions that substantially improved this paper. This research was supported by the Natural Science Foundation of Hebei Province (no.C2024201020), the Advanced Talents Incubation Program of the Hebei University (grant 521100223004), and the National Animal Collection Resource Center of China.

References

- Chamberlin JC (1931) The arachnid order Chelonethida. Stanford University Publications, University Series. Biological Sciences 7: 1–284.
- Feng ZG, Zhang F, Chen J (2023) Cave-dwelling Neobisiidae in South China Karst, with descriptions of twelve new species of *Bisetocreagris* (Pseudoscorpiones, Neobisiidae) from Guizhou Province. *Zootaxa* 5395: 1–77. <https://doi.org/10.11646/zootaxa.5395.1.1>
- Gao ZZ, Wynne JJ, Zhang F (2018) Two new species of cave-adapted pseudoscorpions (Pseudoscorpiones: Neobisiidae, Chthoniidae) from Guangxi, China. *Journal of Arachnology* 46: 345–354. <https://doi.org/10.1636/JoA-S-17-063.1>
- Gao ZZ, Zhang F, Chen H (2020) Two new cave-dwelling species of *Tyrannochthonius* Chamberlin 1929 (Pseudoscorpiones: Chthoniidae) from the Guizhou karst, China. *Zootaxa* 4853: 572–580. <https://doi.org/10.11646/zootaxa.4853.4.6>
- Harvey MS (1992) The phylogeny and classification of the Pseudoscorpionida (Chelicerata: Arachnida). *Invertebrate Taxonomy* 6: 1373–1435. <https://doi.org/10.1071/IT9921373>
- Hou YM, Feng ZG, Zhang F (2023a) Diversity of cave-dwelling pseudoscorpions from Guizhou in China, with the description of twenty-four new species of the genus *Tyrannochthonius* (Pseudoscorpiones, Chthoniidae). *Zootaxa* 5262: 1–158. <https://doi.org/10.11646/zootaxa.5262.1.1>
- Hou YM, Feng ZG, Zhang F (2023b) New cave-dwelling pseudoscorpions of the genus *Lagynochthonius* (Pseudoscorpiones, Chthoniidae) from Guizhou in China. *Zootaxa* 5309: 1–64. <https://doi.org/10.11646/zootaxa.5309.1.1>
- Hou YM, Gao ZZ, Zhang F (2022) Diversity of cave-dwelling pseudoscorpions from eastern Yunnan in China, with the description of eleven new species of the genus *Lagynochthonius* (Pseudoscorpiones, Chthoniidae). *Zootaxa* 5198: 1–65. <https://doi.org/10.11646/zootaxa.5198.1.1>
- Judson MLI (2007) A new and endangered species of the pseudoscorpion genus *Lagynochthonius* from a cave in Vietnam, with notes on chelal morphology and the composition of the Tyrannochthoniini (Arachnida, Chelonethi, Chthoniidae). *Zootaxa* 1627(1): 53–68. <https://doi.org/10.11646/zootaxa.1627.1.4>

- Li YC (2022) Five new troglobitic species of *Tyrannochthonius* (Arachnida, Pseudoscorpiones, Chthoniidae) from the Yunnan, Guizhou and Sichuan Provinces, China. *Zookeys* 1131: 173–195. <https://doi.org/10.3897/zookeys.1131.91235>
- Mahnert V (2009) New species of pseudoscorpions (Arachnida, Pseudoscorpiones: Chthoniidae, Chernetidae) from caves in China. *Revue Suisse de Zoologie* 116: 185–201. <https://doi.org/10.5962/bhl.part.79492>
- Mahnert V, Li YC (2016) Cave-inhabiting Neobisiidae (Arachnida: Pseudoscorpiones) from China, with description of four new species of *Bisetocreagris* Ćurčić. *Revue Suisse de Zoologie* 123: 259–268.
- Schawaller W (1995) Review of the pseudoscorpion fauna of China (Arachnida: Pseudoscorpionida). *Revue Suisse de Zoologie* 102: 1045–1064. <https://doi.org/10.5962/bhl.part.80489>
- Sun JZ, Guo XB, Zhang F (2024) A review of the genus *Lagynochthonius* Beier, 1951 (Pseudoscorpiones, Chthoniidae) from China. *Megataxa* 012(2): 177–250. <https://doi.org/10.11646/megataxa.12.2.1>
- Wang KL, Zhang CH, Chen HS, Yue YM, Zhang W, Zhang MY, Qi XK, Fu ZY (2019) Karst landscapes of China: patterns, ecosystem processes and services. *Landscape Ecology* 34: 2743–2763. <https://doi.org/10.1007/s10980-019-00912-w>
- WPC (2025) World Pseudoscorpiones Catalog. Natural History Museum Bern. <https://wac.nmbe.ch/order/pseudoscorpiones/3> [accessed on 21 March 2025]

***Baeticoniscus carmonaensis* sp. nov. a new Isopod found in an underground aqueduct from the Roman period located in Southwest Spain (Crustacea, Isopoda, Trichoniscidae)**

Julio Cifuentes¹, Enrique Peña Pérez^{2,3}, Álvaro Luna⁴

1 *Departamento de Biología (Zoología), Facultad de Ciencias, Universidad Autónoma de Madrid, 28049 Cantoblanco, Madrid, Spain* **2** *Asociación Andaluza de Exploraciones Subterráneas, Sevilla, Spain* **3** *Universidad Europea de Madrid, 28670 Madrid, Spain* **4** *Department of Biosciences, Faculty of Biomedical and Health Sciences, Universidad Europea de Madrid, 28670 Madrid, Spain*

Corresponding author: Álvaro Luna (alvaro.luna@universidadeuropea.es)

Academic editor: Fabio Stoch | Received 15 October 2024 | Accepted 7 January 2025 | Published 15 May 2025

<https://zoobank.org/92A011F6-CC7E-433A-9D58-9BD37E434C8D>

Citation: Cifuentes J, Peña Pérez E, Luna Á (2025) *Baeticoniscus carmonaensis* sp. nov. a new Isopod found in an underground aqueduct from the Roman period located in Southwest Spain (Crustacea, Isopoda, Trichoniscidae). *Subterranean Biology* 51: 135–146. <https://doi.org/10.3897/subtbiol.51.139380>

Abstract

We use a morphological approach to describe a new species of isopod in the genus *Baeticoniscus*, found so far only in an underground gallery system created during the Roman period, approximately two thousand years ago, located beneath the modern town of Carmona (Seville, Spain). Specimens have been observed inhabiting rotten wood in the aphotic zone. The new species, *Baeticoniscus carmonaensis* **sp. nov.** differs from related species in the presence of the eyes as well as the number and arrangement of the tubercles and ribs on the cephalon and pereon. The description of this new species of *Baeticoniscus* represents one of the few cases worldwide in which the description of a new taxon has been described in a subterranean archaeological site.

Keywords

Crustacea, Iberian Peninsula, Isopoda, taxonomy, Trichoniscidae, urban ecology

Introduction

Nineteen families of terrestrial isopods and 269 species have been recorded in the Ibero-Balearic region, 52 of which were described in the last seven years (unpublished data). Most of these species fit into three families: Armadillidiidae Brandt, 1833, with 41 species; Porcellionidae Brandt & Ratzeburg, 1831, with 76 species; and Trichoniscidae Sars, 1899, with 89 species. Among the trichoniscids, the subfamily Trichoniscinae G.O. Sars, 1899 includes the largest number of species, while the subfamily Haplophthalminae Verhoeff, 1908, is only represented by fourteen species belonging to the following genera: *Baeticoniscus* Garcia, 2020, *Balearonethes* Dalens, 1977, *Graeconiscus* Strouhal, 1940, *Haplophthalmus* Schöbl, 1860, *Iberoniscus* Vandel, 1952 and *Moserius* Strouhal, 1940.

To date, underground ecosystems remain overlooked in conservation policies, and our knowledge of subterranean life is far from complete (Mammola et al. 2019; Nanni et al. 2023). Within these ecosystems, those created by human activities are even less studied, and many of such places often remain unknown. The role that fauna can play in utilizing human-made infrastructures, whether abandoned or still in use, is only now beginning to be properly understood. For example, some amphibians have been detected in abandoned railway tunnels (Herrero and Hinckley 2014), and drainage galleries (Rosa and Penado 2013), and Italian speleologists discovered a new subspecies of beetle, *Boldoria ghidinii ghidinii*, exclusively found in the subterranean dungeons of a castle in Brescia (Giachino and Vailati 2010). In this article, we describe a new terrestrial isopod species based on morphological characters of specimens collected from the only known location for this species, a subterranean gallery system built during the Roman period in Carmona (Seville, Spain). The conservation status of the new species remains unknown, but all specimens were detected at a single point within the artificial gallery system.

Material and methods

Study site and data collection

We conducted this study in the municipality of Carmona (Seville, Spain; 37.472, -5.638; Fig. 1A) (Instituto de Estadística y Cartografía de Andalucía 2022). Here, we specifically explored the so-called ‘*San Antón water mine*’, a complex of underground galleries located beneath the modern town. Designed for the storage and use of groundwater, the system still maintains a permanent stream and was used until recent times to supply water to residents, orchards and hydraulic infrastructures (Naranjo 2017) (Fig. 1B). Recent studies have confirmed the Roman origin of the underground gallery system, possibly dating back to the Republican period, with significant infrastructure development occurring between the 1st and 2nd centuries AD, the peak period of Carmona (the Roman name for present-day Carmona) (Naranjo and Rodríguez 2023a; Naranjo and Rodríguez 2023b). The structure of the mine includes a main gallery or aqueduct, extending 880 meters, which intercepts water currents flowing perpendicularly. It also features five forks and

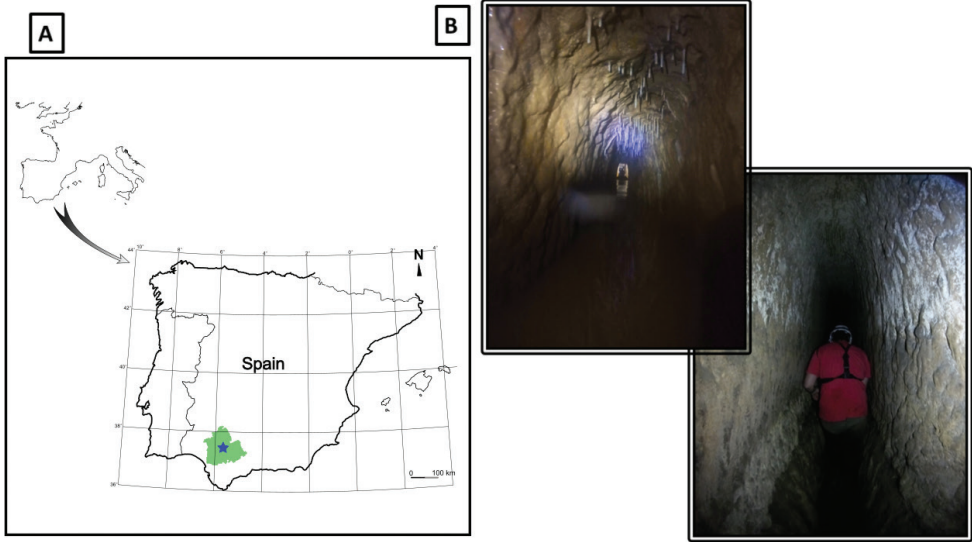


Figure 1. **A** study area, with the province of Seville in color green and the exact location of Carmona represented with a blue star **B** pictures of the location where the specimens described were found.

three short galleries (see Naranjo 2017 for a detailed description of the mine). Studies in galleries located in adjacent areas have revealed the presence of diverse species both terrestrial and aquatic, including the red swamp crayfish (*Procambarus clarkii*), and snakes such as the horseshoe whip snake (*Hemorrhois hippocrepi*) and the ladder snake (*Zamenis scalaris*) (Naranjo and Rodríguez 2023b). During our fieldwork in the ‘San Antón water mine’ we observed Spanish ribbed newts (*Pleurodeles waltl*), the amphipod *Echinogammarus obtusidens* (Gammaridae), American cockroaches (*Periplaneta americana*), the Pholcidae *Pholcus phalangioides* and the exotic spider *Howaia mogera* (Cortés-Fossati et al. 2025).

Morphological analyses and nomenclature

The identification of the specimens was based on bibliographic descriptions. Specimens were collected by hand, without the use of traps, and preserved in 70% ethanol. For microscopic preparations, the synthetic resin DMHF (dimethyl hydantoin formaldehyde) was used. To assist in the identification of the species, several figures were created using both a microscope and a stereomicroscope (Gundlach), each equipped with a 12 MP digital camera (C2CMOS). The drawings were made using the free graphic editor Inkscape (<https://inkscape.org/es/>).

Specimens have been deposited in the isopod collection of the National Museum of Natural Sciences in Madrid (MNCN) and four specimens remain in the personal collection of one of the authors (JC). Specimens of *Baeticoniscus bullonorum* Garcia, 2020 (Fig. 2) were studied to establish the necessary comparisons with the new species described in this work.

Results

Class Malacostraca Latreille, 1802

Orden Isopoda Latreille, 1816

Suborden Oniscidea Latreille, 1802

Family: Trichoniscidae G. O. Sars, 1899

Genus: *Baeticoniscus* Garcia in Garcia et al. 2020

***Baeticoniscus bullonorum* Garcia, 2020**

Material analyzed. • MÁLAGA, Benaoján, Cueva de la Pileta: 1 male and 2 females 04/27/2014, T. Pérez leg., JC402; 5 males and 4 females 04/13/2019, J. Cifuentes and J.T. Bullón leg., JC400.

Remarks. Since this is the other species of the genus to which the new species described belongs, specimens of *B. bullonorum* have been included, along with images (Fig. 2B, C), in order to establish the differences between them.

***Baeticoniscus carmonaensis* sp. nov.**

<https://zoobank.org/974EA5B5-E0E2-4E58-A8A5-E4F3D8D28E22>

Type material. Holotype. • SEVILLE, Carmona, 37.472, -5.638, Mina de San Antón, 07/27/2022, male, A. Luna, A. Adame, D. León and E. Peña leg., MNCN 20.04/20569.

Paratypes: Same locality and collectors as holotype: • 3 males, 03/12/2021, MNCN 20.04/20598 to 20.04/20600; • 1 female 06/11/2021, MNCN 20.04/20601; • 9 males, 07/27/2022, MNCN 20.04/20570 to 20.04/20578; 07/27/2022, • 2 males, 19 females (2 ovigerous) and 1 panga, MNCN 20.04/20579 to 20.04/20597; • 2 females, leg., JC662.

Etymology. The new species name refers to the town where the species was collected, Carmona.

Type locality. Carmona (Seville, Spain); system of underground galleries (37.471111, -5.642222).

Diagnosis. Cephalon with large tubercles, two elongated on the middle zone and four on posterior edge; pereonites 1 to 6 with 4 ribs and two on seventh; smooth pleon. Eyes of large, black ocellus. Pereopods 1 and 7 without sexual differentiation. Male pleopod 1, with endopod long, biarticulated and ending in hollow and striated conical point; exopod triangular, with protrusion near base. Male pleopod 2 with very long endopod ending in one silk; exopod with long rounded inner tip.

Description. Maximum length: 2.5 mm male; 2.7 mm in a female. Coloration: Specimens examined are colorless, with dark pigmented ocellus Somatic characters: **Cephalon** (Figs 2D, E, 3A) with triangular median lobe, large and rounded at end, lateral lobes and mediocre laterals slightly protruding from lateral edge and directed forwards. **Pereon** (Figs 2D, 3A) with the pereonites epimera extended as well as the pleonites epimera in the pleon. **Telson** (Figs 2D, 3A) trapezoidal, much shorter than posterior edge of uropod protopod, with concave sides and broadly rounded end.

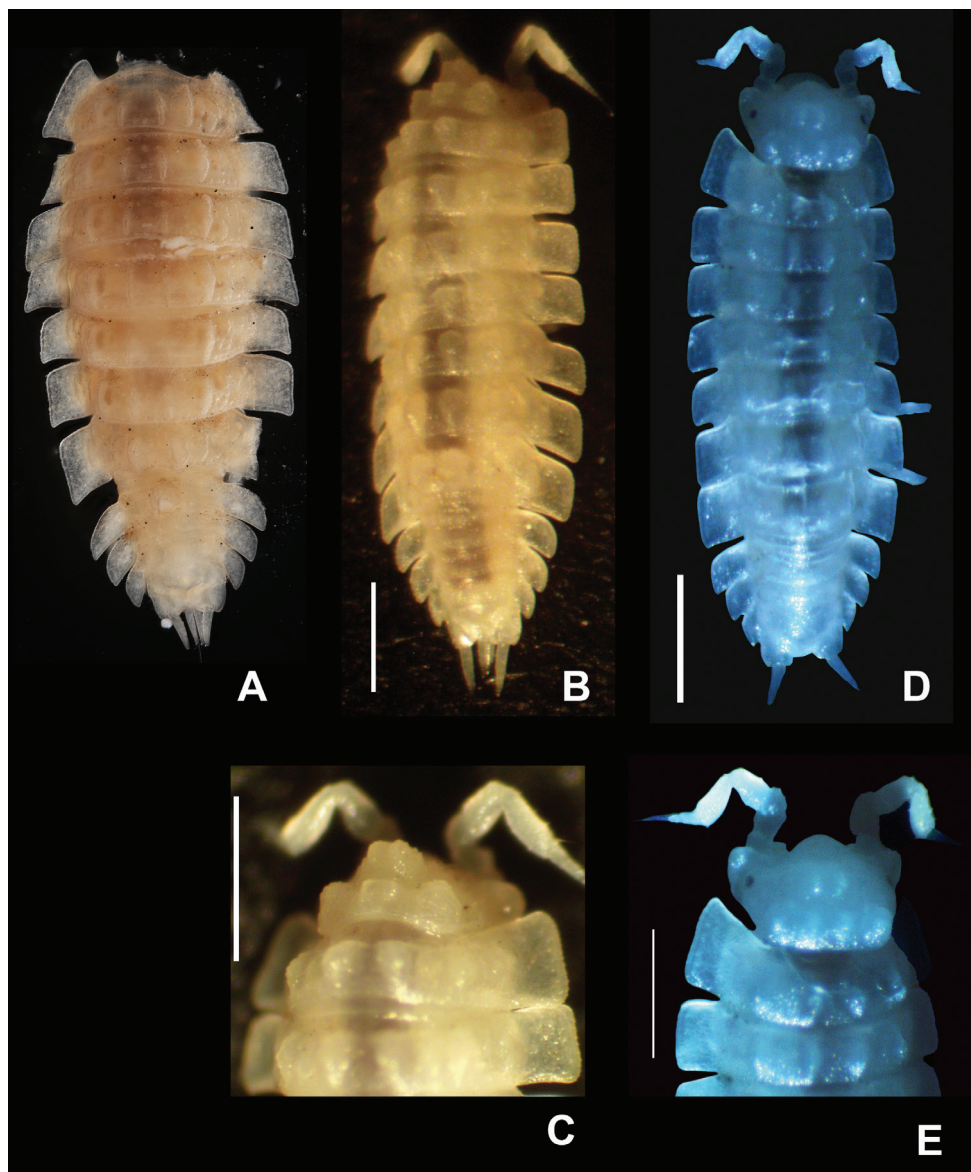


Figure 2. *Iberoniscus breuili* Vandel, 1952, female, MNHN-IU-2013-19986 **A** habitus. *Baeticoniscus bullonorum* Garcia, 2020, male, JC400 **B** habitus **C** cephalon. *Baeticoniscus carmonaensis* sp. nov., male **D** habitus **E** cephalon. Scale bars: 0.5 mm (**B–E**); (**A** sin escala).

Integumentary characters (Figs 2D, E, 3A): cephalon with two small central tubercles, behind median lobe; two large elongated tubercles on middle area and four (2+2) on posterior margin, outer ones larger. Pereonites with four longitudinal ribs (2+2), gradually reducing, pereonite 6 with outer ribes smaller, and pereonite 7 two central ribs pleon. Ocular apparatus (Figs 2D, 3A): formed by large ocellus. Appendages: *Antennula* (Fig. 3B) with three segments, basal one stout, second and third thinner and subequal in length;

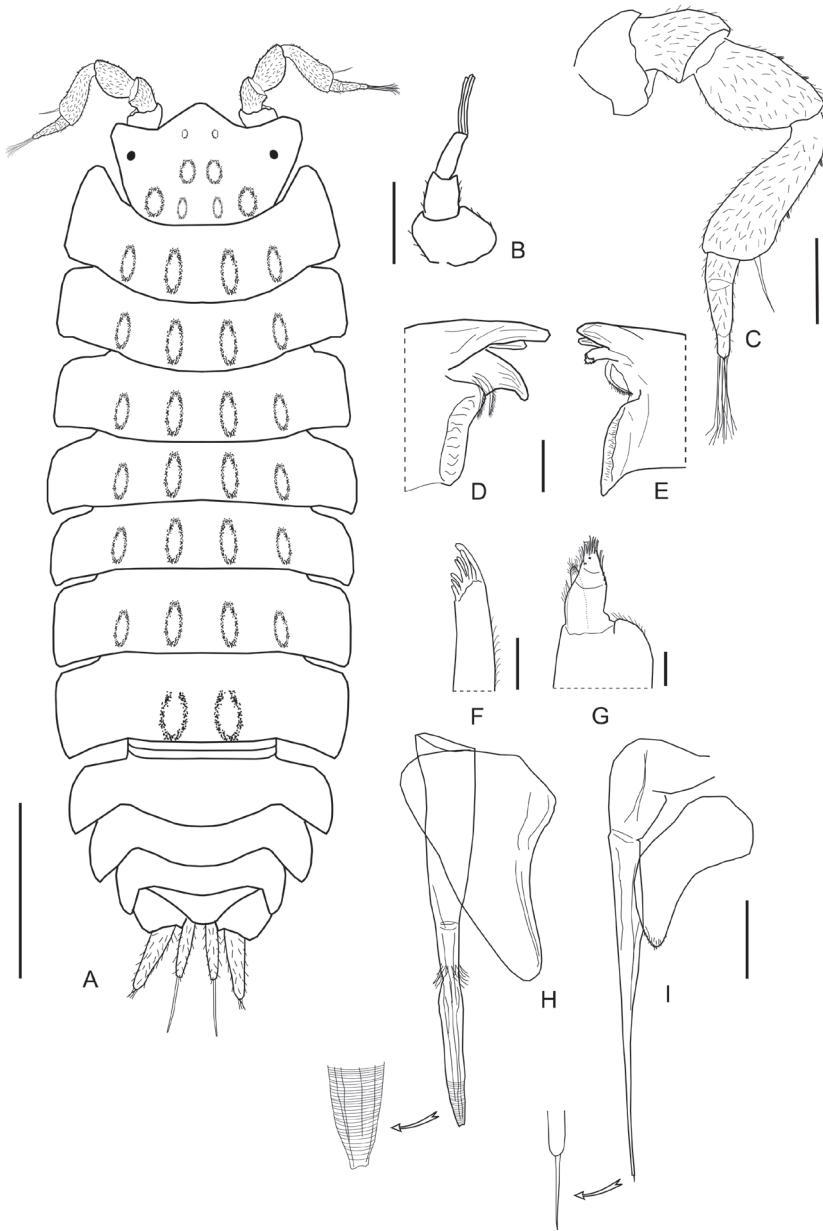


Figure 3. *Baeticonicus carmonaensis* sp. nov., male, MNCN 20.04/20598 **A** habitus **B** antennula **C** antenna MNCN 20.04/20601 **D** left mandible **E** right mandible **F** maxillula **G** maxilliped. MNCN 20.04/20598 **H** Pleopod I **I** Pleopod II. Scale bars: 0.5 mm (**A**); 0.1 mm (**C, H, I**); 0.01 mm (**B, D–G**).

third segment with three long terminal aesthetascs. **Antennas** (Fig. 3C) with fourth segment stout and with some scaly tubercles on fourth and fifth segments; flagellum of three segments, second segment with a group of aesthetascs. **Buccal pieces** (Fig. 3D–G) similar

to that of other species of the genus, with two free penicils on the left mandible (Fig. 3D) and one on the right (Fig. 3E). Maxillula and maxilliped as observed in Fig. 3F, G.

Sexual characteristics of male: Pereopods 1 and 7 without sexual differentiation. Pleopod I (Fig. 3H): endopod long, biarticulated, with long setae at junction of both segments, and ending in hollow and fluted conical point; exopod triangular, elongated, with protruding outer edge near base. Pleopod II (Fig. 3I): endopod very long, sharp and ends in one silk; exopod with long and rounded inner tip; posterior border concave and inner one convex.

Habitat and ecology. Our knowledge of the ecology of *Baeticoniscus carmonaensis* sp. nov. is limited due to the lack of specific studies on the species and the absence of other populations for comparison. *Baeticoniscus carmonaensis* sp. nov., along with others species, thrives in groundwater ecosystems. The only known population of this species has been found in elevated areas within the gallery system, beyond the reach of water floods. All specimens were discovered on or within pieces of rotten wood, likely fallen from wells connected to the underground galleries. When manipulating such wood, specimens were observed moving and hiding within the crevices of this decomposing material.

Conservation. *Baeticoniscus carmonaensis* sp. nov. is known only from the type locality, where the total number of specimens observed by the authors during fieldwork does not exceed 150–200 individuals. The site remains well preserved, as it receives no tourist or other visits, except for those made for scientific purposes, typically between 0 and 5 per year. However, recent surveys have detected microplastics in the water and sediments, suggesting a potential interaction with this species (unpublished data). Any contamination event or alteration of the environmental conditions could severely affect the only known individuals of the species. Moreover, archaeological activities or other environmental transformations could have similar impacts. Thus, the major threats to the species include increased human presence and the associated impacts of habitat transformation and depletion.

Family Platyarthridae Verhoeff, 1949

Genus *Platyarthrus* Brandt, 1833

Platyarthrus caudatus Aubert & Dollfus, 1890

Material examined. • SEVILLE, Carmona, system of underground galleries from the Roman period, 07/27/2022, 3 females and 1 panga, A. Luna, A. Adame, D. León and E. Peña leg., JC663.

Comments. This species is found in Algeria, Tunisia, Spain, France, Italy and the Mediterranean islands of Sardinia, Corsica and Sicily (Vandel 1962; Achouri et al. 2008; Abidi and Hamaied 2023). In the Ibero-Balearic area, it has been cited from Gerona, the Balearic Islands, Jaén and Málaga (Pablos 1964; Cruz 1991b; Garcia and Cruz 1996; Garcia 2009, 2013, 2019). It is cited here for the first time in the province of Seville.

Discussion

The subfamily Haplophthalminae Verhoeff, 1908, within the family Trichoniscidae G.O. Sars, 1899, includes genera whose species exhibit an integument characterized by prominent tubercles. The differences in the ornamentation patterns of many of these species are minimal, which is why Schmalfuss et al. (2004) recommended a review of this subfamily. Additionally, the differences in the secondary sexual characters, mainly in the first two pairs of pleopods of the males, are also usually small, complicating the identification of specimens.

Until now, fourteen species belonging to six genera of this subfamily are known in the Iberian Peninsula:

Balearonethes Dalens, 1977 with *B. sesrodesanus* Dalens, 1977 from the Balearic Islands (Dalens, 1977; Cruz, 1991a).

Graeconiscus Strouhal, 1940 with *G. gevi* Garcia, Miralles-Núñez & Pérez-Fernández, 2020 from Málaga (Garcia et al. 2020).

Haplophthalmus Schöbl, 1860, the most important in terms of the number of species, with *H. alicantinus* Cruz & Dalens, 1989 from Alicante (Cruz and Dalens 1989; González Silvestre 2015); *H. asturicus* Vandel, 1952 from Asturias (Vandel 1952; Cifuentes et al. 2021); *H. chisterai* Cruz & Dalens, 1989 from Alicante and the Balearic Islands (Cruz and Dalens 1989; Cruz 1991a; Cifuentes 2021b); *H. danicus* Budde-Lund, 1880 with a wide distribution area, as it has been reported from Bizkaia, Cantabria, Barcelona, the Balearic Islands, Orense, Pontevedra, Seville, Tarragona and Teruel (Arcangeli 1924; Schmölzer 1955, 1971; Cruz 1991a; Garcia and Cruz 1996; Barrientos 2005; Garcia 2009; Gregory et al. 2012; Cifuentes 2019, 2021a; Cifuentes and Tinaut 2019; Cifuentes et al. 2021); *H. gibbus* Legrand & Vandel, 1950 from the Balearic Islands (Vandel 1960); *H. mengii* (Zaddach, 1844) from Barcelona, Bizkaia, Cantabria, Gipuzkoa Girona and Navarra (Arcangeli 1924; Cifuentes et al. 2021); *H. siculus* Dollfus, 1896 from Girona and Tarragona in Spain, Faro and Setúbal in Portugal (Vandel 1946; Cruz 1991a); *H. transiens* Legrand & Vandel, 1950 from Castellón and Málaga (Vandel 1952, 1960; Cifuentes 2021b) and *H. valenciae* Cruz & Dalens, 1989 only known from Valencia (Cruz and Dalens 1989; González Silvestre 2015).

Iberoniscus Vandel, 1952 with *I. breuili* Vandel, 1952 from Cádiz and Málaga (citation that we consider doubtful as stated below) in Spain, and from Gibraltar (Vandel 1952).

Moserius Strouhal, 1940 with *M. inexpectatus* Reboleira & Taiti, 2015 from Santarém in Portugal (Reboleira et al. 2015).

Finally, the genus *Baeticoniscus* Garcia, 2020, was monospecific until this study, with *B. bullonorum* Garcia, 2020, as its only representative. Garcia (2020) described *B. bullonorum* from 31 specimens, 10 males and 21 females, from Cueva de la Pileta, located in Benaoján, province of Málaga (Spain) (Garcia et al. 2020). *Baeticoniscus bullonorum* is characterized by the presence of prominent tubercles on the cephalon, 4 ridges (2+2) on pereonites 1 to 6, and 2 ridges (1+1) on pereonite 7, a smooth pleon, and striations on the tip of the endopod of the male's first pleopod. All these characteristics are present in *Baeticoniscus carmonaensis* sp. nov., which justifies its classification within this genus.

From the same Cueva de la Pileta, Vandel (1952) studied five specimens, two males and three females, which along with other specimens from the Cueva de las Motillas in Jerez de la Frontera (Cádiz) and from the Old St Michel's Cave in Gibraltar, were used for the description of *Iberoniscus breuili* Vandel, 1952. A comparison between the descriptions of both species, *I. breuili* and *B. bullonorum*, reveals important differences between them in the ornamentation of the integument. *I. breuili* presents five pairs of ribs on the pereion (Fig. 1A) and a tubercle in the pleonite 3, whereas *B. bullonorum* has two pairs of ribs on the pereion and lacks a pleon tubercle (Fig. 2B, C). Note also the presence of a developed carpal lobe on the pereopod 7 of the male in *I. breuili*, which is absent in *B. bullonorum*. However, the drawings of the cephalon tubercles provided by both authors for their respective species are very similar (see Vandel 1952 p. 350 and Garcia 2020 p. 261).

We studied 12 specimens (six males and six females) of *B. bullonorum* from the Cueva de la Pileta, consistent with the description of this species by Garcia (2020). These specimens exhibit the same arrangement of tubercles on the cephalon (Fig. 2C) as *I. breuili* described by Vandel, but without the accessory ribs on the pereion and the large tubercle on pleonite 3 characteristic of that species. In the Vandel collection deposited at the Muséum national d'Histoire naturelle (MNHN) in Paris, under reference MNHN-IU-2013-19986, there is a single tube containing several poorly preserved specimens of *I. breuili* from two of the localities mentioned by Vandel (1952). Of one of these specimens, which lacks the cephalon, have been photographed (Fig. 2A) and the accuracy of Vandel's description can be confirmed in relation to the ribs of the pereion and the tuberculation of the pleon, but as it lacks the cephalon, the tubercles cannot be observed. As noted earlier, since the only preserved specimens belong to the two localities are mixed, it is not possible to determine which cave the specimen in the photograph originates from. We consider it unlikely that two species from different genera, in which the integument ornamentation is a crucial character, would exhibit the same arrangement of tubercles on the cephalon. Since all 43 specimens studied from the Cueva de la Pileta by both Garcia (2020) and us undoubtedly correspond to *B. bullonorum*, it is highly probably that *I. breuili* is not present in the Cueva de la Pileta as Vandel (1952) said. It is likely that the specimens Vandel studied from this locality actually belong to *B. bullonorum*. Thus, until the Cueva de las Motillas in Jerez de la Frontera (Cádiz) and the Old St. Michael's Cave in Gibraltar can be revisited, *I. breuili* would only be known from these caves, not from the Cueva de La Pileta in Málaga.

Baeticoniscus carmonaensis sp. nov. is differentiated from *B. sesrodesanus*, as the latter species has spiny tubercles arranged in several rows, not forming ribs. In *G. gevi* and *I. breuili* there is a large tubercle on the third pleonite, and in *M. inexpectatus* there are two, neither of which are found in *B. carmonaensis* sp. nov. In *Haplophthalmus* species, the tubercles are much weaker than those found in *B. carmonaensis* sp. nov. Finally, *B. carmonaensis* sp. nov. (Figs 2D, E, 3A) differs from other species in the genus *Baeticoniscus* due to the presence of the ocular apparatus, the absence of lateral roughness and the cephalon tubercle, as it only has two elongated median tubercles and four posterior ones, compared to the bilobed frontal tubercles of *B. bullonorum* (Fig. 2B, C).

The description of this new species is significant for different reasons. Beyond enhancing our understanding of underground biodiversity and European terrestrial isopods, this discovery represents one of the few descriptions of a new species in an urbanized area. Considering the growing effort for a greater recognition of subterranean ecology, the discovery of a new species in an urban underground environment- alongside other species as *Platyarthrus caudatus*- can help draw attention to these often overlooked ecosystems, particularly in cities with archaeological sites, canals, and tunnels. Regarding the unknown conservation status of the species, increasing research is demonstrating how cities can play a role in nature conservation, sometimes being the main habitat for species (Luna and Rausell-Moreno 2024). For *Baeticoniscus carmonaensis* sp. nov. future surveys in other underground environments in southern Spain could confirm its presence in new cave systems, both artificial and natural, which would help inform conservation measures with more comprehensive knowledge. In any case, the species is currently only known from a single population, found in decaying wood, consisting of several hundred specimens.

Acknowledgements

We would like to express our gratitude to MR. J.T. Bullón for his generosity in providing specimens, facilitating access and accompanying us during the sampling at the Cueva del Cerro de la Pileta, in Benaoján (Málaga). We also express our gratitude to Paula Rodríguez Moreno, Collection Manager at the Muséum national d'Histoire naturelle de Paris (MNHN) for providing us with the photograph of the Vandel specimen mentioned in the text. Finally, we thank the members of the AAES (Asociación Andaluza de Exploraciones Subterráneas), for their contribution to the broader understanding of the underground system studied in this project. In particular, we wish to express our heartfelt thanks to José Millán for his unwavering dedication to the speleological exploration of the region. Sadly, he passed away during the course of this work.

References

- Abidi S, Hamaied S (2023) A new species of *Platyarthrus* Brandt, 1833 from Tunisia: Morphological description, geographical distribution and ecological remarks. *Biologia* 79: 109–114. <https://doi.org/10.1007/s11756-023-01503-6>
- Achouri MS, Hamaied S, Charfi-Cheikhrouha F (2008) The diversity of terrestrial Isopoda in the Berkoukech area, Kroumirie, Tunisia. *Crustaceana*, 917–929. <https://doi.org/10.1163/156854008X354948>
- Arcangeli A (1924) Contributo alla conoscenza degli isopodi della Catalogna. *Trabajos del Museo de Ciencias naturales de Barcelona* 4(12): 3–29. [5 láms]
- Barrientos JA (2005) Artrópodos no insectos de la provincia de Teruel. Estado de la cuestión. *Revista del instituto de estudios turolenses* 90: 253–294.
- Cifuentes J (2019) Los isópodos terrestres de Galicia, España (Crustacea: Isopoda, Oniscidea). *Graellsia* 75(2): e098. [13 pp] <https://doi.org/10.3989/graeellsia.2019.v75.243>

- Cifuentes J (2021a) Los isópodos terrestres de Andalucía, España (Crustacea: Isopoda, Oniscidea). *Graellsia* 77(1): e133. <https://doi.org/10.3989/graelesia.2021.v77.276>
- Cifuentes J (2021b) Contribución al conocimiento de los isópodos terrestres de la Comunidad Valenciana y de la Región de Murcia, España (Crustacea: Isopoda, Oniscidea). *Graellsia* 77(2): e143. <https://doi.org/10.3989/graelesia.2021.v77.296>
- Cifuentes J, Tinaut A (2019) Isópodos terrestres (Crustacea, Isopoda, Oniscidea) de las cavidades del Parque Natural de la Sierra Norte de Sevilla (España). *Boletín Asociación española de Entomología* 43(1–2): 79–90.
- Cifuentes J, Beruete E, Prieto CE (2021) Isópodos oniscídeos en cuevas de la región Vasco-Cantábrica, España (Crustacea: Isopoda). *Boletín de la Sociedad Entomológica Aragonesa (S.E.A.)* 68: 270–288.
- Cortés-Fossati F, Barrientos JA, González-Moliné AL, Peña Pérez E, Luna Á (2025) A review on the global spread of the non-native spider *Howaia mogera* (Yaginuma, 1972) (Araneae: Nesticidae), with first records for the Iberian Peninsula. *Arachnology* 20(1): 52–59.
- Cruz A (1991a) Isópodos terrestres de la colección del Museu de Zoologia de Barcelona (Crustacea, Oniscidea). *Miscelánea zoológica, Barcelona* 15: 81–102.
- Cruz A, (1991b) Especies nuevas o poco conocidas de isópodos terrestres de la Península Ibérica. II. Isópodos epigeos de España y Portugal (Crustacea, Oniscidea). *Bulletin de la Société d'Histoire naturelle de Toulouse* 127: 71–75.
- Cruz A, Dalens H (1989) Especies nuevas o poco conocidas de isópodos terrestres de la Península Ibérica. I. Isopodos cavernícolas de la España oriental (Crustacea, Oniscidea). *Bulletin de la Société d'Histoire naturelle de Toulouse* 125: 91–98.
- Dalens H (1977) Sur un nouveau genre de Trichoniscidae, *Balearonethes sesrodesanus* n. g., n. sp. (Isopoda, Oniscoidea). *Bulletin de la Société d'Histoire naturelle de Toulouse* 113: 298–302. [1 pl.]
- García L (2009) Les “someretes” (Crustacis isòpodes terrestres: Isopoda, Oniscidea) de la vall de Sóller (Mallorca). Aproximació a una biodiversitat menystinguda. En: III Jornades Estudis Locals a Sóller. Ed. Ajuntament de Sóller, 129–146.
- García L (2013) Isópodos terrestres (Crustacea: Oniscidea) recolectados en cavidades subterráneas de Jaén. En: Los invertebrados de hábitats subterráneos de Jaén, Pérez Fernández, T. y Pérez Ruiz, A. (coord.). Grupo de Espeleología de Villacarrillo (G.E.V.) (Ed.), 78–87.
- García L (2019) Nuevos registros de Isópodos terrestres (Crustacea: Oniscidea) en España meridional (Andalucía y Murcia). *Revista Sociedad Gaditana Historia Natural* 13: 27–32.
- García L, Cruz A (1996) Els isòpodos terrestres (Crustacea: Isopoda: Oniscidea) de les Illes Balears: catàleg d'espècies. *Bolletí de la Societat d' Història natural de les Balears* 39: 77–99.
- García L, Miralles-Núñez A, Pérez-Fernández T (2020) A new genus and species of cave-dwelling terrestrial isopod (Crustacea: Oniscidea: Trichoniscidae) from Southern Spain. *Zootaxa* 4822(2): 257–268. <https://doi.org/10.11646/zootaxa.4822.2.7>
- Giachino PM, Vailati D (2010) The subterranean environment. Hypogean life, concepts and collecting techniques. *WBA Handbooks* 3, Verona, 1–132.
- González Silvestre JV (2015) Memorias del inframundo: Bioespeleología I. *Gota a gota* 7: 1–13.
- Gregory S, Lee P, Read HJ, Richards P (2012) Woodlice (Isopoda: Oniscidea) collected from northwest Spain and northern Portugal in 2004 by the british myriapod and isopod group. *Bulletin of the British Myriapod & Isopod Group* 26: 6–23.

- Herrero D, Hinckley A (2014) First record of a tunnel breeding population of *Pleurodeles waltl* and two other records of Iberian cave dwelling urodeles. *Reptilia* 28: 387–392.
- Instituto de Estadística y Cartografía de Andalucía (2022) Andalucía pueblo a pueblo - Fichas Municipales. <https://www.juntadeandalucia.es/institutodeestadisticaycartografia/sima/ficha.htm?mun=41024> [checked 07/02/2024]
- Luna Á, Rausell-Moreno A (2024) Unveiling the urban colonization of the Asian water monitor (*Varanus salvator*) across its distribution range using citizen science. *PeerJ* 12: e17357. <https://doi.org/10.7717/peerj.17357>
- Mammola S, Cardoso P, Culver Dc, Deharveng L, Ferreira RI, Fišer C, Galassi Dmp, Griebler C, Halse S, Humphreys Wf, Isaia M, Malard F, Martinez A, Moldovan Ot, Niemiller MI, Pavlek M, Reboleira Aspd, Souza-Silva M, Teeling Ec, Wynne Jj, Zagnajster M (2019) Scientists' warning on the conservation of subterranean ecosystems. *BioScience* 69(8): 641–650. <https://doi.org/10.1093/biosci/biz064>
- Nanni V, Piano E, Cardoso P, Isaia M, Mammola S (2023) An expert-based global assessment of threats and conservation measures for subterranean ecosystems. *Biological Conservation* 283: 110136. <https://doi.org/10.1016/j.biocon.2023.110136>
- Naranjo JM (2017) La mina de agua de San Antón (Carmona, Sevilla). *Gota a gota* (14): 40–58.
- Naranjo JM, Rodríguez JMR (2023a) Estudio espeleoarqueológico de la mina de agua de Alcaudete (Carmona), una extraordinaria obra de ingeniería hidráulica romana. 2º parte: Descripción general de la mina. *Gota a Gota* 28: 74–96.
- Naranjo JM, Rodríguez JMR (2023b) Estudio espeleoarqueológico de la mina de agua de Alcaudete (Carmona), una extraordinaria obra de ingeniería hidráulica romana. 3ª parte: Valoraciones finales, cronología, funcionalidad, valores patrimoniales, amenazas y necesidad de protección, agradecimientos. *Gota a Gota* 29: 20–32.
- Pablos F (1964) Isópodos de las islas Medas. *Publicaciones Instituto Biología Aplicada*, Universidad de Barcelona 36: 97–100.
- Reboleira AS, Gonçalves F, Oromí P, Taiti S (2015) The cavernicolous Oniscidea (Crustacea: Isopoda) of Portugal. *European Journal of Taxonomy* 161: 1–61. <https://doi.org/10.5852/ejt.2015.161>
- Rosa G, Penado A (2013) *Rana iberica* (Boulenger, 1879) goes underground: subterranean habitat usage and new insights on natural history. *Subterranean Biology* 11: 15–29. <https://doi.org/10.3897/subtbiol.11.5170>
- Schmalfuss H, Paragamian K, Sfenthourakis S (2004) The terrestrial isopods (Isopoda: Oniscidea) of Crete and the surrounding islands. *Stuttgarter Beiträge zur Naturkunde, Serie A*, 662, 74 pp.
- Schmölzer K (1955) Isopoda terrarum mediterraneorum. 1. Mitteilung: Über neue und bekannte Landasseln der Pyrenaenhalbinsel. *Eos (Madrid)* 31: 155–215.
- Schmölzer K (1971) Die Landisopoden der Iberischen Halbinsel. *Monografías de Ciencia moderna (Madrid)* 80: XI, 161 pp. [10 maps]
- Vandel A (1946) Crustacés isopodes terrestres (Oniscoidea) épigés et cavernicoles du Portugal. *Anais da Faculdade de Ciências do Porto* 30: 135–427.
- Vandel A (1952) Biospeologica LXXIII. Isopodes terrestres (troisième série). *Archives de Zoologie expérimentale et générale* 88: 231–362.
- Vandel A (1960) Faune de France, vol. 64. Isopodes terrestres (première partie), Paris, 1–416.
- Vandel A (1962) Faune de France, 66. Isopodes terrestres (deuxième partie), Paris, 417–931.

***Amphicutis stygobita* (Echinodermata, Ophiuroidea, Amphilepidida, Amphilepididae), a brooding brittle star from anchialine caves in The Bahamas: feeding, reproduction, morphology, paedomorphisms and troglomorphisms**

Jerry H. Carpenter¹

¹ *Department of Biological Sciences, Northern Kentucky University, Highland Heights, Kentucky 41099, USA*

Corresponding author: Jerry H. Carpenter (carpenter@nku.edu)

Academic editor: Elizabeth Borda | Received 10 March 2025 | Accepted 26 April 2025 | Published 16 May 2025

<https://zoobank.org/B7817771-B422-44BE-9F79-6BF76A975382>

Citation: Carpenter JH (2025) *Amphicutis stygobita* (Echinodermata, Ophiuroidea, Amphilepidida, Amphilepididae), a brooding brittle star from anchialine caves in The Bahamas: feeding, reproduction, morphology, paedomorphisms and troglomorphisms. *Subterranean Biology* 51: 147–196. <https://doi.org/10.3897/subtbiol.51.152663>

Abstract

Amphicutis stygobita Pomory, Carpenter & Winter, 2011 was the world's first known cave brittle star. It has been found only in two anchialine caves: Bernier Cave (type locality and current study area) and Lighthouse Cave on San Salvador Island, The Bahamas. Bernier Cave's low salinity (14–28 ppt) reduces ionic precipitation in *A. stygobita*'s endoskeleton to produce fewer and lighter ossicles. Scanning electron microscopy (SEM) revealed details of internal skeletal structures including elongated arm segment ossicles with greatly reduced density and increased fenestration. The large ceiling entrance of Bernier Cave is directly above the water allowing abundant growth of algae and accumulation of detritus. Small (disk diameter = 3–4 mm) microphagous deposit-feeding brittle stars survived and grew in captivity by consuming energy-rich detritus containing algae, bacteria, invertebrates, and a sticky biofilm containing extracellular polymeric substances (EPS). Reproductive structures are described for this hermaphroditic brooding species, as are morphology and growth rates for adults and three babies born in captivity. Comparisons are made to three recently described cave species that appear to be cave endemics and to several epigeal brittle stars including the brackish-water species *Ophiophragmus filigraneus* and two deep-sea species: *Amphilepis patens* and *Amphilepis platytata* herein removed from synonymy. Several of these species show paedomorphy, including reduced mouth structures and arm ossicles. Paedomorphy conserves energy by not producing, maintaining, and transporting adult structures not needed for survival. Paedomorphic traits that are adaptive and occur in cave organisms are considered troglomorphic traits, as in *A. stygobita*. Correlations are made between specific paedomorphisms and environmental features.

Keywords

Amphilepis patens, *Amphilepis platytata*, detritus, energy conservation, extracellular polymeric substances, hermaphroditic, ossicles, streptospondylous

Introduction

Amphicutis stygobita, described by Pomory, Carpenter and Winter in 2011, was the world's first known cave brittle star. Pomory et al. (2011) assigned this new genus and species to the family Amphilepididae in the order Ophiurida, but this family is now placed in the order Amphilepidida, created by O'Hara et al. (2017, 2018). The small family Amphilepididae includes only the cave species *Amphicutis stygobita* and 12 species of *Amphilepis* (Stöhr et al. 2024), which are all deep sea. Caves that are close to oceans typically contain salt water or brackish water; such caves without a surface connection to the ocean are called anchialine (for definitions please see Holthuis 1973; Stock et al. 1986; Bishop et al. 2015; Carpenter 2021). *Amphicutis stygobita* has been found only in two anchialine caves: Bernier Cave (type locality) and nearby Lighthouse Cave on San Salvador Island, The Bahamas (Fig. 1A–E). It is much more abundant in Bernier Cave; to my knowledge, only two specimens have ever been found in Lighthouse Cave, and they were not used in the current study. Carpenter (2016) reported additional observations on the biology and behavior of *A. stygobita*, including apparent cave adaptations (troglomorphisms): no body pigment, reduced body size, elongated arm segments, muted alarm response to light, reduced aggregation, slow movement primarily with podia (rather than by swinging arms forward), and extremely slow regeneration of 0.03 mm/wk (this is about 1% of the average rate for 13 species reported by Clark et al. 2007). Carpenter (2016) also noted that, “They are challenging to maintain in the laboratory because they are susceptible to light, salinity changes, and elevated temperatures, and they don't accept food normally eaten by brittle stars.” The brittle stars survived and grew in captivity using cave detritus as their only food source. Comparisons are made between Bernier Cave and deep-sea environments, since the relatively high richness of detritus is presumed to be one of the main reasons the brittle star population does well in this cave and why there are so many deep-sea brittle star species.

Caves and deep-sea environments are both characterized by low food supplies because they are dark and have no primary production by photosynthesis (Culver and Pippin 2019), but this is not always the case. Bernier Cave is exceptional because the large ceiling entrance allows detritus and sunlight to enter and produce an energy-rich food source for *A. stygobita*. Similarly, some areas of the deep-sea floor are covered by abundant energy-rich phytodetritus which can provide food for brittle stars that are detritivores (Ramirez-Llodra et al. 2010). I contend that high-energy detritus promotes paedomorphy (retention of juvenile traits by adults). In both environments, the soft and sticky detritus contains extracellular polymeric substances (EPS) that provide food and may aid ingestion by brittle stars that have paedomorphically reduced mouthparts.

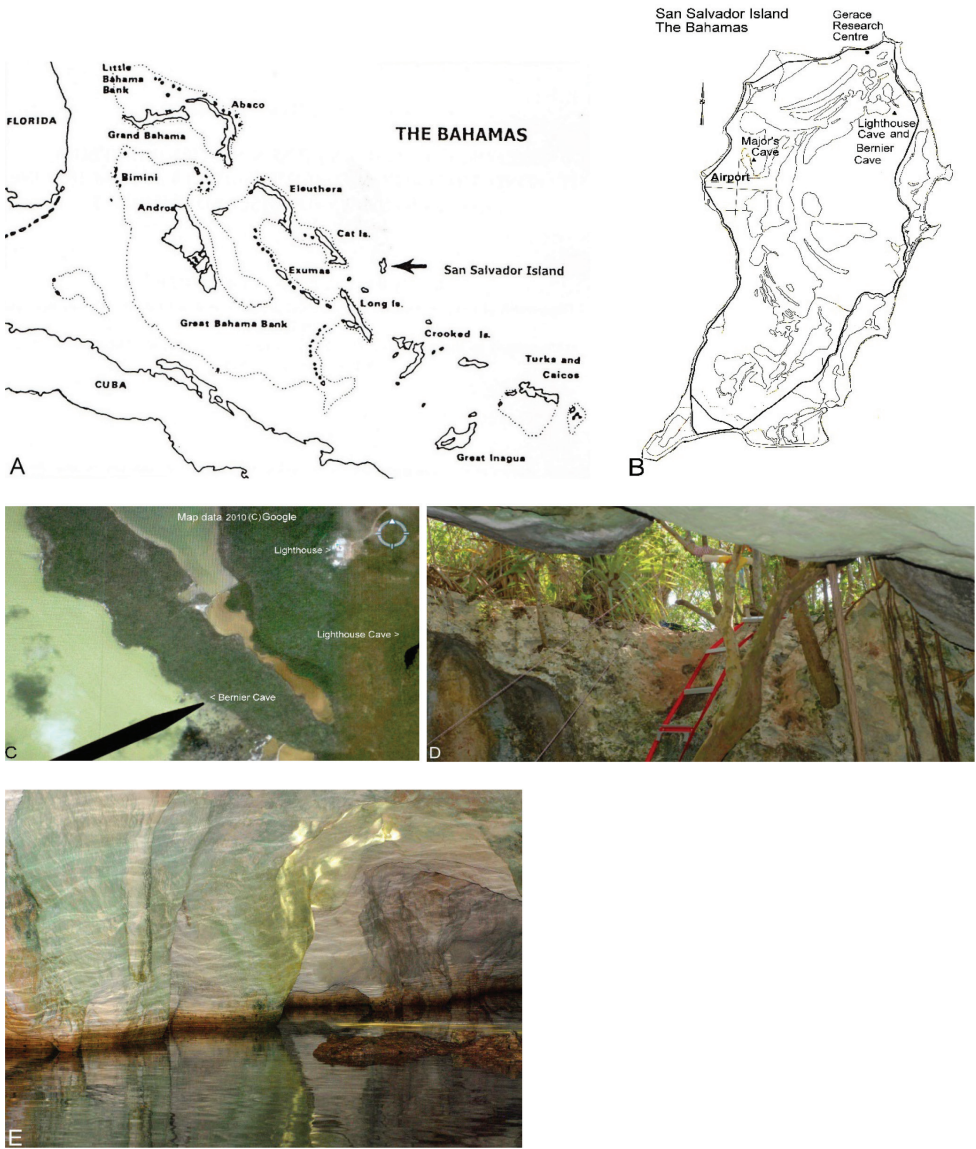


Figure 1. Location **A** map with location of San Salvador Island in The Bahamas (from Carpenter 2021) **B** map of San Salvador Island with locations of Bernier Cave and Lighthouse Cave (modified from Carpenter 2021) **C** Google earth map with location of caves **D** ceiling entrance to Bernier Cave **E** algae-covered wall below entrance to Bernier Cave.

Reproductive structures are described for this brooding species, as are morphology and growth rates for adults and three individuals born in captivity. Only about 3% (~70 species) of the 2000+ species of brittle star species are known to be brooders (Hendler 1975; Hendler et al. 1995; Stöhr 2005). Stöhr et al. (2012) indicated that there were 2064 described species of brittle stars, and “juvenile stages are still only

known for less than 50 species.” There are very few observations on the development and behavior of newly released babies, so keeping *A. stygobita* babies alive for up to 14.5 months provided valuable information.

The original description of *A. stygobita* included many detailed images using light microscopy, and it is expanded herein with descriptions of the internal skeletal structure (stereom) of adults using scanning electron microscopy (SEM). Comparisons are made to several epigeal brittle star species including two deep-sea species, *Amphilepis patens* Lyman, 1879 and *Amphilepis platytata* HL Clark, 1911; although these two species were synonymized in 1917 (Clark 1917), I present evidence for them to be recognized as separate species. Comparisons are also made to the brackish-water species *Ophiophragmus filigraneus* (Lyman, 1875) and to three recently described species that appear to be cave endemics: (1) *Ophiozonella cavernalis* Okanishi & Fujita, 2018 (Japan), (2) *Ophionereis commutabilis* Bribiesca-Contreras et al., 2019 (Mexico), and (3) *Ophiopsila xmasilluminsans* Okanishi, Oba & Fujita, 2019 (Christmas Island, north of Australia).

Because *A. stygobita* has so many unusual traits, I felt it important to include an abundance of photographs of this species and of several species used for comparison. Hopefully, these photographs will help other researchers better understand the unusual traits. The photographs also support rare observations on feeding, birth and growth of three babies, and paedomorphic traits.

Materials and methods

Study area

Bernier Cave (24°05'37"N, 7°27'15"W) is about 1.5 km from the ocean in the north-eastern part of San Salvador Island, The Bahamas (Fig. 1A, B). The entrance is only ~20 m from the northeast arm of Great Lake (Fig. 1C). Near the cave this lake is hypersaline with salinities sometimes measuring > 70 ppt (personal observations), so it is surprising that the water inside Bernier Cave is hyposaline at ~14–28 ppt. Salinities and temperatures were measured at various locations, depths, and times in Bernier Cave using refractometers and hydrometers for salinities and a probe thermometer for temperatures. Pomory et al. (2011) noted that, “It appears meteoric water or water from a subsurface freshwater lens infiltrates Bernier Cave, so that the shallow-water environment may never reach total marine salinity of 35 ppt.” While most anchialine caves in The Bahamas and other locations around the world are stratified with a freshwater layer and halocline layer over a saltwater layer, the anchialine caves on San Salvador Island have salt water or brackish water all the way to the surface (Carpenter 2021).

One of the most important features of Bernier Cave is that the ceiling entrance is large and directly above or near the water (Fig. 1D). This allows considerable detritus to enter the aquatic ecosystem. It also provides an unusual amount of light to reach the walls of the entrance room to create abundant and colorful growth of algae (Fig. 1E), including the large dominant diatom *Campylodiscus neofastuosus* Ruck & Nakov (Ruck

et al. 2016a, 2016b) (Fig. 2A, B). The unusual brackish-water environment in Bernier Cave, along with adequate sunlight, provides an ideal habitat for *Campylodiscus* diatoms. The companion paper in this issue (Steinitz-Kannan et al. 2025) describes this diatom population from Bernier Cave and its special adaptations to thrive in low light. The detritus also contained nematodes, ostracods, harpacticoid copepods, ciliates, dinoflagellates, foraminiferans, cyanobacteria, other bacteria, and a sticky biofilm containing extracellular polymeric substances (EPS).



Figure 2. Large diatoms, macroinvertebrates, fish, and bats found in Bernier Cave **A** 40 × dissecting microscope view of *Campylodiscus neofastuosus* diatoms **B** compound microscope view of *C. neofastuosus* with branching chloroplast and oil droplets **C** 7.5 mm cirranean isopod *Babalana geracei* with ~12 eggs **D** mangrove killifish *Kryptolebias marmoratus* watching brittle star **E** 9 mm diameter hydromedusa *Vallerinina gabriellae* **F** colony of buffy flower bats *Erophylla sezekorni*, mostly females with babies, roosting in dark area of cave.

Tidal fluctuations (changes in water depth between low and high tide) are relatively slight compared to Lighthouse Cave and the ocean water surrounding the island. This results in very slow movement of water during tidal flows and allows sizeable accumulations of detritus, some of which is distributed throughout the cave with each tidal flow.

Besides *A. stygobita*, other small animals we found in Bernier Cave include the cirrolanid isopod *Bahalana geracei* Carpenter, 1981 (Fig. 2C), and mangrove killifish *Kryptolebias marmoratus* (Poey, 1880) (Fig. 2D). Carpenter (2016) found that neither of these predators appeared to show interest in preying on *A. stygobita* in laboratory experiments. In 2015 my research team collected three specimens of the rare hydromedusa *Vallentinia gabriellae* Vannucci Mendes, 1848 (Fig. 2E) in Bernier Cave's entrance room; this appears to be the first record of this species in The Bahamas. Birds occasionally flew through the entrance room. Female buffy flower bats *Erophylla sezekorni* (Gundlach, 1861) with babies sometimes roosted in dark areas of the cave (Fig. 2F).

Sampling

All specimens of *A. stygobita* were found in shallow water 10–40 cm deep in dark areas of Bernier Cave using underwater flashlights. It was challenging to find specimens because this species is exceptionally small, with disk diameters (dd) of only 3–4 mm and short arms to 10 mm, and their lack of pigment helps them blend into the detritus. Our fingers and spatulas were usually used to scoot specimens into 35 mm film canisters or small clear jars; pipettes were used to transfer detritus from the substrate to small jars. Each specimen was kept in a separate container to reduce oxygen depletion and damage to arms from entangling with other specimens. They were taken to the Gerace Research Centre for short-term observation, then to Kentucky for long-term observation and experimentation. Collections were made in 2011, 2013, 2014, 2015, 2016, 2018. In most years, fewer than 6 specimens were collected, so there are insufficient numbers to warrant traditional statistical tests; however, the few specimens collected provided valuable support of observations on the biological phenomena reported herein.

Culture methods

The following culture techniques were used as reported by Carpenter (2016):

“Each specimen was kept in a small jar with ~30 ml of brackish water (20–28 ppt), similar to that of Bernier Cave. Depth in each jar was kept shallow (1–2 cm) for a high surface area to volume ratio to keep oxygen levels high. Jars had tight-fitting lids (rather than loose lids as with Petri plates) to limit evaporation that could increase salinity. Salinities were checked weekly with a refractometer. If salinity increased, it was reduced slightly by adding 1–2 ml of water at a slightly lower salinity; drops were added slowly and away from specimens to avoid salinity shock. A thin layer of detritus

from Bernier Cave was kept on the bottom of each jar to provide food and to help stabilize levels of oxygen and salinity. An additional 8–15 drops of new Bernier Cave detritus were added every 4–7 days. Animals ignored or rejected other foods offered including small pieces of TetraMin© fish flakes, shrimp, boiled egg, and boiled lettuce. Each specimen jar was labeled so individual records could be kept of maintenance, experiments, and general observations. Animals were kept in darkness except during observations and maintenance. Observations and maintenance were done at night or in a room without windows to avoid even weak sunlight, and jars were shaded from direct overhead lights and microscope lights.”

Specimens were kept near Bernier Cave temperatures of 23–25 °C (73–77 °F) by using either a 10-gallon tank with a heating pad below, or a water bath with an aquarium heater. Jars of Bernier Cave detritus were also kept in darkness at cave temperatures and salinities to try to keep them viable and to avoid temperature or salinity shock when detritus was added to specimen jars.

Photographic and SEM methods

All photos were taken by the author. Except for SEM images and one light microscope image (Fig. 4F), photographs of *A. stygobita* in this paper are of live specimens using various Nikon cameras with built-in flashes and a 60 mm micro-Nikkor lens, either shot through an Olympus dissecting microscope or directly. Photographs of some individuals were shot approximately weekly to record feeding activities, growth, and regeneration progress. The camera's built-in flash was dimmed by setting it on ½ power and using a diffuser to reduce possible disturbance or damage to specimens. Two preserved specimens were sent to Excalibur Pathology for decalcification, serial sectioning, and staining before I examined and shot photos of sections (e.g., Fig. 4F).

Several methods were used to prepare SEM specimens. Some were prepared in the traditional way of removing preserved specimens from ethanol, removing soft tissue with dilute sodium hypochlorite solution, rinsing the remaining ossicles with tap water, and mounting them on stubs. Bleaching was sometimes minimized or omitted to leave parts of specimens intact. Parts of dried museum specimens were mounted directly on stubs without bleaching. In some cases, parts of *A. stygobita* were preserved in alcohol after specimens had died and partly decomposed, and bleaching was not necessary to disarticulate ossicles. Sputter coating was not used. Northern Kentucky University's FEI Quanta 200 scanning electron microscope was used to take SEM images of more than 20 species, including *Amphilepis patens* and *Amphilepis platytata*.

Abbreviations used in text

CP - clock position; **DAP** - dorsal arm plate; **dd** - disk diameter; **DOM** - dissolved organic matter; **EPS** - extracellular polymeric substances; **LAP** - lateral arm plate; **ppt** - parts per thousand; **SEM** - scanning electron microscopy; **V** - vertebra; **VAP** - ventral arm plate.

Results

Feeding on detritus

While in Bernier Cave, the disks of *A. stygobita* took on the color of the detritus they consumed (Fig. 3A). Detritus from Bernier Cave was used successfully as food for the brittle stars in the laboratory. Before eating, adult *A. stygobita* usually had central disks that were pale yellow (Fig. 3B) and clear enough to see internal structures such as gonads (Fig. 3C, D). When a few drops of fresh detritus were added to their culture jars, they often started consuming it within minutes and their disks turned brown (Fig. 3E). They usually fed while nearly flat on the surface of the detritus, only occasionally with disk partly buried, but not with arm tips above the detritus. When new detritus was added near the edge of specimen jars, brittle stars sometimes moved to the edge and side of the jar and could be seen pulling detritus into the mouth with tube feet (Fig. 3C, D, 90 sec. apart). There seemed to be no chewing and no selection or filtering of the various light and dark components as detritus streamed into the mouth. This microphagous detritus feeding was accomplished with mouth papillae reduced in number and density, as described in the morphology section.

Reproduction, birth and growth of babies

Although gonads were not visible in preserved *A. stygobita*, in July 2018, four of the five adult *A. stygobita* that survived the 6–14 July collecting trip were each observed to contain 5–7 gonads inside their disks (Fig. 4A–D); only specimen #7 had no gonads clearly visible (Fig. 4E). The four adults with gonads (#1, 4, 5, and 6) did not appear to have gonads in their interbrachial area with a madreporite (M), which was gray and located proximal to a genital slit and near mouth structures; madreporite locations are indicated in captions for Fig. 4A–E by clock position (CP) (e.g., CP 12 is straight up, CP 6 is straight down). Most non-madreporite interbrachial areas each had 1–2 ovaries close to the genital slits near base of arms; a total of 4–5 egg-bearing ovaries appeared in most individuals; similar arrangements of gonads appeared in adults collected in previous years (e.g., Fig. 3C, D), but gonads were not counted or measured. Ovaries from the four 2018 specimens were ~0.25 to 0.75 mm in diameter, with up to 5 eggs and/or embryos visible in various stages of development, ranging in size from 0.20 to 0.35 mm. Horizontal serial sections revealed that testes and ovaries were both present in the same specimen indicating hermaphroditism (Fig. 4F).

On 17 July 2018, one adult (#5) released a baby (Fig. 5A), another emerged on 31 July, and a third appeared on 6 August. I use the term “babies” for these individuals newly released from their mother, instead of a broader term such as young or juveniles, because it better describes the specific time in their development as relatively soon after birth. Unfortunately, we don’t have a specific term for newly released brittle star babies, such as the term “mancas” used for isopods. Stöhr (2005) used the term baby in her title, “Who’s who among baby brittle stars (Echinodermata: Ophiuroidea):

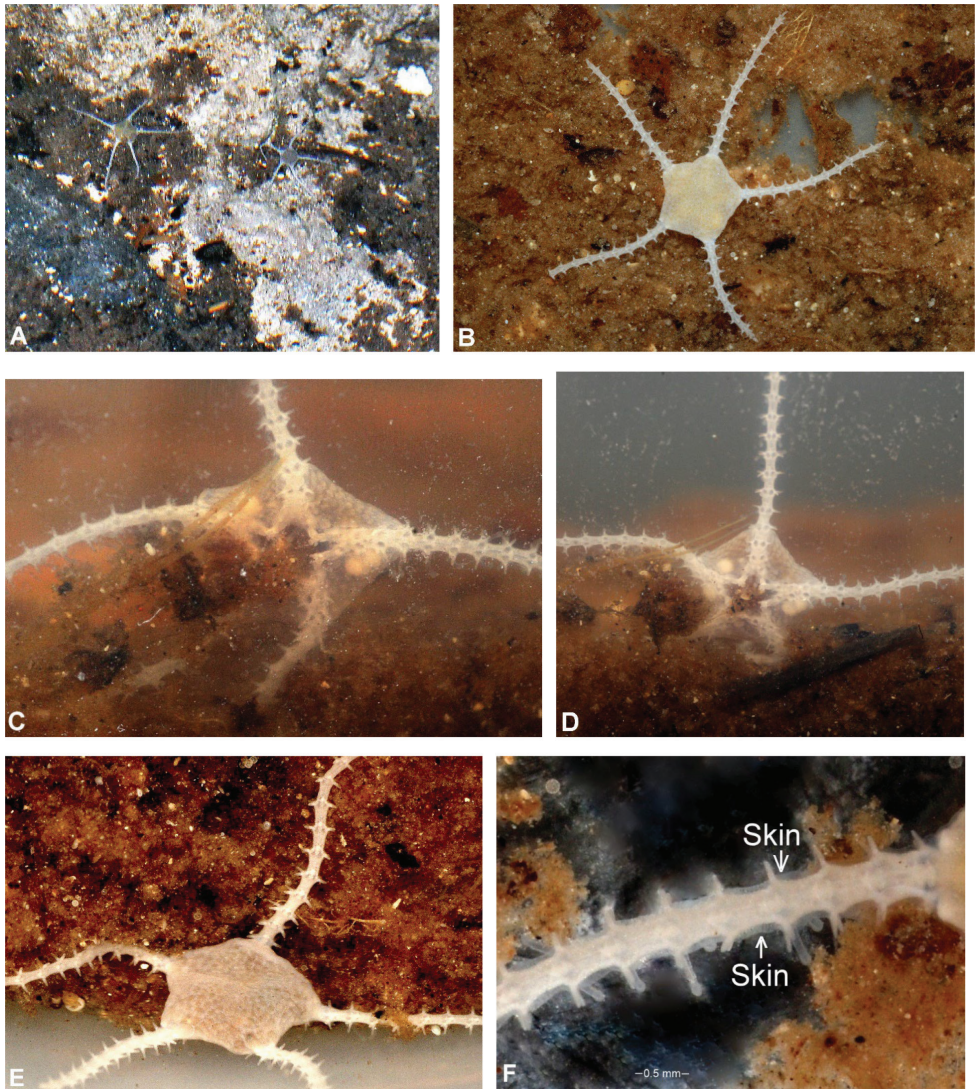


Figure 3. *Amphicutis stygobita* feeding **A** two dark adults in cave on dark substrate **B** light-colored adult before feeding **C** same animal on side of jar feeding on detritus streaming into mouth **D** same animal, 90 sec. later, with detritus in stomach **E** same animal with brown disk 25 min. after eating detritus **F** arm of adult showing skin layer.

Postmetamorphic development of some North Atlantic forms.” Stöhr (2005) noted that “the term ‘juvenile’ has been used interchangeably with ‘postlarva’ in the literature for newly metamorphosed animals to sizes of at least 2 mm disc diameter (Webb & Tyler, 1985).” Thus, the term juvenile was convenient for Stöhr (2005) and others to use for any small sexually immature individual, regardless of age. The term newborn might be appropriate for individuals shortly after being released, but it does not seem

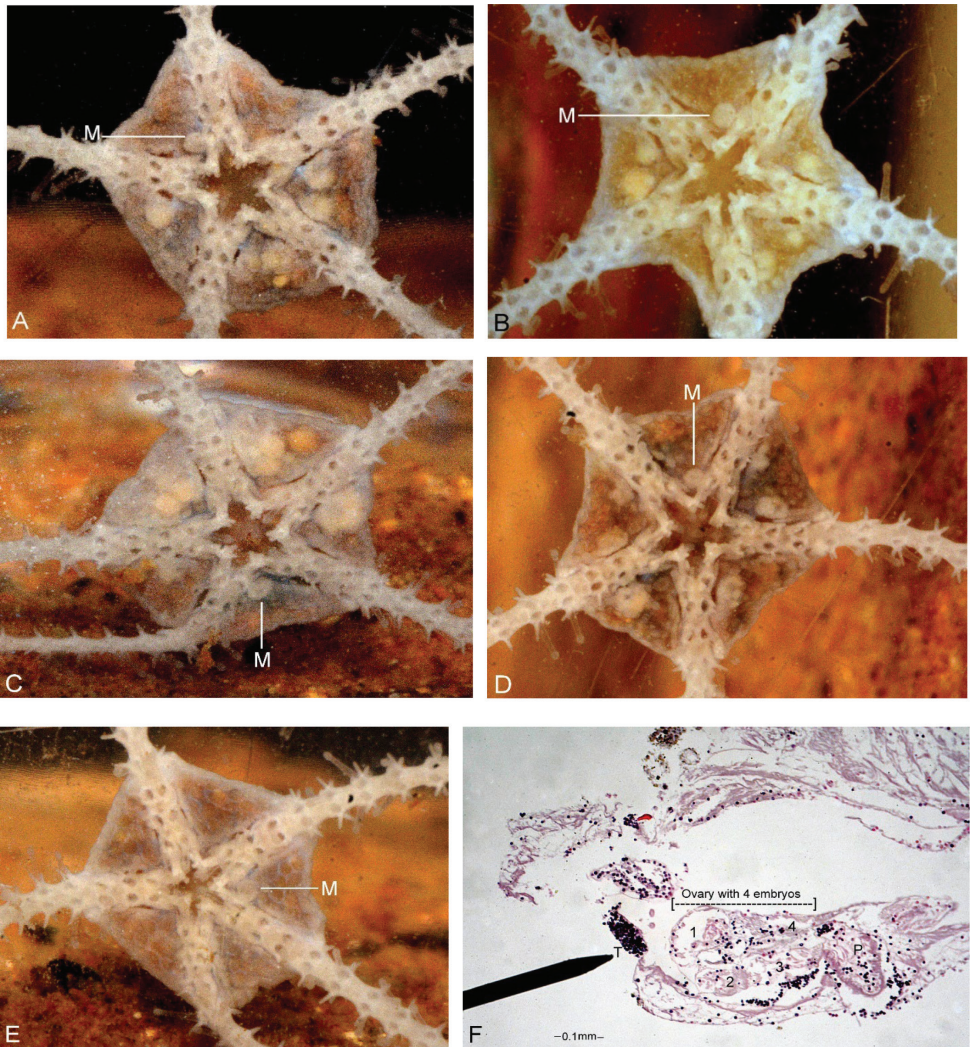


Figure 4. *Amphicutis stygobita* with gonads; all specimens with dd = 3-4 mm **A** specimen #1 with 5 gonads, madreporite (M) at clock position (CP) 11, 8 August 2018 **B** specimen #4 with 5 gonads, madreporite at CP 12, 30 July 2018 **C** specimen #5 with 5-7 gonads, madreporite at CP 6, 7 August 2018 **D** specimen #6 with 5-7 gonads, madreporite at CP 1, 30 July 2018 **E** specimen #7 with no discernible gonads, madreporite at CP 3, 24 July 2018 **F** 40 × light microscope view of horizontal section showing testis at pointer, ovary with 4 embryos (1, 2, 3, 4) near podium. Abbreviations: M – madreporite, P – podium, T – testis.

to be accurate for the same individuals after several months of growth. While some might suggest that baby seems less technical than juvenile or newborn, I contend that it is the most appropriate and accurate term for the three individuals born in this study.

Newborn babies had the following anatomical traits: disk all white (no pigment) except when brown detritus was eaten and showed through surfaces (Figs 5C, 6D);

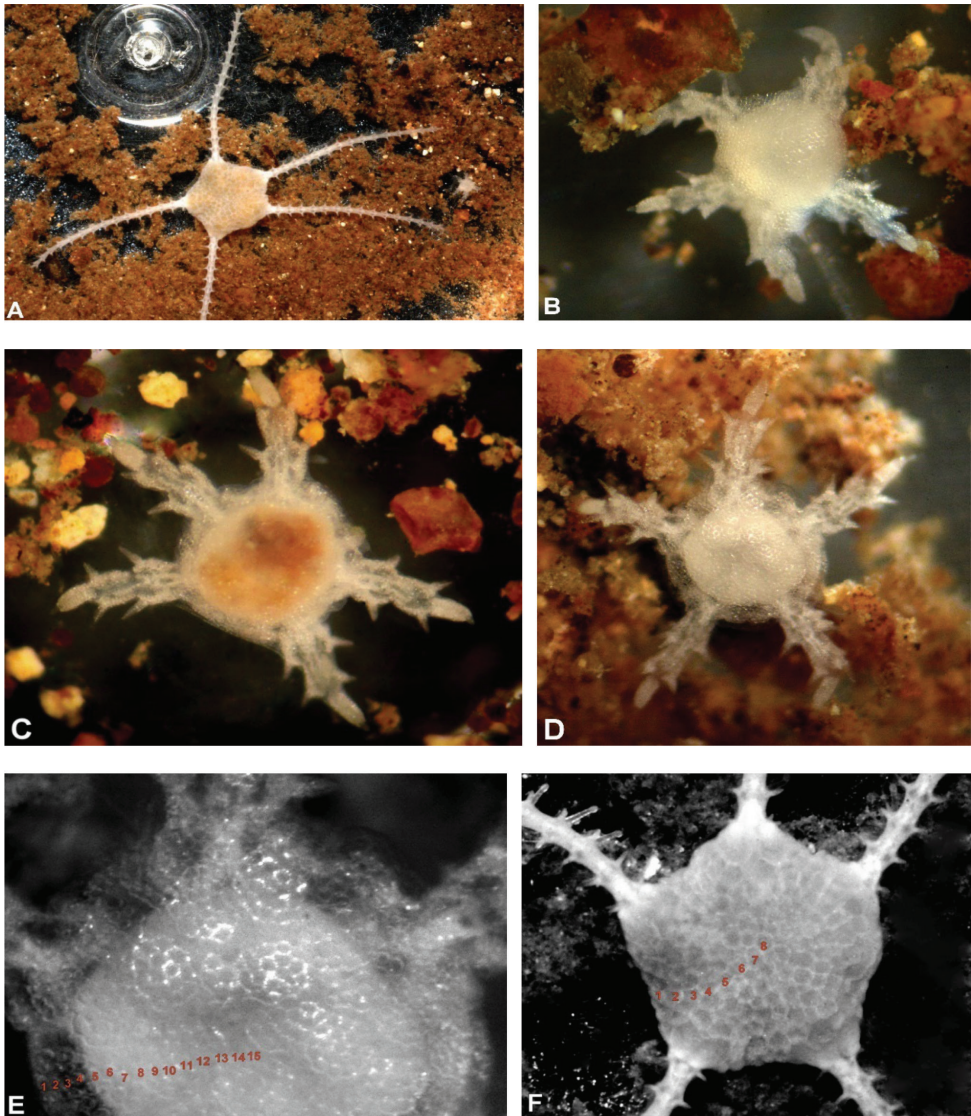


Figure 5. *Amphicutis stygobita* mother (dd = 4 mm) and babies (dd = 0.8 mm) **A** mother (adult #5) with baby #1 on right, 17 July 2028 **B** baby #1, arm at CP 4 with partially developed 3rd segment, 4 days old, 21 July 2028 **C** baby #2, food in stomach, 7 days old, 6 August 2018 **D** baby #3, clear skirt around disk, 3 days old, 8 August 2018 **E** baby #3, disk radius with ~15 scales, 8 August 2018 **F** adult #5, disk radius with ~8 scales, 17 July 2018.

disk diameter (dd) was ~0.8 mm with ~30 rows of disk scale rows (Fig. 5E), more than in adults with ~17 rows (Fig. 5F); skirt of skin with disk scales surrounded the white central disk (Fig. 5B–E); disk rounded at first (Fig. 5B–D) and became more pentagonal in a few weeks (Fig. 6C–F). Possible central and radial primary plates were visible in some images of baby #3's disk (Figs 5D–E, 6A), but if they were actually present, they

were often obscured by disk scales. Only 1 arm segment was within disk (Fig. 6F). All three babies had only 2 segments per arm beyond disk, except for baby #1 that had the beginning of a third segment on 1 arm (Fig. 5B). Each arm segment was ~ 0.2 mm long, then a cream-colored terminal plate ~ 0.2 mm long with a groove at the end bearing a short clear terminal tube foot ~ 0.04 mm long (Figs 5B, 6A–C); each arm was ~ 0.6 mm long; arm segments were flared at distal ends to accommodate podia, podian basins, and spines (Figs 5B, 6A–F); arm segments near disk were covered by small scales similar to those on disk (Figs 5B–D, 6A–C). Lateral arm plates (LAPs) were well developed to support the 2 arm segments, with each LAP bearing 2 distal spines (Figs 5B–D, 6B); dorsal arm plates (DAPs) appeared to be absent, although tiny white structures visible between segments 1–2 could have been either DAPs or part of the vertebral joints (Fig. 5C, D); good ventral views of babies were not available in their first few months, but VAPs were clearly visible when baby #2 was 8.5 months old (Fig. 6F). Developing vertebrae (Vs) were visible inside the 2 arm segments; the most apparent vertebral structures were the 2 parallel ambulacral plates that form support for adjoining parts (Figs 5B–D, 6B–F).

The behaviors of all 3 babies were similar, except that baby #1 hardly moved for several days; the other two were moderately active from near birth. They all started eating detritus within a few days of birth (Fig. 5C); detritus continued to be their only food source for as long as they lived, which was up to 14.5 months. They reacted negatively to the weak lights used to observe them (otherwise, they were in total darkness); they moved away from the light and sometimes hid under or behind detritus to stay out of direct light. Each baby was often found in the same area of its jar several days in a row, indicating they didn't move much in the dark. Arms were too short to effectively move babies forward by swinging arms, so they glided slowly on their podia (podial walking); however, they did move arms from side to side, especially the distal segment and terminal plate (Figs 5B, 6A, B). All three babies grew very slowly. The beginning of third segments could be seen developing within 2–4 months of birth (Fig. 6B). Lateral arm plates appeared to be the first arm ossicles to form in new segments, followed by VAPs and Vs (Fig. 6F). Baby #2 lived the longest (from 31 July 2018 to 14 Oct. 2019 = 14.5 months). Its dd increased from ~ 0.80 to 0.85 mm, arm length increased from ~ 0.6 to ~ 0.8 mm, and three arms each added a third segment with distal spines (Fig. 6E); third segments were ~ 0.2 mm long when distal spines developed, but they were narrower than the first two segments (Fig. 6E, F).

Morphology of adult *Amphicutis stygobita*

John Winter collected the first specimens of brittle stars from newly discovered Bernier Cave in 2009, which he sent to me. I was struck by their lack of color, very small size, and arm segments that were proportionately longer (L:W ~ 1.5) than those of all the other 13 genera illustrated in a key (Pomory 2007). These unusual traits were confirmed by Pomory et al. (2011) and are still worth emphasizing. When Pomory et al. (2011) described *Amphicutis stygobita* as a new genus and species, SEM images were not available for the description, but they now supplement the original description and confirm some of its unusual traits.

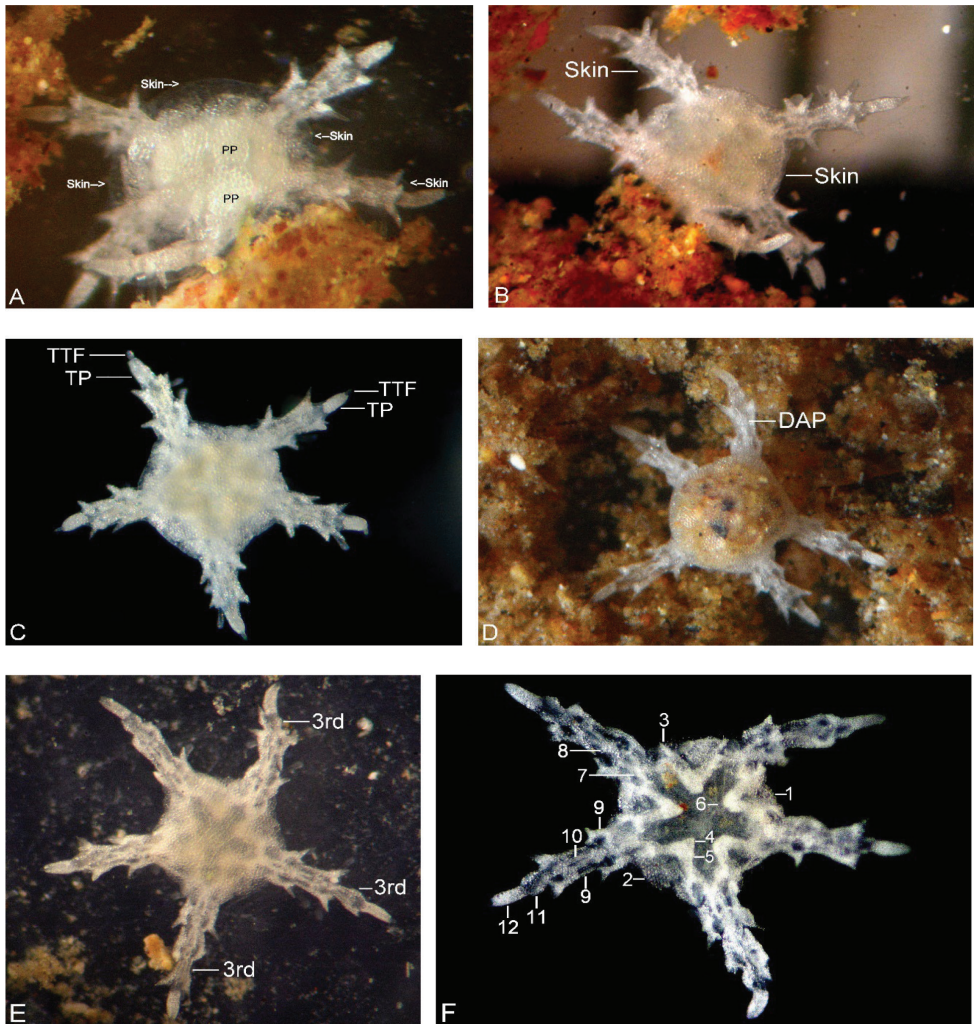


Figure 6. *Amphicutis stygobita* development, all dorsal (aboral) except 6F **A** baby #3 with skin and possible primary plates, 19 September 2018 **B** baby #3, skin on disk and arm, 31 December 2018 **C** baby #2, disk pentagonal, arms with grooved terminal plate and terminal tube foot, 30 October 2018 **D** baby #2 full of detritus, probable DAP, 29 December 2018 **E** baby #2, 13.5 months old, some arms have 3rd arm segments with 1-2 terminal spines, 14 September 2019 **F** baby #2 ventral (oral) surface showing parts of stereom, 9 April 2019: 1 madreporite, 2 disk scales, 3 adoral shield spine, 4 ventral tooth, 5 dental plate, 6 oral tentacle, 7 VAP #1, 8 VAP #2, 9 LAP, 10 ambulacral plate, 11 3rd segment outside disk, 12 terminal plate. Abbreviations: DAP – dorsal arm plate, PP – primary plates, TP – terminal plate, TTF – terminal tube foot.

The dorsal side of the disk of *A. stygobita* is covered by highly fenestrated scales (Fig. 7A, B). SEMs of the ventral disk (Figs 8A–C, 9) show the extreme variability of ossicles that was expressed by Pomory et al. (2011), “except for the distal large papillae, no two jaws have the same papillae arrangement” and “many missing due partly to

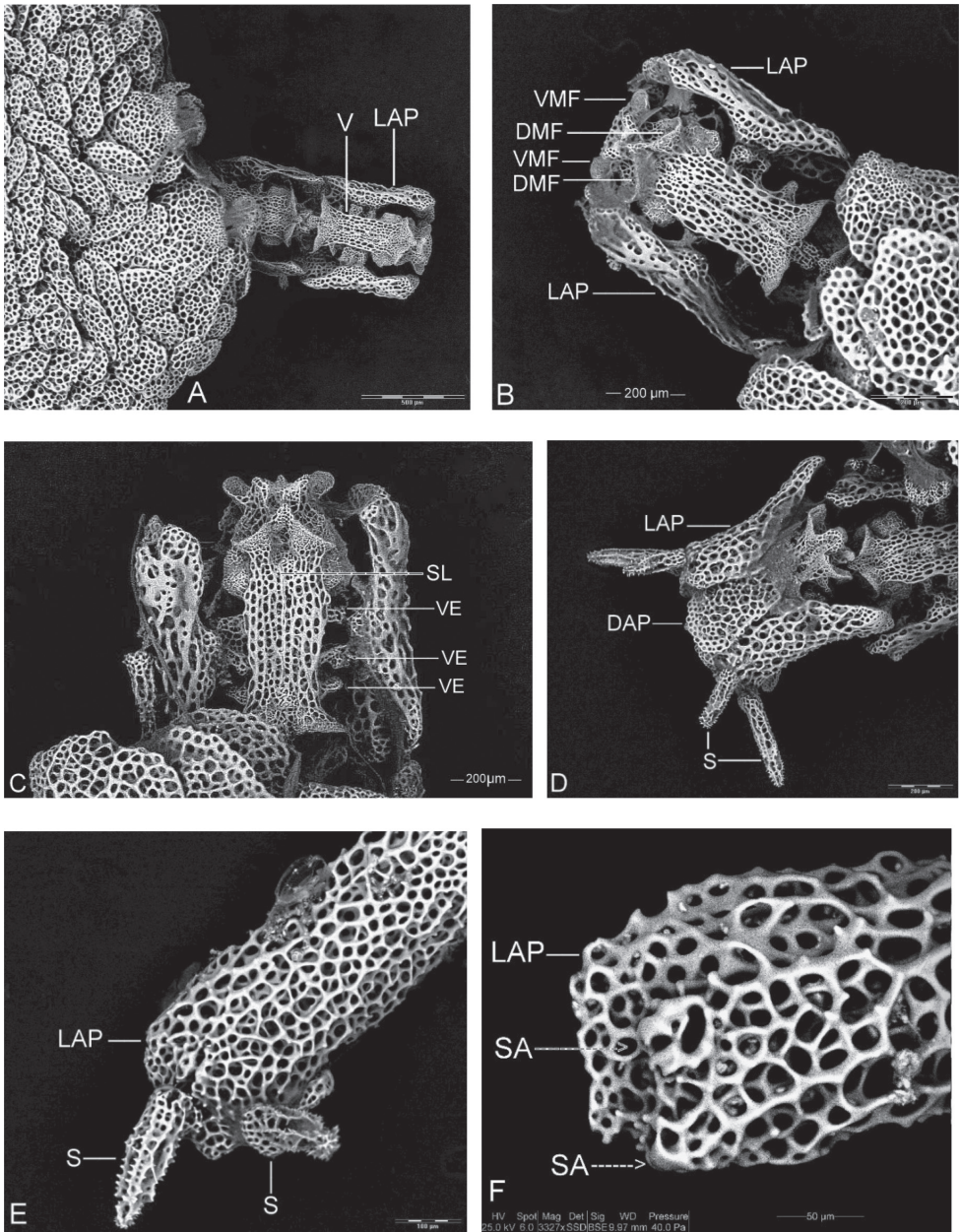


Figure 7. *Amphicutis stygobita* dorsal (aboral) SEMs **A** disk with fenestrated scales, 1st 2 arm segments, Vs with lateral extensions **B** 1st arm segment, ventral muscle flange extends past dorsal muscle flange **C** 1st arm segment, middle of LAPs curve inward to meet 3-4 vertebral extensions **D** 1st arm segment, dorsal arm plate, LAP with 2 spines **E** LAP with 2 fenestrated spines **F** LAP with 2 spine articulations. Abbreviations: DAP – dorsal arm plate, DMF – dorsal muscle flange, LAP – lateral arm plate, PB – podian basin, S – spine, SA – spine articulation, SL – suture line, V – vertebra, VAP – ventral arm plate, VE – vertebral extension, VMF - ventral muscle flange.

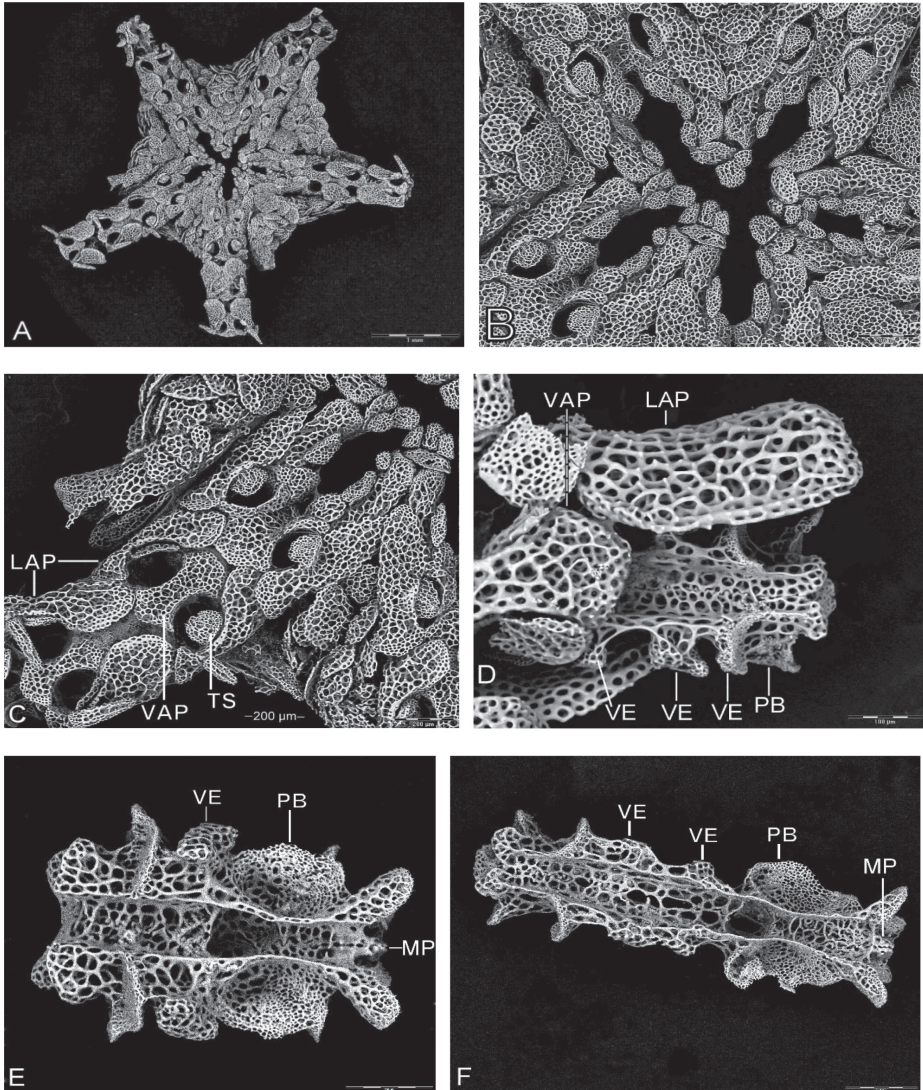


Figure 8. *Amphicutis stygobita* ventral SEMs **A** disk and 1 or 2 segments of each arm distal to disk, 1 complete segment within disk but outside mouth slit at CP6 and CP 8, 1.5–2 segments within disk at CP 11, CP 1, and CP 3 **B** oral frame showing mouth structures (see Fig 9 for labelled structures) **C** base of arm at CP8 from Fig 8A, 1 complete segment within disk with LAPs, tentacle scales, and VAPs, interbranchial areas with scales **D** 1st segment beyond disk with LAP, V with lateral extensions **E** V from proximal area of arm, large podian basin, distal to right, length 1.4 × width **F** V from mid-section of arm, distal to right, length ~3 × width. Abbreviations as in Fig. 7 plus TS - tentacle scale.

uncalcified state.” This uncalcified state relates to the extreme fenestration of ossicles seen in SEMs (Figs 7–11). Several other key morphological traits are associated with the oral frame, including: ventral tooth shape, oral plates, oral shields, location of 2nd

tentacle pore, and number of arm segments within disk. Most of these oral frame features can be seen in SEM images (Figs 8A–C, 9); their significance is covered in the Discussion of Adult Morphology.

The ossicles of brittle star arm segments consist of a central vertebra (V) enclosed by a dorsal arm plate (DAP), a ventral arm plate (VAP), and 2 lateral arm plates (LAPs) (one on each side) (Fig. 10D). One of the most extraordinary features of *A. stygobita* is the arrangement of arm segment ossicles, with reduced DAPs and VAPs, and elongated LAPs (Figs 7A–D, 8B, C) that run parallel to Vs and connect directly to them. This is in contrast to most brittle stars that have LAPs that extend laterally from the vertebral plane. The arm ossicles of *A. stygobita* are also unusual because they are highly fenestrated with a net-like lattice of bones (trabeculae) around large open spaces where soft tissue (stroma) was before SEM preparation, similar to those seen in disk ossicles. Tentacle pores are relatively large with one large tentacle scale on the lateral side (Fig. 8A–C). Two spines are located near the distal end of LAPs (Figs 7D, E, 10D). Arm spine articulations are nearly round with 2–3 openings for muscles and nerves to pass through to the spine (Fig. 7F).

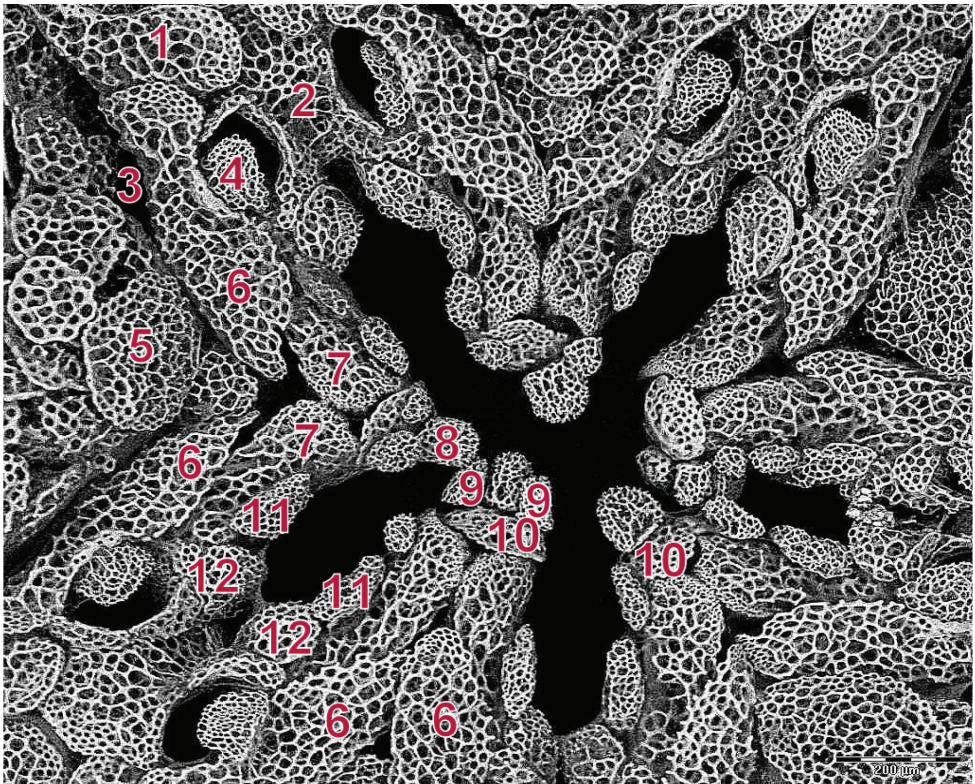


Figure 9. *Amphicetus stygobita* ventral SEM, oral frame enlargement of Fig. 8B. Numbers: 1 - 1st lateral arm plate, 2 - 1st ventral arm plate, 3 - genital slit, 4 - 2nd tentacle scale, 5 - oral shield, 6 - adoral shields, 7 - oral plates, 8 - ventral tooth, 9 - infradental papillae, 10 - dental plate, 11 - 2nd oral papillae, 12 - distal oral papillae.

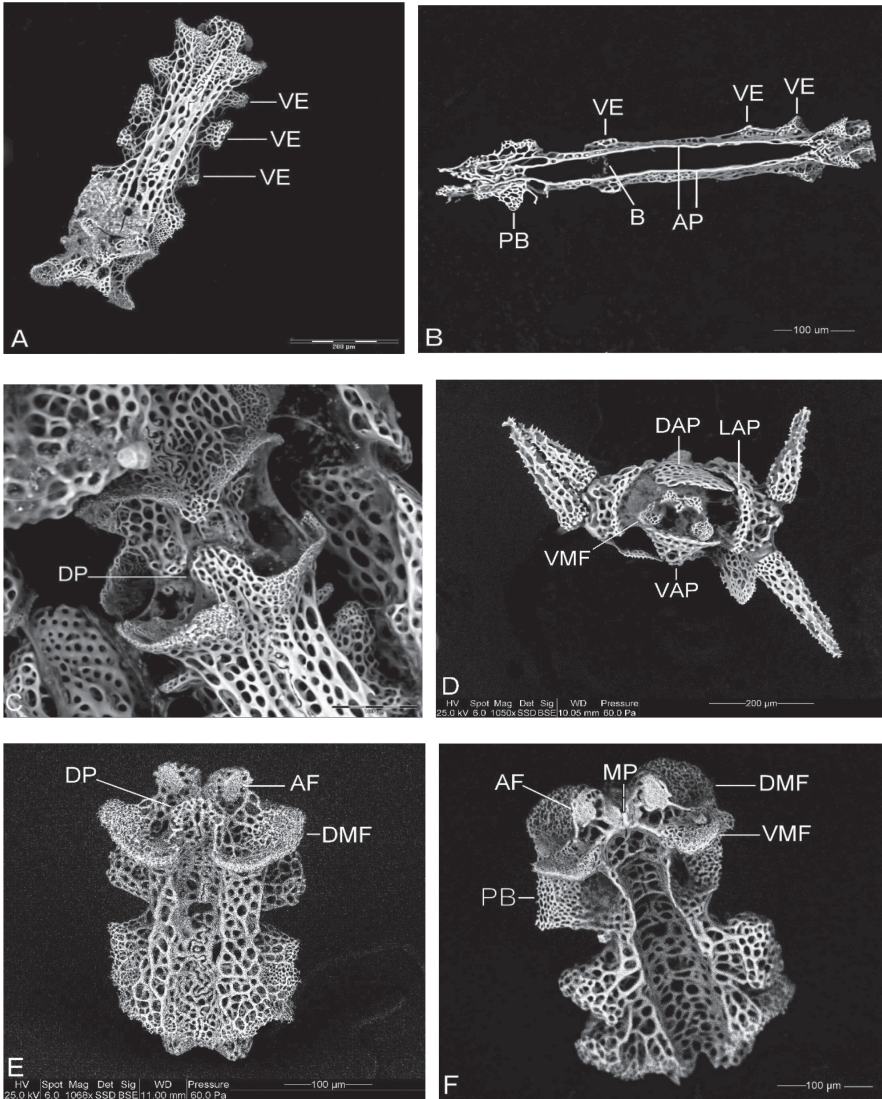
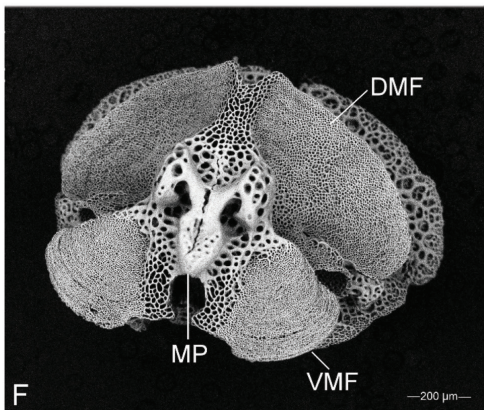
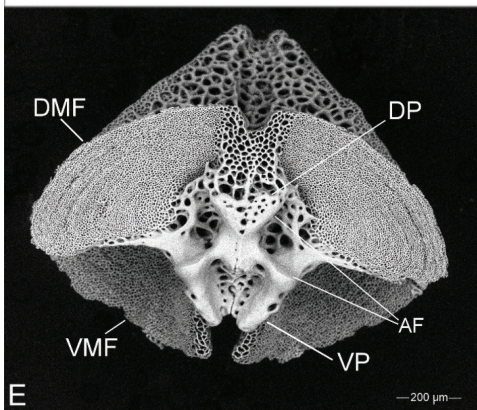
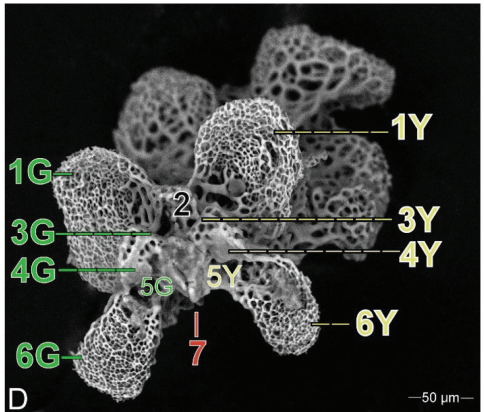
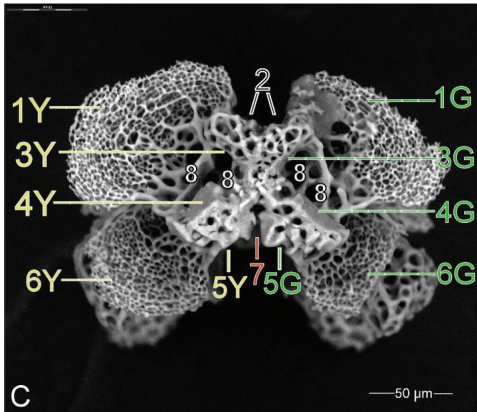
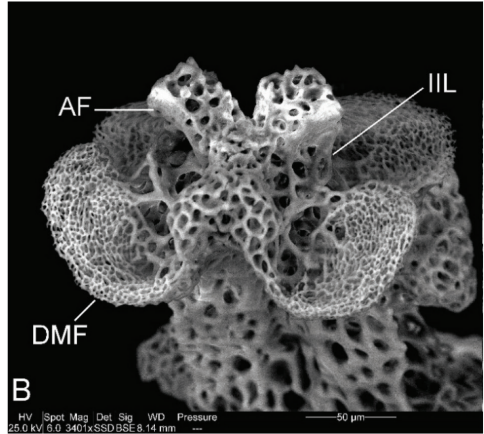
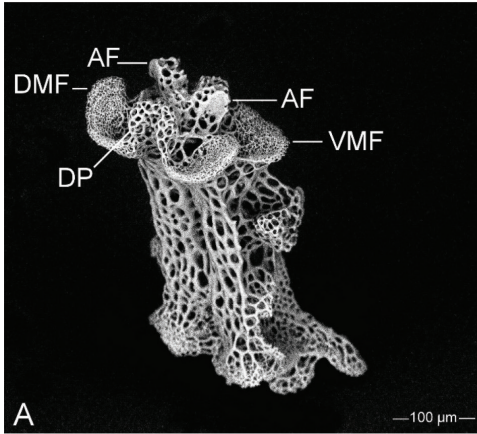


Figure 10. *Amphicutis stygobita* SEMs of vertebrae (Vs) **A** V from mid-section of arm with lateral extensions, length $\sim 3 \times$ width, dorsal view, distal down **B** V from distal area of arm, length $\sim 6 \times$ width, ventral view, distal left, bridge formed between ambulacra **C** joint between 1st 2 Vs outside disk, dorsal, distal down **D** distal face of segment showing V enclosed by DAP, VAP, and 2 LAPs with spines **E** dorsal/proximal end view of V tilted ~ 40 degrees showing proximal end (up) with large dorsal muscle flanges and 2 articulating facets (top) **F** ventral view of V rotated to show distal end with dorsal and ventral muscle flanges, 2 articulating facets, and median process. Abbreviations as in Fig. 7 plus: AF- articulating facet, DP – dorsal process, MP – median process.

Since Pomory et al. (2011) did not have access to SEM, our description emphasized external structures, and vertebrae were little mentioned. Some unusual features of the Vs were revealed by SEMs. Arm segments of brittle stars are often shortest near

the disk and are elongated distally where new segments are produced, so it is useful to indicate location of segments and Vs in SEM images. Figs 7A–D, 8D, and 10C are from *A. stygobita* segments near disk; Figs 8E, F, 10A, E, F are Vs from near the middle of arms; Fig. 10B is a very narrow V from the distal end of arm with a thin bridge formed between the 2 central ambulacral plates.



Length of Vs varies with location on arm, but in most species the length is seldom more than twice the width. However, Vs of *A. stygobita* are about 2 to 8 times longer than wide (narrowest near distal ends of arms) (Fig. 10B). Lateral extensions of Vs connect with LAPs; Vs near disk have 3–4 narrow extensions on each side, most of which connect to protrusions near the middle of LAPs (Figs 7A–C, 8D). Lateral extensions on some Vs are flared or knobbed to form wider attachment points to LAPs (Figs 8D, 10A, E), and some lateral extensions form interrupted ridges for attachment points (Figs 8E, 10F). A pair of large podian basins near distal ends of oral surfaces of each V serve as bases for podia (Figs 8E, F, 10F). These large podian basins with their accompanying podia result in flared distal ends of segments (Figs 5A, 7A, 8A). LAPs twist around lateral sides of podia, and hourglass-shaped VAPs curve around the medial sides of podia (Fig. 8A–C). A suture line is visible along the middle of each V on both the dorsal and ventral surfaces (Figs 7A–C, 8D–F, 10A). Sutures result from the joining of the 2 ambulacral plates that are prominent in newly generated Vs in adults (Fig. 10B) and are detectable in babies (Fig. 6B–F).

The distal ends of Vs near disk have dorsal muscle flanges (= aboral muscle areas, or fossae) that are more proximal than ventral flanges and are arrow-shaped (Figs 7A–C, 10A) with arrow tips forming part of dorsal articulating projections (= dorsal processes) (Figs 8E, F, 10E, 11C). The ventral muscle flanges on distal ends of Vs extend more distally than dorsal muscle flanges (Figs 7A–C, 10A, F) with the ventral processes extending furthest (Figs 7C, 8E, F). The proximal ends of Vs near disk have dorsal muscle flanges with faces that appear to be perpendicular to the vertebral axis in dorsal view (Figs 7A–C, 10A), but they actually curve proximally and ventrally (Figs 7D, 10C, E,

Figure 11. SEMs of vertebrae ends, *Amphicutis stygobita* **A–D**, *Amphilepis patens* **E–F**. **A** dorsal/side view, proximal end up showing muscle flanges, articulating facets (top) and proximal extension of center of dorsal muscle flanges (upper left) to form dorsal process that supports dorsal articulating facets (on opposite side, out of view) **B** tilted proximal end showing dorsal muscle flanges in front, 2 ventral articulating facets behind, insertion point for intervertebral ligaments, dorsal view **C** proximal face showing: 1Y (yellow) left dorsal muscle flange, 1G (green) right dorsal muscle flange, 2 (black) dorsal process, 3Y (yellow) left dorsal articulating facet, 3G (green) right dorsal articulating facet, 4Y (yellow) left ventral articulating facet, 4G (green) right ventral articulating facet, 5Y (yellow) left side of ventral process, 5G (green) right side of ventral process, 6Y (yellow) left ventral muscle flange, 6G (green) right ventral muscle flange, 7 (red) median socket, 8 (white) insertion points for intervertebral ligaments **D** distal face showing: 1G (green) right dorsal muscle flange, 1Y (yellow) left dorsal muscle flange, 2 (black) median depression, 3G (green) right dorsal articulating facet, 3Y (yellow) left dorsal articulating facet, 4G (green) right ventral articulating facet, 4Y (yellow) left ventral articulating facet, 5G (green) right side of ventral depression, 5Y (yellow) left side of ventral depression, 6G (green) right ventral muscle flange, 6Y (yellow) left ventral muscle flange, 7 (red) median process. (If image **D** is turned over face down to left to meet image **C**, green structures connect with corresponding green structures, yellow with yellow, red with red, and black with black), **E** proximal face of *Amphilepis patens* vertebra, large dorsal muscle flanges with growth rings, thick dorsal and ventral processes with articulating facets, **F** distal face of *A. patens* vertebra, large dorsal and ventral muscle flanges with growth rings, thick rounded tongue-shaped median process. Abbreviations as in Fig. 7 plus: ILL – insertion for intervertebral ligaments, MP – median process, VP – ventral process.

11A, B). Vertebrae are very narrow so their ends are greatly reduced in surface area, and the projections and depressions that fit into the complimentary articulating surfaces of adjacent ossicles are highly modified (Figs 10E, F, 11A–D). Ventral processes extend beyond muscle flanges and contain the ventral articulating facets; these processes appear as posts in Fig. 11A. The median process (on distal end view, Fig. 11D) is thin and wedge shaped; it fits into the corresponding median socket (on proximal end view, Fig. 11C). The complex arrangement of these vertebral projections and depressions can be better visualized by imagining the connections resulting if Fig. 11D is turned over face down to meet Fig. 11C; then the green structures would connect with corresponding green structures, yellow with yellow, red with red, and black with black. The strong fenestration appearing in other body parts of *A. stygobita* are also prominent in the ends of Vs, including muscle flanges and the post-like processes holding dorsal and ventral articulating facets (Figs 10E, F, 11A–D). Insertion points for intervertebral ligaments are trabeculae located between dorsal muscle flanges and the dorsal process (8's in Fig. 11C) and are reduced in size and number compared to other species such as *Amphilepis patens* (Fig. 11E).

Morphology of *Amphilepis patens* and *Amphilepis platytata*

Amphilepis patens Lyman, 1879 (Figs 11E, F, 12A–F, 13A–F) and *Amphilepis platytata* HL Clark, 1911 (Figs 14A–F, 15A–F) were selected for comparisons to *A. stygobita* because they are in the family Amphilepididae, as is *A. stygobita*, according to O'Hara et al. (2018). In the original description of *A. stygobita*, Pomory et al. (2011) compared the new genus *Amphicutis* to *Amphilepis*, the only other genus in the family Amphilepididae, with 12 species of *Amphilepis* considered valid (Stöhr et al. 2024).

Gordon Hendler kindly sent me four *Amphilepis* specimens from the Natural History Museum of Los Angeles County: two (10–12 mm dd) were labelled “*Amphilepis patens* Lyman, 1879, 26 OCT 1989” (Fig. 12A, B); two (both ~9.0 mm dd) were labelled “*Amphilepis platytata* HL Clark, 1911, 2 MAR 1992” (Fig. 14A, B). My SEMs of these specimens showed several distinct differences, so it is interesting to note that *Amphilepis platytata* was synonymized with *Amphilepis patens* by HL Clark (1917); apparently this was not widely known or recognized until reported relatively recently in the World Ophiuroidea Databases by Stöhr et al. (e.g., 2024 and earlier). Clark (1917), while examining 550 specimens from deep-sea samples (to 2235 fathoms = 4087 m), made his decision on synonymy because 2 small specimens “6.5–8 mm dd” had traits of *A. platytata* (“no tentacle scales and the interbrachial areas below are perfectly naked”), while 8 others (10–12.5 mm dd, and apparently from different locations) had traits of *A. patens* (“interbrachial areas below are fully covered with scales”); he concluded that the morphological differences were probably due to “growth-stages and at any rate a matter of individual diversity.” Based on my SEM specimens, it is my opinion that Clark (1917) should not have synonymized *A. platytata* with *A. patens*, and I consider them to be separate species in this paper. Hopefully, other researchers will examine additional specimens to confirm this.

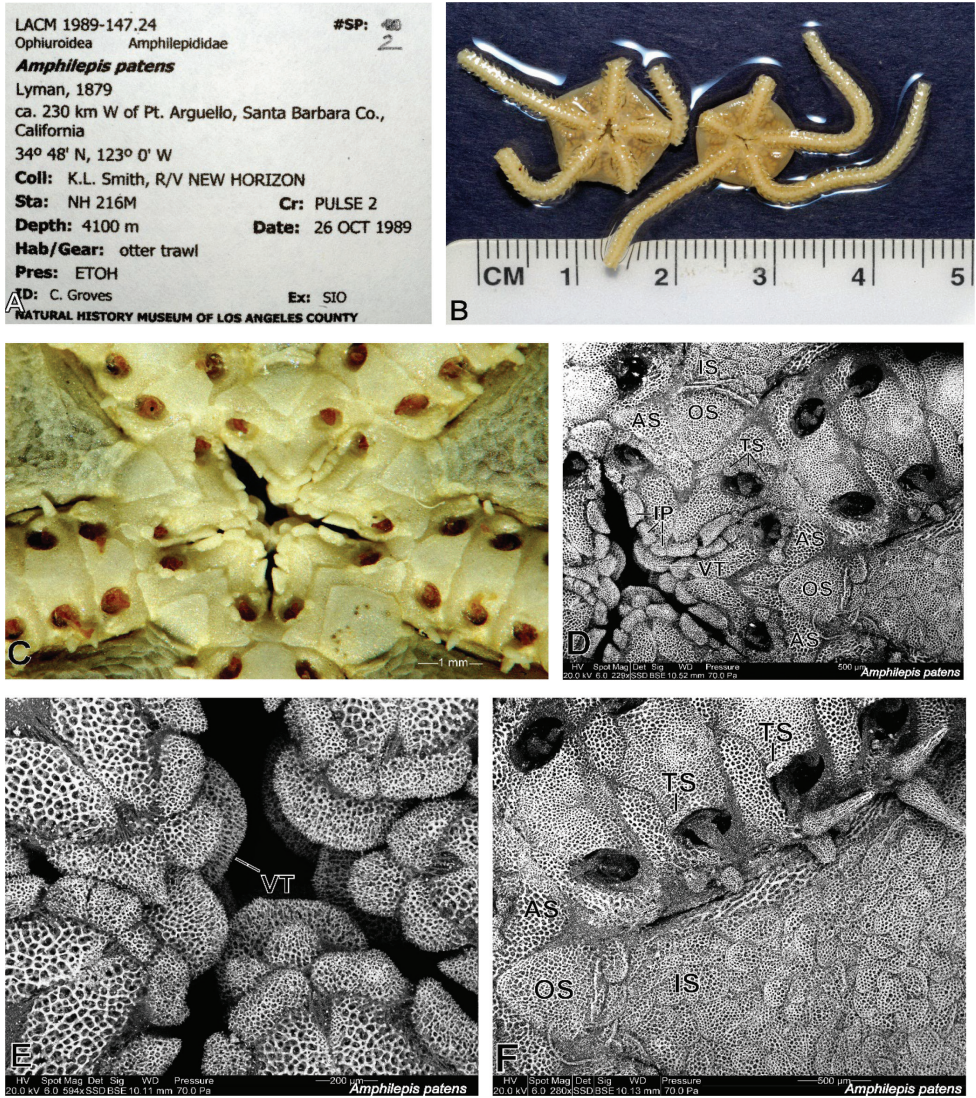


Figure 12. *Amphilepis patens* **A** museum label **B** ventral view of two preserved specimens, arms with many short segments, 4-5 arm segments within disk **C** mouth area before SEM preparation **D** SEM of mouth area and disk arm segments lightly bleached, triangular oral shields, interbranchial scales, rounded ventral teeth, elongated infradental papillae, 3 scales on oral tentacle pores **E** SEM of mouth area with rounded ventral teeth, elongated infradental papillae **F** SEM of disk arm segments with small tentacle pore scales, triangular oral shield, interbranchial scales. Abbreviations: AS – adoral shields, IP – infradental papillae, IS – interbranchial scales, OS – oral shields, TS – tentacle scales, VT – ventral teeth.

Here are three important differences I noticed on my SEMs of these two species, along with comments from the original descriptions. (1) *A. patens* has 3-4 tentacle scales adjacent to adoral shields near mouth slit (Fig. 12C–E), 1 small tentacle scale on lateral side of some VAPs distal to adoral shields (Fig. 12F) (Lyman 1879: “one minute

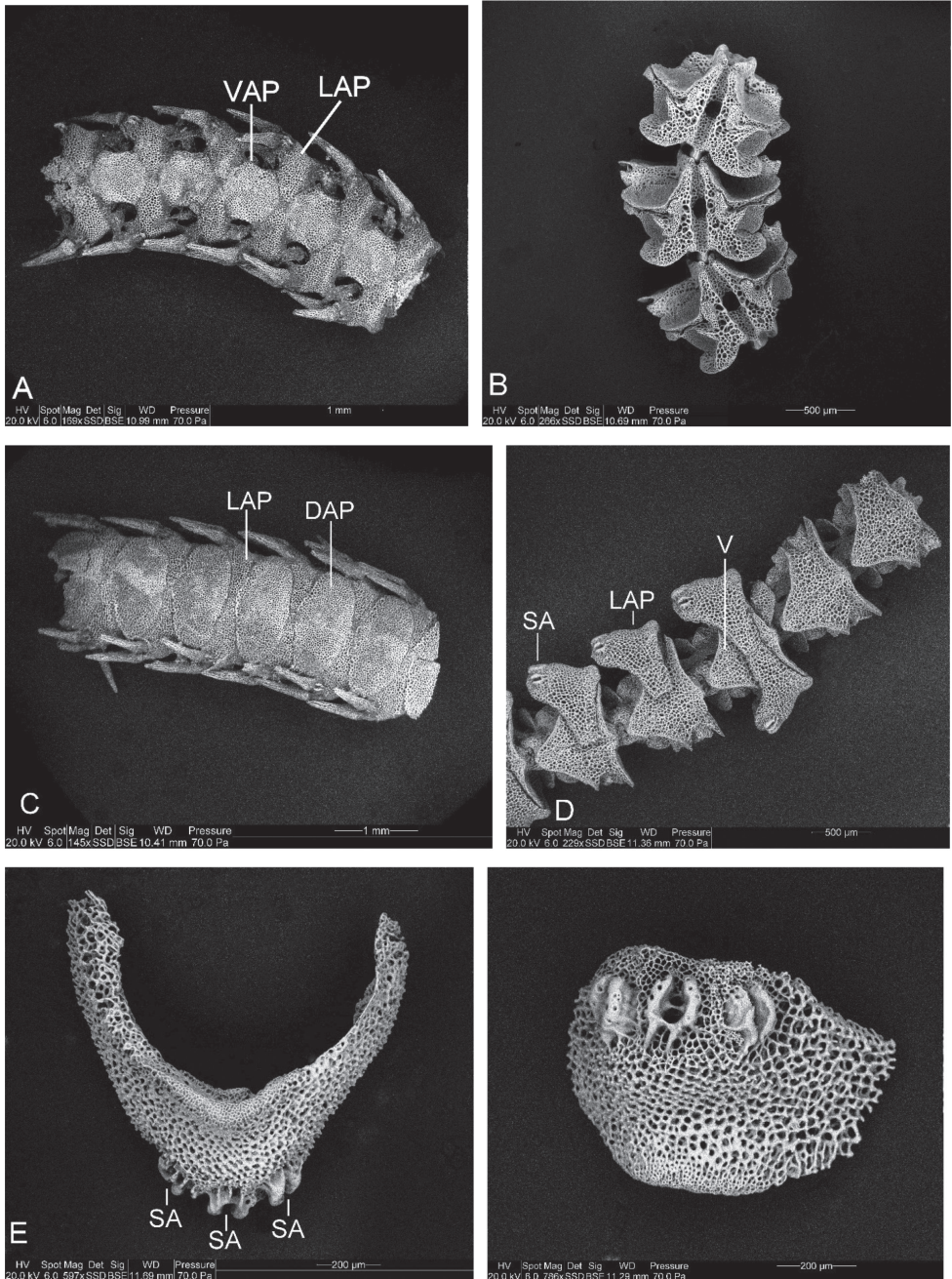


Figure 13. SEMs of *Amphilepis patens* **A** ventral view of 5 segments partially bleached, VAPs hexagonal, large LAPs with spines **B** ventral view of 3 bleached Vs **C** dorsal view of 6 wide arm segments partially bleached, LAPs between DAPs **D** dorsal view of 5 partially bleached Vs, 3 LAPs with 2 spine articulations visible, LPs attached atop Vs **E** LAP side view of 3 spine articulations **F** LAP dorsal view of 3 spine articulations. Abbreviations as in Fig. 12.

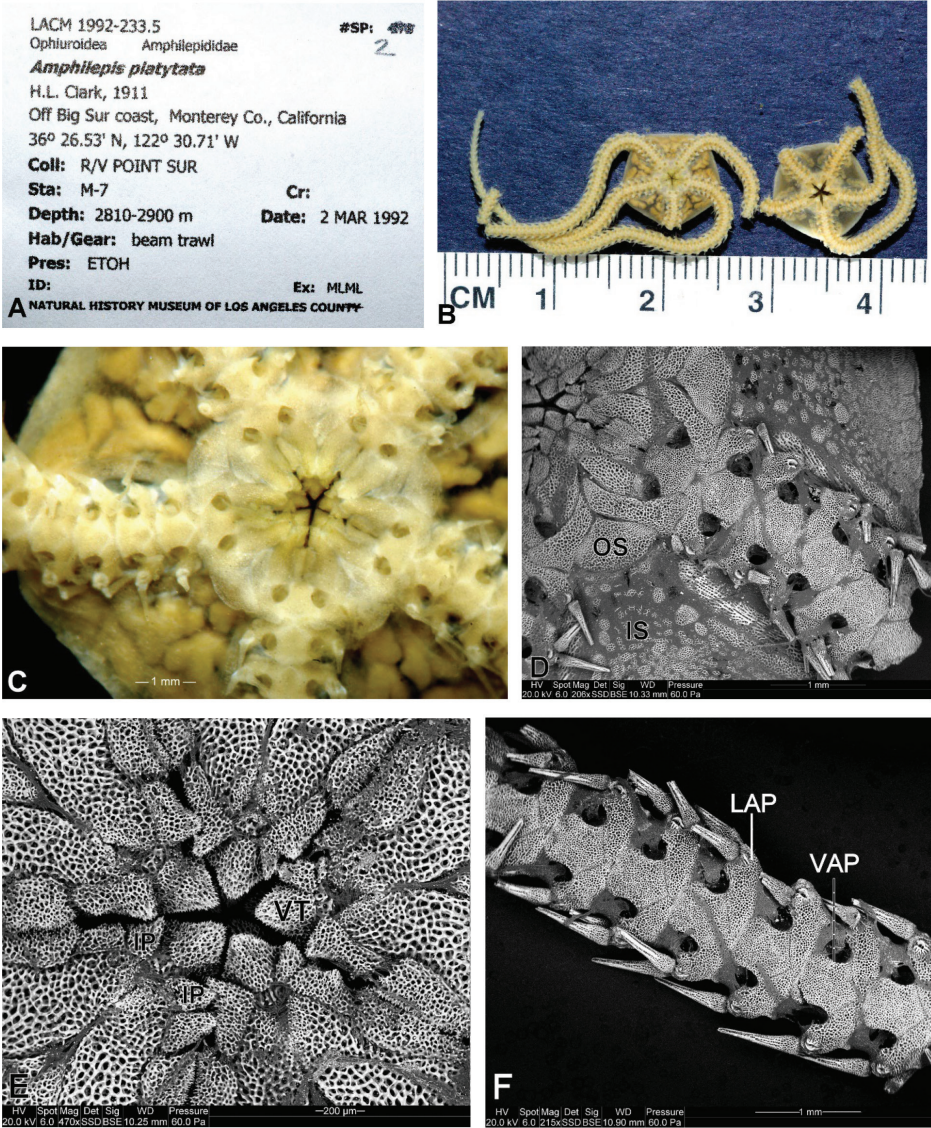


Figure 14. *Amphilepis platytata* **A** museum label **B** ventral view of two preserved specimens, arms with many short segments, 4-5 arm segments within disk **C** mouth area before SEM preparation **D** SEM of mouth area and proximal arm segments, triangular oral shields, sparse interbranchial scales, no tentacle pore scales **E** SEM of mouth area with pointed ventral teeth and infradental papillae **F** SEM of 7 arm segments partially bleached, VAPs nearly pentagonal, no tentacle pore scales, ventral, distal left. Abbreviations as in Fig. 12.

scale on lateral side of underarm-plate”); *A. platytata* has no tentacle scales (Figs 14C, 15A, B), which agrees with Clark’s 1911 original description of a single 8.0 mm dd specimen, (2) *A. patens* has disk covered above and below with translucent scales, as described by Lyman (1879) (Fig. 12C, D, F); in *A. platytata* the ventral interbranchial

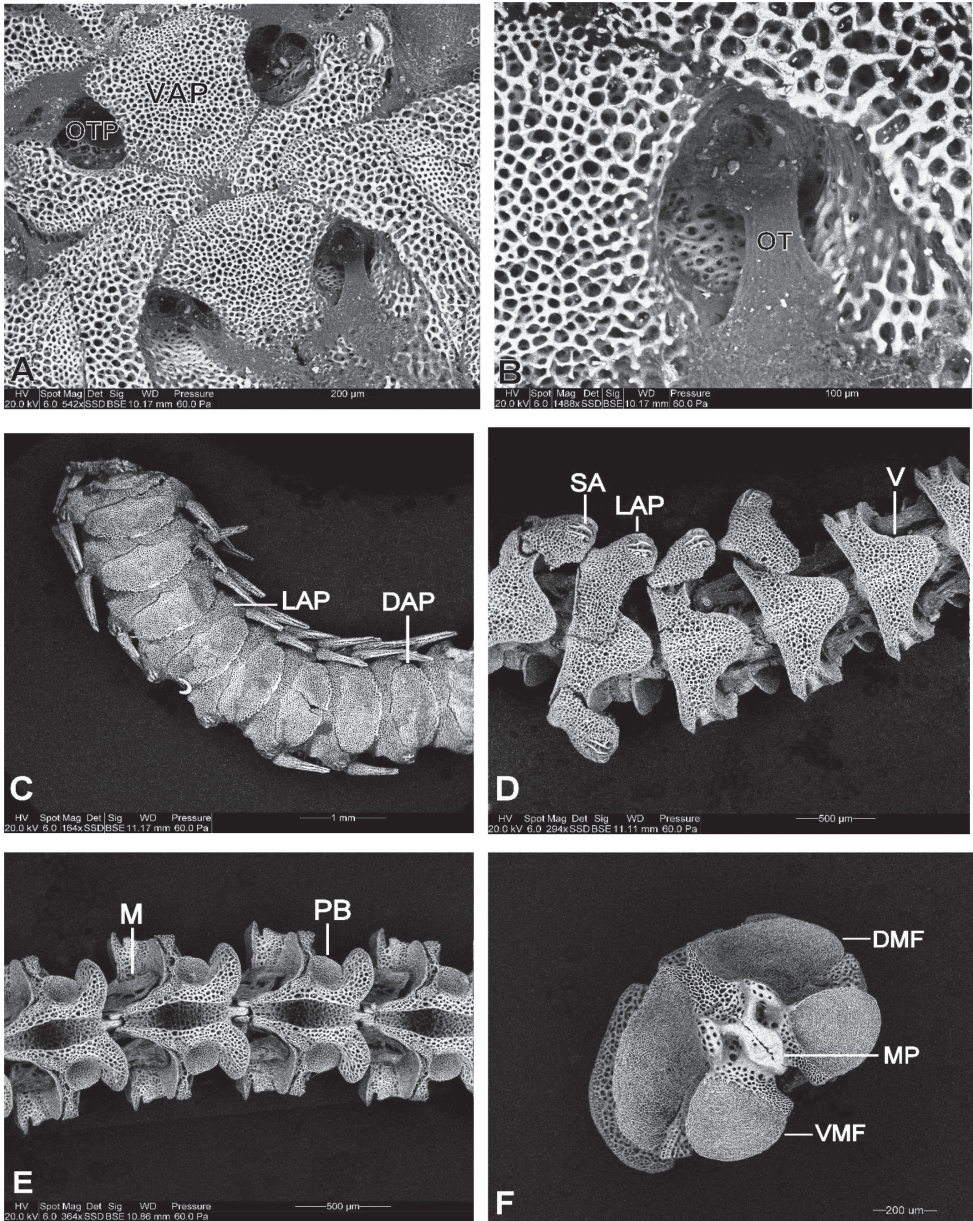


Figure 15. SEMs of *Amphilepis platytata* **A** enlarged view of mouth area in Fig. 14D, oral tentacle pores without scales **B** oracle tentacle inside tentacle pore, no scales **C** partially bleached string of 8 arm segments, broad DAPs and LAPs, dorsal, distal right **D** bleached string of vertebrae, spine articulations on LAPs, dorsal, distal right **E** string of 4 vertebrae with muscles connecting flanges, ventral, distal right **F** distal face of proximal vertebra showing muscle flanges, median process, and articulating surfaces. Abbreviations as in Fig. 12 plus: DMF – dorsal muscle flange, M – muscle, MP – median process, OT – oral tentacle, OTP – oral tentacle pore, PB – podian basin, VMF – ventral muscle flange.

spaces are sparsely covered with small scales (Fig. 14D), as described by Clark (1911), and (3) *A. patens* has ventral teeth broadly rounded (Fig. 12C–E) and infradental papillae elongated along the adoral shields (Lyman 1879: “mouth papillae broad and irregular; on either side of the large prominent mouth-angle, at the outer corner, are two more or less closely joined; and, at the apex, a larger pair which, through the gap between them, show the small lowest tooth”); *A. platytata* has ventral teeth and infradental papillae pointed toward mouth opening (Fig. 14C–E), as described by Clark (1911), “Oral plates large, each carrying two low wide, truncate papillae. Teeth nearly triangular.” While Pomory et al. (2011) suggested that “Amphilepidids have triangular teeth,” this is not the case for *A. patens*. The shape of ventral teeth was not mentioned by O’Hara et al. (2018) as a trait for Amphilepidida, Amphilepididae, or Amphieuridae.

Morphology of *Ophiophragmus filigraneus*

The *Amphilepis* species above were examined because of their close taxonomic relationship to *Amphicutis*. The species *Ophiophragmus filigraneus* (Figs 16A–F, 17A–F) was examined primarily because it lives in organically rich sediments in estuaries of Florida (USA) with brackish water (Turner and Meyer 1980); salinity ranges there are near or below those of Bernier Cave. Since the low salinity of Bernier Cave probably contributes to the reduced stereom of *A. stygobita*, it is surprising that the stereoms of my *O. filigraneus* SEMs (Figs 16A–F, 17A–F) are not reduced as much as those of *A. stygobita*.

Discussion

Feeding on detritus with EPS, skin may absorb DOM or EPS

While the types of food consumed by brittle stars may be determined by examining food in stomachs of preserved and dissected specimens, the actual feeding process of many brittle stars is unknown, especially for species like *A. stygobita* that consume detritus and for species in certain families. For instance, according to Hendler (2018), “the feeding behavior of Amphilepididae is an enigma.” So, the feeding behaviors of *A. stygobita* (family Amphilepididae) provide valuable insight for this group. This species ignored or rejected foods that are often fed to other brittle stars, including boiled egg, boiled lettuce, shrimp, fish, and TetraMin© fish flakes. Instead, they fed exclusively on cave detritus which they consumed while nearly flat on the surface of the detritus, occasionally with disk partly buried, but not with arms raised above the detritus the way passive suspension feeders collect particulate matter from the water (Hendler 2018).

Captive *A. stygobita* pulled fresh detritus into the mouth with their oral tentacles (Fig. 3C, D, 90 sec. apart) and without masticating or closing the mouth. In fact, live *A. stygobita* always had their mouths open whenever I observed or photographed their oral surfaces (Figs 3C, D, 4A–F, 6E). There appeared to be no selection or filtering of the various detritus components as they streamed into the mouth. This stream of detritus

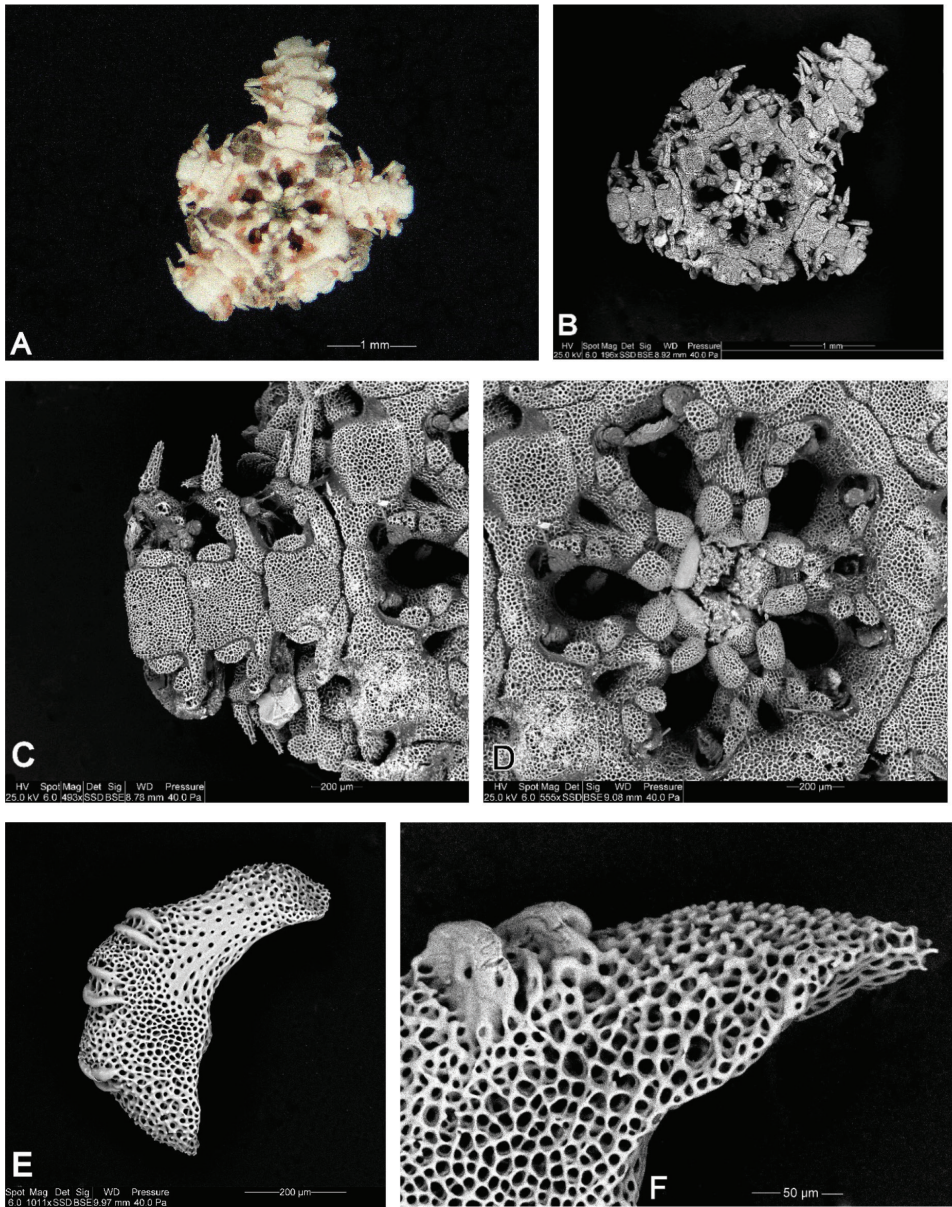


Figure 16. *Ophiophragmus filigraneus* **A** ventral view of disk and mouth area before bleaching, buccal funnel **B** lightly bleached SEM of disk and mouth area **C** SEM of 3 arm segments, wide VAPs and LAPs **D** SEM of mouth area **E** LAP with 3 spine articulation sockets with parallel sides **F** LAP with thick raised lobes of spine articulation.

was part of a sticky biofilm mass. It is not uncommon for caves to have phototrophic biofilms that are held together by extracellular polymeric substances (EPS), and for these EPS to be produced mainly by cyanobacteria and diatoms (Roldán and Hernández-Maríné 2009; Falasco et al. 2014). Not only did this biofilm help hold detritus

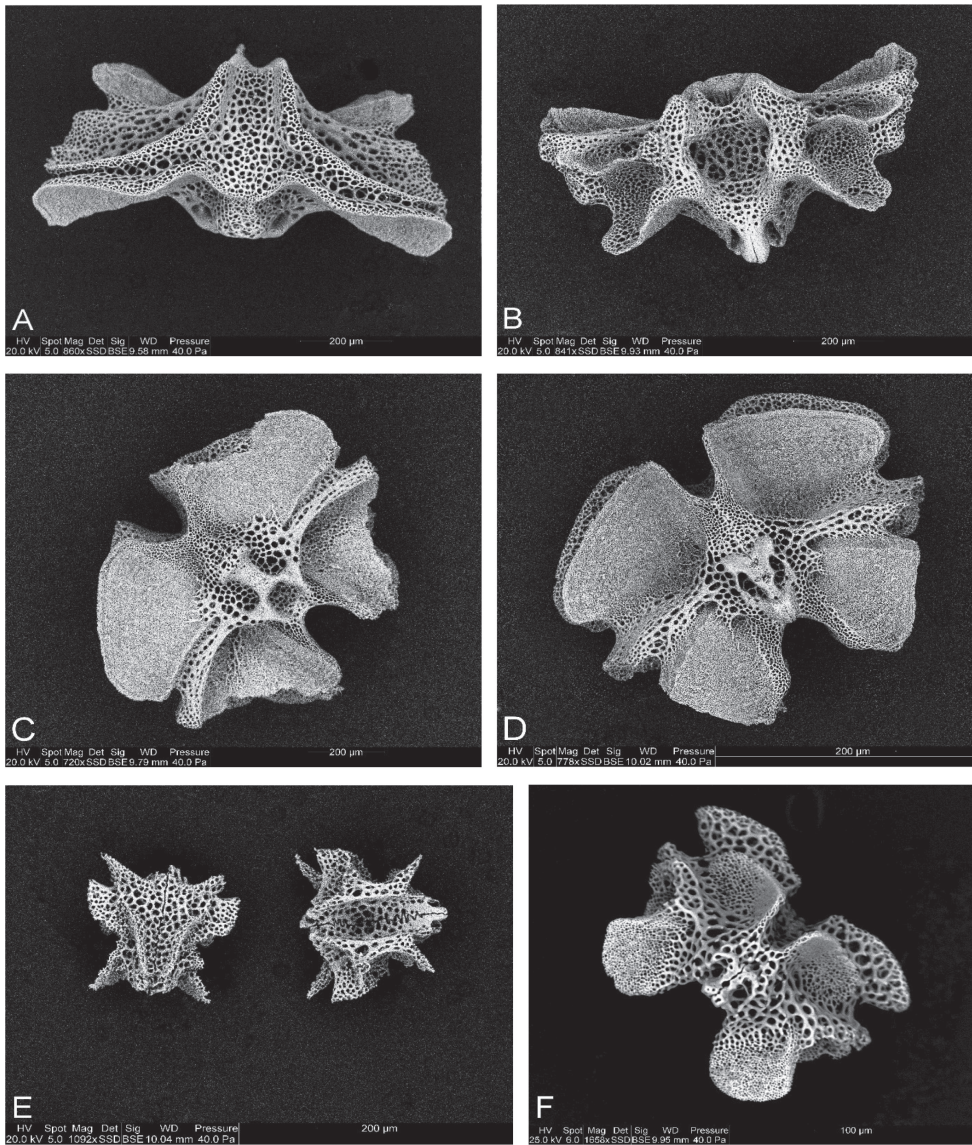


Figure 17. SEMs of *Ophiophragmus filograneus* **A** dorsal view of vertebra near disk, width $2 \times$ length and moderately fenestrated **B** ventral view of vertebra near disk, wide and fenestrated, elongated median process **C** proximal face of vertebra from near disk, arches radiate outward from ventral processes **D** distal face of vertebra from near disk, arches radiate outward from dorsal processes **E** dorsal (left) and ventral (right) views of vertebrae from near distal end of arm, width nearly same as length **F** distal face of vertebra from near distal end of arm, more fenestrated than proximal vertebrae.

together for easier manipulation by *A. stygobita*, it probably provided significant additional nutrients since such biofilms are composed of polysaccharides, proteins, lipids and nucleic acids (Falasco et al. 2014). Hoskins et al. (2003) studied the utilization of algal and bacterial EPS by the deposit-feeding brittle star *Amphipholis gracillima*

(Stimpson, 1854) and suggested that “EPS may represent a significant energy source for this deposit-feeding ophiuroid and other organisms with similar feeding habits. Additionally, *A. gracillima* appears to be especially adept at utilizing EPS resources from benthic diatom communities.” Sköld and Gunnarsson (1996) also found that the two detritus-consuming brittle star species, *Amphiura filiformis* (OF Müller, 1776) and *Amphiura chiajei* Forbes, 1843, were capable of increasing their growth and gonad development in response to short-term organic enrichment with concentrated diatoms. Large marine diatoms such as *Campylodiscus* are particularly good producers of EPS (Shnyukova and Zolotariova 2017). The substantial population of *C. neofastuosus* was probably a large contributor to the EPS in Bernier Cave detritus. Bruckner et al. (2011) found that the release of EPS by benthic diatoms depends on interactions with bacteria.

Hendler (2018) indicated that, “Two principal feeding modes of ophiuroids, macrophagy and microphagy, are distinguished according to the type of food consumed and manner in which it is acquired (reviewed by Warner, 1982). Generally, macrophagous species are carnivores and carrion feeders that grasp prey in loops of their arms, whereas microphagous species are deposit feeders and passive suspension feeders that gather particulate material with their tube feet.” It is clear that *A. stygobita* is a microphagous deposit feeder. The discussion of “feeding adaptations of microphagous ophiuroids” in Hendler (2018) concentrated on passive suspension feeders such as *Ophiothrix spiculata* LeConte, 1851, whose anatomy and feeding behavior are much different from that of the detritus feeding *A. stygobita*. Feeding behaviors of *Ophiothrix* species include: directing the ambulacral surfaces of raised arms toward the current, using tube feet to accumulate particulate material that they bind into a bolus, and moving the bolus toward the mouth where oral tentacles push the bolus through the buccal funnel as jaws open and close (Hendler 2018). The specialized tube feet and buccal funnel distinguish *Ophiothrix* species from macrophagous species; several other species have similar feeding behaviors and buccal funnels (Hendler 2018). Thus, it is important to visualize the buccal funnel described by Hendler (2018) as a funnel-shaped complex feeding apparatus that comprises a graduated series of oral papillae on the jaws and surrounded by radiating spindle-shaped oral slits between the jaws. Included in this paper are digital light microscope photos and SEMs of buccal funnels of three species to compare to *A. stygobita*, which does not have a buccal funnel: *Ophiophragmus filograneus* (Fig. 16A, B, D), *Ophiophragmus wurdemanii* (Lyman, 1860) (Fig. 18A), and *Ophiomastix wendtii* (Müller & Troschel, 1842) (Fig. 18B).

Compared to most other species such as *Ophiophragmus filograneus* (Fig. 16B), *Ophiophragmus wurdemanii* (Fig. 18A), and *Ophiomastix wendtii* (Fig. 18B), the oral frame ossicles of *A. stygobita* are reduced in number, highly variable, highly fenestrated, and loosely organized. In fact, the teeth and most oral papillae that would normally be used by most species for masticating or swallowing food appear to be missing or so fenestrated that this species may have difficulty manipulating food other than soft detritus. This appears to be another energy-saving feature used by *A. stygobita* because more complex mouthparts are not needed for microphagous detritus feeding. O’Hara et al. (2018) considered reduced or absent tooth clusters and reduced skeletons to be paedomorphic traits.

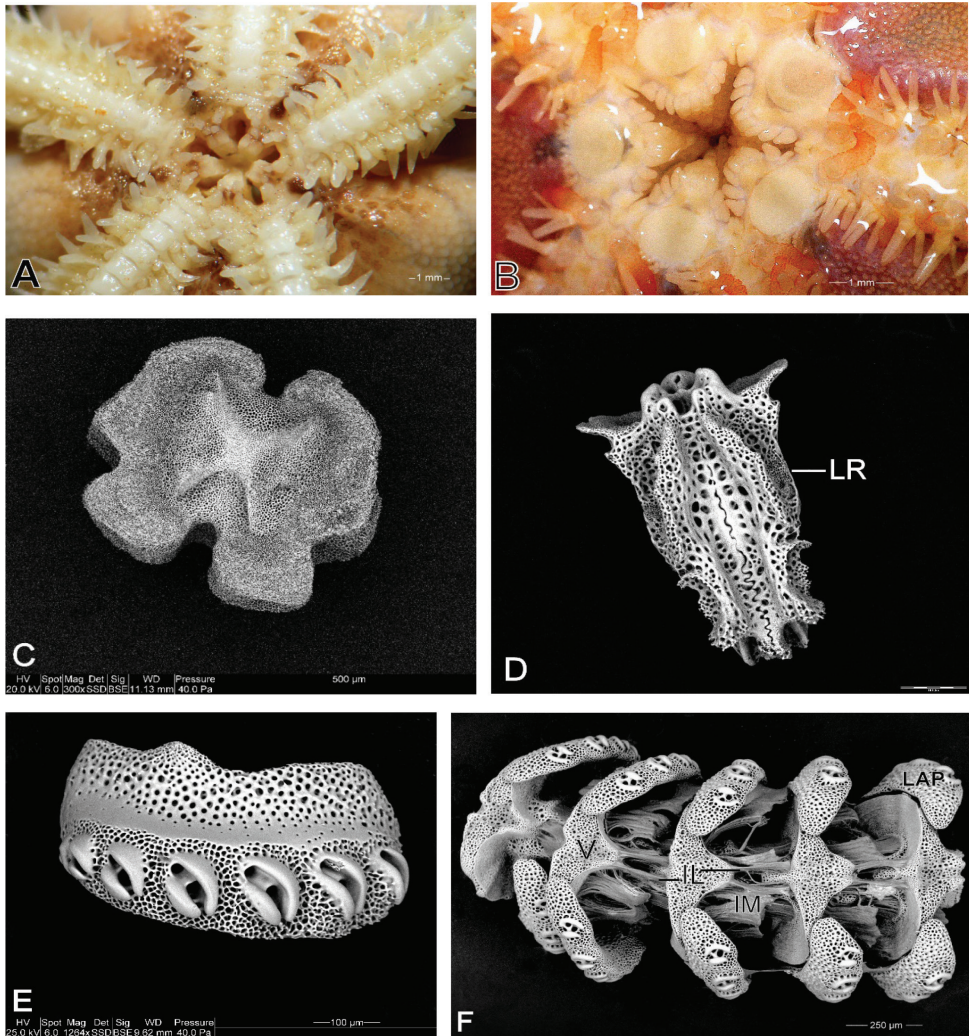


Figure 18. Miscellaneous morphological features for comparisons **A** preserved *Ophiophragmus wurdemanii*, mouth with buccal funnel **B** live *Ophiomastix wendtii*, mouth with buccal funnel **C** SEM of *Asteroschema brachiatum* proximal vertebra end, hourglass-shaped streptospondylous articulation **D** SEM of mid-arm vertebra of *Ophiocomella sexradiata*, ventral, with lateral ridges for connections to VAP **E** SEM of LAP of *Ophiothrix angulata*, 6 thick spine articulation lobes oriented diagonally **F** SEM of *Ophiactis savignyi* string of 5 pairs of very wide LAPs attached to Vs with intervertebral muscles, Vs attached to Vs with ligaments. Abbreviations: IL – intervertebral ligaments, IM – intervertebral muscles, LAP – lateral arm plate, LR – lateral ridge, V – vertebra.

The generic epithet *Amphicutis* (= around skin) was given to this cave brittle star because it has a translucent layer of skin raised above the surface of arms that persists after calcification (Pomory et al. 2011) (Fig. 3F). Pomory et al. (2011) speculated that this species may feed on dissolved organic matter (DOM), and the soft tissue might improve absorption of DOM, since other brittle stars are

known to use DOM (Clements et al. 1988). The fact that *A. stygobita* is a detritus feeder does not exclude the possibility that absorption of DOM and EPS by the skin might provide additional nutrients.

Reproduction and development of babies

Pomory et al. (2011) indicated that *A. stygobita* appeared to have spawned (to produce developing larvae externally) soon after being collected, but that observation was obviously incorrect, since three babies born in 2018 showed that this is a brooder instead of a spawner. Hendler (1975) indicated that only about 55 species, or about 3% of approximately 2000 species of ophiuroids, had been reported as brooding, although the reproductive mode of many other species is unknown and additional species may be recognized as brooding (Hendler et al. 1995; Stöhr 2005). Table II in Hendler (1991) indicates about 69 species are brooders. The birth of three *A. stygobita* babies confirms that this species is another brooder.

Gonads and developing embryos were visible in most adult *A. stygobita*. Horizontal serial sections revealed that both testes and ovaries were present in the same specimen indicating hermaphroditism. Hendler (1975) suggested that the high occurrence of hermaphroditism in viviparous ophiuroids may be “a function of the relatively inefficient dispersal of these forms,” and hermaphroditism ensures both sexes to be present “in newly settled areas with low population density.” This corresponds to the difficulty for a cave endemic brittle star to disperse and to the apparently low population of *A. stygobita* in the two caves it is known to inhabit. However, the populations of *A. stygobita* could be much larger than they seem since individuals are difficult to find with their very small disks that are usually filled with detritus so they are camouflaged by the surrounding detritus. Babies would be even more difficult to find in the detritus because they are microscopic (dd = 0.8 mm), as well as camouflaged. Since adults have relatively few ovaries and embryos, reproduction would seem to be slow, which is typical of cave adapted animals (Culver and Pipan 2019).

Brooding in *A. stygobita* appears to take place within the ovaries since bursae could not be identified in this study, nor in dissections done for the original description (Pomory et al. 2011). Hendler (1975) discussed various locations for brooding, including: within bursae, within ovaries, beneath the disk in *Ophiophycis gracilis* (Mortensen, 1933), and on the oral surface of the arms in *Astrotoma waitei*, now *Astrothorax waitei* (Bonham, 1909). Hendler (1975) noted that *Ophiophycis* (dd ~2 mm) “is among the smallest of ophiuroids and its 10 eggs, each 0.15 to 0.20 mm in diameter could conceivably be too large for bursal brooding, hence external brooding.” This same phenomenon may help explain the intraovarian brooding of *A. stygobita*, which is very small (dd = 3–4 mm) with relatively large eggs and developing embryos 0.20 to 0.35 mm. Although pre-released embryos may be only 0.35 mm, it is likely that newly released babies with 0.8 mm dd and arms of 0.6 mm could result from a 0.35 mm embryo unfolding. The length of time for egg and embryo development in *A. stygobita* appears to be greater than 1 year, since several adults showed little change in ovaries during this amount of time in captivity.

This corresponds to the slow growth rates observed in adult regeneration experiments (Carpenter 2016) and slow growth of babies in the current study.

As noted in Results section, if central and radial primary plates were present in disks of the three babies, they were obscured by disk scales (Fig. 5E). Stöhr and Martynov (2016) said “primary plates seem to have been lost completely (not just in adults), several times independently on species level in several families.”

Babies were born with LAPs well developed to support the 2 arm segments, while dorsal arm plates appeared to be absent (Fig. 5B–D); ventral arm plates were not easily viewed on the ventral side of the tiny babies. Based on their study of ophiuroid ontogeny, Stöhr and Martynov (2016) indicated that, “Dorsal arm plates are at first absent and develop gradually, starting on the proximalmost joints. Of the ventral arm plates the first one is always present from the youngest stages as part of the mouth frame, while the following develop gradually, but usually before the corresponding dorsal plate.” Stöhr and Martynov (2016) also said that, at the 2-3 arm joint stage, the arms are formed by joined pairs of lateral plates and bear two spines. It appears that *A. stygobita* follows this same pattern of arm development, starting with LAPs and Vs, followed by proximal VAPs, then DAPs.

As noted in Results section, babies were born with disk diameters of ~0.8 mm (adults have ~4 mm dd) and the number of segments per arm was very small for a brooding species, with only 2 arm segments. According to Hendler (1975), newly hatched young of viviparous species range from 0.6 to 5.0 mm dd and have 8 to 40 arm segments, and “the major limitation on size for brooded young appears to be the size of the parent.” Stöhr (2005) provided descriptions and SEM images of small juveniles of 17 ophiuroids, including three brooding species: *Ophiomitrella clavigera* (Ljungman, 1885) (smallest free-living juveniles had 1.5 mm dd and 13 arm segments), *Ophiacantha anomala* GO Sars, 1871 (smallest free-living juveniles had 2.0 mm dd and > 8 arm segments, and *Amphiura borealis* (GO Sars, 1871) (smallest free-living specimen had 0.7 mm dd and 5-6 arm segments). Byrne (1991) reported that adult *Ophionereis olivacea* HL Clark, 1900 with a maximum dd of 5.2 mm had juveniles emerge from the bursae at 0.48 mm dd and each arm had three segments. Even though *A. stygobita* babies were born with larger disks than *O. olivacea* (0.8 vs. 0.48 mm), the relatively fewer segments (2 vs. 3) is consistent with adult *A. stygobita* having fewer segments than adult *O. olivacea*.

Since *A. stygobita* babies and adults have relatively few segments, they have fewer joints in each arm, which makes it more difficult for them to use the normal brittle star mode of walking by bending the arms. As a result, adults and babies of this species were observed to move primarily by podial walking, which is common in asteroids (e.g., sea stars) but not in brittle stars (Carpenter 2011; Pomory et al. 2011; current study). Stöhr et al. (2012) said, “Ophiuroid tube feet lack suction cups and are rarely used for locomotion. Instead, ophiuroids move by twisting and coiling their arms, pushing against the surface like a snake or gripping objects and pulling themselves forward.” However, podial walking is typical of baby brittle stars because they have relatively short arms with few segments and joints, and since adult *A. stygobita* have short arms with few segments and joints, they would tend to use podial walking as well.

According to Stöhr and Martynov (2016), “arm segments are relatively longer in juveniles than in adults, but adult distal arms are similar to juvenile arms, because the arms grow at the tip, proximal to the terminal plate, and thus the distal part is younger and less developed than the proximal part. Growth occurs first lengthwise, later widthwise.” The first two arm segments of *A. stygobita* babies are also relatively longer than segments in adults; baby arm segment length/dd (= 0.2 mm/0.8 mm) = 25%, while adult arm segment length/dd (= 0.6 mm/4.0 mm) = 15%. These segment lengths of ~0.2 mm in babies (Figs 5B–D, 6A–E) and ~0.6 mm in adults (Figs 3A, 5A) are rather uniform except at distal ends where segments may be shorter while being produced (Figs 3B, 6E). This means that dd increases 5-fold (4.0 mm in adults/0.8 mm in babies), while segment length increases only 3-fold (0.6 mm in adults/0.2 mm in babies) during a lifetime. The width of arm segments in adults varies considerably near distal ends, being relatively narrow when segments are first produced (Fig. 10B) and increasing more in width than in length during their lives. On the other hand, the first 2 segments of *A. stygobita* babies were relatively wide, with the greatest width near distal ends of segments being nearly as wide as long. In this respect, the very narrow adult distal arm segments are very much different from the very wide first arm segments of babies.

Developing Vs were visible inside the two segments of babies; the most apparent vertebral structures were the 2 parallel ambulacral plates that eventually form support for adjoining parts (Figs 5B–D, 6B–F). *Amphicutis stygobita* babies were kept alive as long as possible to provide valuable information on development and behavior; unfortunately, they were not available for SEM study of their ossicles since they disintegrated soon after dying.

Growth rates

As noted in the results section, two adult *A. stygobita* were observed to regenerate arm tips at a rate of up to 1 mm in 24 weeks (Carpenter 2016). This is one of the slowest regeneration rates reported for any brittle star species with several possible contributing factors mentioned by Carpenter (2016). In the current study, babies also had a very slow growth rate; arm length increase of baby #2 was only ~0.2 mm (from ~0.6 to ~0.8 mm) in 13.5 months (Fig. 6E). At this growth rate of ~0.1 mm/yr. for dd and ~0.2 mm/yr. for arms, it would take about 30–40 years to reach the size of adults we have collected. Of course, growth rates in nature could be considerably faster with a better, fresher supply of detritus for food. In comparison, two adult specimens were observed to regenerate arm tips at a rate of up to 1 mm in 24 weeks (Carpenter 2016), which is about 12 times faster than growth in baby #2 (0.2 mm/13.5 mo. = 0.08 mm/24 wks.). However, baby growth and adult regeneration rates were somewhat closer if relative sizes are compared: dd of babies were 0.8 mm and adults were 4 mm (= 5 times as large), and growth rates may not be comparable to regeneration rates in the same species.

In contrast to the slow growth of *A. stygobita* babies, Gage (1984) observed that postlarvae and juveniles of non-brooders initially grow quickly. Ravelo et al. (2017) indicated that the growth curves of two continental shelf brittle stars from Alaska, *Ophiura sarsii* Lutken, 1855 and *Ophiocten sericeum* (Forbes, 1852), had “initial fast

growth, with an inflection period followed by a second phase of fast growth” and with maximum ages of 27 for *O. sarsii* and 20 years for *O. sericeum*. These growth patterns and ages were determined using annual growth bands on muscle flanges (fossae) of Vs as described by Gage (1990). Similar growth bands can be seen in the muscle flanges of *Amphilepis patens* (Fig. 11E, F), *Amphilepis platytata* (Fig. 15F), and *Ophiophragmus filograneus* (Fig. 17C, D). One reason I started using SEM was to look for growth rings in *A. stygobita*, but their highly fenestrated Vs did not display any distinguishable growth rings (Fig. 11A–D), and Gage (2003) indicated that it was difficult to find growth rings on specimens with dd less than ~5 mm because “the small overall size of the ossicle in relation to its mesh-like microstructure did not allow differences in surface relief or stereom density to be as easily recognizable as in other species.”

Morphology of adult *A. stygobita* compared to other species

Several morphological features of *A. stygobita* are quite extraordinary. To compare SEMs of *A. stygobita* to those of other species, SEMs of many epigeal brittle star species have been published; some of the most extensive include: Sumida and Tyler 1998; Stöhr 2005; Stöhr et al. 2012; Stöhr and Martynov 2016; Hendler 2018; O’Hara et al. 2018. Included here are my own SEMs of a few species selected from more than 20 that I prepared for comparison to *A. stygobita*.

Taxonomic considerations: *Amphilepis patens* and *Amphilepis platytata*

When *A. stygobita* was described by Pomory et al. (2011), its traits were distinctive enough to create the new genus *Amphicutis*. However, it was difficult to decide what family to place it in because it has some traits of Amphiuroidae, some traits of Amphilepididae, some in between, and some unique. The decision was made to place this species in the family Amphilepididae, but that decision was considered tentative. Family placement remained uncertain (“incertae sedis”) in the taxonomic revision by O’Hara et al. (2018) since they did not have tissue from *A. stygobita* for molecular analysis; however, they did move the families Amphilepididae and Amphiuroidae from the order Ophiurida to the order Amphilepida. O’Hara et al. (2018) commented that the large family Amphiuroidae requires revision and, “Preliminary findings (O’Hara et al. 2017) indicate that there are at least three major clades within the group that fit our criteria for family status.” They also remarked that the family Amphilepididae “is a paedomorphic family with reduced characters.” The following discussion may help resolve these family issues in the future.

The oral frame features in SEM images of *A. stygobita* (Figs 8A–C, 9) show some key traits, most of which were described by Pomory et al. (2011) as follows. (1) The ventral tooth at the apex of each jaw is broadly rounded, rather than triangular as in most other amphilepidids (triangular in *A. platytata*, rounded in *A. patens*), (2) oral plates are blunt ended as in amphiuroids, rather than pointed as in amphilepidids (including *A. patens* and *A. platytata*), (3) the 2nd tentacle pore (= 1st tentacle pore visible in ventral view) of the oral frame is outside mouth slit as in most amphilepidids, including *A. platytata* (Fig. 14D),

but inside (or even with distal ends of slit) in *A. patens* (Fig. 12C–E), while most amphiuroids have it inside the mouth slit, (4) oral shields are small and oval, similar to disk scales in appearance (usually triangular, sometimes diamond or heart shaped in *Amphilepis*), (5) lateral arm plates (LAPs) within the disk have large indentations on the ventral surface to partially encompass lateral edges of podial pores, and ventral arm plates are figure-8 shaped to partially encompass medial edges of podial pores (Fig. 8A–C), which seems to be unusual since it does not appear in any figures in Pomory's (2007) key, and (6) disk contains either 2 arm segments with LAPs distal to plates bounding end of mouth slit at (CP1 and CP3 in Fig. 8A), or 1.5 arm segments (CP 11 in Fig. 8A) or only 1 arm segment (CP6, Fig. 8A; CP8, Fig. 8A, C). This last trait differs from the original description (Pomory et al. 2011), "Three arm segments with lateral plates distal to plate bounding end of mouth slit on ventral side of disk." Whether the number of arm segments within the disk is 2, 1.5, or 1, the number is unusually small. For comparison, Pomory's (2007) taxonomic key illustrated 13 common genera, all with 3 to 7 arm segments within the disk; only *Ophiostigma* had 3, 2 genera had 4, 8 genera had 5, and 2 had 7. The number of arm segments within the disk may have relatively little taxonomic value, since Pomory (2007) did not mention or use it in his key, nor is it consistently mentioned in descriptions of new species. However, the low number of 1-2 segments within the disk corresponds well with the relatively low number of ~10–20 arm segments outside the disk.

One reason the two deep-sea *Amphilepis* species were examined was to compare their possible paedomorphisms to those of *A. stygobita*. The mouth features in all three species appear to be somewhat reduced (paedomorphic), especially in the number of oral papillae; however, the papillae seem to be more variable and less defined in *A. stygobita* (Figs 9, 12E, 14E), perhaps due to variable calcification states. The reduction in trabeculae and corresponding increase in fenestration are greater in *A. stygobita* and are especially noticeable in LAPs and Vs (Figs 8A, 11C, vs. 11E, 13D, 15D–F).

Salinity considerations: *Ophiophragmus filigraneus*

Considering that *A. stygobita* and *O. filigraneus* both live in low salinity environments, it is surprising that the stereoms of my *O. filigraneus* SEMs (Figs 16A–F, 17A–F) are not reduced as much as those of *A. stygobita*. This may be partly because my *O. filigraneus* specimen was considerably larger (dd = 8 mm) than my *A. stygobita* specimens (dd = 3–4 mm). A study by LaFace (2019) confirmed that reduced salinity can result in reduced ossicles with greater fenestration. LaFace (2019) found that regenerating arm ossicles of *Amphipholis squamata* maintained at ~25 ppt had "thinner ridges and less pronounced trabeculae than the regenerated ossicles of the brittlestars in the control condition." LaFace (2019) noted that "the stroma was also more elongated at day 28 so the shape resembled ovals rather than circles." Donachy and Watanabe (1986) found that length of regenerated arms and number of ossicles formed in *Ophiothrix angulata* were significantly less at 23 ppt than at 28–38 ppt; they correlated this with reduced calcium concentrations at lower salinities. Other traits of *O. filigraneus* are compared to *A. stygobita*'s in the following pages comparing anatomies.

Anatomy of arm segments

In their original description, Pomory et al. (2011) noted the unusual arm segment anatomy, “The dorsal and ventral arm plates of most ophiuroids are typically large and in contact, or nearly in contact, in sequence along the length of the arm. The lateral arm plates are usually small and separated from one another across an arm. The new species has the exact opposite arrangement. The dorsal and ventral arm plates are small and distinctly separated from one another along the length of the arm with the lateral arm plates large and broadly in contact across an arm. No shallow-water Caribbean species has this character as an adult.” SEM images of *A. stygobita* (Figs 7–10) confirm this unusual arrangement of segment ossicles, which effectively reduces weight but retains strength. Especially note that elongated LAPs almost completely encompass Vs and provide strength for arm segments, in conjunction with lateral extensions to Vs. This results in LAPs that are oriented parallel to the vertebral axis, comparable to splints used to stabilize a human broken arm. In contrast, many species have heavy LAPs extending laterally and supporting several spines pointing distally or laterally to provide protection from predators and to grip the substrate to help them move forward as they swing arms. Examples include: *Amphilepis patens* (Fig. 13A, C, E), *Amphilepis platytata* (Figs 14C, E, 15C, D), *Ophiophragmus filograneus* (Fig. 16A–C), and *Ophiactis savignyi* (Müller & Troschel, 1842) (Fig. 18F).

Amphicutis stygobita is unusual in having only two spines which are near the end of LAPs (Fig. 7D, E). Pomory et al. (2011) indicated that, “Only one other shallow-water Caribbean species in a different family, *Ophiolepis paucispina* (Say), consistently has only two arm spines (Hendler et al. 1995; Pomory 2007).” Arm spine articulations in *A. stygobita* are nearly round with 2–3 openings for muscles and nerves to pass through to the spine; lobes are only slightly raised (Fig. 7F). This type of spine articulation appears to be unusual, since O’Hara et al. (2018) included in their diagnosis of the order Amphilepidida (which they created in O’Hara et al. 2017), “Dorsal and ventral lobes of arm spine articulations parallel (except in Ophiotrichidae).” This parallel arrangement is seen in my other specimens in the order Amphilepidida: *Amphilepis patens* (Fig. 13D–F), *Amphilepis platytata* (Fig. 15D), *Ophiophragmus filograneus* (Fig. 16E, F), and *Ophiactis savignyi* (Fig. 18F). In contrast, *Ophiotrix angulata* (Say, 1825) (family Ophiotrichidae, order Amphilepidida) has thick spine articulation lobes oriented diagonally (Fig. 18E). The reduced number of spines and shallow arrangement of spine articulations in *A. stygobita* may be the result of the overall reduction in stereom density, which provides additional energy conservation.

Anatomy of vertebrae

Stöhr and Martynov (2016) concluded, “It is clear that species in which adults have vertebrae with a L:W ratio below 1 are well developed, whereas species with values close to 10 are strongly paedomorphic.” Of course, it depends on the technique used to measure Vs and on which Vs are measured since distal ones tend to be much narrower

than ones near the disk. Nevertheless, the L:W ratio of *A. stygobita* Vs (Figs 8F, 10A, B) is in the upper part of this paedomorphic range, and it is much greater than most species, including most deep sea paedomorphic species such as *Amphilepis* species.

Lateral extensions of Vs in *A. stygobita* connect with LAPs; some Vs have 3–4 narrow extensions on each side (Fig. 7C), some are flared or knobbed to form wider attachment points to LAPs (Figs 8D, 10A), and some form interrupted ridges for attachment points (Figs 8F, 10E). Other species with elongated Vs often have lateral ridges that connect to LAPs as in *Ophiocomella sexradiata* (Duncan, 1887) (Fig. 18D). Several families of ophiuroids (e.g., Ophiopsilidae, Amphilimnidae, and Amphiuroidae) have the inner side of LAPs with two, three, or more merged knobs instead of a ridge to connect to Vs (O’Hara et al. 2018). The very narrow Vs at the distal ends of arms of *A. stygobita* have short lateral extensions (Fig. 10B), indicating they lengthen as Vs widen.

Since Vs and LAPs of *A. stygobita* are very narrow, there is less surface area on ends of Vs and LAPs to form connections to adjoining Vs and LAPs. For comparison to the very narrow segments of *A. stygobita*, please note the very wide segments of *Ophiactis savignyi* (Duncan, 1887) (Fig. 18F); muscles and ligaments between segments were left intact to show how adjoining LAPs connect with each other along their length, and Vs have large areas of connections to adjoining Vs.

Irimura and Fujita (2003) observed that, “Two morphological types of the vertebral articulation, streptospondylous and zygospondylous, have been traditionally used by many taxonomists to classify ophiuroids into separate orders or suborders.” However, O’Hara et al. (2018) noted that, “Arm vertebrae are subject to ecological adaptation and show convergent evolution. This character cannot therefore be used on its own but it is helpful in combination with other characters or to differentiate closely related groups.” Streptospondylous articulations are hourglass-shaped (Fig. 18C), both proximally and distally, that give great arm joint flexibility that allow arm loops and coils characteristic of gorgonocephalids (e.g., basket stars) (LeClair 1996). The zygospondylous type of articulation is more mechanically limited and has vertebral surfaces bearing a complex set of projections and depressions that fit into the complimentary articulating surfaces of the adjacent V; this is typical of most brittle stars (LeClair 1996). Articulations in *A. stygobita* are zygospondylous but are significantly modified compared to most species.

The connections of Vs in *A. stygobita* are different from other species in several ways. The median socket is thinner and the median process is thinner and more pointed (Fig. 11 C, D) in comparison to *Amphilepis patens* (Fig. 11E, F) and *O. filigraneus* (Fig. 17C, D). The muscle flanges, dorsal processes, and ventral processes at the ends of *A. stygobita* segments are not only relatively small, they are also highly fenestrated; please compare these structures in *A. stygobita* (Fig. 11C, D), *Amphilepis patens* (Fig. 11E, F), and *O. filigraneus* (Fig. 17C, D). In *O. filigraneus* the Vs that are early in development near distal ends of arms (Fig. 17F) are similar to more proximal Vs in *A. stygobita* (Fig. 11C, D). Although strong fenestration might provide better attachment for individual muscle fibers, it probably creates joints that are weaker and less flexible, which could result in reduced capability to move arms forward and contribute to the tendency to use podial walking. Individual tube feet of *A. stygobita* are very large with an enlarged

smooth knob on the end and 2-3 rings/ridges below knobbed end (Pomory et al. 2011). The large podian basins on the ventral surfaces of Vs (Fig. 8 E, F) provide space for the large podia. The weakness in arm joint articulation structure may be partly compensated for by multiple connections between Vs and LAPs to hold segment ossicles together.

Highly fenestrated ossicles

The ossicles of *A. stygobita* (including disk scales, Vs, LAPs, and other arm components) are highly fenestrated with a net-like lattice around larger open spaces, more than in *O. filigraneus* (Figs 16C–F, 17A–F) and other species I have examined. One of the distinctive traits of the genus *Amphicutis* described by Pomory et al. (2011) is that the “disk and arms are often formed by soft tissue outlining plates and scales but lacking significant calcification,” and “the soft tissue creates up to 13 arm segments with just a thin axial center of calcium carbonate.” Apparently, the highly fenestrated ossicles seen in SEMs correspond to this lack of calcification, which seems to be at a greater extent than in other brittle star species. Pomory et al. (2011) suggested that the soft tissue-calcification differences may be a paedomorphic trait.

Paedomorphism advantages

Paedomorphic traits have been mentioned several times in this paper. Probable reasons for why ophiuroid paedomorphic traits occur are usually not explained in other papers. For instance, O’Hara et al. (2017) described various taxonomic groups (e.g., Amphilepididae) as being paedomorphic, with little explanation about how and why. It is interesting to note that the family Amphilepididae consists of only 2 genera: *Amphicutis* (with *A. stygobita* being the only species) and *Amphilepis* with about 12 species (Stöhr et al. 2024), all of which appear to be deep-sea dwellers. This may explain why the family Amphilepididae is considered paedomorphic: living in caves and the deep sea can promote paedomorphy due to evolutionary pressure to conserve energy in relatively low nutrient environments. In their study of paedomorphosis in deep-sea brittle stars, Stöhr and Martynov (2016) listed 29 morphological features they considered paedomorphic; however, they provided little explanation of why paedomorphisms occur in the deep sea, except that the paedomorphic morphology of deep-sea brittle stars “may be linked to low nutrient and energy potential of the bathyal and abyssal environments.” Here I would like to expand on this explanation for the occurrence of ophiuroid paedomorphisms in the deep sea and in *A. stygobita* in Bernier Cave.

Apparently it is well known that several cave dwelling salamander species are permanently aquatic and retain their larval gills into adulthood (i.e., paedomorphy) because they have access to a richer food source in the water than in the terrestrial cave habitat (Recknagel and Trontelj 2022). The explanation for paedomorphy in ophiuroids is much different. In most cases, paedomorphic species conserve energy by not producing, maintaining, and transporting fully developed adult body parts, and these reductions would be retained in populations if they are not disadvantageous. The survival

advantage of a specific paedomorphic trait can often be correlated with certain environmental circumstances that allow animals with juvenile traits to survive. For instance, brittle stars that are microphagous detritivores may be able to survive well with reduced mouthparts, since adults and babies can more easily consume soft detritus than passive suspension feeders that gather particulate material with their tube feet or macrophagous carnivores that grasp prey with their arms. Similarly, species with reduced arm stereoms save energy by not producing, maintaining, and transporting heavy adult ossicles if they do not need them to catch food or to survive predation or strong water flow. According to Harper and Peck (2016) there is a general paradigm that marine predation pressure decreases with depth, which they confirmed in their study of shell repair in brachiopods. In addition, ocean currents generally diminish in intensity with increasing depth (Faugères and Mulder 2011), which enables fine particles to settle out of suspension as detritus (Dutkiewics et al. 2016). Seasonal deposition of phytodetritus below productive surface areas provides abyssal communities with a high-quality food resource (Tyler 1988; Gage 2003; Ramirez-Llodra et al. 2010). Deep-sea detritus is also enriched by EPS (Thornton 2002), as it is in Bernier Cave. According to Ramirez-Llodra et al. (2010), “Much of the sediment-covered abyssal seafloor is characterized by sluggish bottom currents and little current scouring” and “the top centimetres of sediments of abyssal plains are colonized by very rich communities of macro- and meiofauna with very high biodiversity levels.” Thus, it seems likely that many deep-sea brittle star species are able to find microhabitats with slight currents, few predators, and abundant energy-rich detritus where they can survive with paedomorphic traits. More than half of the 2300 brittle star species are found in the deep sea (Stöhr et al. 2012). I contend that most of them are probably paedomorphic at least partly because of their intake of soft high-energy detritus, not by the “low nutrient and energy potential of the bathyal and abyssal environments,” as suggested by Stöhr and Martynov (2016). The cold temperatures of the deep sea may also contribute to paedomorphosis since brittle stars and their predators would have lower metabolic rates, and they would move more slowly, which could reduce chances of predation and the need for stronger stereoms.

Size appears to have a significant effect on the number and strength of certain paedomorphic traits. Stöhr and Martynov (2016) examined paedomorphic traits of 40 deep-sea species in the families Ophiuridae and Ophiolepididae which “are often quite small, with disk diameters of a few millimetres, and their skeleton consists of fewer elements than in the majority of extant species.” This could be because: (1) small species tend to be detritivores, so they can survive with reduced mouthparts, (2) they may be able to better avoid predators if they hide within the detritus, and (3) stereoms need to be stronger in larger brittle stars to support and move their heavier bodies.

Another situation in which a reduced stereom is advantageous is in swimming brittle stars. A few species are known to use swimming as a defensive escape mechanism, and a lighter body facilitates swimming (Hendler and Miller 1991). Hendler and Miller (1991) found that, “The skeletal ossicles of swimming ophiuroids are thinner and more porous than non-swimmers’ ossicles,” and the few species of “known swimming ophiuroids are deep-water species and several are widely distributed.”

Adaptations to cave environments are known as troglomorphisms, and many of these adaptations are related to ways that cave animals conserve energy in a low nutrient environment. Paedomorphisms offer an excellent way to conserve energy, both in caves (where they may be recognized as troglomorphisms) and in the deep sea; in both environments brittle stars do not need to spend energy producing adult structures that they do not need to survive. While humans generally want their offspring to grow up big and strong, in nature these traits do not always contribute to a species' survival and may even be detrimental.

Summarized here are the presumptive correlations between paedomorphisms in *A. stygobita* and its environment. The Bernier Cave environment has a remarkable set of characteristics that have provided the circumstances for *A. stygobita* to develop several sets of paedomorphic and troglomorphic traits. (1) Although most of the cave is in total darkness, the ceiling entrance is large and near the water which allows considerable detritus to enter the aquatic ecosystem. It also provides light for abundant growth of algae. These algae, in conjunction with bacteria to make EPS, help provide detritus sufficiently rich for detritivores to survive. This soft detritus can be consumed with reduced and fenestrated mouthparts. (2) The water inside Bernier Cave is hyposaline at ~14–28 ppt, which facilitates the reduced stereom of *A. stygobita* by reducing ionic precipitation. (3) The reduced water flow in this cave keeps detritus relatively stationary, which allows *A. stygobita* to reduce its ossicle weight as ballast and not get washed away. Ossicle weight is lost by greatly increasing fenestration in virtually all ossicles, including mouth and arm structures. In addition, several body parts have been reduced in size and/or changed in proportion. Most notably are the narrowed arms with strongly reduced DAPs and VAPs, reduced total arm length, but increased arm segment length (LAPs and Vs). This results in fewer arm joints, reduced arm swinging, and more podial walking (supported by enlarged podia). It also permits significant changes in structure of Vs with reduced articulation areas and muscle flanges. The LAPs and Vs have lateral extensions that hold them together while reducing weight, and (4) *A. stygobita* does not appear to have any major predators in Bernier Cave, which allows it to survive with a smaller body, reduced ossicle strength, and reduced spine number and size. The abundant detritus containing few predators should also provide a favorable environment for newly released brooded offspring, which may increase their survival rate and conserve energy for the population compared to producing many free-living larvae.

Culver (1982) mentioned that paedomorphosis “has been reported for a variety of cave organisms. For example, *Speoplatyrhinus poulsoni*, the most cave modified amblyopsid fish, shares some characters, such as body size and head size, with immature *Typhlichthys subterraneus*.” Also, Langecker and Longley (1993) found that two Texas blind catfishes exhibit “a series of apparently paedomorphic traits: a small body size, an enlarged head, a weakly ossified skeleton, and reduced muscles.” However, it appears that the significance of paedomorphisms as troglomorphisms has not been widely recognized. Although paedomorphy is not the same as troglomorphy, when paedomorphic traits occur in cave animals they should also be recognized as troglomorphisms. Perhaps it is easier to recognize paedomorphy in cave brittle stars than in many other cave animals since brittle stars do not have obvious eyes, so loss of eyes is not easily

observed in them, and other traits are more closely examined. In addition, the relationship of morphological traits to the environmental niche may not be as apparent as it is with *A. stygobita* in the unusual environment of Bernier Cave. Paedomorphisms may be more common in caves than in other habitats because the relatively stable environment and relaxed predation and competition in caves allow survival without adult structures.

Conservation of energy is a driving force in the evolution of many traits found in nature including: mammal hair and bird feathers to conserve heat energy, streamlined bodies of aquatic animals and light weight bones of birds and bats to conserve energy while moving, and paedomorphic traits of brittle stars to conserve energy of producing, maintaining, and transporting heavy adult structures. In general, paedomorphy should be a very effective way to conserve energy in a variety of animals, especially cave animals, by not having to produce and transport the many structures found in adults. Thus, it is surprising that paedomorphisms are not predominant troglomorphisms, but apparently for many species the adult structures are so valuable for protection from predators, competitors, and strong water movements that they are still produced. It seems that echinoderms may be unusual in their plasticity with many ways to produce a body that can survive in various environments.

Emson (1984) proposed the important concept of “Bone Idle.” He suggested that echinoderms are a “highly successful group in the marine environment” partly because they are the only invertebrates with an endoskeleton, which requires less energy to build and maintain than soft tissue due to its formation by ionic precipitation. Emson (1984) speculated that being “bone idle” may have been the recipe for success of echinoderms.

Even though the endoskeleton apparently gives echinoderms a competitive advantage over other invertebrates, it could still be advantageous to reduce their skeleton in certain environments. The body plan in *A. stygobita* seems to follow a modified recipe for success by having a greatly reduced endoskeleton that it uses effectively in this special cave environment with sufficient light to stimulate growth of energy-rich diatoms, few predators, and brackish water that reduces ionic precipitation.

Probable paedomorphisms and troglomorphisms in 4 cave brittle species

Since *A. stygobita* was the first known cave brittle star, Carpenter (2016) compiled a list of probable troglomorphisms that he had observed in this species, including: (1) no body pigment, (2) reduced body size, (3) elongated arm segments, (4) raised skin possibly for enhanced chemoreception, (5) muted alarm response to light, (6) reduced aggregation, (7) reduced fecundity, and (8) slow metabolism (movement and regeneration). Since SEMs show a greatly reduced density of the stereom with increased fenestration of ossicles, this trait is now added to the list (Table 1) of probable troglomorphisms for *A. stygobita*, along with other morphological features described in the above Discussion of Paedomorphisms and Troglomorphisms. Carpenter (2016) remarked in his study of *A. stygobita* that it was surprising that more brittle stars had not been found in caves, considering that brittle stars are generally photonegative, and it seemed likely that more species do live in marine caves. Three other brittle star species that are

Table 1. Probable troglomorphisms compared in four cave species. T: troglomorphism; dd: disk diameter; ND: no data.

Troglomorphism	<i>A. stygobita</i>	<i>O. cavernalis</i>	<i>O. commutabilis</i>	<i>O. xmasilluminans</i>
Body pigment	Absent (T)	Mottled/bands	Brown blotches	Creamy, bands, spots
Mouth parts	Very reduced (T)	Normal	Buccal funnel	Normal
Ossicle density	Very reduced (T)	Normal	Some reduced (T)	Normal
Disk diameter	Small, 3–4 mm (T)	Small, 5.3 mm	Normal, 11.4 mm	Small, 6.3 mm
Arm length	Short, 2.5 × dd (T)	Medium, 9 × dd	Long, 20 × dd (T)	Long, 18 × dd (T)
Arm seg. number	Reduced (-18) (T)	Normal (-75)	Many (-150) (T)	Many (-150) (T)
Arm spines	Few, short (T)	Few, short (T)	Normal	Many, long
Podia	Enlarged (T)	ND	Long, many (T)	Many (T)
Regeneration rate	Very slow (T)	ND	ND	ND

apparently cave endemics have recently been described and are compared below and in Table 1. In addition, Márques-Borrás (2020) indicated that 39 brittle star species have been reported from caves, including many that are not endemic to caves; this includes Okanishi and Fujita's (2019) listing of 20 species of brittle stars from 8 families collected in submarine caves of the Ryukyu Islands, southwestern Japan.

Ophiozonella cavernalis. Okanishi and Fujita (2018) described two new species from specimens collected in submarine caves in Ryukyu Islands, southwestern Japan: *Ophiolepis cavitata* and *Ophiozonella cavernalis*. The authors did not claim that *O. cavitata* was a cave endemic because their “only 2 specimens were found in a single cave despite extensive searching, which suggests that this occurrence may have been random.” Also, the specimens were very similar to a non-cave specimen from northeastern Australia that was identified by Baker (1979) as *Ophiolepis rugosa* Koehler, 1898. Okanishi and Fujita (2019) later reported that 4 additional specimens of *O. cavitata* were found in another cave about 60 km from the original collection site, this time in the “entrance zone” with coral rubble, thus confirming that this species is probably not a cave endemic. However, this points out the difficulty of conclusively identifying brittle star species as cave endemics.

Okanishi and Fujita (2018) did claim that *O. cavernalis* is “an anchialine-endemic ophiuroid and the first finding from the Pacific Ocean.” They made this claim partly because “the number of *O. cavernalis* specimens is large and its presence in 4 caves suggest that it is indeed a cave endemic species with self-recruiting population.” Okanishi and Fujita (2018) said *O. cavernalis* (Amphilepidida) was found in four caves with an “anchialine environment (low salinity and water temperature).” Unfortunately, they did not indicate how low the salinity was, and they did not identify any troglomorphic traits. *Ophiozonella cavernalis* does not appear to have most of the prominent paedomorphic or troglomorphic traits seen in *A. stygobita* (e.g., reduced mouth parts, reduced stereom, and elongated arm segments), but it does have spines that are slightly reduced in size and number (3 vs. > 3 in the 31 congeners) (Okanishi and Fujita (2018). From examining the SEM images of Okanishi and Fujita (2018), it appears that LAPs of *O. cavernalis* have substantial EPTs (extra peripheral trabeculae) that may be related to a photoreceptor system, which is described in more detail in the section below on

Ophionereis commutabilis. The lack of paedomorphic mouth structures in *O. cavernalis* may be related to the shallow habitat (8–27 m) composed of a silty-muddy bottom (Okanishi and Fujita 2018), instead of detritus. One prominent troglomorphic trait found in many cave-adapted organisms is the loss of pigment, and *O. cavernalis* has a significant color pattern described by Okanishi and Fujita (2018) as: “mottled light and dark brown on aboral disc, radial shields darker, arms variegated light brown with dark bands, a darker brown band on proximal portion of each arm spine.”

Ophionereis commutabilis Bribiesca-Contreras et al., 2019 was originally identified as an undescribed species from Mexico in the family Ophionereididae and barcoded by Bribiesca-Contreras et al. (2013). It was formally described and named in a phylogenetic paper by Bribiesca-Contreras et al. (2019). Márques-Borrás et al. (2020) meticulously compared morphologies of *O. commutabilis* to a close surface relative *Ophionereis reticulata* (Say, 1825) and determined “some characters representing potential morphological cave adaptations in *O. commutabilis*: bigger sizes, elongation of arms and tube feet and the presence of traits potentially paedomorphic.” Particularly notable was that arm lengths of *O. commutabilis* were “up to 20 times the disc diameter and a mean of 13.2 in comparison to 6.6 of *O. reticulata*.” Although Márques-Borrás et al. (2020) cited “bigger sizes” as a potential cave adaptation, their Fig. 5 indicates that both *O. commutabilis* and *O. reticulata* had exactly the same dd of 11.4 mm; but when they compared ratios of arm length/dd, *O. commutabilis* was much “bigger” (13.2 vs. 6.6) because of the greatly elongated arms of *O. commutabilis*. So, bigger size is only relevant when elongated arms are included. Feeding was not observed in this species, but the presence of elongated arms and tube feet, a well-developed buccal funnel, and a cave floor covered by soft sediments (Márques-Borrás et al. 2020) all indicate that this species is a passive suspension feeder or benthic deposit feeder.

Márques-Borrás et al. (2020) observed that the ossicles they examined with SEM were more porous in *O. commutabilis*, which they considered being potentially paedomorphic and troglomorphic; they did not mention the increased porosity as a possible way to reduce weight and conserve energy. They indicated that the salinity was 30–31 ppt where *O. commutabilis* were found, which may partly explain the more porous ossicles.

Márques-Borrás et al. (2020) made the important point that the increased porosity of dorsal arm plates (DAP) in *O. commutabilis* resulted in a partial reduction of its photoreceptor system, compared to *O. reticulata*. A brittle star photoreceptor system was first described by Hendler and Byrne (1987) for *Ophiocoma wendtii*, which (according to O’Hara et al. 2018) is now recognized as *Ophiomastix wendtii* (Müller & Troschei, 1842). This photoreceptor system included light sensitive nerve bundles below hemispheres on the outer surface of dorsal arm plates; they called these hemispheres EPTs (expanded peripheral trabeculae), which presumably concentrate light on the nerve bundles. EPTs appear in distinctive patterns in SEMs of those brittle star species that have EPTs, including *O. commutabilis* and *O. reticulata*. Márques-Borrás et al. (2020) found that “this pattern decreases the EPT density (increasing in size) on the stygobiotic specimens in comparison to its epigeic congeners.” Hendler and Byrne (1987) and Hendler (2004) indicated that *Ophiocoma wendtii* has a well-developed

photoreception system, “but not every *Ophiocoma* species has a *wendtii*-type system with interactive microlens, chromatophore, and photoreceptor structures. There are species with markedly different capacities for color-change and differing lens morphology and light sensitivity among the four subgeneric groups of *Ophiocoma*.” Hendler (2004) noted that such optically efficient lenses are restricted to the relatively animated Ophiuroidea. However, Sumner-Rooney et al. (2018) were skeptical of the Hendler and Byrne (1987) photoreceptor system with microlenses, and they presented evidence that “whole-body photoreceptor networks are independent of ‘lenses’ in brittle stars.” Because EPT’s are restricted to certain groups of ophiuroids, and their potential use in photoreception in cave brittle stars has not been tested, I chose to not use their reduction or absence as a troglomorphism in comparing cave species in Table 1.

Márques-Borrás et al. (2020) did not discuss the fact that *O. commutabilis* appears to lack the common troglomorphic feature of pigmentation loss. Bribiesca-Contreras et al. (2019) described the coloration in *O. commutabilis* as “brown on the dorsal surface of the disc, with scattered large pale blotches” and “patterns were quite variable, resembling those described of other species of the genus.” Bribiesca-Contreras et al. (2019) suggested “that this diversity of colouration patterns could be a result of inhabiting a low-light environment, where pigmentation is extraneous and there might be no selective pressures for this trait.”

Ophiopsila xmasillumins Okanishi, Oba & Fujita, 2019 was described from a cave on Christmas Island, northwestern Australia. According to Okanishi et al. (2019), specimens occur on sandy bottoms with “disc buried and arms extended above the substratum.” This is consistent with passive suspension feeding behaviors described by Hendler (2018), although photos of the oral frame presented by Okanishi et al. (2019) do not clearly show a buccal funnel as illustrated by Hendler (2018) for *Ophiopsila californica* A.H. Clark, 1921, which frequently accompanies passive suspension feeding.

Arms of *O. xmasillumins* are approximately 18 times longer than disk diameter (Okanishi et al. 2019); a medium-length arm in their Fig. 2 has ~150 segments. Okanishi et al. (2019) noted that, “As suggested in previous studies of ophiuroids (Bribiesca-Contreras et al. 2013), extraordinarily long arms of species could be an adaptation to cave life.” The color is generally creamy white with yellowish bands, green bands, and yellowish spots in various locations (Okanishi et al. 2019).

Okanishi et al. (2019) also “describe bioluminescence and burying behaviour, which suggest adaptation to submarine cave environments.” Bioluminescence in *O. xmasillumins* could be useful in either attracting prey or scaring predators, including decapods and fishes that are known to inhabit this same cave (Okanishi et al. 2019). Protection from predators might also be provided by the numerous spines encircling each of the many short arm segments. Okanishi et al. (2019) observed that “other coastal congeners also show the same bioluminescence” and “it is difficult to say whether *O. xmasillumins* new species is a cave-endemic, since adequate inventory surveys around the cave have not yet been done.” Unfortunately, Okanishi et al. (2019) did not mention any probable cave adaptations for this species except for the long arms and bioluminescence, and they did not mention or make comparisons to *A. stygobita*,

O. cavernalis, or *O. commutabilis*. Although evidence for cave endemism in this species is sparse, it is still worthy of comparison to other species found in caves.

It is interesting to compare possible troglomorphisms of the three recently (2018, 2019) described species to those of *A. stygobita*. These four cave-dwelling species are greatly separated geographically and are in different taxonomic families, which indicates their troglomorphic traits evolved independently. This may partially explain why their apparent troglomorphisms vary widely. Also, since many brittle stars are photonegative and often live in dark environments, it is difficult to identify traits of cave-dwelling brittle stars as being definite troglomorphisms, rather than simply being traits of photonegative benthic animals. Table 1 compares probable troglomorphisms for the four cave species.

Troglomorphisms are often described as either regressive or constructive (Culver and Pippin 2019). The most obvious regressive traits in most cave animals are reduction in eyes and body pigment, while constructive traits include enhanced sensory structures or behaviors to help find or capture food (Culver 1982; Culver and Pippin 2019; Romero 2009). In cave brittle stars, probable regressive traits are loss or reduction in body pigment, mouth parts, ossicle density, disk diameter, arm length, arm segment number, and spine length and number; most of these regressive troglomorphic traits are also pedomorphic traits. Constructive traits in cave brittle stars may include elongated arms and enlarged or more podia to help sense and/or capture food in the substrate or suspended in the cave water; podia are larger in *A. stygobita* and more numerous in *O. commutabilis* and *O. xmasillumians* by virtue of their having much longer arms. On the other hand, the short arms of *A. stygobita* apparently are an advantageous pedomorphic trait because less energy is needed to produce them, and long arms are not needed to eat soft detritus. Most brittle stars have many short arm segments resulting in many podia (2 per segment) and many joints that give arm flexibility. In *A. stygobita*, energy is conserved by reducing arm segment number, which reduces total number of podia and joints; each segment is relatively long, but energy is conserved by producing fenestrated ossicles, with LAPs and Vs reinforced by lateral extensions.

Note that there is little consistency in the presence or absence of any of the troglomorphisms across the four species. Thus, it is challenging to find definite troglomorphic traits in the three ophiuroid species described after *A. stygobita* in 2011. All have pigment, and the loss of microlenses as light-detecting structures is not clear. Romero (2009) pointed out that troglomorphisms can be highly variable, blindness and depigmentation do not occur in parallel among most cave species, and “This disparity in character development among species suggest that both the evolutionary history of the species involved and the peculiar characteristics of the environment in which they live must be taken into consideration to explain such a mosaic of character development.” Several of the troglomorphic traits for *A. stygobita* described by Carpenter (2016) including a very slow regeneration rate and behavioral traits (e.g., muted alarm response to light and slow movement with podial walking) were not reported and were apparently not observed in the other three cave species; hopefully, live specimens of these three species will be studied in the future to look for such traits. Brooding, the extreme fenestration of ossicles, and elongated vertebrae with extra lateral extensions in *A. stygobita*

appear to be additional energy conserving traits. So, it appears that *A. stygobita* has more troglomorphisms and paedomorphisms than the other three species, which may be the result of a longer evolutionary history in cave habitats and/or of the special characteristics of Bernier Cave, especially low salinity and abundant detritus.

Conclusions

The cave brittle star *A. stygobita* is a small (adult dd = 3–4 mm) microphagous deposit-feeding brittle star that survived and grew in captivity by consuming detritus rich in microorganisms and a sticky biofilm containing extracellular polymeric substances (EPS). They can feed with reduced mouth parts because the detritus is soft and easy to consume. This hermaphroditic intraovarian brooding species had only ~5–7 gonads per individual with relatively large eggs and developing embryos 0.20 to 0.35 mm. Three babies born in captivity each had only two segments per arm outside the disk and produced only one additional segment per arm in about a year. The slow growth rate of babies corresponds to the very slow regeneration rate of adults.

This species has numerous paedomorphisms and troglomorphisms that appear to be related to its unusual cave habitat with reduced salinity, little tidal movement, reduced predation, and abundant detritus enriched by diatoms, EPS, and bacteria. Three other cave endemic brittle stars have much fewer troglomorphisms probably because salinity in their caves was not reduced as much, and energy-rich detritus was not available. Many deep-sea brittle star species have numerous paedomorphisms probably because some areas of the deep sea provide energy-rich detritus, along with reduced currents and predation pressure. Conservation of energy is a driving force in the evolution of many traits found in nature including reduced mouthparts and arm ossicles in brittle stars; this conserves energy by not producing, maintaining, and transporting these adult structures. Although *A. stygobita* has been found only in Bernier Cave and Lighthouse Cave and only in low numbers, it does not seem to be endangered. Few people visit Bernier Cave because it is a challenge to hike to, and the administrators at the Gerace Research Centre limit visits to protect this unusual habitat and its rare brittle stars. This species probably exists in other subterranean habitats that humans have not been able to explore. Ideally, the DNA sequence of *A. stygobita* should be analyzed for phylogenetic studies, and eDNA might be used to determine if populations of *A. stygobita* occur in other caves in the region.

Acknowledgements

I thank the Bahamian government, the Gerace Research Centre on San Salvador Island, and Executive Director Troy Dexter for logistic support and making specimens available. Special thanks to John Winter for discovering and collecting the first cave brittle stars and sending them to me; Li Newton for her many hours of cutting trails and collecting specimens; other colleagues who helped collect specimens, especially

Mark Lewin, Patty Lewin, David Cunningham, Ben Crossley, Nick Callahan, Cliff Hart, Reeda Hart, Billy Stafford, Julie Moses, and Ramamurthi Kannan; Brenda Racke for assistance with NKU's scanning electron microscope; Paula Keene Pierce of Excalibur Pathology for preparing serial sections; Chris Pomory for his excellent work on our original 2011 paper and for helpful comments on this paper; Joan Herrera and Laura Wiggins for providing preserved specimens from collections of the Florida Fish and Wildlife; Gordon Hendler for providing preserved specimens from the Natural History Museum of Los Angeles County and for sharing his extensive knowledge on brittle stars; Richard Turner for help interpreting SEM images; Miriam Closer for carefully editing the manuscript; Academic editor Fabio Stoch and Subject editor Elizabeth Borda for their encouragement and guidance during the review process; Jill Yager, Francisco Solís-Marín, and an anonymous reviewer for their valuable suggestions that improved the manuscript; and my wife Rhonda for assisting with the manuscript and for her many years of patience during this long project.

Northern Kentucky University provided financial support for my associate Julie Moses.

References

- Baker AN (1979) Some Ophiuroidea from the Tasman Sea and adjacent waters. *New Zealand Journal of Zoology* 6: 21–51. <https://doi.org/10.1080/03014223.1979.10428345>
- Bishop RE, Humphreys WF, Cukrov N, Žic V, Boxshall GA, Cukrov M, Iliffe TM, Kršinić F, Moore WS, Pohlman JW, Sket B (2015) “Anchialine” redefined as a subterranean estuary in a crevicular or cavernous geologic setting. *Journal of Crustacean Biology* 35(4): 511–514. <https://doi.org/10.1163/1937240X-00002335>
- Bribiesca-Contreras G, Solís-Marín FA, Laguarda-Figueras A, Zaldivar-Riveron A (2013) Identification of echinoderms (Echinodermata) from an anchialine cave in Cozumel Island, Mexico, using DNA barcodes. *Molecular Ecology Resources* 13(6): 1137–1145. <https://doi.org/10.1111/1755-0998.12098>
- Bribiesca-Contreras G, Pineda-Enríquez T, Márques-Borrás F, Solís-Marín FA, Verbruggen H, Hugall AF, O'Hara T (2019) Dark offshoot: phylogenomic data sheds light on the evolutionary history of a new species of cave brittle star. *Molecular Phylogenetics and Evolution* 136: 151–163. <https://doi.org/10.1016/j.ympev.2019.04.014>
- Bruckner CG, Rehm C, Grossart H, Kroth PG (2011) Growth and release of extracellular organic compounds by benthic diatoms depend on interactions with bacteria. *Environmental Microbiology* 13(4): 1052–1063. <https://doi.org/10.1111/j.1462-2920.2010.02411.x>
- Byrne M (1991) Reproduction, development and population biology of the Caribbean ophiuroid *Ophionereis olivacea*, a protandric hermaphrodite that broods its young. *Marine Biology* 111(3): 387–399. <https://doi.org/10.1007/BF01319411>
- Carpenter JH (1981) *Bahalana geracei*, n. gen., n. sp., a troglobitic marine cirrolanid isopod from Lighthouse Cave, San Salvador Island, Bahamas. *Bijdragen tot de Dierkunde* 51(2): 259–267.
- Carpenter JH (2016) Observations on the biology and behavior of *Amphicutis stygobita*, a rare cave brittle star (Echinodermata: Ophiuroidea) from Bernier Cave, San Salvador Island,

- Bahamas. In: Erdman R, Morrison R (Eds) Proceedings of the 15th Symposium on the natural history of The Bahamas. June 2013. Gerace Research Centre, San Salvador.
- Carpenter JH (2021) Forty-year natural history study of *Bahalana geracei* Carpenter, 1981, an anchialine cave-dwelling isopod (Crustacea, Isopoda, Cirolanidae) from San Salvador Island, Bahamas: reproduction, growth, longevity, and population structure. *Subterranean Biology* 37: 105–156. <https://doi.org/10.3897/subtbiol.37.60653>
- Clark HL (1911) North Pacific ophiurans in the collection of the United States National Museum. *United States National Museum Bulletin* 75: 1–302.
- Clark HL (1917) Reports on the scientific results of the Albatross Expedition to the Tropical Pacific, 1899–1900 (Part 18). Reports on the scientific results of the Albatross Expedition to the Eastern Tropical Pacific, 1904–1905 (Part 30). Ophiuroidea. *Bulletin of the Museum of Comparative Zoology at Harvard* 61(12): 429–453.
- Clark MS, Dupont S, Rossetti H, Burns G, Thorndyke MC, Peck LS (2007) Delayed arm regeneration in the Antarctic brittle star *Ophionotus victoriae*. *Aquatic Biology* 1: 45–53. <https://doi.org/10.3354/ab00004>
- Clements LAJ, Fielman KT, Stancyk SE (1988) Regeneration by an amphiid brittlestar exposed to different concentrations of dissolved organic material. *Journal of Experimental Marine Biology and Ecology* 122: 47–61. [https://doi.org/10.1016/0022-0981\(88\)90211-0](https://doi.org/10.1016/0022-0981(88)90211-0)
- Culver DC (1982) *Cave Life: Evolution and Ecology*: Harvard University Press, Cambridge 189 pp. <https://doi.org/10.4159/harvard.9780674330214>
- Culver DC, Pippan T (2019) *The biology of caves and other subterranean habitats*. Oxford University Press, New York, 301 pp. <https://doi.org/10.1093/oso/9780198820765.001.0001>
- Donachy JE, Watanabe N (1986) Effects of salinity and calcium concentration on arm regeneration by *Ophiothrix angulata* (Echinodermata: Ophiuroidea). *Marine Biology* 91: 253–257. <https://doi.org/10.1007/BF00569441>
- Dutkiewics A, Müller RD, Hogg MA, Spence P (2016) Vigorous deep-sea currents cause global anomaly in sediment accumulation in the Southern Ocean. *Geology* 44(8): 663–666. <https://doi.org/10.1130/G38143.1>
- Emson RH (1984) Bone idle – A recipe for success? Proceedings of the Fifth International Echinoderm Conference / Galway, 25–30. <https://doi.org/10.1201/9781003079224-5>
- Falasco E, Ector L, Isaia M, Wetzel CE, Hoffmann L, Bona F (2014) Diatom flora in subterranean ecosystems: a review. *International Journal of Speleology* 43(3): 231–251. Tampa, FL (USA) ISSN 0392-6672. <https://doi.org/10.5038/1827-806X.43.3.1>
- Faugères J, Mulder T (2011) Contour currents and contourites. In: Hüneke H, Mulder T (Eds) *Developments in deep-sea sedimentology deep-sea sediments*. Amsterdam, Elsevier: 149–214. [https://doi.org/10.1016/500-70.4571\(11\)63003-3](https://doi.org/10.1016/500-70.4571(11)63003-3)
- Gage JD (1984) On the status of the deep-sea echinoids, *Echinosigra phiale* and *E. paradoxa*. *Journal of the Marine Biological Association of the United Kingdom* 64: 157–170. <https://doi.org/10.1017/S0025315400059701>
- Gage JD (1990) Skeletal growth markers in the deep-sea brittle stars *Ophiura ljungmani* and *Ophiomusium lymani*. *Marine Biology* 104: 427–435. <https://doi.org/10.1007/BF01314346>
- Gage JD (2003) Growth and production of *Ophiocten gracilis* (Ophiuroidea: Echinodermata) on the Scottish continental slope. *Marine Biology* 143: 85–97.

- Harper EM, Peck LS (2016) Latitudinal and depth gradients in marine predation pressure. *Global Ecology and Biogeography* 25(6): 670–678. <https://doi.org/10.1111/geb.12444>
- Hendler G (1975) Adaptational significance of the patterns of ophiuroid development. *American Zoologist* 15: 691–715. <https://doi.org/10.1093/icb/15.3.691>
- Hendler G (1991) Echinodermata: Ophiuroidea. In: Gies AC, Pearse JS, Pearse VB (Eds) *Reproduction of marine invertebrates*. Vol. VI. Echinoderms and Lophophorates. Pacific Grove, California: Boxwood Press, 355–511.
- Hendler G (2004) An echinoderm's eye view of photoreception and vision. In: Heinzelner T, Nebelsick JH (Eds) *Echinoderms Munchen: proceedings of the 11th international echinoderm conference*. AA Balkema Publishers, Leiden, 339–349. <https://doi.org/10.1201/9780203970881.ch56>
- Hendler G (2018) Armed to the teeth: a new paradigm for the buccal skeleton of brittle stars (Echinodermata: Ophiuroidea). *Contributions in science* 526: 189–311. <https://doi.org/10.5962/p.324539>
- Hendler G, Byrne M (1987) Fine structure of the dorsal arm plate of *Ophiocoma wendtii*: evidence for a photoreceptor system. *Zoomorphology* 107: 261–272. <https://doi.org/10.1007/BF00312172>
- Hendler G, Miller JE (1991) Swimming ophiuroids – real and imagined. *Biology of Echinodermata* (1st edn.), 179–190. <https://doi.org/10.1201/9781003077565-41>
- Hendler G, Miller JE, Pawson DL, Kier PM (1995) *Sea stars, sea urchins, and allies*. Echinodermata of Florida and the Caribbean. Smithsonian Institution Press, Washington DC, 390 pp.
- Holthuis LB (1973) Caridean shrimps found in land-locked saltwater pools at four Indo-West Pacific localities (Sinai Peninsula, Funafuti Atoll, Maui and Hawaii Islands), with the description of one new genus and four new species. *Zoologische Verhandelingen* 128: 1–48 [pls. 1–7].
- Hoskins DL, Stancyk SE, Decho AW (2003) Utilization of algal and bacterial extracellular polymeric secretions (EPS) by the deposit-feeding brittlestar *Amphipholis gracillima* (Echinodermata). *Marine Ecology Progress Series* 247: 93–101. <https://doi.org/10.3354/meps247093>
- Irimura S, Fujita T (2003) Interspecific variation of vertebral ossicle morphology in the Ophiuroidea. In: Feral JP, David B (Eds) *Echinoderm Research 2001: Proceedings of the 6th European Conference on Echinoderm Research, Banyuls-sur-me, 3–7 September 2001*, Lisse: Netherlands: AA Balkema, 161–167.
- LaFace KMP (2019) Assessing the impact of climate-change related lower pH and lower salinity conditions on the physiology and behavior of a luminous marine invertebrate. Master of Science thesis, University of California San Diego. 86 pp.
- Langecker TG, Longley G (1993) Morphological adaptations of the Texas blind catfishes *Trogloglanis pattersoni* and *Satan eurystomus* (Siluriformes: Ictaluridae) to their underground environment. *Copeia* 1993(4): 976–686. <https://doi.org/10.2307/1447075>
- LeClair EE (1996) Arm joint articulations in the ophiuran brittlestars (Echinodermata: Ophiuroidea): a morphometric analysis of ontogenetic, serial, and interspecific variation. *Journal Zoological Society of London* 240: 245–275. <https://doi.org/10.1111/j.1469-7998.1996.th05283.x>
- Márquez-Borrás F, Solís-Marín FA, Mejía-Ortiz LM (2020) Troglomorphism in the brittle star *Ophionereis commutabilis* Bribiesca-Contreras et al., 2019 (Echinodermata,

- Ophiuroidea, Ophionereididae). *Subterranean Biology* 33: 87–108. <https://doi.org/10.3897/subtbiol.33.48721>
- O'Hara TD, Hugall AF, Thuy B, Stöhr S., Martynov AV (2017) Restructuring higher taxonomy using broad-scale phylogenomics: The living Ophiuroidea. *Molecular Phylogenetics and Evolution* 107: 415–430. <https://doi.org/10.1016/j.ympev.2016.12.006>
- O'Hara TD, Stöhr S, Hugall AF, Thuy B, Martynov A (2018) Morphological diagnoses of higher taxa in Ophiuroidea (Echinodermata) in support of a new classification. *European Journal of Taxonomy* 416: 1–35. <https://doi.org/10.5852/ejt.2018.416>
- Okanishi M, Fujita Y (2018) First finding of anchialine and submarine cave dwelling brittle stars from the Pacific Ocean, with descriptions of new species of *Ophiolepis* and *Ophiozonella* (Echinodermata: Ophiuroidea: Amphilepidida). *Zootaxa* 4377(1): 001–020. <https://doi.org/10.11646/zootaxa.4377.1.1>
- Okanishi M, Fujita Y (2019) A comprehensive taxonomic list of brittle stars (Echinodermata: Ophiuroidea) from submarine caves of the Ryukyu Islands, southwestern Japan, with a description of a rare species, *Dougaloplus echinatus* (Amphiuridae). *Zootaxa* 4571(1): 73–98. <https://doi.org/10.11646/zootaxa.4571.1.5>
- Okanishi M, Oba Y, Fujita Y (2019) Brittle stars from a submarine cave of Christmas Island, northwestern Australia, with description of a new bioluminescent species *Ophiopsila xmas-illuminaans* (Echinodermata: Ophiuroidea) and notes on its behaviour. *Raffles Bulletin of Zoology* 67: 421–439. <https://doi.org/10.26107/RBZ-2019-0034>
- Pomory CM (2007) Key to the common shallow water brittle stars (Echinodermata: Ophiuroidea) of the Gulf of Mexico and Caribbean Sea. *Caribbean Journal of Science Special Publication*, 10, 42 pp. <http://caribjsci.org/epub10.pdf>
- Pomory CM, Carpenter JH, Winter JH (2011) *Amphicutis stygobita*, a new genus and new species of brittle star (Echinodermata: Ophiuroidea: Ophiurida: Amphilepididae) found in Bernier Cave, an anchialine cave on San Salvador Island, Bahamas. *Zootaxa* 3133: 50–68. <https://doi.org/10.11646/zootaxa.3133.1.3>
- Ramirez-Llodra E, Brandt A, Danovaro R, De Mol B, Escobar E, German CR, Levin LA, Martinez Arbizu P, Menot L, Buhl-Mortensen P, Narayanaswamy BE, Smith CR, Tittensor DP, Tyler PA, Vanreusel A, Vecchione M (2010) Deep, diverse and definitely different: unique attributes of the world's largest ecosystem. *Biogeosciences* 7: 2851–2899. <https://doi.org/10.5194/bg-7-2851-2010>
- Ravelo AM, Konar B, Bluhm B, Iken K (2017) Growth and reproduction of the brittle stars *Ophiura sarsii* and *Ophiocten sericeum* (Echinodermata: Ophiuroidea). *Continental Shelf Research* 139: 9–20. <https://doi.org/10.1016/j.csr.2017.03.011>
- Recknagel H, Trontelj P (2022) From cave dragons to genomics: advancements in the study of subterranean tetrapods. *Bioscience* 72(3): 254–266. <https://doi.org/10.1093/biosci/biab117>
- Roldán M, Hernández-Mariné M (2009) Exploring the secrets of the three-dimensional architecture of phototrophic biofilms in caves. *International Journal of Speleology* 38: 41–53. <https://doi.org/10.5038/1827-806X.38.1.5>
- Romero A (2009) *Cave biology, life in darkness*. Cambridge University Press, 291 pp. <https://doi.org/10.1017/CBO9780511596841>

- Ruck E, Nakov T, Alverson AJ, Theriot EC (2016a) Phylogeny, ecology, morphological evolution, and reclassification of the diatom orders Surirellales and Rhopalodiales. *Molecular Phylogenetics and Evolution* 103: 155–171. <https://doi.org/10.1016/j.ympev.2016.07.023>
- Ruck EC, Nakov T, Alverson AJ, Theriot EC (2016b) Nomenclatural transfers associated with the phylogenetic reclassification of the Surirellales and Rhopalodiales. *Notulae Algarum* 10: 1–4.
- Shnyukova EI, Zolotariova EK (2017) Ecological role of exopolysaccharides of Bacillariophyta: A review. *International Journal on Algae* 19: 5–24. <https://doi.org/10.1615/InterJAlgae.v19.i1.10>
- Sköld M, Gunnarsson SG (1996) Somatic and germinal growth of the infaunal brittle stars *Amphiura filiformis* and *A. chiajei* in response to organic enrichment. *Marine Ecology Progress Series* 142: 203–214. <https://doi.org/10.3354/meps142203>
- Steinitz-Kannan M, Carpenter JH, Nienaber MA (2025) A biofilm micro-community dominated by the diatom *Campylodiscus neofastuosus* (Surirellales) binds detritus used as food source for rare brittle stars endemic to two Bahamian caves. *Subterranean Biology* 51: 197–212. <https://doi.org/10.3897/subtbiol.51.141192>
- Stock JH, Illife TM, Williams D (1986) The concept “anchialine” reconsidered. *Stygologia* 2: 90–92.
- Stöhr S (2005) Who’s who among baby brittle stars (Echinodermata: Ophiuroidea): Postmetamorphic development of some North Atlantic forms. *Zoological Society of the Linnean Society* 143: 543–576. <https://doi.org/10.1111/j.1096-3642.2005.00155.x>
- Stöhr S, Martynov A (2016) Paedomorphosis as an evolutionary driving force: insights from deep-sea brittle stars. *PLoS ONE* 11(11): e0164562. <https://doi.org/10.1371/journal.pone.0164562>
- Stöhr S, O’Hara TD, Thuy B (2012) Global diversity of brittle stars (Echinodermata: Ophiuroidea). *PLoS ONE* 7(3): e31940. <https://doi.org/10.1371/journal.pone.0031940>
- Stöhr S, O’Hara TD, Thuy B (Eds) (2024) World Ophiuroidea Database. *Amphilepis platytata* H.L. Clark, 1911. World Register of Marine Species. <https://www.marinespecies.org/aphia.php?p=taxdetails&id=242633> [2024-03-27]
- Sumida YG, Tyler PA (1998) Postlarval development in shallow and deep-sea ophiuroids (Echinodermata: Ophiuroidea) of the NE Atlantic Ocean. *Zoological Society of the Linnean Society* 124: 267–300. <https://doi.org/10.1111/j.1096-3642.1998.tb00577.x>
- Sumner-Rooney L, Rahman IA, Sigwart JD, Ullrich-Lüter E (2018) Whole-body photoreceptor networks are independent of ‘lenses’ in brittle stars. *Proceedings Royal Society B* 285: 20172590. <https://doi.org/10.1098/rspb.2017.2590>
- Thornton D (2002) Diatom aggregation in the sea: mechanisms and ecological implications. *European Journal of Phycology* 37: 149–161. <https://doi.org/10.1017/S0967026202003657>
- Turner RL, Meyer CE (1980) Salinity tolerance of the brackish-water echinoderm *Ophiophragmus filigraneus* (Ophiuroidea). *Marine Ecology Progress Series* 2: 249–256. <https://doi.org/10.3354/meps002249>
- Tyler PA (1988) Seasonality in the deep-sea. *Marine Biology* 26: 227–258.
- Webb PM, Tyler PA (1985) Post-larval development of the common north-west European brittle stars *Ophiura ophiura*, *O. albida* and *Acrocnida brachiata* (Echinodermata: Ophiuroidea). *Marine Biology* 89: 281–292. <https://doi.org/10.1007/BF00393662>

A biofilm micro-community dominated by the diatom *Campylodiscus neofastuosus* (Suriellales) binds detritus used as food source for rare brittle stars endemic to two Bahamian caves

Miriam Steinitz-Kannan¹, Jerry H. Carpenter¹, Mark A. Nienaber¹

¹ Department of Biological Sciences, Northern Kentucky University, Highland Heights, KY 41099, USA

Corresponding author: Miriam Steinitz-Kannan (Kannan@nku.edu)

Academic editor: Fabio Stoch | Received 6 November 2024 | Accepted 17 February 2025 | Published 16 May 2025

<https://zoobank.org/4DC92A8B-27AD-41CD-8A88-86D6B00CD104>

Citation: Steinitz-Kannan M, Carpenter JH, Nienaber MA (2025) A biofilm micro-community dominated by the diatom *Campylodiscus neofastuosus* (Suriellales) binds detritus used as food source for rare brittle stars endemic to two Bahamian caves. *Subterranean Biology* 51: 197–212. <https://doi.org/10.3897/subtbiol.51.141192>

Abstract

The rare endemic brittle star *Amphicutis stygobita* (Echinodermata: Ophiuroidea: Amphilepididae) is found in Bernier Cave on San Salvador Island in The Bahamas. We report here on the diatom-rich detritus on which the brittle star feeds. The detritus contains a microbial biofilm dominated by a large diatom *Campylodiscus neofastuosus* Ruck & Nakov that thrives in the cave's brackish water. The biofilm diatoms and bacteria produce sticky, carbohydrate-rich, extracellular polymeric substances (EPS) that add to the detritus' nutritional value and help give the detritus a consistency for *A. stygobita* to pull it into its mouth. Of particular interest is that *Campylodiscus neofastuosus* has distinct cell wall features that make efficient use of the limited light in the cave. It appears these morphological adaptations might focus light onto the chloroplasts increasing light capture. Furthermore, large, dark, and highly lobed chloroplasts serve as an additional low-light adaptation. This is a rare instance where efficient photosynthetic activity by diatoms produces a complex biofilm that feeds an endemic cave species population.

Keywords

Amphicutis, anchialine, Bernier Cave, diatom adaptations for low light, epipellic diatoms, EPS, extracellular polymeric substances, Ophiuroidea

Introduction

Bernier Cave on San Salvador Island in the Bahamas (24°05'37"N, 74°27'15"W) is the type locality for the rare cave brittle star, *Amphicutis stygobita*, described by Pomory, Carpenter and Winter (2011). This was the world's first known cave brittle star and is only found in Bernier Cave and in nearby Lighthouse Cave (Carpenter 2025). It is much more abundant in Bernier Cave; to our knowledge, only two specimens have ever been found in Lighthouse Cave. Although the brittle star population appears to be small, individuals of *A. stygobita* are difficult to find because their small disks (3–4 mm diameter) are filled with brown detritus. Therefore, their populations could be much larger than they seem, as they are camouflaged by the surrounding brown detritus.

In the laboratory *A. stygobita* did not accept food normally eaten by brittle stars but readily consumed detritus collected from the cave that contained diatoms (Carpenter 2016; Carpenter 2025). In 2013 our examination of the diatoms in cave microbial mats (Figs 1, 2D, E) and detritus showed the dominant species to be *Campylodiscus neofastuosus* Ruck & Nakov (Ruck et al. 2016a, 2016b). This species thrives in the cave's brackish water (salinity 14–28 ppt). We collected and studied the organisms in the cave detritus to be used as a food source in the laboratory for the brittle stars. We believe that the main reason the brittle star population does well in this cave is because of the diatom rich detritus it feeds on.

Detritus and epilithic biofilms have been recognized as important energy sources for cave invertebrates (Simon et al. 2003). However, because cave ecosystems are normally light-limited, these are nutritionally poor food sources. This results in low population numbers and slow growth rates of the organisms they support. A cave with a light-filled entrance allowing substantial photosynthesis should be able to support greater biomass including diatoms.

Phototrophic biofilms containing diatoms are not uncommon in caves. They also consist of filamentous and coccoid cyanobacteria, chlorophytes, and other Protista, which are all held together by the extracellular polymeric substances (EPS) they produce (Roldán and Hernández-Mariné 2009). Such biofilms have been studied in caves with artificial lights visited by tourists, where they are referred to as "lampenflora" (Popović et al. 2023). The diatom composition of phototrophic biofilms is reviewed in Falasco et al. 2014 who list 363 species belonging to 82 genera, most of them cosmopolitan in distribution and usually aerophilic. Most recently Winsborough and Sudbury (2024) described seventy diatom taxa from Hall's Cave, a limestone cave in central Texas, USA. Both Falasco et al. (2014) and Winsborough and Sudbury (2024) found mostly very small freshwater species that are highly resistant to desiccation and tolerate low levels of nutrients and high conductivity. The most common genera were *Hantzschia*, *Diademesmia*, *Orthoseira*, *Luticola*, and *Pinnularia* (Falasco et al. 2014) and in Hall's Cave *Nitzschia palmida* (Winsborough and Sudbury 2024). This diatom composition, except for a few genera, is very different from what we found in the detritus of Bernier Cave. There, the dominant diatoms are large *Campylodiscus neofastuosus*. This species is not mentioned in Falasco et al. (2014) or in Winsborough and Sudbury (2024).

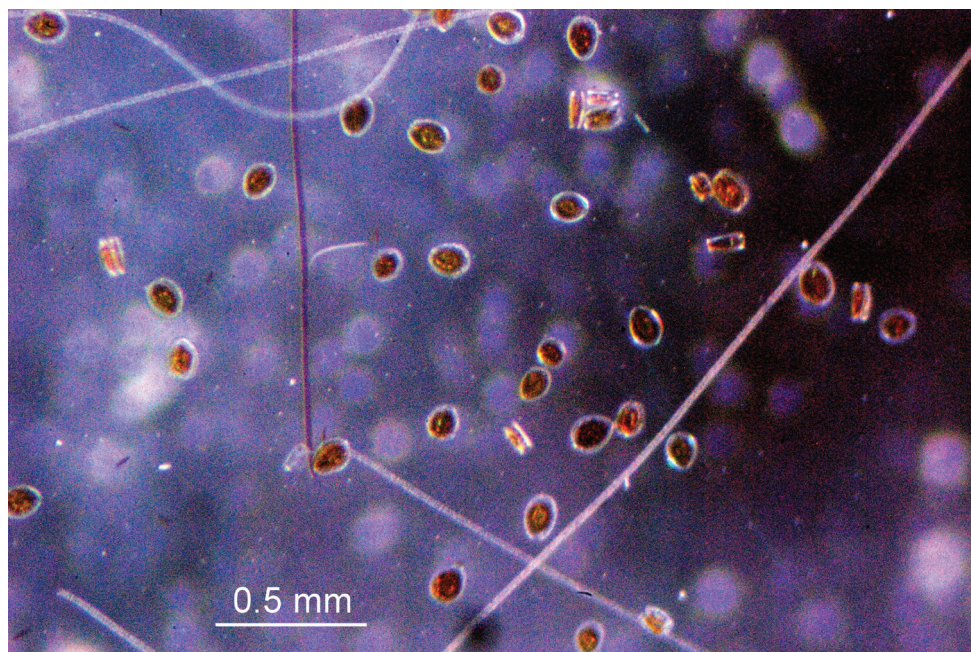


Figure 1. Dissecting microscope view (40X) of microbial mat from entrance room of cave after 9 hours in black film cannister, showing diatoms identified as *Campylodiscus neofastuosus* (from Carpenter 2025).

It is usually found in brackish water and apparently has never been reported from caves. This paper describes this population, its uncommon adaptations to thrive in the low light of the cave, and why it can provide a rich food source for the endemic brittle star.

Materials and methods

Study site

The location of Bernier Cave is described in the companion paper in this issue (Carpenter 2025). One of the most important features of Bernier Cave is that the ceiling entrance is large and directly above or near the water (Fig. 2A). This allows considerable detritus to enter the aquatic ecosystem. It also provides an unusual amount of light to reach the walls of the entrance room to create abundant and colorful growth of algae (Fig. 2B). Water in the cave is brackish with salinities of 14–28 ppt (Carpenter 2025). Tidal fluctuations (changes in water depth between low and high tide) are relatively slight compared to Lighthouse Cave and the ocean water surrounding the island (Fig. 2C). This results in very slow movement of water during tidal flows and allows sizeable accumulations of detritus, some of which is distributed throughout the cave with each tidal flow. The tide line can be seen as a distinctive brown area extending a few centimeters above the water (Fig. 2B, C); we observed that this brown line is a result of prolific

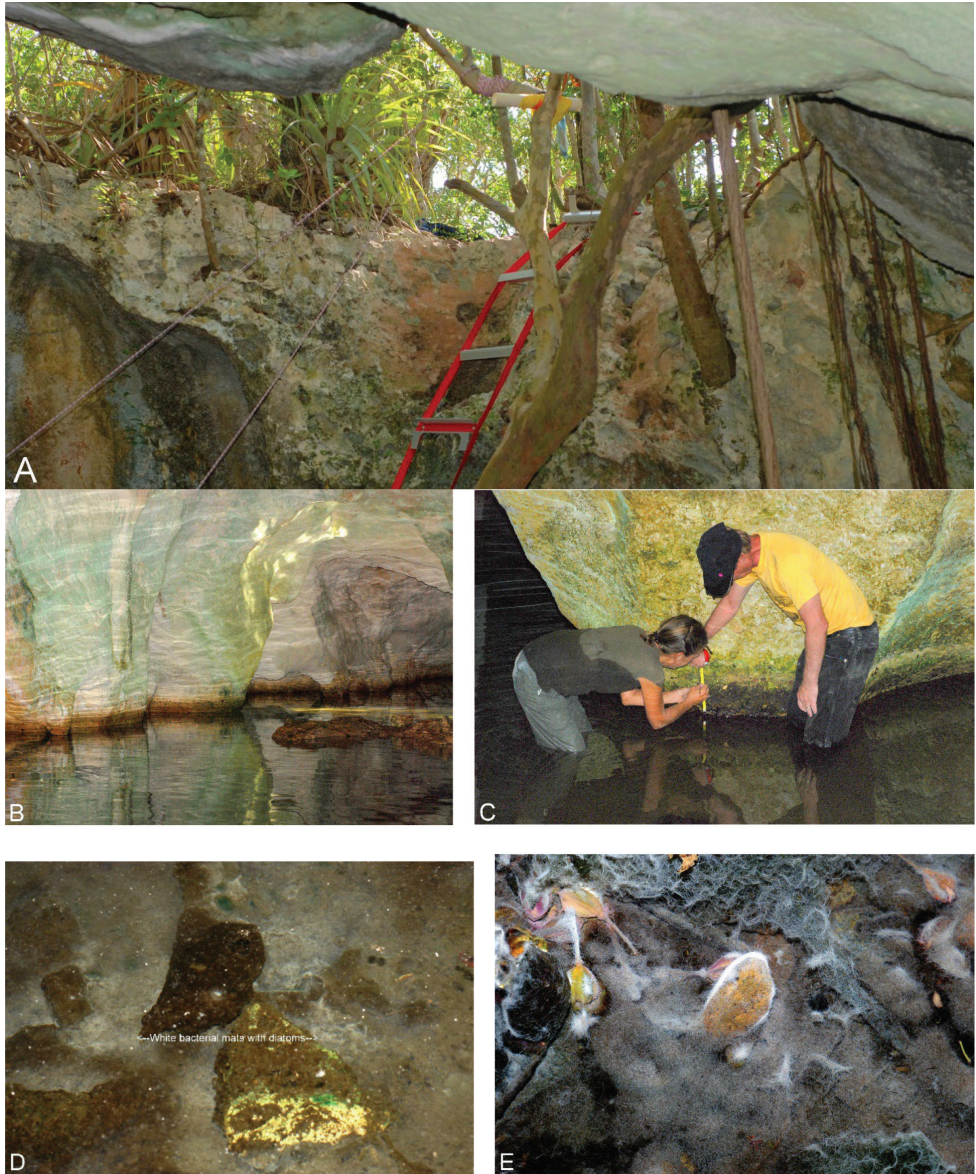


Figure 2. Study site: Bernier Cave, San Salvador Island in The Bahamas (from Carpenter 2025) **A** ceiling entrance **B** algae-covered wall below ceiling entrance **C** tide line composed mostly of *Campylodiscus neofastuosus* in entrance room **D** white bacterial mats in entrance room containing diatoms (brown areas) **E** white bacterial growths on detritus in entrance room.

growth of the diatom *Campylodiscus neofastuosus* and other microbes. The water in the entrance room has a diverse microbial community growing on the walls, the detritus, and in large white mats (Fig. 2D, E). The white mats consisted of filamentous bacteria (mainly *Beggiatoa* and actinomycetes) growing on the organic matter produced, at least in part, by the diatoms seen in Fig. 1.

Collection of detritus with diatoms

In 2013 JHC collected and examined white bacterial mats in Bernier Cave that contained numerous large diatoms (Fig. 1). Samples were given to MSK for identification as described below. Additional collections were made in 2014, 2015, 2016, and 2018 with cave wall scrapings placed in microcentrifuge tubes (Fig. 3B), which were then kept in black film cannisters for later examination and experimentation. In 2015 MSK collected plankton samples (Fig. 3A) and fresh wall scrapings for microscopic examination at the Gerace Research Centre located about 5 km from the cave. Some samples were preserved in Lugol's iodine; these preserved samples and fresh samples (for food for the brittle stars) were brought back to Northern Kentucky University (NKU) for continued study.

Observations of detritus microbial community

All three authors examined detritus samples for composition of diatoms, other microbes, and invertebrates. Detritus was fed to cave brittle stars approximately weekly by JHC (Carpenter 2025). However, adults regenerated very slowly (Carpenter 2016), and babies born in 2018 grew very slowly (Carpenter 2025), possibly because the cave detritus was losing some of its nutritional value as the diatoms in it died. Sköld and Gunnarsson (1996) described the positive effect of diatom supplementation on feeding brittle stars. Therefore, to improve the nutritional quality of the detritus, we experimented with culturing it under different light conditions to try to stimulate the growth of diatoms.

One ml of a well-mixed suspension of cave detritus was placed in standard 6-well tissue culture plates containing 9 ml artificial sea water with salinity adjusted by dilution with distilled water to 30 ppt and 35 ppt. Salinity was measured with a refractometer. Duplicates were made for each plate and identical set ups were kept in (1) an environmental chamber with fluorescent light at 28 °C, (2) a bench next to a lab window at room temperature, and (3) inside a box in the dark at the same room temperature.

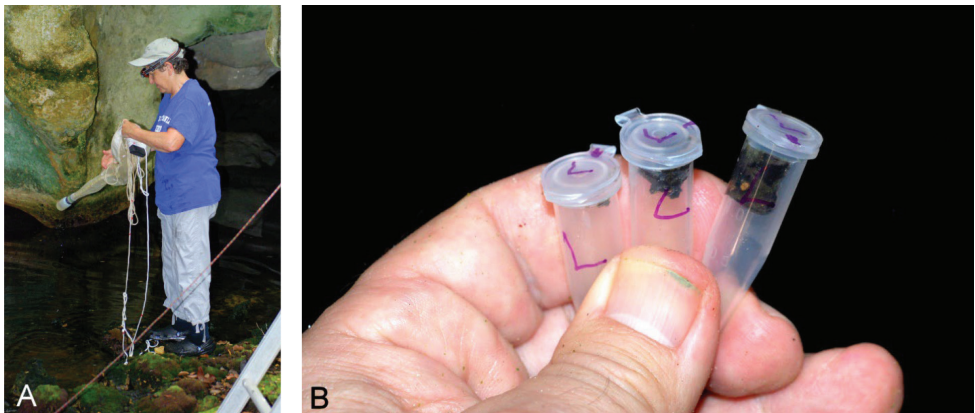


Figure 3. Collection methods **A** MSK with plankton net in Bernier Cave entrance room **B** centrifuge tubes with wall scrapings from entrance room.

Care was taken to ensure *Campylodiscus* frustules were present in each well at the start of the experiment. Plates were examined using a Nikon inverted microscope daily for 6 days noting diversity of species, changes to the initial community, and changes in *Campylodiscus*' chloroplast morphology.

Diatom identification, quantification, and description

For identification purposes, diatoms were examined with an Olympus dissecting microscope, a Nikon inverted microscope, and a Motic compound microscope equipped with a digital camera. SEM images were taken with NKU's FEI Quanta 200 scanning electron microscope. Literature available at the NKU Diatom Herbarium was used to identify the diatoms in our samples. We initially identified the dominant species as *Surirella fastuosa* (Goldman et al. 1990). Regional floras including "Diatoms of Cuba" (Foged 1984) mention this species as commonly found in benthic habitats of brackish ecosystems in the Caribbean. In 2016 *Surirella fastuosa* was renamed *Campylodiscus neofastuosus* Ruck & Nakov (Ruck et al. 2016a, 2016b). Elizabeth Ruck confirmed this identification after examining our cave specimens. Although we did not collect quantitative samples of the detritus, microscopic examination of a well-mixed sample of detritus collected with a plankton net was used to estimate biomass and percentage composition of diatoms.

Results

Detritus as brittle star food

Detritus samples from Bernier Cave were used successfully as food for the brittle stars. Before eating, adult *A. stygobita* usually had central disks that were pale yellow (Fig. 4A) and clear enough to see internal structures such as gonads (Fig. 4B, C). When a few drops of fresh detritus were added to their culture jars, they often started pulling it into the mouth within minutes (Fig. 4B, C) and their disks turned brown (Fig. 4D).

In July 2018 four of the five live adult *A. stygobita* that survived the 6–14 July collecting trip were each observed to contain five to seven broods or gonads inside their disks. On 17 July, one adult released a baby, another was born 31 July, and a third appeared on 6 August. All three babies started consuming detritus when only a few days old (Carpenter 2025). Detritus continued to be their only food source for as long as they lived, which was up to 14.5 months. This feeding behavior drove us to investigate the detritus composition and diversity and to study the chloroplasts and EPS of *Campylodiscus*.

Detritus composition and diversity

Examination of a well-mixed 5 ml sample of detritus under a dissecting microscope at 40X magnification revealed that the detritus micro-community was dominated by *C. neofastuosus*. Observations with a compound microscope at 400X and 1000X

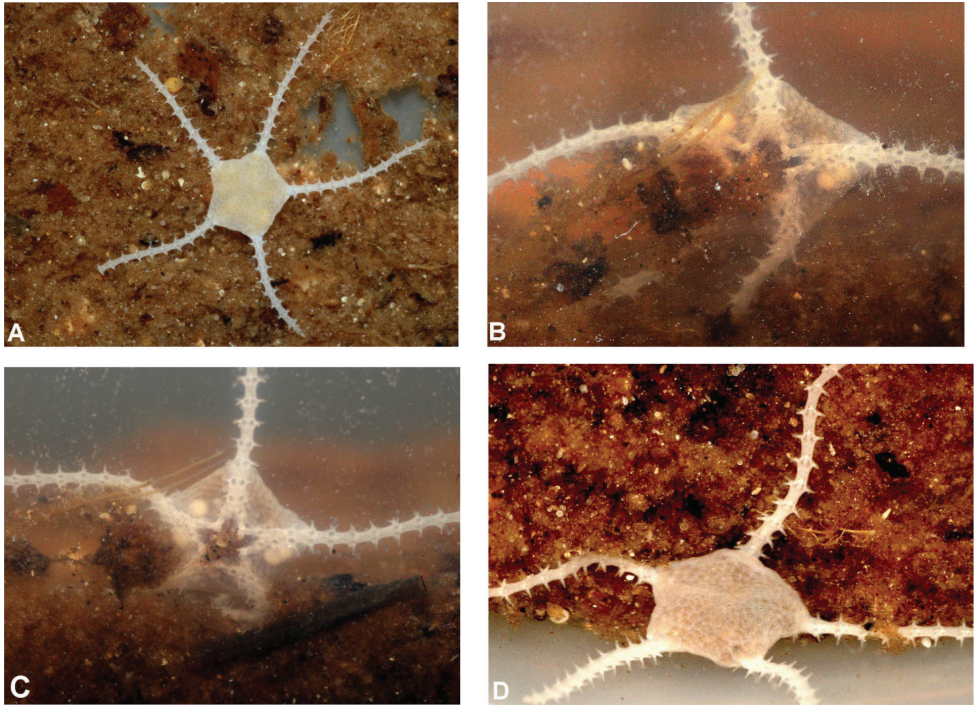


Figure 4. *Amphicutis stygobita* feeding (from Carpenter 2025) **A** light-colored adult with 4mm disk diameter before feeding **B** same animal on side of jar feeding on detritus streaming into mouth **C** same animal, 90 sec. later, with detritus in stomach **D** same animal with brown disk 25 min. after eating detritus.

magnification revealed that other, smaller diatom species were more abundant in the sample, comprising about 70% of all the diatoms. They included the genera *Amphora*, *Achnanthes*, *Achnantheidium*, *Orthoseira*, and *Staurosira* (Fig. 5A–D). In addition to diatoms there were filamentous Chlorophyta, nematodes, ostracods, harpacticoid copepods, ciliates, dinoflagellates, foraminifera, cyanobacteria, and other bacteria. The white mats in Fig. 2D, E consisted mainly of *Beggiatoa*. These are large filamentous sulfur bacteria commonly found in caves (Macalady et al. 2008). However, *C. neofastuosus*, was also abundantly associated with these mats.

Observations of chloroplast morphology under different light conditions

We observed changes in *Campylodiscus* chloroplast shape over the 6-day culture of detritus under various light conditions. In the plates placed in total darkness the chloroplasts filled almost the entire cell. This is just like in the diatoms in the fresh collection from the cave after being kept in black film cannisters for 9 hours (Figs 1, 6A). In the detritus community, kept at low light (close to a window), each chloroplast appeared to be lobed (Fig. 6B). The chloroplasts appear to follow the costae and concentrate pigment in the lens-shaped interior area (Fig. 6C). In the high light treatment group

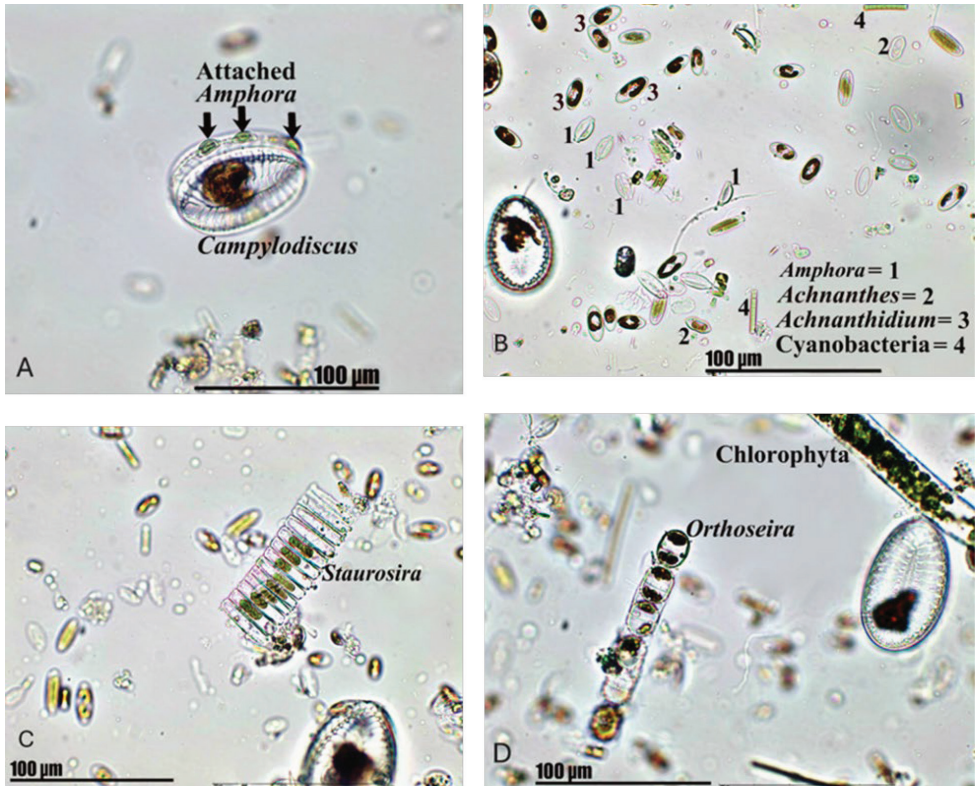


Figure 5. Algae in the detritus collected with a plankton net in Bernier Cave; all images at 400X but identifications were made at 1000X **A** *Campylodiscus neofastuosus* with *Amphora* attached to the girdle band **B** *Amphora*, *Achnanthes*, *Achnanthidium* and Cyanobacteria. Note relative abundance of the very small diatoms **C** *Staurosira* colony **D** *Orthoseira* colony.

(fluorescent light in an environmental chamber) the chloroplasts became compacted around the nucleus (Fig. 6D). No pure cultures of *C. neofastuosus* were attempted. No cultured detritus in this experiment was fed to the brittle stars.

Discussion

Cave environment

As described above, the brown detritus in Bernier Cave that successfully fed *A. stygobita* had an abundance of *C. neofastuosus*. The brown coloration was due partly to the diatom chloroplasts. Samples collected by scraping the brown coloration of the cave walls at the water line (Fig. 3B) were also dominated by this diatom. Several adaptations make *C. neofastuosus* ideal for growing in this specialized niche. There is light in the entrance room of the cave, but it is relatively low light, so we believe that it is the efficient light capturing morphology and chloroplast coloration and shape that make

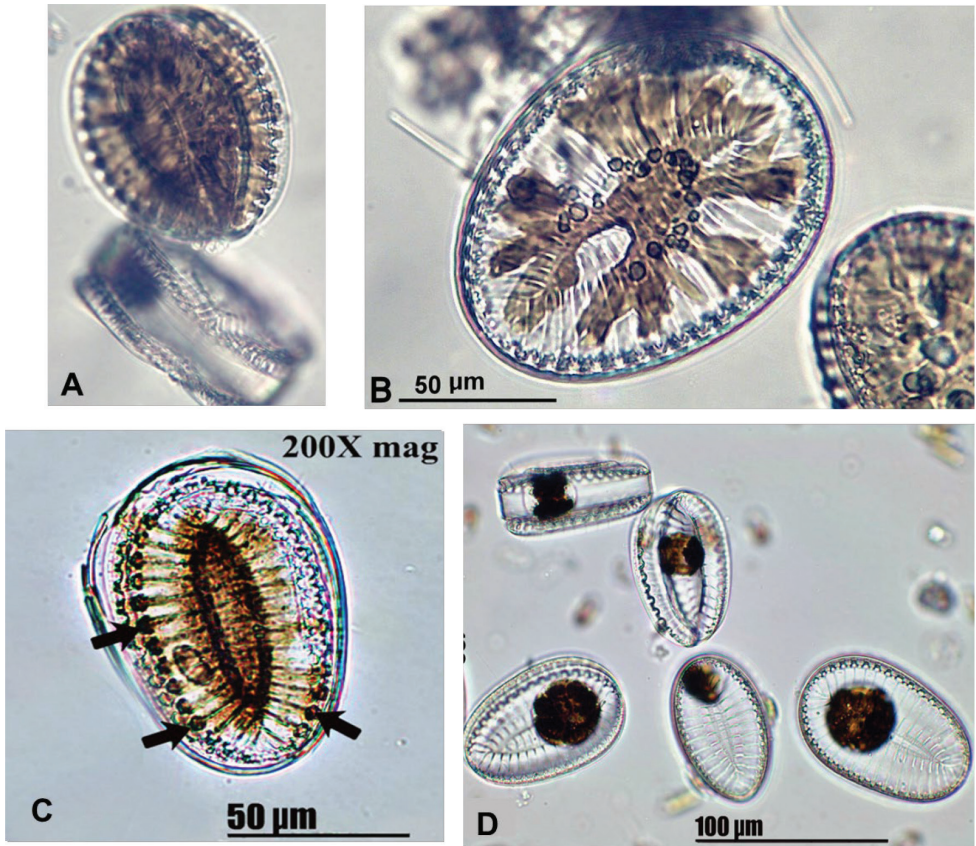


Figure 6. Light micrographs of *Campylodiscus neofastuosus* (100X mag. except for **C**) **A** dark brown chloroplast covering the interior of cell kept in total darkness **B** lobed chloroplast of cells kept in low light **C** chloroplast follows the costae and concentrates in the lens-shaped interior area **D** compact rounded chloroplasts in cells grown in bright light.

the population of *C. neofastuosus* dominate the detritus community found in Bernier Cave. Many diatoms thrive in benthic habitats where light is limited, including species in the genera *Campylodiscus* and *Surirella*. These genera are usually epipelagic diatoms, which are diatoms that live attached to sediment particles or at the interface of water and sediment; thus, epipelagic diatoms have evolved adaptations to efficiently capture light in such environments (Round et al. 1990). We discuss below specific adaptations that *C. neofastuosus* has for the low-light environment of Bernier Cave.

Chloroplast morphology

The pigments in diatom chloroplasts, particularly the dark brown fucoxanthins, are most efficient at harvesting light and transferring excitation energy to chlorophyll a (Büchel 2020). *Campylodiscus* examined in the field and in preserved samples collected from dimly lit areas of the cave show a lobed very dark chloroplast cover-

ing almost the entire cell (Fig. 6A). Such a chloroplast efficiently collects light. It is composed of mostly fucoxanthin-chlorophyll *a/c* binding protein constituting the light harvesting complex that transfers photons to chlorophyll *a*, close to the center of the cell (Scarsini et al. 2019; Büchel 2020). When the detritus was kept close to a window or under a fluorescent light in an environmental chamber the shape of the chloroplast changed. Near the window at low light chloroplasts appeared lobed (Fig. 6B). Fig. 6C shows the chloroplast following the costae that may act as tunnels shuttling photons to the lens-shaped interior area to maximize photosynthesis. With more light the chloroplast became rounder and less lobed and centered around the nucleus, presumably protecting the DNA from UV (Fig. 6D). Such motile or shape-shifting chloroplasts in response to light are common features in diatoms (Mann 1996). Based on chloroplast morphology and cell architecture, *C. neofastuosus* is remarkably adapted to grow in the conditions of Bernier Cave.

Frustule architecture

A distinctive feature of diatoms is the silicon cell wall or frustule. The intricate architecture of the frustule has not only made diatoms famous for their beauty, but its function has been suggested as providing mechanical protection from predators (Hamm et al. 2003), and most importantly providing a device of efficient light capture (for examples see Goessling et al. 2018, 2021; Ghobara et al. 2019; Svetlana et al. 2022). The optical properties of the frustule have inspired their use in nanotechnology and more specifically in applications in material sciences to produce photonic materials and devices (see for example De Stefano et al. 2007). It is therefore not surprising that a diatom species with remarkable adaptive morphology for more efficient light capture is found in the low light environmental niche of Bernier Cave.

The genus *Campylodiscus* is characterized by valves that are large (76–136 μm long), with the apical axis (Fig. 7A) just slightly longer than the transapical axis. The frustule is usually saddle-shaped, with an elliptical area in the center (Spaulding and Edlund 2009). *Surirella* valves are usually heteropolar, with one rounded end and one pointed end (Spaulding and Edlund 2010). The shape of *C. neofastuosus* as described by Ruck et al. (2016a) and in our collections from Bernier Cave is intermediate between these two forms. Rather than being saddle shaped, it is concave and only slightly heteropolar (Fig. 7A, B). It is shaped like a plano-concave lens consisting of one flat and one inward curved surface (Fig. 7B). This type of lens is ideal for projecting light and expanding the focal length of an optical system (Hradaynath and Singh 2015). The concavity and morphology of the frustule acts as a lens to concentrate the light and focus it onto the lens-shaped central area. The costae (Figs 7A, 8) extend from the margins to the apical axis (Fig. 7A). This diatom has a canal raphe (Figs 7A, 8), well known to enhance motility, allowing the diatom to position itself at an angle best for light capture (Ruck and Theriot 2011). It is also through this canal raphe that the diatom EPS are secreted (Poulsen et al. 2022).

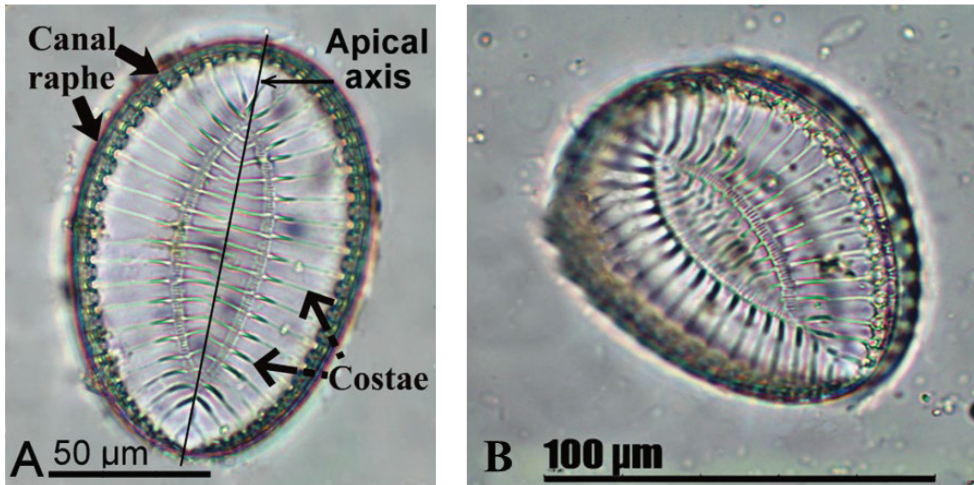


Figure 7. Light micrographs of *Campylodiscus neofastuosus* showing morphology of the valves, including lens-shaped central area **A** shows apical axis in relation to the canal raphe and costae **B** shows concavity of frustule.

Extracellular polymeric substances layer or phycosphere of *C. neofastuosus*

The detritus in Bernier cave is bound by a multi-species microbial biofilm consisting of EPS. Diatom-produced EPS are rich in polysaccharides, monosaccharides and proteins (Zhang et al. 2008). They also contain diatom oils including Omega 3 fatty acids (Oliver et al. 2020). The importance of diatom-produced EPS was not immediately apparent to us when we collected detritus from the cave. However, a recently published book chapter (Underwood 2024) made it clear that the role of EPS as a food source for the cave brittle star should not be ignored. It also called attention to the large amount of literature available on diatom EPS and the need to further study the EPS in Bernier cave.

The EPS layer surrounding diatom cells is known as the diatom phycosphere. The phycosphere is key to symbiotic exchanges where diatom secretions attract a variety of heterotrophic bacteria. These bacteria supply diatoms with nutrients and cofactors essential for their survival. One example is vitamin B12 which diatoms cannot make on their own (Bruckner et al. 2008; Helliwell et al. 2022; Perera et al. 2022). The EPS contributes to the dissolved organic matter (DOM) and particulate organic matter (POM) that are integral parts of food webs in oligotrophic environments (Bhaskar and Bhosle 2006). Our examination of the diatom-rich EPS in the cave detritus revealed a complex microbial community containing, in addition to the diatoms, a diversity of bacteria, protozoans and nematodes. This detritus is likely to be a high-quality food source for *A. stygobita*, just like the energy-rich phycodetritus is for brittle stars in the deep-sea (Ramirez-Llodra et al. 2010).

Abyssal communities feed on diatom-rich biofilm aggregates, called marine snow, that transport nutrients from surface blooms and from resuspension of benthic biofilms (Thornton, 2002). The diatom EPS contributes the stickiness responsible for diatom adhesion to surfaces and to diatom motility (Poulsen et al. 2022), and in doing so, also agglutinates

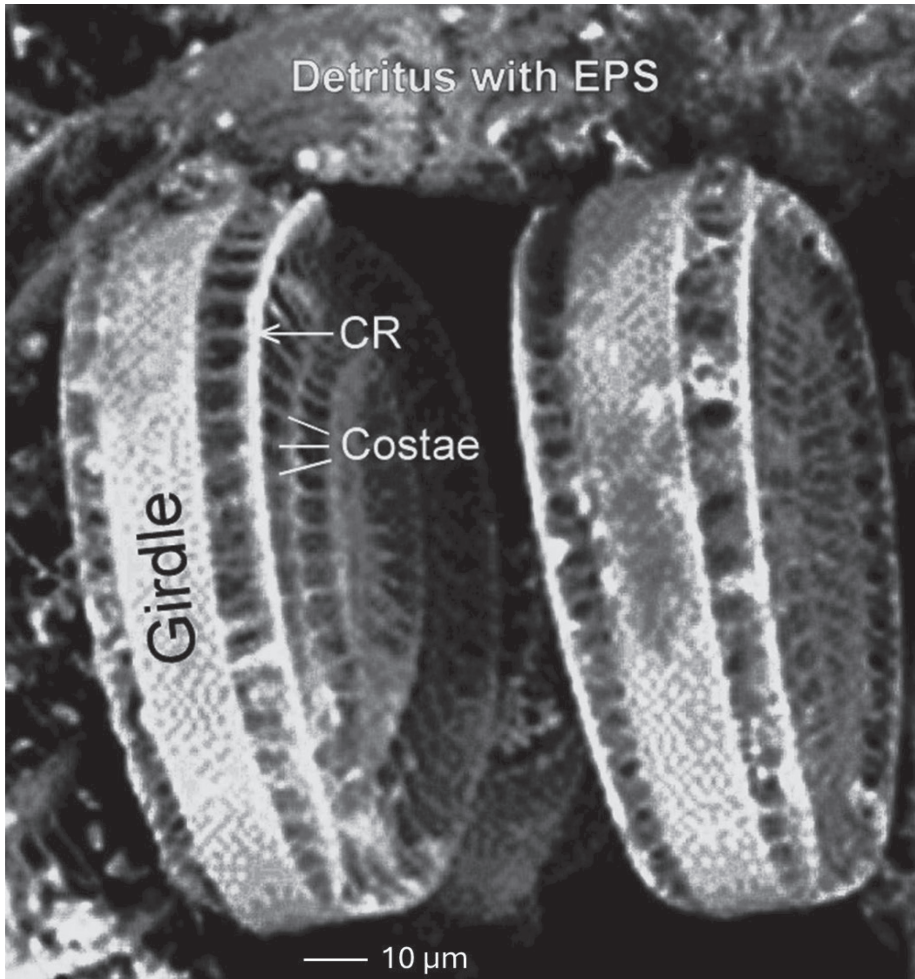


Figure 8. Electron micrograph of *Campylodiscus neofastuosus* from Bernier Cave positioned in girdle view and showing the detritus. Note the fabric-like consistency of the detritus. This is due to it being bound by the extracellular polymeric substances (EPS) secreted from the canal raphe (CR).

particles leading to marine snow aggregates. So, as with marine snow, the diatom EPS in the cave glues together material in the detritus converting it into a loose biofilm easily managed as a food source by the brittle star. The consistency of this loose biofilm is fabric-like (Fig. 8), similar to that described in Heissenberger et al. (1996) for marine snow.

Conclusion

Bernier Cave contains a rare and possibly unique niche that has allowed for the evolution and survival of the endemic brittle star *A. stygobita*. The cave's large ceiling entrance allows both detritus and enough light to reach the walls and water in the

entrance room for microbial communities to thrive. These communities are dominated by large diatoms *Campylodiscus neofastuosus* that have distinct morphological adaptations in their cell wall architecture and chloroplast morphology to make efficient use of the limited light. The diatoms release substantial EPS rich in polysaccharides that bind the detritus (Shnyukova and Zolotariova 2017) and gives it the consistency that allows the brittle star to feed on it. The presence of *C. neofastuosus* makes the detritus in Bernier Cave different from detritus in other caves. These large diatoms enrich and modify the detritus to support a diverse population of detritivores (nematodes, ostracods, copepods, ciliates) and particularly a population of the endemic cave brittle star *Amphicutis stygobita*.

Acknowledgements

We thank the Bahamian government, the Gerace Research Centre on Salvador Island, and Executive Director Troy Dexter for logistic support. Special thanks for field and laboratory assistance to Julie Moses. Millicent Frimpong-Manso cultured the detritus and made observations of the organisms in the detritus. For field assistance we thank Ramamurthi Kannan, Mark Lewin, Patty Lewin, David Cunningham, Ben Crossley, Nick Callahan, Cliff Hart, Reeda Hart and Billy Stafford; Brenda Racke for assistance with NKU's scanning electron microscope. We also thank Melanie Riedinger-Whitmore, Rebecca Bixby and an anonymous reviewer who made valuable comments and suggestions that improved the manuscript.

Northern Kentucky University provided financial support for our research associates Julie Moses and Millicent Frimpong-Manso.

References

- Bhaskar PV, Bhosle NB (2006) Dynamics of transparent exopolymeric particles (TEP) and particle-associated carbohydrates in the Dona Paula Bay, west coast of India. *Journal of Earth System Science* 115: 403–413. <https://doi.org/10.1007/BF02702869>
- Büchel C (2020) Light-Harvesting Complexes of Diatoms: Fucoxanthin-Chlorophyll Proteins. In: Larkum A, Grossman A, Raven J (Eds) *Photosynthesis in Algae: Biochemical and Physiological Mechanisms*. *Advances in Photosynthesis and Respiration*, vol 45. Springer, Cham. <https://doi.org/10.1007/978-3-030-33397-3>
- Bruckner CG, Bahulikar R, Rahalkar M, Schink B, Kroth PG (2008) Bacteria associated with benthic diatoms from Lake Constance: phylogeny and influences on diatom growth and secretion of extracellular polymeric substances. *Applied and Environmental Microbiology* 74: 7740–7749. <https://doi.org/10.1128/AEM.01399-08>
- Carpenter JH (2016) Observations on the biology and behavior of *Amphicutis stygobita*, a rare cave brittle star (Echinodermata: Ophiuroidea) from Bernier Cave, San Salvador Island, Bahamas. *Proceedings of the 15th Symposium on the natural history of The Bahamas*. June 2013. Gerace Research Centre, San Salvador, 31–44.

- Carpenter JH (2025) *Amphicutis stygobita* (Echinodermata, Ophiuroidea, Amphilepidida, Amphilepididae), a brooding brittle star from anchialine caves in The Bahamas: feeding, reproduction, morphology, paedomorphisms and troglomorphisms. *Subterranean Biology* 51: 147–196. <https://doi.org/10.3897/subtbiol.51.152663>
- De Stefano L, De Stefano M, Maddalena P, Moretti L, Rea I, Mocella V, Rendina I (2007) Playing with light in diatoms: small water organisms with a natural photonic crystal structure. *Photonic Materials, Devices, and Applications II 6593*: 305–313. <https://doi.org/10.1117/12.723987>
- Falasco E, Ector L, Isaia M, Wetzel CE, Hoffmann L, Bona F (2014) Diatom flora in subterranean ecosystems: a review. *International Journal of Speleology* 43: 231–251. <https://doi.org/10.5038/1827-806X.43.3.1>
- Foged N (1984) *Freshwater and Littoral Diatoms from Cuba*. Bibliotheca Diatomologica, J. Cramer, Berlin, Germany.
- Ghobara MM, Mazumder N, Vinayak V, Reissig L, Gebeshuber IC, Tiffany MA, Gordon R (2019) On light and diatoms: A photonics and photobiology review. In: Seckbach J, Gordon R (Eds) *Diatoms: fundamentals and applications*, 129–189. <https://doi.org/10.1002/9781119370741.ch7>
- Goessling JW, Su Y, Cartaxana P, Maibohm C, Rickelt LF, Trampe EC, Walby SL, Wangpra-seurt D, Wu X, Ellegaard M, Kühl M (2018) Structure-based optics of centric diatom frustules: modulation of the in vivo light field for efficient diatom photosynthesis. *New Phytologist* 219: 122–134. <https://doi.org/10.1111/nph.15149>
- Goessling JW, Yanyan S, Kühl M, Ellegaard M (2021) Frustule photonics and light harvesting strategies in diatoms. In: Annenkov V, Seckback J, Gordon R (Eds) *Diatom morphogenesis*, 269–300.
- Goldman N, Paddock TBB, Shaw KM (1990) Quantitative analysis of shape variation in populations of *Surirella fastuosa*. *Diatom Research* 5: 25–42. <https://doi.org/10.1080/0269249X.1990.9705090>
- Hamm CE, Merkel R, Springer O, Jurkojc P, Maier C, Prechtel K, Smetacek V (2003) Architecture and material properties of diatom shells provide effective mechanical protection. *Nature* 421: 841–843. <https://doi.org/10.1038/nature01416>
- Heissenberger A, Leppard GG, Herndl GJ (1996) Ultrastructure of marine snow. II. Microbiological considerations. *Marine Ecology Progress Series* 135: 299–308. <https://doi.org/10.3354/meps135299>
- Helliwell KE, Ahmed AS, Shady AA (2022) The diatom microbiome: new perspectives for diatom-bacteria symbioses. In: Falcatore A, Mock T (Eds) *The Molecular Life of Diatoms*. Cham: Springer International Publishing, 679–712. https://doi.org/10.1007/978-3-030-92499-7_23
- Hradaynath R, Singh I (2015) Lenses, Mirrors and Prisms. In: *Encyclopedia of Optical and Photonic Engineering (Print)-Five Volume Set* CRC Press, 20 pp.
- Macalady JL, Dattagupta S, Schaperdoth I, Jones DS, Druschel GK, Eastman D (2008) Niche differentiation among sulfur-oxidizing bacterial populations in cave waters. *The ISME Journal* 2: 590–601 <https://doi.org/10.1038/ismej.2008.25>
- Mann DG (1996) Chloroplast morphology, movements, and inheritance in diatoms. In: Chaudhary BR, Agrawal SB (Eds) *Cytology, Genetics and Molecular Biology of Algae*. SPB Academic Publishing, Amsterdam, 249–274.

- Oliver L, Dietrich T, Marañón I, Villarán MC, Barrio RJ (2020) Producing omega-3 polyunsaturated fatty acids: A review of sustainable sources and future trends for the EPA and DHA market. *Resources* 9: 148. <https://doi.org/10.3390/resources9120148/>
- Perera IA, Abinandan S, Subashchandrabose SR, Venkateswarlu K, Cole N, Naidu R, Megharaj M (2022) Extracellular polymeric substances drive symbiotic interactions in bacterial–microalgal consortia. *Microbial Ecology* 83: 596–607. <https://doi.org/10.1007/s00248-021-01772-1>
- Popović SS, Nikolić NV, Pečić MN, Anđelković AA, Subakov Simić GV (2023) First report on a 5-year monitoring of lampenflora in a famous show cave in Serbia. *Geoheritage* 15: 14. <https://doi.org/10.1007/s12371-022-00771-z/>
- Pomory CM, Carpenter JH, Winter JH (2011) *Amphicutis stygobita*, a new genus and new species of brittle star (Echinodermata: Ophiuroidea: Ophiurida: Amphilepididae) found in Bernier Cave, an anchialine cave on San Salvador Island, Bahamas. *Zootaxa* 3133: 50–68. <https://doi.org/10.11646/zootaxa.3133.1.3>
- Poulsen N, Davutoglu MG, Zackova Suchanova J (2022) Diatom adhesion and motility. In: Falciatore A, Mock T (Eds) *The molecular life of diatoms*. Cham: Springer International Publishing, 367–393. https://doi.org/10.1007/978-3-030-92499-7_14
- Ramirez-Llodra E, Brandt A, Danovaro R, De Mol B, Escobar E, German CR, Levin LA, Martinez Arbizu P, Menot L, Buhl-Mortensen P, Narayanaswamy BE, Smith CR, Tittensor DP, Tyler PA, Vanreusel A, Vecchione M (2010) Deep, diverse and definitely different: unique attributes of the world's largest ecosystem. *Biogeosciences* 7: 2851–2899. <https://doi.org/10.5194/bg-7-2851-2010>
- Roldán M, Hernández-Mariné M (2009) Exploring the secrets of the three-dimensional architecture of phototrophic biofilms in caves. *International Journal of Speleology* 38: 41–53. <https://doi.org/10.5038/1827-806X.38.1.5>
- Round FE, Crawford RM, Mann DG (1990) *Diatoms: Biology and Morphology of the Genera*. Cambridge University Press.
- Ruck E, Theriot EC (2011) Origin and Evolution of the Canal Raphe System in Diatoms. *Protist* 162: 723–737. <https://doi.org/10.1016/j.protis.2011.02.003>
- Ruck E, Nakov T, Alverson AJ, Theriot EC (2016a) Phylogeny, ecology, morphological evolution, and reclassification of the diatom orders Surirellales and Rhopalodiales. *Molecular Phylogenetics and Evolution* 103: 155–171. <https://doi.org/10.1016/j.ympev.2016.07.023>
- Ruck EC, Nakov T, Alverson AJ, Theriot EC (2016b) Nomenclatural transfers associated with the phylogenetic reclassification of the Surirellales and Rhopalodiales. *Notulae Algarum* 10: 1–4.
- Scarsini M, Marchand J, Manoylov KM, Schoefs B (2019) Photosynthesis in diatoms. In: Seckbach J, Gordon R (Eds) *Diatoms: fundamentals and Applications*, 191–211. <https://doi.org/10.1002/9781119370741.ch8>
- Sköld M, Gunnarsson JS (1996) Somatic and germinal growth of the infaunal brittle stars *Amphiura filiformis* and *A. chiajei* in response to organic enrichment. *Marine Ecology Progress Series* 142: 203–214. <https://doi.org/10.3354/meps142203>
- Shnyukova EI, Zolotariova EK (2017) Ecological role of exopolysaccharides of Bacillariophyta: A review. *International Journal on Algae* 19: 5–24. <https://doi.org/10.1615/InterJAlgae.v19.i1.10>
- Simon KS, Benfield EF, Macko SA (2003) Food web structure and the role of epilithic biofilms in cave streams. *Ecology* 84: 2395–2406. <https://doi.org/10.1890/02-334>

- Spaulding S, Edlund M (2009) *Campylodiscus*. In: Diatoms of North America. Guide to Campylodiscus | Genera - Diatoms of North America. [Retrieved 9/22/2024]
- Spaulding S, Edlund M (2010) *Surirella*. In: Diatoms of North America. Guide to Surirella | Genera - Diatoms of North America. [Retrieved 9/22/2024]
- Svetlana NK, Andrey VU, Porfirev AP (2022) Diatom optical element: a quantized version of the generalized spiral lens. *Optics Letters* 47: 3988–3991. <https://doi.org/10.1364/OL.469113>
- Thornton DC (2002) Diatom aggregation in the sea: mechanisms and ecological implications. *European Journal of Phycology* 37: 149–161. <https://doi.org/10.1017/S0967026202003657>
- Underwood GJ (2024) Extracellular polymeric substance production by benthic pennate diatoms. In: Goessling Jw, Serôdio J, Lavaud J (Eds) *Diatom Photosynthesis: From Primary Production to High-Value Molecules*, 301–326. <https://doi.org/10.1002/9781119842156.ch10>
- Winsborough B, Sudbury JB (2024) The Diatom Flora of Hall's Cave, Kerr County, Texas. *Journal of Cave and Karst Studies* 86: 37–56. <https://doi.org/10.4311/2019PA0104>
- Zhang S, Xu C, Santschi PH (2008) Chemical composition and ^{234}Th (IV) binding of extracellular polymeric substances (EPS) produced by the marine diatom *Amphora* sp. *Marine Chemistry* 112: 81–92. <https://doi.org/10.1016/j.marchem.2008.05.009>